

A novel mechanism for centrosome expulsion ensures metabolic activity in polyploid cells

Riham Salame

▶ **To cite this version:**

Riham Salame. A novel mechanism for centrosome expulsion ensures metabolic activity in polyploid cells. Development Biology. Université Paris sciences et lettres, 2025. English. ⟨NNT : 2025UPSLS040⟩. ⟨tel-05559281⟩

HAL Id: tel-05559281

https://theses.hal.science/tel-05559281v1

Submitted on 19 Mar 2026

HAL is a multi-disciplinary open access archive for the deposit and dissemination of scientific research documents, whether they are published or not. The documents may come from teaching and research institutions in France or abroad, or from public or private research centers.

L'archive ouverte pluridisciplinaire **HAL**, est destinée au dépôt et à la diffusion de documents scientifiques de niveau recherche, publiés ou non, émanant des établissements d'enseignement et de recherche français ou étrangers, des laboratoires publics ou privés.



HAL Authorization

PSL UNIVERSITÉ PARIS

THÈSE DE DOCTORAT
DE L'UNIVERSITÉ PSL

Préparée à l'Institut Curie
UMR144 – Biologie Cellulaire et Cancer

Un nouveau mécanisme d'expulsion des centrosomes est nécessaire au maintien de l'activité métabolique dans les cellules polyploïdes

A novel mechanism for centrosome expulsion ensures metabolic activity in polyploid cells

Soutenue par
Riham SALAME
Le 08 septembre 2025

Ecole doctorale n° 515
Complexité du vivant

Spécialité
Biologie cellulaire et développement

Composition du jury :

Manuel, THERY PhD, CEA	*Président*
Katja, RÖPER PhD, MRC	*Rapporteure*
Benedicte, DURAND PhD, Claude Bernard University	*Rapporteure*
Véronique, BRODU PhD, Institut Jacques Monod	*Examinatrice*
Ishier, RAOTE PhD, Institut Jacques Monod	*Examinateur*
Renata, BASTO PhD, Institut Curie	*Directrice de thèse*

institutCurie | PSL

Acknowledgment

Thursday 22. May 2025 – 1:30 pm: The first day I started writing this thesis. I am not sure that anything I wrote that day is actually kept in this version! But I will never forget what I felt that day. And from that date, everyday I sit in front of my computer to write a new sentence, chapter or even just stare at the screen, and everyday I think what should I write in this part. I am sorry in advance that this will be long, because I am so lucky to have so many people that I love and that contributed to this thesis. I really hope I don't forget anyone, but I am writing this at 8 in the morning after not sleeping for an entire day, so….

First, I would like to thank **Renata**, for her supervision and for her help throughout my whole thesis. Thank you for your guidance and for sharing all your great Drosophila knowledge with me and for seeing potential in me and giving me this opportunity. I want to thank you for all your help and reading over and over and over this manuscript to be sure that it is flawless, (at least I hope it is!). I will always remember our late discussion on Friday when we start brainstorming and throw hypothesis, that I am not sure we remember all of them, but these were great moments.

Now our precious lab member, I want to write to all of you that is still in the lab and those who left and those who are not in the team but feels like they are! You are the best team that anyone can ask for!! Believe it or not but without you guys, I don't think this thesis would have been as it is now.. Thank you endlessly for that!

Anthony, our superhero, magician and angel that find a solution for anything and is always there to help! I don't think I ever met someone with such energy and memory.. Thank you so much for all your help during the molecular biology (the hell experiments), and I will always be gratefull for you because you told me about la SPA and let me meet Zaytoun!!!!

Simon, one of the smartest and calmest person that I ever met! I can't count the amount of time I was impressed by how much information you know in very different domains. Thank you for sharing the work on salivary gland, even if in different project but I am no longer lonely working on SGs!!

Veronique, the great mom! Sharing the office with you was amazing, we talked and discussed science, and talked, and shared therapy sessions, and talked!!! I love how we turn around at the same moment and just start talking!! Discussing science with you is another experience that every single person in the lab should have it at least once!

Antonia, my lab bestie!! You are the most adventurous person that I ever met!! I love your energie and how strong and talented you are.. I miss so much our talks in the fly room and mounting your brains just for fun!! Thank you so much for sharing so many moments with me during this thesis, and for your support during work and personal time!! Thank you for coming to protest with me and for your support!! And I promise one day I will be in the crowd watching you dance like a star! And next year we paint more eggs!!!

Corentin, my dear!! We didn't know each other for long time but you became my favorite so fast! I love how smiley and histérique you are (but I don't love how you scare me!!!!).. Thank you so much for making me laugh and enjoy the lab even more!! And thank you for trying to speak in arabic whenever you can!! I am sure that you will do great things and that you are so smart that you can get and do anything even going to space!!!!

Hugo, the energy bomb! Another person who decided to get as a hobby scarring me!! Not appreciated!! But I love your smiley face and your energy and how much positive vibes you can give! Thank you that in such a short periode, you lightened the lab and made everything happier!! I am sure that you will have a great future full of energy!!!

Alima, I know it will sound weird but you are my salivary gland buddy!! I love the way that you are always smiling… Thank you for being so nice and for staying with me in the fly room dissecting together!! I wish that you will achieve all what you want and I hope we will see each other again!

Lin, the nicest and most innocent person I know! Thank you so much for just being in the lab, talking in arabic together and understanding each other so fast! Don't let

anyone change or ruin your nice heart!! I am sure that you will reach and achieve all what you want so fast!!

Neda, my mirror! I don't know if it is because we were going through the same thesis process, or because we are just so similar in behavior, but what I am sure of is that you were the perfect emotional support and friend in this road! Can't wait for our next panda wok meal!!

Etienne, the destroyer of vine leaves!! Thank you for always enjoying my food and giving the greatest expression!! You know that I will always save for you a plate of vine leaves! Thank you for sharing very deep and important conversations! You are next!!!

Margaux, the runner! although we didn't talk that much and we were in separate offices but I always see you smiling and positive! I can't believe how much you run and the fact that you actually love it!!!!! I wish for you all the best and that you get all what you want!

Sandrine, actually you are the calmest person I ever knew! Thank you so much for helping me with my medical issues and for sharing our love to dance in Turkey!

Céline, the savior! Thank you so much for helping me and everyone with all the administrative puzzle that we face!!

Althought these people left the lab long time ago, but their influence on me and on my thesis is unforgettable…

Agata, droso queen! Sharing the hidden office at the corner with you was amazing!! Thank you for always supporting me and for giving me confidence and great discussion!

Guilya, the star! I really wish that we went to Marseille much earlier! I really admire how strong you are.. no matter what happens you continue and you find a way! I learned so much from you! I can't wait to see you again in Paris or maybe in Nice! Maybe then we continue that UNO game!!

Clément, the food lover!! I love your passion for cooking and how much similar we are in that!! Thank you for always saying that I should rest and that I doing good!! I am still waiting for use to cook together one day!

Federica, the fashionista! The most elegant person I ever saw! Always flawless and on point! Thank you so much for all the support and for always saying something nice that will definetly comfort me! I will always remember you from the pillows!! I am sure that you are and will be even better and great PI…

Margot, the artist! I am sure you know that I am not the only one who love your drawing!! Thank you for always giving new movies suggestion with rating…

Manon, the energetic parisian! I love that everytime you start speaking in french slowly and then go as fast as light! Thank you so much for the discussion we had and the support after long day at work!

Oumou and **Frances**, thank you for all the discussion and suggestion that you gave me at the start of my thesis!

I am the luckiest person on earth to have such beautiful gifts from Paris to make my life here much easier and fun!!

Alice, **Giammarco**, **Magui** and **Mateus**: You are the best group that I can ever ask for!! Our boardgame nights, sharing food, roadtrips, travels, I cherish every single moment of these!! You made Paris a much better and happier place for me! I love you endlessly and I will be there for all of you forever!!

Now, let's go back in time. I am lebanese, more than half of me is still there somewhere in my bedroom, under any random tree from my village, in a small cafeteria… And although I am very far away from there, and I did my thesis here in Paris, but each one of my familly and friends were with me at every single moment!

Sara, who is the best to start with than my forever bestfriend and twinzy! 11 years and still counting! Thank you for always being there for me, for being on video call for 6

hours while I am working and quantifying!! For crying with me, laughing with me and being angry with me!!! For hating the same people that I hate even if you never met them!! (Sadek bi2ellik abdo btw) Ok ktir sa3eb eno le2e l kalimet bl english la elik li bade ellik ye! Merci baby 3ala kel shi 3njd, enik tkoune mawjoude hade 3atoul w tesma3e na2ee w tet7ammale hormonete w ka2abte w 3atoul ta3erfe t5alline erja3 ed7ak!! B3rf bt3rfe hal shi bs ha ellik yeha anw, ente ekhte li ma jebeta emme w shrike b hayete la e5ir nafas!!

Rany, **Rouba** and **Mohsen**: The rest of the gang! Although we are very busy but you always find time when I come to Lebanon so that we all sit together like we used to! I love you so much my second familly!!

Hsein and **Rana**: my protectors and saving angels! My brother and sister! I love you so much and I will never thank you enough for being my brother and sister and for giving me the best gifts in my entire life: Talia, Touline, Elena and Mostafa!!!

ماما و بابا، شكرا إنكم أمي وابي، شكرا لكل ما فعلتموه من أجلنا في هذه الحياة. شكرا خصيصا أنكم أمنتم لي هذه الفرصة لأحقق أحلامي وهدفي في حياتي. لم يكن سهلا أن أكون بعيدة عنكم كل هذه المدة ولكن تهون علي هذه المسافة عندما أراكم فخورين وسعداء بكل ما حققته باسمكم. أحبكم كثيرا

I know it will be weird, but I definetly want to thank my **Zaytoun**!! My little cat, my emotional support! I think he is the most who really saw every single moment of this final process! And always stayed next or even on my desk while writing this thesis!

Finally, I want to thank the person that sum up all the previous characteristic that I mentioned in just one person, **Sadek**. Writing for you a thank you is not enough to all what you did for me! But I couldn't thank everyone and not you! Actually if I am asked to only thank one person, it will be you! You were always there! When I am crying, screaming, depressed, crazy, happy, lazy… You were always there and always supprotive! Thank you for that!

Now you can go read the actual thesis. Thank you!

Table of Content

List of abbreviations ***5***

Chapter 1 - Introduction ***9***

1. Diploidy, Polyploidy and the cell cycle **10**

1.1. Diploidy 10

1.1.1. The cell cycle 10

Interphase 11

Mitosis 13

1.1.2. Cell cycle regulators 17

Cyclin-CDKs 17

1.1.3. Cell cycle checkpoints 20

1.2. Polyploidy 21

1.2.1. Endomitosis 22

Mitotic slippage 23

Cytokinesis Failure 23

1.2.2. Cell-cell Fusion 23

1.2.3. Endoreplication/ Endocycle 24

Endoreplication in *Drosophila* salivary glands 26

2. Scheduled and Unscheduled Polyploidy **31**

2.1. Advantages of scheduled polyploidy 31

2.1.1. Increase in cell size 31

2.1.2. Increase of metabolic activity 32

2.1.3. Barrier function 33

2.1.4. Stress response: regeneration and inhibition of apoptosis 33

2.2. Disadvantages of unscheduled polyploidy 35

2.2.1. Cancer 35

2.2.2. Genetic and chromosomal instability 36

3. Centrosomes **38**

3.1. Centrosome structure 38

3.1.1. Centrioles 39

3.1.2. Pericentriolar material – PCM 41

3.2. Centrosome duplication cycle 42

Initiation of duplication - G1/early S 42

Procentriole formation – S-phase 43

Centriole elongation –S/G2 44

Centriole to centrosome maturation – G2/M 44

3.3. Centrosome function 44

Non-centrosomal microtubule organizing centers (ncMTOCs) 46

3.4. Centrosome number 48

3.4.1. Centrosome number regulation 48

3.4.2. Centrosome amplification 48

Centrosome amplification in cancer 49

Centrosome amplification beyond cancer 50

Centrosome amplification and mitochondria 50

Centrosome amplification in programmed polyploid cells 55

Centrosome amplification control 55

3.4.3. Centrosome loss 56

Naegleria gruberi 57

Starfish oocytes 57

C. elegans 58

Drosophila melanogaster 59

Vertebrates: human and mouse 60

4. Myosin II 63
4.1. MyoII structure 63
4.1.1. Motor domain 64
4.1.2. Neck domain 65
4.1.3. Tail domain 67
4.2. MyoII mechanochemical cycle 68
4.3. MyoII function 70
4.3.1. Morphogenesis 70
4.3.2. Secretion 72
4.3.3. Activation of phagophore formation 73

5. Cellular trafficking and secretion 74
5.1. ESCRT-dependent membrane dynamics 74
5.1.1. ESCRT complex composition 74
5.1.2. ESCRT function and pathway 76
MVB formation process 76
Cytokinesis 76
5.2. Rab-mediated secretion 77
5.3. Autophagy 79
5.3.1. Molecular mechanisms 79
Induction of autophagy 80
Initiation - Phagophore formation 81
Elongation - Autophagosome closure 81
Fusion with the lysosome - Autolysosome 81
5.3.2. Outcome of the autophagic pathway 82

6. *Drosophila* Salivary glands 83
6.1. *Drosophila* as a model system 83
6.1.1. *Drosophila* genome 83
6.1.2. *Drosophila* life cycle 83
6.1.3. Genetic tools 85
UAS-GAL4 system 85
Balancer Chromosomes 86
6.2. Salivary glands 86
6.2.1. SG development 87
During Embryogenesis (Figure 24) 87
During larval stages (Figure 26) 90
During pupation 91
During adulthood (Figure 27) 92
6.2.2. SG function 92
Growth factors 93
Glue proteins 93
Apocrine secretion 94

Thesis outlines 95

Chapter 2 – Material and Methods 97

1. Fly husbandry 98
1.1. Fly culture 98
1.2. Fly stocks 99

2. Immunofluorescence experiments 100
2.1. Immunofluorescence of *Drosophila* SGs whole mount preparations 100
2.2. Clearing experiment on L3 SGs for microtubule staining 100
2.3. Embryo culture and collection 101
2.4. DNA Fluorescent In Situ Hybridization (FISH) 102

3. Primary and secondary antibodies 103

4. MG-132 treatment for proteasome activity inhibition 105

5. SeaHorse Assays 105

6. Conventional transmission electron microscopy (EM) 105

7. Molecular Biology 106

7.1. Molecular cloning 106

7.2. Synthetized/mutagenized sequences: 107

7.2.1. For WT MyoII-mCherry: 107

7.2.2. For MyoII AA - mCherry: (Inactive MyoII - iMyoII) 108

7.2.3. For MyoII EE - mCherry: (Constitutively active MyoII - aMyoII) 109

8. Live imaging of *Drosophila* embryos 110

9. Image acquisition and analysis 110

9.1. L3 SGs Image acquisition and super-resolution 110

9.2. Embryonic SGs Images acquisition 111

9.3. Imaris 111

9.4. Analysis 111

9.4.1. Quantification of the frequency of events 111

9.4.2. Characterization of centrosomes in L3 SGs 112

9.4.3. Mitochondria characterization 112

9.4.4. Ubiquitin fluorescence signal quantification 112

9.4.5. Statistical analysis 113

Chapter 3 - Results 114

1. Abstract: 116

2. Introduction 117

3. Results 118

3.1. Centrosomes are released into the salivary gland lumen during embryonic development 118

3.2. Centrosome expulsion depends on MyoII activity 119

3.3. Centrosome release into the SG lumen does not require loss of Polo kinase activity 120

3.4. Increasing MyoII activity can overcome the presence of extra centrosomes in SG cells .. 121

3.5. Luminal centrosomes are targeted for proteasome degradation 121

3.6. Secretory autophagy coupled with autolysosome exocytosis promotes centrosome expulsion from the cell 123

3.7. Centrosome elimination is required for proper mitochondria organization and respiratory activity 124

4. Discussion 126

Chapter 4 - Figures 129

Chapter 5 - Discussion 150

1. Why reaching such high level of ploidy? 151

2. Is there a relation between centrosome elimination and endoreplication? 152

3. Similar mechanisms for centrosome elimination in the fat body and ring gland polyploid cells? 153

4. Direct function of MyoII on centrosomes? 153

5. Why are centrosomes degraded in the lumen? Is there a function in glue biogenesis? 154

6. MyoII role in MT nucleation from the NE? 154

7. **How do centrosomes influence the mitochondrial network? 155**
8. **Do centrosomes disrupt mitochondrial function by altering the MT cytoskeleton? 156**

References 157

List of abbreviations

ADP	Adenosine diphosphate
ALIX	Apoptosis-linked gene-2 interacting protein X
aMyoII	Hyperactive (constitutively active) Myosin II
Ana1	Anastral spindle1
Ana2	Anastral spindle 2
APC/C	Anaphase-promoting complex or cyclosome
Asl	Asterless
ATM	Ataxia-telangiectasia mutated
ATP	Adenosine triphosphate
ATR	Ataxia telangiectasia and Rad3 related
CAK	CDK-activating kinase
Cdc45	Cell division cycle protein 45
CDKs	Cyclin-dependent kinases
ChII/III	Chromosome II/III
CHMP	Charged multivesicular body protein
CIP/KIP	CDK interacting protein/Kinase inhibitory protein family
Cnn	Centrosomin
CP110	Centriolar Protein of 110 kDa
Crb	Crumbs
CyO	Curly of Oster
Dapi	4′,6-diamidino-2-phenylindole
Dl	Dorsal
Dpp	Decapentaplegic
Duf	Dumbfounded
ELCs	Essential light chain
EM	Electron microscopy
ESCRT	Endosomal sorting complex required for transport
FADH2	Flavin adenine dinucleotide
FEN1	Flap endonuclease-1
Fkh	Fork head
FM7	First Multiple 7

Fzr	Fizzy-related
G0 phase	Gap0 phase
G1 phase	Gap1 phase
G2 phase	Gap2 phase
GAP	GTPase-activating protein
GDI	Rab GDP dissociation inhibitor
GEFs	Guanine exchange factors
GGT	Geranylgeranyl transferase
GSK-3β	Glycogen synthase kinase-3β
HMMM	Homemade mounting media
HRS	Hepatocyte growth factor regulated tyrosine kinase substrate
iMyoII	Inactive Myosin II
K48	Proteasome-promoting Lysine 48 polyubiquitination
K63	Autophagy-linked Lysine 63 polyubiquitination
Klp10A	Kinesin-like protein 10A
L1/ L2/ L3	First/ Second/ Third larval stages
L50	Lower 50 kDa subdomain
LAMP1/2	Lysosomal-associated membrane protein 1/2
LSVs	Large secretory vesicles
MBS	Myosin-binding subunit
MCM	Mini-chromosome maintenance
MHC	Myosin heavy chain
MIM	Microtubule interacting and trafficking domain-interacting motif
MIT	Microtubule interacting and trafficking domain
MLCK	Myosin light chain kinase
MLCP	Myosin light chain phosphatase
Msp300	Muscle-specific protein 300 kDa
Msps	Minispindles
mtDNA	Mitochondrial DNA
MTOC	Microtubule organizing center
MTs	Microtubules
MVBs	Multivesicular bodies
MyoII	Non-muscle myosin II

MYPT1	Myosin phosphatase target subunit 1
NADH	Nicotinamide adenine dinucleotide
Ncd	Non-claret disjunctional
ncMTOC	Non-centrosomal microtubule organizing center
NE	Nuclear envelope
Nin	Ninein
Nter	N-terminal subdomain
ON	Overnight
ORCs	Origin Recognition complexes
OXPHOS	Oxidative phosphorylation
P-loop	Phosphate-binding loop
p-MyoII	Phospho-Myosin II
PBS	Phosphate-Buffered Saline
PCD	Programmed cell death
PCM	Pericentriolar material
PCNA	Proliferating cell nuclear antigen
Pi	Inorganic phosphate
PI3K	Phosphatidylinositol-3-kinase
Plk4	Polo like kinase 4
Plp	Pericentrin-like protein
Pol δ	DNA polymerase epsilon δ
Polα	DNA polymerase α
Polε	DNA polymerase epsilon ε
PP1	Protein phosphatase
Pre-RC	pre-replication complex (pre-RC)
PS	Parasegment
Rab	Ras-related protein in brain
Ran	Ras-related nuclear protein
RB	Retinoblastoma
RhoGAP	Rho GTPase activating protein
Rif1	Rap1-interacting factor 1
RLCs	Regulatory light chain
RNAi	RNA interference

ROCK	Rho-associated protein kinase
RPA	Replication protein A
Rst	Roughest
S phase	Synthesis phase
SAC	Spindle assembly checkpoint
Sas-4	Spindle assembly abnormal-4
Sas-6	Spindle assembly abnormal-6
SCF	Skp1-Cullin1-F-box
Scr	Sex combs reduced
Sgs	Salivary gland secretion protein
SGs	Salivary glands
Sgsf	SG-derived secreted factor
SNARE	Soluble NSF Attachment Protein Receptor
Sns	Sticks and stones
Spd-2	Spindle defective-2
SPG	Sub-perineurial glia
Sqa	Spaghetti-squash activator
sqh	Spaghetti squash
SSB	Single-strand DNA-binding proteins
ssDNA	Single-stranded DNA
STAM	Signal transducing adaptor molecule
SuUR	Suppressor of Under-replication
Syx16	Syntaxin 16
TGN	Trans-Golgi network
TM6	Third Multiple 6
TOR	Target of rapamycin
Tsh	Teashirt
U50	Upper 50 kDa subdomain
UB	Ubiquitin P4D1
Vps4	Vacuolar protein sorting
WGD	Whole genome duplication
WT	Wildtype
γ-TuRC	γ-Tubulin ring complex
γ-TuSC	γ-tubulin small complexes

Chapter 1 - Introduction

1. Diploidy, Polyploidy and the cell cycle

1.1. Diploidy

Diploidy is defined by the presence of two sets of each chromosome, which are inherited from each parent. Diploidy is hallmark of most animal cells, including humans, but also for many plants and other eukaryotic organisms such as *Drosophila melanogaster* (Fuse et al., 1994; Goldstein, 1992). Maintenance of the diploid status requires genetic stability, which is possible thanks to a regulated cell cycle, allowing the birth of identical diploid cells from a pre-existing cell.

1.1.1. The cell cycle

Cell biology went through many debatable theories through history, until the 19th century when the “cell theory” was proposed and described by Mathias Jacob Schleiden, a German botanist, and Theodor Schwann, a German physiologist (Ribatti, 2018; Scott and Logan, 2004). This theory acknowledged that the cell is the basic unit of all organisms and that cells arise from pre-existing parental cells after division. A process now known to be possible thanks to a tight regulation of the cell cycle.

The cell cycle varies from one organism to another. Further, even among the same organism, cell cycles can vary substantially however, several common characteristics can be found (Figure 1). Generally, the cell cycle consists of two major phases, a long phase allowing cell growth both in size and DNA content, known as Interphase, and a second shorter phase that allows cell division into two genetically identical daughter cells, known as Mitosis (Norbury and Nurse, 1992). Each phase is divided into several steps, regulated by cyclin-dependent kinases (CDKs) and monitored by cell cycle checkpoints (Summarized in Table 1).

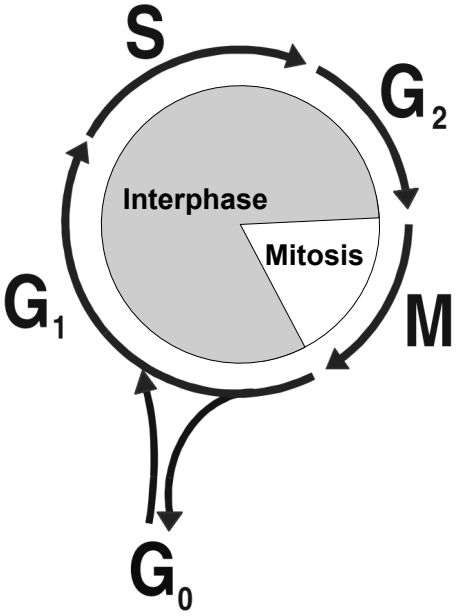


Figure 1. The cell cycle

The cell cycle consists of a growth and replication phase called interphase and a mitotic phase (M). Interphase is divided into three distinct phases, G1, S and G2, while M-phase is the phase of division. Modified from (Vermeulen et al., 2003).

Interphase

Interphase starts with the pre-replicative growth phase, also known as Gap1 (G1) phase, to prepare cells for DNA synthesis. During this first phase, the cell increases in size and becomes metabolically active enabling the synthesis of nutrients, RNA and proteins required for the accomplishment of the following phases (Pardee, 1989). If the cell is not ready to proceed to the next phase, it may exit the G1 phase and enters in a non-proliferative G0 phase, remaining quiescent until further reactivation (Pardee, 1989).

When the conditions are favorable or when there is stimulation by growth factors, cells progress through the commitment point (also known as the restriction point) and enter the Synthesis (S) phase. In this phase, DNA replication takes place (Figure 2). One critical step that should occur during G1 to ensure DNA replication, is the assembly of replication origins at specific DNA regions (Fangman and Brewer, 1992). Origin Recognition complexes (ORCs) bind to these replication origins, followed by the recruitment of proteins like Cdc6 and Cdt1, responsible to recruit and load a complex of helicases- mini-chromosome maintenance (MCM) in its inactive

state. Helicases are proteins involved in DNA unwinding (Bell and Botchan, 2013; Fragkos et al., 2015; Masai et al., 2010). This entire complex, comprising ORCs, Cdc6, Cdt1 and MCM is also called the pre-replication complex (pre-RC), which marks the licensing process required for the initiation of DNA synthesis.

At the onset of S-phase, ORCs are phosphorylated by CDKs, inhibiting its capacity to load new MCM helicases until the next G1 and thus ensuring that the DNA is replicated only once per cell cycle (Arias and Walter, 2007). The MCM complex is then activated by the assembly of two helicase activator proteins, a tetrameric protein complex, GINS, that stabilize the association of another activator, the Cell division cycle protein 45 (Cdc45), forming the CMG helicase (Aparicio et al., 2006; Takayama et al., 2003; Zou et al., 1997). This CMG helicase is responsible to unwinds the DNA double-helix by breaking the hydrogen bonds generating single-stranded DNA (ssDNA) (Abdel-Monem et al., 1976; Li and O'Donnell, 2018; Tanaka and Araki, 2013).

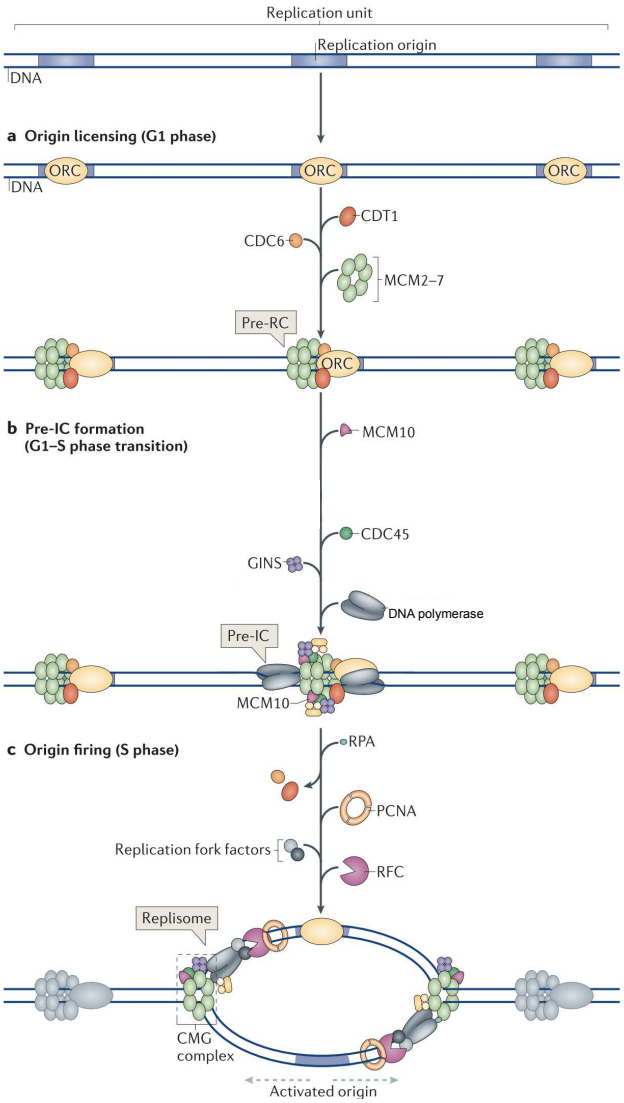


Figure 2. The machinery involved in DNA replication

During G1, the pre-RC complex is recruited to replication origins triggering their "licensing". Then the MCM helicase unwinds the DNA, which allows the recruitment of DNA polymerases generating origin firing. At this point, new DNA starts to be synthesized, marking the beginning of S-phase. Modified from (Fragkos et al., 2015).

This marks the formation of the replication fork, and the initiation of DNA synthesis through the firing process. All regions of the single-stranded DNA are then straightened by the cooperative binding of single-strand DNA-binding proteins (SSB), such as the replication protein A (RPA), preventing short region base-paired matching, known as short hairpin helices (Wold, 2025).

Initiation of DNA synthesis requires DNA polymerase α (Polα). DNA Polα -the DNA primase- binds to the DNA strand and uses it as a template to synthetize a short ribonucleotide primer in the leading strand and at the beginning of all the Okazaki fragments on the lagging strand (Burgers, 2009; Dewar and Walter, 2017; Friedberg, 2006). DNA Polα synthesizes only a short sequence of nucleotides however, this problem is overcome by the association of a sliding clamp, such as proliferating cell nuclear antigen (PCNA) protein, that catches the polymerase on the DNA using a clamp loader, until it reaches a 5'-end (Burgers, 2009). Thanks to DNA polymerase epsilon ε and delta δ and (Polε and Pol δ), the leading strand is continuously synthetized from 5' → 3', while the lagging strand will be discontinuously synthetized mainly by Pol δ (Burgers, 2009; Zheng and Shen, 2011). With the activity of Flap endonuclease-1 (FEN1), all RNA primers are removed and replaced with DNA by Polδ. These new DNA fragments are then joined and sealed by a DNA ligase.

The last phase of interphase is another growth phase- G2 phase, where both cell mass and organelle number increase in order to prepare the cell for mitosis (Norbury and Nurse, 1992).

Mitosis

Mitosis, the process of cell division was firstly described by Walther Flemming in 1882 (Flemming Walther, 1882), using his developed staining techniques that showed subcellular structures throughout the cell cycle. Based on his observations, he illustrated cell cycle progression by describing a filamentous structure, later known as

the chromosomes. He found that chromosomes were localized within the nucleus and that changes in size and shape, prior cell division could be noticed (Flemming Walther, 1882; Uzbekov and Prigent, 2022).

Mitosis starts with chromosome condensation, which is dependent on the condensin complex. In the cytoplasm, the mitotic spindle is assembled with the nucleation of microtubules (MTs) from the two centrosomes, which are the main microtubule organizing center (MTOCs) of animal cells (Figure 3). Centrosomes also nucleate astral MTs that radiate and connect the poles to the cell cortex, ensuring correct spindle positioning. This represents the first phase of mitosis, and it is known as prophase (Peter et al., 1990; Sedat and Manuelidis, 1977). Nuclear envelope (NE) breakdown allows MTs to capture chromosomes by binding to kinetochores, a protein complex recruited at the centromere that connects the sister chromatids (Walczak et al., 2010; Walczak and Heald, 2008; Zhai et al., 1996). This represents the second phase of mitosis- prometaphase. Once all chromosomes are captured by MTs emanating from opposite poles and aligned normally at the center of the cell, a metaphase phase can be noticed (Walczak et al., 2010). During anaphase, sister chromatids separate synchronously and are pulled apart to opposite poles. Chromosome segregation is initiated by cleavage of cohesion proteins that hold sister chromatids together, by a protease called Separase (Uhlmann, 2001). In addition to cohesion cleavage, sister chromatids are pulled apart to opposite poles due to forces exerted on chromosomes and the shortening of kinetochore MTs by depolymerizing kinesins. Further, the elongation of interpolar MTs, trigger spindle pole outward movement (Batty and Gerlich, 2019; Hopfner, 2003; Nishiyama, 2018; Walczak et al., 2010). Telophase is initiated with chromosome decondensation, mitotic spindle disassembly, and NE reformation. Cytokinesis allows the physical separation of the cytoplasm, and the assembly of two genetically identical daughter cells. In animal cells, cytokinesis requires actin filaments, myosin II and other proteins that will assemble into a contractile ring allowing the formation of a cleavage furrow (Gatti et al., 2000; Karess et al., 1991; Schroeder, 1973; Williams et al., 1995).

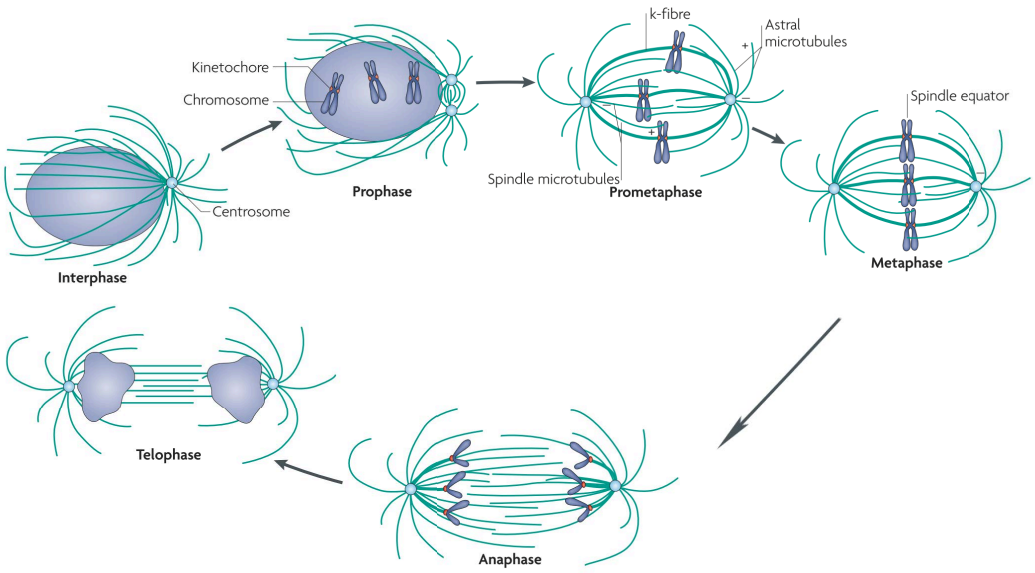


Figure 3. Different phases of mitosis

Mitosis is divided into five distinct phases. Prophase is initiated when chromosomes start condensing forming their typical shape and the NE breaks down. During prometaphase, the centrosomes have separated and are actively nucleating MTs, leading to the establishment of kinetochore-MT attachments. Metaphase is recognized by the chromosome alignment on the equatorial plate of the cell due to their bipolar attachment status. During Anaphase sister chromatids segregate to opposite poles of the spindle. In telophase, the NE is reformed and with cytokinesis, cells became physically separated. Modified from (Walczak et al., 2010).

Table 1. Summary of the key events during each phase of the cell cycle

	Phase	Main events
Interphase	G1 phase	Cell size increase RNA and protein synthesis Fate decision Origin of Replication assembly Pre-replication complex (Pre-RC) assembly: ORCs bind to replication origins Cdc6 and Cdt1 bind to ORCs Recruitment and loading of MCM helicases
	S phase	Phosphorylation of ORCs by CDK Recruitment of Cdc45 and GINS MCM activation Synthesis of short Ribonucleotides by DNA primases Association of PCNA with replicative regions <u>Leading strand:</u> Polε recognition catalyzing synthesis from 5' → 3' direction <u>Lagging strand:</u> Polα discontinuously synthetizes Okazaki fragments Polδ synthesis of Okazaki fragments DNA ligase joins the DNA fragments together
	G2 phase	Growth phase Cell mass increase Organelle number increase
Mitosis	Prophase	Chromosome condensation Bipolar mitotic spindle assembly
	Prometaphase	Nuclear envelope breakdown Chromosomes captured by MTs
	Metaphase	Chromosomes alignment
	Anaphase	Cohesion cleavage Chromosome segregation towards the poles
	Telophase	Chromosome decondensation Disassembly of the mitotic spindle Nuclear envelope reformation Cytokinesis

1.1.2. Cell cycle regulators

Cyclin-CDKs

The passage from one phase to another is tightly regulated by CDKs, which are a family of serine/threonine protein kinases (Morgan, 1995; Pines, 1995; Uzbekov and Prigent, 2022; Vermeulen et al., 2003). CDKs are normally present throughout the cell cycle, but their activity is tightly controlled by the oscillation of the levels of cyclins (Figure 4) (Glotzer et al., 1991; Vermeulen et al., 2003). Cyclin binding is not the only factor that activates CDKs. Frequently, this requires the phosphorylation of CDKs near its active site by a CDK-activating kinase (CAK). In G1, Cyclin D starts to accumulate in the cell which will form a complex with CDK4 or CDK6 (Sherr, 1994; Vermeulen et al., 2003). This complex allows CDK4/6 to partially phosphorylate the retinoblastoma tumor suppressor protein (RB) (Arroyo and Raychaudhuri, 1992; Weinberg, 1995). In its unphosphorylated status, RB binds and inhibits the S-Phase promoting E2F transcription factor (Rubin et al., 2020; Weintraub et al., 1992). Once phosphorylated, RB releases E2F allowing transcriptional activation of factors essential for G1/S transition, such as cyclin E (Bertoli et al., 2013; Foster et al., 2010). Cyclin E binds CDK2 to form an active complex that fully phosphorylate RB leading to the activation of genes required for DNA replication by E2F (Girard et al., 1991; Ohtsubo et al., 1995).

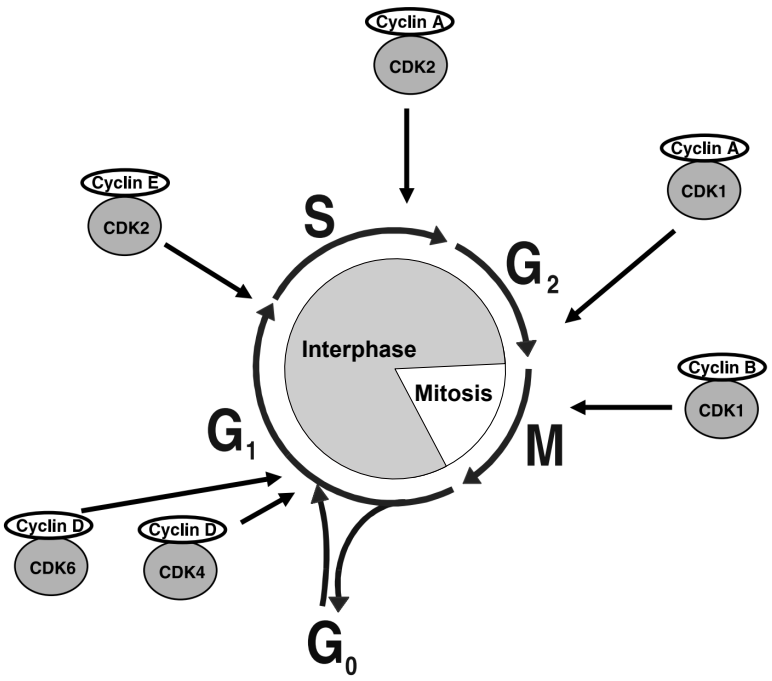


Figure 4. The cell cycle and its regulators - CDKs and Cyclins

The cell cycle is regulated by different type of cyclins. These are synthesized and degraded in a cell cycle phase distinctive manner. The binding of cyclins to a specific CDK is permissive to CDK activation (Vermeulen et al., 2003).

E2F also promotes transcription of cyclin A. Cyclin A is the only cyclin that promotes transition through different cell cycle phases by binding to different CDKs. First, cyclin A replaces cyclin E and associates with CDK2 which is essential for completion of DNA replication and S-phase progression (Duncan H. Walker & James L. Maller, 1991). Cyclin A binds to CDK1 in order to prepare cells for mitotic entry, by favoring the accumulation and activation of cyclin B/CDK1 complexes. Lastly, the activation of cyclin B/CDK1 allows mitotic entry and progression (Gavet and Pines, 2010). Importantly, the activity of cyclin B/CDK1 complex is further regulated by CDK1 phosphorylation/dephosphorylation forms. Outside of mitosis, CDK1 is phosphorylated by a protein kinase known as Wee1 which keeps it in an inhibitory mode. Once the cell is ready to transition from G2 to mitosis, the CDC25 phosphatase, dephosphorylates CDK1 to increase its activity.

Interestingly, as mentioned before, the levels of cyclins oscillate throughout the cell cycle, and this is established by cyclin degradation by ubiquitin-mediated proteolysis (Figure 5) (Craney and Rape, 2013; Dang et al., 2021). This process starts first by ubiquitination of the selected cyclin which marks it to be degraded by a multiprotein complex carrying protease activity, the 26S proteasome (Grice and Nathan, 2016; Peters et al., 1994). The ubiquitination process is divided into 3 main steps, (1) activation step of the ubiquitin protein by an E1-ubiquitin activating enzyme; (2) conjugation step where the ubiquitin protein is transferred from E1 to E2 ubiquitin-conjugating enzyme and finally (3) ligation step of the ubiquitin with the substrate by an E3 ubiquitin ligase (Dang et al., 2021).

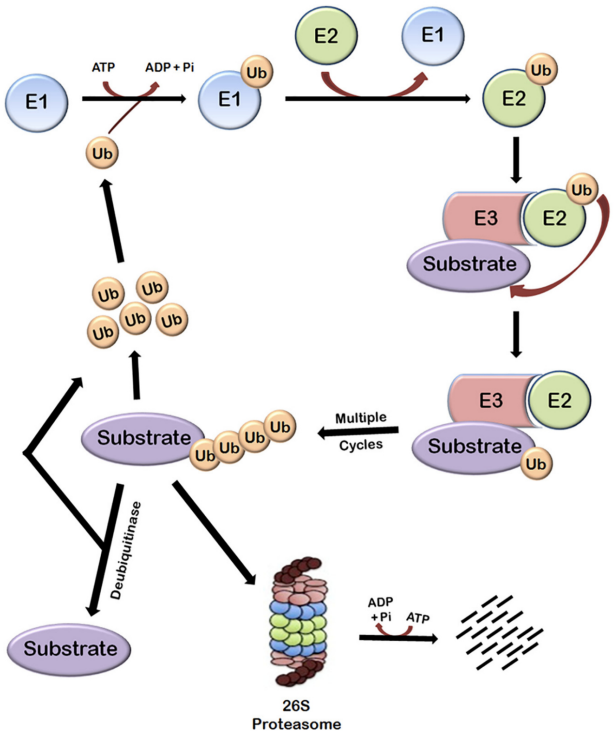


Figure 5. Mechanisms of protein ubiquitination and proteasome degradation

The small Ubiquitin protein is activated by E1 enzymes and conjugated by E2 enzymes. The final step allows the transfer to the substrate by E3 ubiquitin ligases. Substrates containing ubiquitin chains are recognized by the proteasome for degradation (Lata et al., 2018).

Two main E3 ligases promote cyclin degradation. The Skp1-Cullin1-F-box (SCF) complex and the anaphase-promoting complex or cyclosome (APC/C). Cyclin D is first phosphorylated at Threonine 286 (Thr286) by a glycogen synthase kinase-3β (GSK-3β) (Diehl et al., 1995). After its phosphorylation, cyclin D is exported from the nucleus towards the cytoplasm where it is poly-ubiquitinated by the SCF E3 ligase complex, targeting it for proteasome degradation (Lin et al., 2006). Cyclin E phosphorylated by GSK-3 and CDK2 itself (Clurman et al., 1995; Welcker et al., 2003), is poly-ubiquitinated by the SCF E3 ligase complex, to be then degraded by the proteasome (Koepp DM et al., 2001). Finally, the APC/C is activated by Cdc20 or Cdh1 to mediate ubiquitination and proteasomal degradation of both cyclin A and cyclin B, at specific time regulated by different checkpoints (Hershko et al., 1999; Wolthuis et al., 2008). APC/C activated by Cdc20, also leads to the ubiquitylation and degradation of securin,

a protein that binds to separase to inhibit its activity in order to maintain chromatid connection, which will then allow the cleavage of cohesion molecules (Schrock et al., 2020).

1.1.3. Cell cycle checkpoints

Checkpoints are surveillance mechanisms required to ensure that both DNA replication and cell division are carried out correctly and efficiently (Figure 6) (Barnum and O'Connell, 2014; Hartwell and Weinert, 1989; Vermeulen et al., 2003). One example of a cell cycle checkpoint is the restriction point in G1 phase, that control cell size, nutrient availability and DNA integrity before commitment to S-phase. During S-phase, DNA damage will activate the Ataxia-telangiectasia mutated/ Ataxia telangiectasia and Rad3 related (ATM/ATR) kinases. ATM/ATR downstream effector such as Chk2 phosphorylates p53, which results in the upregulation of p21. P21 can form stable complexes with CDKs, to block cell cycle progression (Bertoli et al., 2013; Giono and Manfredi, 2006). During DNA replication, the intra-S checkpoint ensure proper DNA synthesis by blocking late replication or DNA re-replication by activation of ATR kinase and downstream effector such as Chk1 (Bertoli et al., 2013). At the end of G2 and right before entering mitosis, the G2/M checkpoint prevents cells with unreplicated or damaged DNA to enter mitosis. This is achieved by activation of ATM kinase and Chk1, to inhibit Cdc25, the phosphatase responsible of the activation of Cyclin B/CDK1 complexes (Donzelli and Draetta, 2003; Vermeulen et al., 2003).

During mitosis, and more specifically at the metaphase/anaphase transition, the spindle assembly checkpoint (SAC) ensure that all chromosomes are properly attached to the mitotic spindle. In case of defects in kinetochore- MT attachment, the checkpoint inhibits Cdc20 to prevent activation of APC/C, thereby preventing the transition to anaphase (Geley et al., 2001; Lara-Gonzalez et al., 2012; Yamano, 2019).

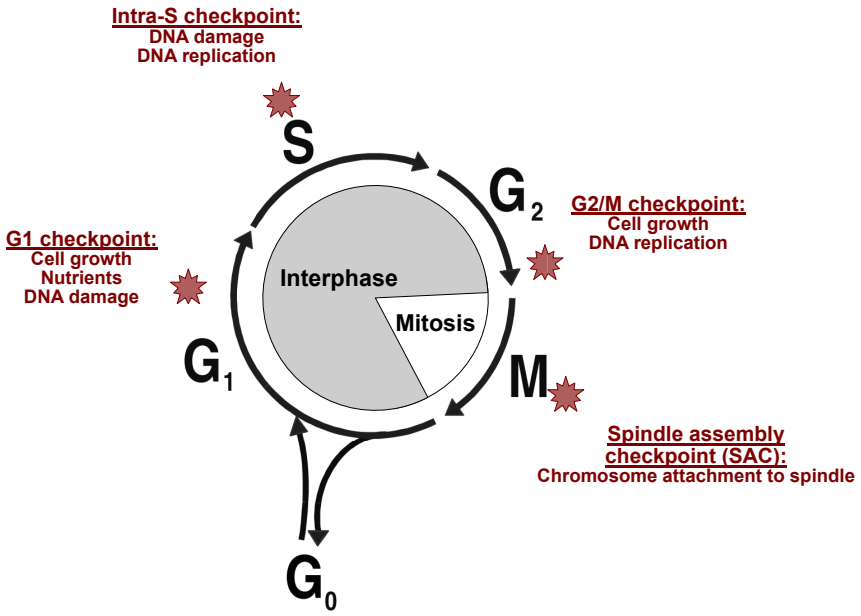


Figure 6. The cell cycle and its regulators - Checkpoints

Four main cell cycle checkpoints have been described. These monitor different types of processes, such as the presence of DNA damage or unattached chromosomes to promote cell cycle arrest allowing time to repair. Modified from (Vermeulen et al., 2003).

1.2. Polyploidy

Polyploidy is defined by the presence of more than two copies of all chromosomes. It has been studied for more than 100 years and it was initially described by Hugo de Vries and G. Ledyard Stebbins Jr, in plant evolution (Soltis et al., 2014; Stebbins, 1938; Van De Peer et al., 2017). However, polyploidy is now known to be present across most eukaryotic organisms (Frawley and Orr-Weaver, 2015; Orr-Weaver, 2015; Van De Peer et al., 2017). In *Drosophila*, most of the differentiated larval tissues and part of adult tissues are polyploid (Almeida et al., 2021; Edgar, 2006; Orr-Weaver, 2015; Smith and Orr-Weaver, 1991). In mammals, many examples of polyploidy have been described such as megakaryocytes (Ravid et al., 2002), hepatocytes (Guidotti et al., 2003; Kudryavtsev et al., 1993), trophoblast giant cells (Barlow and Sherman, 1974) and muscle cells (Mccrann et al., 2008; Quinn et al., 2017). In human differentiating epidermis for example, it has been postulated that the polyploid frequency at a given time, may be around 50–60% (Gandarillas and Freije, 2014).

When discussing polyploidy, the notion of N and C have to be included. N relates to the number of chromosomes sets in a given cell. For a diploid cell, N=2, for a triploid cell, N=3, for a tetraploid cell, N=4 and so on. C, on the other hand is defined as the amount of DNA content in the haploid genome (Orr-Weaver, 2015).

Polyploidization can be achieved through different routes (Figure 7 and summarized in Table 2).

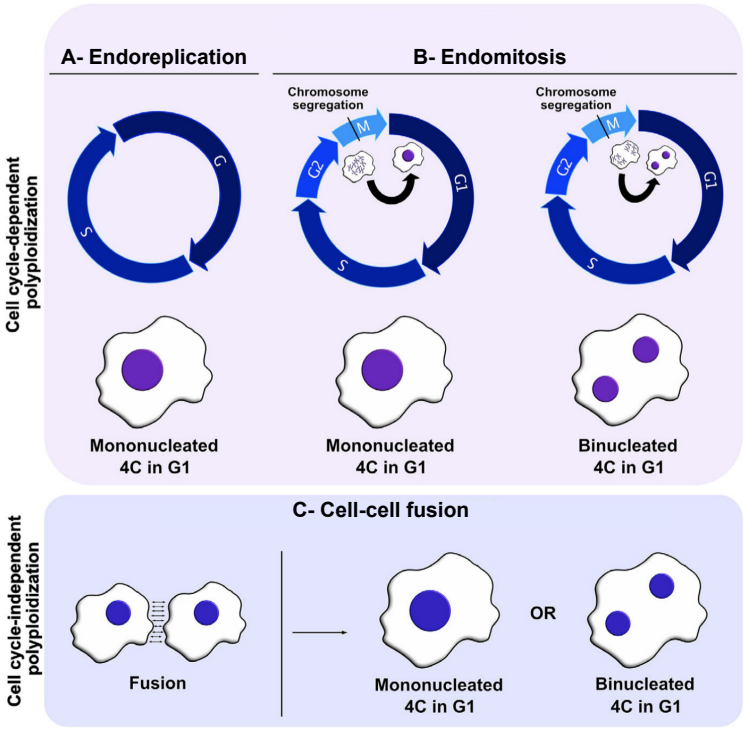


Figure 7. Different routes to polyploidization

During endoreplication, the cell alternates between G and S phases without entering mitosis, resulting in a mononucleated polyploid cell. During endomitosis, the cell enters and exits mitosis before completing chromosome segregation- known as mitotic slippage, or cytokinesis- known as cytokinesis failure. In this case mitotic slippage generates a mononucleated cell, while cytokinesis failure generates a binucleated cell. Cell-cell fusion relies of the fusion of two diploid cells. Modified from (Gemble and Basto, 2020).

1.2.1. Endomitosis

Endomitosis is the process by which cells enter mitosis but exit without completing cell division. Depending on the stage of mitotic exit, endomitosis can generate mono- or

bi-nucleated polyploid cells. Therefore, there are two subtypes of endomitotic cells - cells that undergo mitotic slippage and cells that undergo cytokinesis failure.

Mitotic slippage

In this condition, cells exit mitosis before chromosome segregation by a mechanism based on the premature ubiquitin-proteosome degradation of cyclin B1, via the ubiquitin-conjugating enzyme Ubc4 (Mazzi et al., 2018; Ravid et al., 2002; Zhang et al., 1998). This mechanism was mainly described in mammalian megakaryocytes. Megakaryocytes are polyploid cells (128C) with key functions in platelet production. Megakaryocytes are derived from hematopoietic stem cells and normally exhibit very large sizes containing a single multilobate nucleus (Mazzi et al., 2018; Ravid et al., 2002). Megakaryocytes undergo around 6 rounds of polyploidization, controlled by thrombopoietin (a hormonal factor) signaling pathway, reaching their final ploidy levels (Orr-Weaver, 2015; Ravid et al., 2002; Rojnuckarin et al., 1999; Zhang et al., 1998).

Cytokinesis Failure

Cytokinesis failure refers to the process by which cells exit mitosis after chromosome segregation without undergoing cytokinesis. In this situation, endomitosis results in a binucleated polyploid cell, like for example mammalian hepatocytes. Cytokinesis failure in hepatocytes has been postulated to be induced by external stresses such as oxidative stress, telomere damage or partial hepatectomy. In more detail, defects in the delivery of molecules essential for furrow induction (such as Aurora B) impairs the activation of key regulators of cytokinesis such as RhoA (Gentric and Desdouets, 2014; Guidotti et al., 2003). It has been shown that hepatocyte polyploidization is controlled by the atypical transcriptional repressor E2F8, that downregulates genes that promote cytokinesis (Pandit et al., 2012).

1.2.2. Cell-cell Fusion

Cell fusion is independent of the cell cycle machinery and can give rise to mono- or multinucleated polyploid cells. Cell-cell fusion occurs in tissues like bone, skeletal muscle and the syncytiotrophoblast of the mammalian placenta. In more detail, macrophages fused to produce osteoblasts, myoblasts fuse to form multinucleated muscle fibers and cytotrophoblasts fuse during pregnancy in order to assemble the

syncytiotrophoblast (Abmayr and Pavlath, 2012; Chen and Olson, 2004; Soysa et al., 2012; Zybina and Zybina, 2005). The steps of cell-cell fusion are thought to be conserved in different cell types. First, cell recognition and adhesion, followed by cytoskeleton rearrangement. Further, the assembly of fusion pores and mixing of cytoplasmic content allow the two cells to become a functional cell. Different tissue-specific regulators and receptors mediate each step. For example, *Drosophila* myoblast fusion starts with cell recognition and adhesion, mediated by cell-type-specific transmembrane receptor, such as Dumbfounded (Duf), Roughest (Rst) and Sticks and stones (Sns). After cell-cell adhesion, both membranes and the actin cytoskeleton undergo several rearrangements allowing myoblast fusion. This cytoskeleton rearrangement is promoted by an adaptor protein, Ants/Rols7, that links fusion receptors to the cytoskeleton forming an electron-dense plaque along the membrane. Finally, both cells align allowing membrane breakdown and the formation of fusion pores resulting in the final formation of the myotube (Brukman et al., 2019; Chen and Olson, 2004).

1.2.3. Endoreplication/ Endocycle

In this section, I will first provide a general overview of endoreplication and then elaborate endoreplication in more detail when describing *Drosophila* salivary glands (SGs).

Endoreplication is achieved by alternating G and S- phases without mitosis. This type of cycle generates a mononucleated polyploid cell (Edgar et al., 2014; Edgar and Orr-Weaver, 2001; Lee et al., 2009). To switch from a canonical cell cycle to endoreplication, mitosis has to be bypassed, which is achieved through downregulation of G2/M- CDK1, promoting the degradation of mitotic cyclins (Figure 8) (Edgar et al., 2014; Gemble and Basto, 2020; Øvrebø and Edgar, 2018). In parallel, S-CDK activity must be periodically inactivated to allow the transition to G-phase, allowing the assembly of PreRCs at origins of replication (Figure 8) (Edgar et al., 2014).

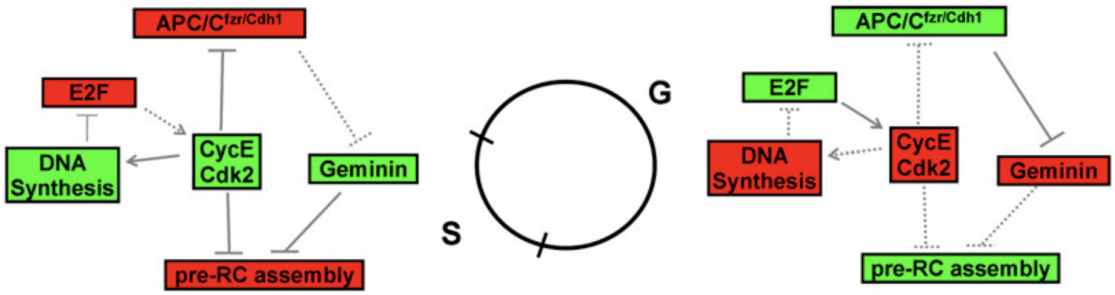


Figure 8. The major regulators of Endoreplication

CyclinE/CDK2 oscillatory activity is the key regulator of endoreplication. With low activity in G1, APC/C$^{fzr/Cdh1}$ represses Geminin accumulation allowing pre-RC assembly. High levels of E2F then stimulates CyclinE transcription, thus activating CyclinE/CDK2 and the initiation of S phase (Lee et al., 2009).

Endoreplication is found in many plants (Øvrebø and Edgar, 2018) as well as different organisms such as *Caenorhabditis elegans* (*C. elegans*) intestinal cells (32C) (Hedgecock' And and White, 1985). It also marks the most used polyploidization route in many *Drosophila* tissues such as the larval sub-perineurial glia (SPG) cells (22C) (Unhavaithaya and Orr-Weaver, 2012), fat body (256C) , salivary glands (1024-2048C) (Pierce et al., 2004), follicle cells of the adult ovary (16C) (Calvi et al., 1998), nurse cells of the adult ovary (512-1024C) (Dej and Spradling, 1998), adult midgut (64C) (Xiang et al., 2017) as well as mammalian trophoblast giant cells (512C in rodents) (Zybina and Zybina, 2005).

In mammals, endoreplication mainly depends on the downregulation of CDK1 by cyclin-dependent kinase inhibitors (CKIs), specially by the CDK interacting protein/Kinase inhibitory protein family (CIP/KIP), such as p21^{CIP1} and p57^{KIP2}, to prevent the transition into mitosis (Ullah et al., 2009). This pathway mediates fibroblast endocycling and differentiation into trophoblast giant cells (Ullah et al., 2008). However, in follicle cells of the *Drosophila* adult ovary, endoreplication is executed by activating Notch signaling, regulating three major cell cycle transitions (Shcherbata et al., 2004). The binding of Notch to Delta (a transmembrane ligand for Notch) promotes transcriptional inhibition of String, the fly CDC25 orthologue, which results in blocking transition into mitosis (López-Schier and St. Johnston, 2001; Shcherbata et al., 2004). On the other hand, Notch activates transcription of the APC/C activator Fizzy-related, Fzr (Cdh1 in mammals), allowing G1 progression (Schaeffer et al., 2004). Finally,

endoreplication is regulated by repression of Dacapo, a CIP/KIP-type inhibitor of the CyclinE/CDK2 complex, promoting entry into the S-phase (Shcherbata et al., 2004). This signaling pathway also regulates the endoreplication cycle in the adult gut (Xiang et al., 2017) and subperineurial glia (SPG) cells in the larval brain (Von Stetina et al., 2018).

Endoreplication in *Drosophila* fat body cells is not completely understood, however, many studies pointed out the similarity between these cells and the *Drosophila* SGs endoreplication machinery (described below) (Maqbool et al., 2010; Zielke et al., 2011). One important difference is the implication of dimerization partner (dDP) of dE2F in regulating endoreplication in the fat body and not in the SGs. dDP is a transcription factor that is associated with dE2F required for high affinity DNA-binding. dE2F/dDP mediates suppression of DNA damage responses (DDR) targeting dATM, to block cell cycle progression (Guarner et al., 2017).

Endoreplication in *Drosophila* salivary glands

Drosophila SG secretory cells (described more in detail in section 6) can be divided into two cell populations. One present at the proximal region which undergoes up to 10 rounds of DNA replication. The second population, positioned more distally can undergo additional cycles, generating cells with 1024C-2048C (Edgar and Orr-Weaver, 2001; Hammond and Laird, 1985; Nordman et al., 2011; Pierce et al., 2004). Previous studies showed that SG cells undergo endoreplication to achieve high levels of polyploidy, which made this tissue a great model to study endoreplication and its regulators (Edgar et al., 2014; Hammond and Laird, 1985; Rudkin, 1972; Smith and Orr-Weaver, 1991).

Endoreplication progression depends on the fluctuation in the levels of different molecules generating pulses of S-CDK to allow G and S phases. In more detail, the molecules responsible for this process are the E2F activator transcription factor (E2F1), Cyclin E and $CRL4^{Cdt2}$. $CRL4^{Cdt2}$ is an S-phase dependent E3 ubiquitin ligase composed of a scaffold for the E3 ligase complex (Cul4), linked by an adapter (DDB1) to a substrate receptor (Cdt2), that recognizes proteins bound to PCNA, and a catalytic subunit ensuring E3 ligase activity (Rbx1). The activity of $CRL4^{Cdt2}$ depends on DNA replication, by its association to the replication fork through PCNA (Zielke et al., 2011). Once activated it can target E2F1 for degradation (Shibutani et al., 2008). Experiments on SGs have demonstrated that endoreplication was blocked after the depletion of

$CRL4^{Cdt2}$ and after the stabilization of E2F1, concluding that E2F1 should oscillate in order to maintain endoreplication (Zielke et al., 2011). This is also true for Cyclin E, as its over-expression also blocks endoreplication (Andreas Weiss, 1999; Follette et al., 1998).

Endoreplication is initiated with the accumulation of E2F1 (late G- phase), which stimulates the transcription of Cyclin E among other S-Phase genes and so the activation of the S- phase CDK. As this phase is completed, $CRL4^{Cdt2}$ activity triggers E2F1 degradation, preventing the accumulation of Cyclin E and so S-phase exit (Edgar et al., 2014; Lee et al., 2009; Zielke et al., 2011). During G phase, APC/C^{Fzr} activity promotes the degradation of the Pre-RCs inhibitor Geminin, allowing Pre-RCs assembly, as well as mitotic cyclins and thus prevents entry in mitosis (Narbonne-Reveau et al., 2008; Sigrist and Lehner, 1997). During S-phase, high levels of Cyclin E/CDK2 represse APC/C^{Fzr} activity to prevents re-licensing of replication origins (Narbonne-Reveau et al., 2008).

In SGs, growth factors represent the upstream regulators of endoreplication. One well studied example is dMyc, the homologue of human Myc, a transcription factor required for cell growth and proliferation. Cell growth and endoreplication are both regulated by dMyc, since studies showed that loss of dMyc in *Drosophila* SGs, leads to endocycle inhibition and generation of small tissue and cells (Edgar et al., 2014; Pierce et al., 2004).

SGs exhibit polytene chromosomes, where all copies of sister-chromatids remained attached together and aligned to form large chromosomes with banded patterns (Hammond and Laird, 1985; Spradling, 2017). One important feature of polytene chromosomes is that 20-30% of the whole genome remains under-replicated (Edgar and Orr-Weaver, 2001; Hammond and Laird, 1985; Smith and Orr-Weaver, 1991). This event concerns the centromeric, certain euchromatin and many late-replicated heterochromatin regions (Edgar et al., 2014; Edgar and Orr-Weaver, 2001). Common and tissue-specific under-replicated region are dependent on a protein called Suppressor of Under-replication (SuUR), since in its absence, the vast majority of under-replicated region become fully replicated (Belyaeva et al., 1998; Nordman et al., 2011). In more recent studies, it has been reported that SuUR localizes to specific regions on the chromosome, and this binding is dependent of a key component of the replicative helicase, Cdc45 (Nordman et al., 2014). The SuUR protein is then recruited to active replication forks mediating Rap1-interacting factor 1 (Rif1) recruitment to

replication forks. Importantly, Rif1 contains a protein phosphatase (PP1) interaction motif, and thus recruit PP1 to the replication origin. Then Rif1/PP1 inhibits replication fork progression through dephosphorylation of MCM, generating therefore under-replicated regions (Munden Alexander et al., 2018; Nordman et al., 2014).

Table 2. Summary of the different routes used to increase DNA content through polyploidization

Routes to polyploidization		Main events	Regulators	Examples
Endomitosis	Mitotic slippage	Cells exit mitosis before chromosome segregation	Premature Cyclin B1 ubiquitin proteosome degradation via the Ubc4	Mammalian Megakaryocytes (128C)
	Cytokinesis failure	Cells exit mitosis after chromosome segregation without undergoing cytokinesis	Defects in Aurora B localization; Inhibition of key cytokinesis regulators such as RhoA; Downregulation of genes that promote cytokinesis by E2F8	Mammalian Hepatocytes (8C for each nucleus)
Cell fusion		(1) Cell recognition and adhesion (2) Cytoskeleton rearrangement (3) Assembly of fusion pores (4) Mixing of cytoplasmic content	Tissue-specific regulators	Bone Skeletal muscle Syncytiotrophoblast of the mammalian placenta
Endoreplication		Alternating G and S-phases without entering mitosis:	CKIs: $p21^{CIP1}$/ $p57^{KIP2}$ → downregulation of CDK1 → prevent transition into mitosis	Trophoblast giant cells (512C in rodents)

Endoreplication	- Mitosis bypass - Transition to G- phase, allowing the assembly of pre-replication complexes (PreRCs)	Notch binds to Delta → inhibition of String (Cdc25 in mammals) → blocks transition into mitosis Notch activates transcription of Fzr (Cdh1 in mammals) → G1 progression Repression of Dacapo → entry into S-phase	*Drosophila* follicle cells of the adult ovary (16C) *Drosophila* sub-perineurial glia (SPG) cells (22C) *Drosophila* adult midgut (64C)
		Accumulation of E2F1 →transcription of Cyclin E →activation of the S-phase CDK $CRL4^{Cdt2}$ activity → E2F1 degradation → S-phase exit Active APC/C^{Fzr} →degradation of Geminin → Pre-RCs assembly; →degradation of mitotic cyclins → no entry in mitosis	*Drosophila* salivary glands (1024-2048C) *Drosophila* fat body (256C) “dE2F/dDP targets dATM → block cell cycle progression”

2. Scheduled and Unscheduled Polyploidy

2.1. Advantages of scheduled polyploidy

Many cells from different organisms are programmed to undergo polyploidization, this is known as programmed polyploidy or scheduled polyploidy. In this context the cell uses this process to gain several advantages required to accomplish their function in the organism. In this section, I will describe the most common and essential functions gained through scheduled polyploidization.

2.1.1. Increase in cell size

One main benefit of polyploidization is the increase in both cell size and biomass production, all without perturbing cell and tissue structure. Polyploid cells increase their DNA content without division, which may support higher transcriptional output and thus enabling the cell to accomplish several functions by the production of more proteins (Øvrebø and Edgar, 2018; Schoenfelder and Fox, 2015). Increase in cell size could be considered as the first advantage gained by polyploidization, which seems to be used in some cells to increase their metabolic activity, as in megakaryocytes (Trakala et al., 2015), trophoblasts (Baines and Renaud, 2017), *Drosophila* nurse and follicle cells (Bastock and St Johnston, 2008) or *Drosophila* SGs (Farkaš et al., 2014; Kerman et al., 2006). In another context, cells might need to increase their size to occupy a larger surface area without increasing cell number and affecting cell-cell junctions, for efficient barrier function as in trophoblast giant cells (Barlow and Sherman, 1974; Watson and Cross, 2005; Zybina and Zybina, 2005) or *Drosophila* SPG (Desalvo et al., 2011; Limmer et al., 2014; Stork et al., 2008; Unhavaithaya and Orr-Weaver, 2012). Interestingly, during stress responses, certain cells use polyploidy and the inherent size increase to regenerate as in hepatocytes (Bailey et al., 2021; Gerlyng et al., 1993; Miyaoka et al., 2012) or *Drosophila* abdominal epithelia (Losick et al., 2013; Tamori and Deng, 2013).

2.1.2. Increase of metabolic activity

Increase in DNA content can result in an increase in protein production and therefore this might lead to increased metabolic activity. This is indeed the case found in examples like in *Drosophila* oogenesis, where the nurse cells synthesize maternal nutrients such as mRNAs, proteins and even mitochondria to feed the oocyte (Bastock and St Johnston, 2008; Dej and Spradling, 1998; Melissa E. Pepling, 2016). Defects in polyploidization of nurse cells induced through mutations in *morula*, resulted in both nurse cell and oocyte degeneration (Reed and Orr-Weaver, 1997). Another example is the follicle cells that produce the eggshell surface, encapsulating the egg chamber. Follicle cells undergo polyploidization in order to over-replicate a specific genome region essential for eggshell formation the chorion gene (Calvi et al., 1998). Any disruption of this amplification results in the formation of thin eggshells leading to embryo lethality (Herriage and Calvi, 2024). Still in *Drosophila*, the SGs at late larval stage reach their highest ploidy level upon several round of endoreplication. At this stage, high levels of an adhesive glue, essential allowing pupae to adhere to a dry surface, have to be secreted (Beňo et al., 2024; Borne et al., 2020; Fraenkel and Brookes, 1953; Gregg et al., 1990). There has been no direct correlation established between polyploid levels and secretion in this tissue, but this could be explained by the fact that suppressing endoreplication in the SG cells causes an important reduction in both cell and tissue size resulting in cell death (Binh et al., 2022; Nguyen et al., 2024; Weng Li et al., 2003).

In mammals, megakaryocytes are known for their capacity to produce many platelets once they reach high ploidy levels (Liu et al., 2021; Zimmet and Ravid, 2000). Reduction of ploidy levels in these cells, which can be induced by arresting cells in mitosis with Cdc20 ablation, causes the formation of smaller megakaryocytes decreasing the number of circulating platelets (Trakala et al., 2015). Another example in mammals, are cardiomyocytes that become polyploid during their normal differentiation program resulting in the variation of both nuclear number and ploidy level in different species. Human cardiomyocytes can be mononucleated (around 57%) or multinucleated, however in mice, 78% of polyploid cardiomyocytes are multinucleated (Bailey et al., 2021). Interestingly, the metabolic rate in cardiomyocytes scales with body mass, as animals with lower metabolic rates, presented more diploid cardiomyocytes than polyploid ones (Hirose et al., 2019).

2.1.3. Barrier function

Another important aspect of polyploidization is related with barrier function, as the increase in cell size allows the cell to cover larger spaces maintaining the integrity of intercellular junctions and ensuring the formation of a barrier-like region. This is the case in the *Drosophila* SPG cells, which undergo polyploidization to sustain the formation of a glial tissue layer, composed of flat cells attached through septate junctions, in the brain serving as a blood-brain barrier (Desalvo et al., 2011; Limmer et al., 2014; Stork et al., 2008). This correlation was tested by decreasing ploidy levels through Cdt1 depletion and thus inhibition of DNA replication, which lead to a decrease in cell size and thus rupture of septate junction (Unhavaithaya and Orr-Weaver, 2012).

In mammals, trophoblast giant cells play an important role in the separation of the maternal and fetal compartments of the placenta (Barlow and Sherman, 1974; Edgar and Orr-Weaver, 2001; Watson and Cross, 2005; Zybina and Zybina, 2005). Another example polyploid cell functioning as barriers are keratinocytes, epithelial cells that compose the epidermis of mammalian skin, which undergo endoreplication and/or mitotic slippage (Gandarillas et al., 2019; Zanet et al., 2010). With higher ploidy levels, these cells increase in size and thus cover a larger area in the skin making the skin more resistant to possible insults as mutations or defects induced by DNA damage (Gandarillas and Freije, 2014).

2.1.4. Stress response: regeneration and inhibition of apoptosis

In addition to the implication of polyploidy in developmental programs, polyploidy can also function as a system of protection upon stress, aging or injury, as increase in DNA content favor resistance and correction of DNA damage. For example, in the adult *Drosophila* abdomen, epithelial cells use a combination of endoreplication and cell fusion as a mechanism to heal after wounding induced by a needle puncture (Losick et al., 2013). In this case, around 100 cells are destroyed, and the dying cells are replaced by surrounding cells that undergo endoreplication compensating therefore for cell loss (Losick et al., 2016, 2013). This switch to polyploidy is regulated by a transcriptional activator Yorkie (Yki) that induces activation of Yki-dependent genes, such as Myc and E2F1, promoting entry into the endocycle (Grendler et al., 2019). In this context, forcing injured epithelial cells to enter mitosis, by expressing String

(Cdc25 in mammals) and genetically removing one copy of Fzr, caused accumulation of DNA damage and mitotic errors (Grendler et al., 2019).

In aging *Drosophila*, DNA damage is accumulated in different tissues like in the brain. Neurons and glia cells use polyploidy, mainly endoreplication, as a strategy to ensure tissue repair by compensating cell loss while maintaining established cell-cell contacts (Nandakumar et al., 2020).

In mammals, upon pathological conditions, such as congenital heart disease or valvular heart disease, cardiomyocytes undergo polyploidization generating multinucleated cells to adapt and for maintaining contractile function under cardiac stress (Bailey et al., 2021; Pandit et al., 2013).

Another example concerns liver hepatocytes that use polyploidization as a way to regenerate tissue mass and restore organ size upon insults. The best-known example of polyploidization, without proliferation, was induced to promote an increase in cell size leading to tissue enlargement, hypertrophic growth in response to partial hepatectomy, surgical removal of a part of the liver in mice (Miyaoka et al., 2012). It has been shown that blocking polyploidization, by E2F7/8 knockout caused the liver to develop tumors more frequently when compared to wild type livers (Pandit et al., 2012; Zhang et al., 2018). The same experimental set up was used in conditions where the levels of ploidy increased through the knockdown of Anilin, a protein required for cytokinesis. In this case, the percentage of tumors decreased (Lin et al., 2020). This role for polyploidy in the liver has been controversial, as recent studies on ploidy reduction has shown that it can initiate tumorigenesis in the liver (Matsumoto et al., 2021).

Still on the advantages of polyploidization in conditions of stress is the capacity to inhibit apoptosis. It is well known that many cellular insults lead to the generation of DNA damage, including double-stranded breaks, which activates a p53-dependent DNA damage response. Several studies have shown that polyploidization serve as a way of resisting apoptosis, maintaining cell growth even in the presence of DNA damage (Mehrotra et al., 2008). For example, endocycling cells in *Drosophila*, such as nurse and follicle cells, were more resistant to irradiation compared to other dividing cells that entered apoptosis (Hassel et al., 2014). In more details, studies showed that in these endocycling cells, p53 signaling is reduced via proteolytical degradation of p53 itself to prevent apoptosis (Hassel et al., 2014). Interestingly, p53 signaling seems to be reduced in these endocycling cells, in mammals, multinucleated polyploid

cardiomyocytes also adapt better to chronic hypoxia stress by decreasing the degree of apoptosis when compared to the diploid cells (Jiang et al., 2020).

2.2. Disadvantages of unscheduled polyploidy

Although polyploidization is crucial for the integrity and function of many tissues, this is mostly the case when it is programmed or scheduled, following a pre-determined program, occurring during development, as described above. However, several studies have showed that a large variety of cancers present genomes that can only be explained by events of whole genome duplication (WGD) (Bielski et al., 2018; Ganem et al., 2007; López, 2020; Storchova and Pellman, 2004; Zack et al., 2013). Interestingly, unscheduled polyploid could act as a strong source of genetic instability, due to the accumulation of high level of DNA damage and errors in mitosis (Ganem et al., 2009; Gemble et al., 2022; Gemble and Basto, 2020; Goupil et al., 2020; Kirsch-Volders et al., 2025; Kuznetsova et al., 2015; Nano et al., 2019).

2.2.1. Cancer

Several studies documented the link between WGD and cancer initiation and proliferation. The first link was made after showing that more than 40% of human tumors are near tetraploid, this rate can even reach up to 70% in specific tumor subtypes such as non-small cell lung carcinomas (Carter et al., 2012; Davoli and De Lange, 2011; Dewhurst et al., 2014; Zack et al., 2013). Bioinformatic analysis reported that polyploidy is most likely an early event that promotes cancer initiation, although metastasis and drug resistance may also be fueled by WGD (Blakely et al., 2017; Erenpreisa et al., 2015; Kirsch-Volders et al., 2025; Liu, 2022; Loftus et al., 2022). It has been proposed that in normal conditions, p53 prevents non-programmed polyploid cell evolution by inhibiting their proliferation leading to elimination (Ganem et al., 2014; Ganem and Pellman, 2007). However, p53 is the most frequently mutated gene in cancer; for example, 42% of Pan-Cancer, 95% of serous ovarian cancer and 89% of serous endometrial carcinomas; which explain the maintenance of polyploid cells arising in response to different insults, promoting therefore tumorigenesis (Baker S J et al., 1987; Fujiwara et al., 2005; Kandoth et al., 2013).

2.2.2. Genetic and chromosomal instability

Most tetraploid cells not only duplicated their DNA but also duplicate different organelle numbers, such as centrosomes. One of the main functions of centrosomes is MT nucleation to assemble a stable bipolar spindle ensuring proper chromosome segregation during cell division. After polyploidization, centrosome amplification represents a challenge as it can result in multipolar spindles and therefore chromosome mis-segregation. Division of a mother cell in more than two daughter cells leads to abnormal chromosome numbers -aneuploidy- defined by the gain or loss of at least one chromosome. Aneuploid cells may subsequently undergo chromosomal instability (CIN), which plays a key role in tumor evolution and resistance (Basto et al., 2008; D'assoro et al., 2002; Dewhurst et al., 2014; Ganem et al., 2007; Goupil et al., 2020; Kuznetsova et al., 2015; Lingle et al., 2002; Morretton et al., 2022; Pihan German A. et al., 1998; Sato et al., 1999; Saunders, 2005; Yongsheng Chan and Yongsheng Chan MBBS, 2011).

In multinucleated unscheduled polyploid cells, it has been shown that cell cycle asynchrony is responsible for the accumulation of high level of DNA damage during mitosis This asynchrony is reasoned to be caused by the fact that each nucleus receives different signals for cell cycle progression. In our lab, recent studies highlighted the effect of unscheduled multinucleated polyploidy effect *in vivo* (Goupil et al., 2020; Nano et al., 2019). By inducing cytokinesis failure in *Drosophila* larval neural stem cells, also called neuroblasts (NBs), the fate of polyploid cells can be studied *in vivo*, Interestingly, these polyploid NBs continued dividing generating even bigger multinucleated polyploid cells while accumulating more centrosomes as well (Goupil et al., 2020; Karess et al., 1991; Nano et al., 2019; Reed and Orr-Weaver, 1997). Surprisingly, it was noticed that the tolerance for unscheduled polyploidy was tissue-dependent, as induction of cytokinesis failure in the *Drosophila* wing disc lead to the elimination of these cells by apoptosis (Gerlach et al., 2018). However, similar to the *Drosophila* neuroblasts, mouse neural stem cells and human cancer cells generated asynchronus polyploid cells with high levels of DNA damage upon cytokinesis failure (Nano et al., 2019).

Importantly, recent work from our lab provided an additional explanation on the orgins of genetic instability upon unscheduled polyploidy (Gemble et al., 2022). By inducing tetraploidy in human cells, high levels of DNA damage were generated during

DNA replication in the first S-phase. This results from the fact that these tetraploid cells do not express suficient DNA replication factors, while duplicating their DNA content. In these cells, under- and over-replicated regions were identified. The levels of DNA damage were decreased after upregulating DNA replication factors by overexpressing E2F1 or by extending the length of the first G1, preceeding S-phase (Gemble et al., 2022).

3. Centrosomes

Centrosomes are organelles described by Edouard van Beneden and Theodor Boveri, in the late 19th century by analyzing the fertilized eggs of the nematode *Ascaris megalocephala* (Boveri Theodor, 1887; Scheer, 2014; van Beneden E, 1887). During their observations, they describe an organelle that replicate itself and is involved in successful chromosome segregation. This organelle was then named by Boveri, as centrosome (central body).

3.1. Centrosome structure

The structure of centrosomes was revealed by electron microscopy (EM) techniques showing its composition of two nine-fold symmetrical MT-based cylindrical centrioles surrounded by an electron-dense matrix called pericentriolar material (PCM) (Figure 9A-C) (Anderson, 1972; Ibrahim et al., 2009; Paintrand et al., 1992). The centrosome proteome comprises more than 100 core centrosome proteins, with many of these proteins conserved across species (Andersen Jens S. et al., 2003; Müller et al., 2010).

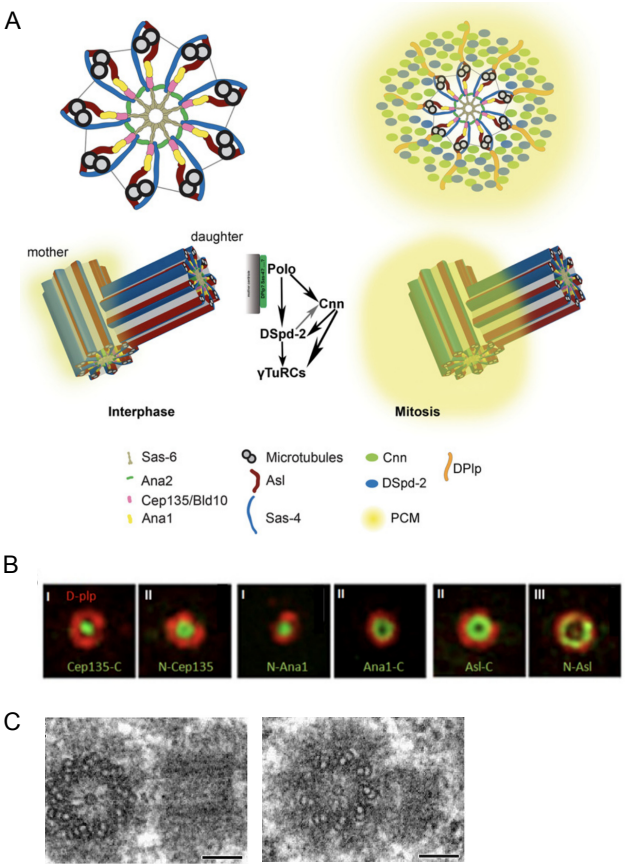


Figure 9. Centrosome structure

A- Ninefold symmetry structure of the centriole and its surrounding PCM (yellow cloud) (left) that expands during mitosis (right) (Lattao et al., 2017). The main proteins involved in centriole and PCM assembly are depicted as indicated in the figure legend. B- Supper-resolution images of D.Mel-2 cells, a Drosophila cell line showing the centrosome structure using both centriolar and PCM markers (Fu et al., 2016). C- EM images of centrioles from Drosophila sperm stem cells containing MT-triplets (left) and MT-doublets (right)(Gottardo et al., 2015).

3.1.1. Centrioles

Centriole architecture is largely conserved among organisms; however, some structural features, such as the central cartwheel or MT walls, vary across species and cell types (Figure 9C). For example, in *C. elegans*, centrioles are composed of nine MT singlets, reaching a length of ~150nm and a diameter of ~100nm (Pelletier et al., 2006). However, in *Drosophila*, centrioles in somatic cells are composed of nine MT doublets which differ from the centrioles in male germ stem cells (mGSCs) that present a mixture of MT doublets and triplets (Debec et al., 1999; Gottardo et al., 2015). In general, in *Drosophila*, centrioles exhibit a length of ~100-200nm and a diameter of ~200-250nm. Finally, in humans, centrioles are composed of MT triplets, ~400-500nm in length and ~250nm in diameter (Chrétien et al., 1997; Paintrand et al., 1992). In vertebrates, centrioles present at their distal end additional structures, subdistal and distal appendages which helps regulating cilia positioning and ciliogenesis respectively (Paintrand et al., 1992; Tanos et al., 2013).

Interestingly, according to the moment centrioles were assembled- born, there is an asymmetry in age that can be translated in certain cell types by an asymmetry in morphology and structure. Based on this difference, the older centriole is called mother centriole, and the younger centriole called daughter centriole is positioned perpendicularly at its proximal end (Figure 9A) (Anderson and Stearns, 2009; Chen and Yamashita, 2021; Vorobjev and Chentsov, 1982). Since there are clear differences between centrosomal proteins involved in centriole duplication and function, I restrict this chapter to *Drosophila*, while referring to their human counterparts.

Centrioles contain a “cartwheel” structure composed of a central hub and nine radially arranged spokes (Callaini et al., 1997; Debec et al., 1999). Two zones (I and II) are distinguished in the core centriole, where a conserved coiled-coil protein, the Spindle assembly abnormal-6 (Sas-6) is localized in the center Zone I. Sas-6 forms homodimers that dimerize through their N-terminal domains to establish the ninefold symmetrical cartwheel (Kitagawa et al., 2011; Van Breugel et al., 2011). Sas-6 interacts with two proteins, a coiled-coil protein, the Anastral spindle 2 protein (Ana2/ human homologue of STIL) that can also homo-oligomerize (Stevens et al., 2010a). The homo-oligomerization of Sas-6 and Ana2 ensures proper centriole assembly, as flies carrying mutations in these genes cannot assemble a normal centriole (Cottee M A et al., 2015; Stevens et al., 2010b). Sas-6 also interacts with the Centrosomal protein Bld10 (human homologue of Cep135), which is not required for the formation of the cartwheel but only to its stabilization. Indeed, mutations in Bld10 showed that the cartwheel can be normally formed but then exhibits increased width and structural instability over time (Roque et al., 2012). Bld10 is also required for the maturation of daughter centrioles (described in section 3.2) (Fu et al., 2016).

The zone II is composed of many proteins, each required for a specific function in centriole organization, that also provide the connection between the cartwheel and the MT wall. The spindle assembly abnormal-4 (Sas-4/ human homologue of CPAP) protein is the primary component of Zone II, that ensure this connection while interacting with both Ana2 and Bld10, as well as physical interaction with MTs (Galletta et al., 2016; Gartenmann et al., 2020; Gopalakrishnan et al., 2011; Hsu et al., 2008). Sas-4 plays a critical role in the formation and maintenance of centrioles, as its absence prevents PCM assembly and blocks centriole duplication, resulting in the loss of centrosome in the following generations (Basto et al., 2006; Gopalakrishnan et al., 2011). Other proteins, such as Polo kinase (Polo/ human homologue of PLK1) and the spindle defective-2 (Spd-2/ human homologue of CEP192) are involved in PCM recruitment (Conduit et al., 2014a; Dix and Raff, 2007; Giansanti et al., 2008). Another protein that is required for PCM recruitment is the Anastral spindle1 (Ana1/ human homologue of CEP295) protein, that is also involved in centrosome assembly and maintenance since cells depleted of Ana1 showed reduction in centrosome number (Dobbelaere et al., 2008; Fu et al., 2016; Saurya et al., 2016). Additionally, the centriolar Protein of 110 kDa (CP110) localized at the distal end of the centriole forms a complex that acts as a cap or plug controlling centriole length, in cooperation with

the MT-depolymerizing Kinesin-like protein 10A (Klp10A) (Delgehyr et al., 2012; Schmidt et al., 2009).

3.1.2. Pericentriolar material – PCM

The PCM is a dense and highly organized matrix of more than 100 proteins that envelops the two centrioles (Andersen Jens S. et al., 2003; Mennella et al., 2012). Importantly, mitotic centrosomes present a significant increase in PCM size due to accumulation of more proteins during centrosome maturation that serves to increase the MT nucleation capacity of the centrosomes (described in section 3.2 and 3.3) (Jens S. Andersen, 2003; Khodjakov and Rieder, 1999; Mennella et al., 2012; Moritz Michelle et al., 1995; Palazzo et al., 2000; Yixian Zheng, 1995).

One of the well-known PCM proteins, is the coiled-coil Pericentrin-like protein (Plp/ human homologue of pericentrin-PCNT) that is organized in clusters with its C-terminus positioned at the centriole wall and its N-terminus radiating outward into the PCM (Mennella et al., 2012). Plp is required for proper PCM assembly and centrosome function as its absence causes defects in the centrosome structure with decrease in PCM size and reduction in centrosome capacity to nucleate MTs (Roque et al., 2018). Spd-2 ensures the incorporation of another protein essential for PCM assembly, Centrosomin (Cnn/ human homologue of CDK5RAP2), that forms a scaffold required to assemble the expanded mitotic PCM (Conduit et al., 2014b; Feng et al., 2017; Lerit et al., 2015; Lucas and Raff, 2007). Asterless (Asl/ human homologue of Cep152) is an important PCM protein during the duplication cycle by recruiting essential protein kinases for this process (Dzhindzhev et al., 2010; Fu et al., 2016; Novak et al., 2014). Polo kinase (human homologue of Plk1) is a major regulator of PCM recruitment to the centriole by phosphorylating several PCM proteins, such as Cnn promoting PCM assembly and (Conduit et al., 2014a; Dobbelaere et al., 2008; Mahen et al., 2011) expansion. Another protein kinase recruited to the PCM during its assembly is Aurora-A, which is required for many functions in the cell including proper centrosome organization and function (Barr and Gergely, 2007; Berdnik and Knoblich, 2002; Magnaghi-Jaulin et al., 2019). Aurora-A is involved in recruiting essential PCM proteins such as γ-Tubulin, which is a core component of the γ-Tubulin ring complex (γ-TuRC) that ensures MT nucleation from the centrosomes (Berdnik and Knoblich, 2002; Magnaghi-Jaulin et al., 2019).

3.2. Centrosome duplication cycle

During the cell cycle, centrosomes undergo a highly regulated duplication cycle in order to generate two centrosomes ensuring bipolar mitotic spindle formation. Centrosome duplication is divided into four distinct steps at different phases of the cell cycle (Figure 10), (1) initiation of duplication in G1/S; (2) procentriole formation during S-phase; (3) centriole elongation in S/G2 and (4) centriole maturation and centrosome separation in G2/M. While the fundamental steps of centrosome duplication are conserved among organisms, there are species-specific proteins and regulatory mechanisms. Here I will describe the process in *Drosophila* (Conduit et al., 2015; Fu et al., 2016, 2015; Lattao et al., 2017).

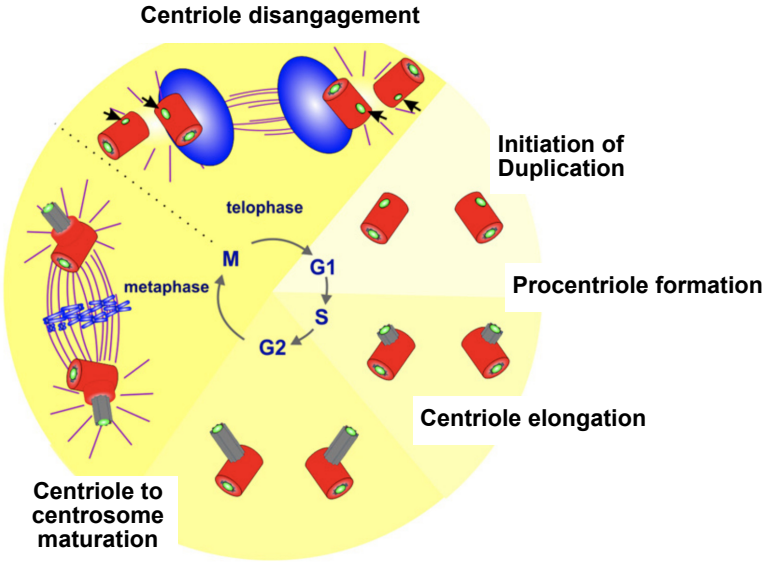


Figure 10. The centriole duplication cycle

Centriole disengagement occurs during late mitosis/early G1. Pro-centriole assembly occurs during G1 or S-phase, next to pre-existing centrioles. Pro- centrioles elongate during S-phase and G2. Centriole to centrosome conversion occurs just before M-phase. As the recruitment of PCM increases at mitotic entry, the capacity to nucleate MTs also increases. Modified from (Lattao et al., 2017).

Initiation of duplication - G1/early S

The first step required for centrosome duplication occurs prior G1, at late mitosis, in coordination with the drop in Cyclin B/Cdk1 activity that allows centrioles

disengagement (Oliveira Raquel A. and Nasmyth Kim, 2013). After disengagement, both centrioles are now defined as mother centrioles that will constitute the template from which two new daughter centrioles will be formed. Centrosome duplication is initiated once Asl with its N-terminal domain interacts with a protein kinase, Polo-like kinase-4 (Sak/Plk4), by recruiting and stabilizing it next to the mother centriole, to ensure proper centriole duplication (Dzhindzhev et al., 2010; Fu et al., 2016; Novak et al., 2014). Thus, Plk4 is considered the master regulator of centriole duplication. After its recruitment, Plk4 localizes around the mother centriole in a ring-like structure (Dzhindzhev et al., 2017; Hamzah et al., 2025).

Procentriole formation – S-phase

Plk4 phosphorylates Ana2 on its STAN domain marking the beginning of procentriole assembly (Figure 11) (Dzhindzhev et al., 2014; Kim Minhee, 2014). This interaction activates Plk4 and stabilizes it into a single focused point at the duplication site, which becomes the site where the daughter centriole is initiated (Dzhindzhev et al., 2017; Ohta et al., 2018, 2014). This step ensures that each mother centriole produces only one procentriole. Once Ana2 is phosphorylated, it is able to bind and recruit the essential cartwheel component, Sas-6, serving as the scaffold for the new centriole (Cottee M A et al., 2015; Dzhindzhev et al., 2014; Kitagawa et al., 2011; Stevens et al., 2010b; Van Breugel et al., 2011).

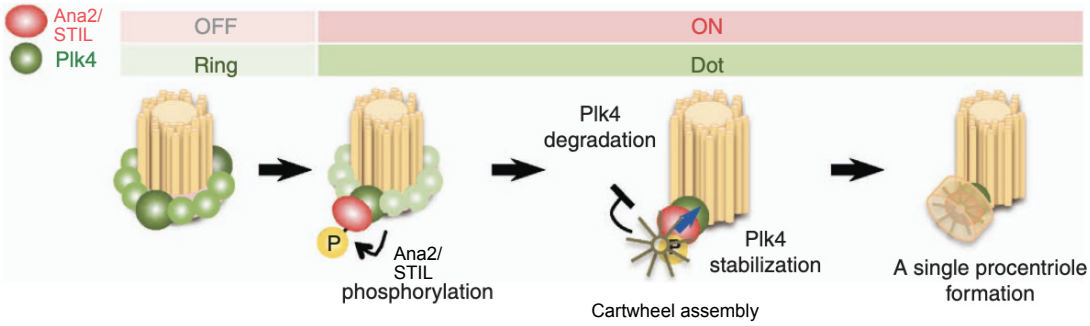


Figure 11. The role of Plk4 in centrosome duplication

Plk4 initially forms a ring at the basis of the mother centriole. Plk4 recruits and phosphorylates Ana2/STIL, marking the site for cartwheel assembly. The initiation of cartwheel assembly limits the centriolar distribution of Plk4 to a single site, thus restricting the assembly of a single procentriole per each parental centriole. Plk4 is

degraded soon after, inhibiting the assembly of other cartwheels. Modified from (Ohta et al., 2014).

Centriole elongation –S/G2

The Bld10 protein is then recruited to stabilize the cartwheel structure to ensure proper centriole elongation, promoted by Sas-4 association and polymerization of centriolar MTs in cooperation with other proteins, such as Ana1 (Fu et al., 2016; Gopalakrishnan et al., 2011; Kohlmaier et al., 2009; Roque et al., 2012; Saurya et al., 2016; Schmidt et al., 2009). As mentioned previously, once the centriole reaches its designated size, CP110 and Klp10A act as negative regulators of centriole elongation to prevent centrioles from becoming abnormally long (Delgehyr et al., 2012; Schmidt et al., 2009).

Centriole to centrosome maturation – G2/M

After centriole elongation, centrioles undergo a conversion process to become functional centrosomes, in a process called centriole maturation. This process is based on the recruitment of PCM by Ana1 and Asl, and the acquisition of MT-nucleating activity, by recruiting γ-Tubulin that will form γ-TuRCs to nucleate MTs from the centrosomes (Fu et al., 2016; Michelle Moritz, 1995; Yixian Zheng, 1995). This marks PCM expansion and activation of the centrosome to nucleate MTs and forming mitotic spindle during mitosis.

3.3. Centrosome function

Centrosomes acts as the main MT-organizing center (MTOC) in many animal cells. The capacity of the centrosome to organize MTs relies on its ability to nucleate, anchor and release MTs. As mentioned previously, γ-TuRCs recruited to the PCM are a key structure that anchors and nucleates MTs. To from this complex, γ-Tubulin composes the γ-tubulin small complexes (γ-TuSC), a core tetrameric complex that comprises two γ-tubulin molecules and two γ-tubulin ring complex proteins called in *Drosophila* Dgrip84 and Dgrip91 (human homologue of GCP2 and GCP3) (Figure 12) (Bettencourt-Dias and Glover, 2007; Gunawardane et al., 2000; Petry and Vale, 2015; Tillery et al., 2018; Vérollet et al., 2006). γ-TuRCs assemble through oligomerization multiple γ-TuSCs and associate with other proteins (Dgrip75, Dgrip128, Dgrip163, and

Dgp71WD), that assembles in the form of a ring forming a cone structure (Figure 12) (Bettencourt-Dias and Glover, 2007; Gunawardane et al., 2000; Petry and Vale, 2015; Tillery et al., 2018; Vérollet et al., 2006; Wiese and Zheng, 2006).

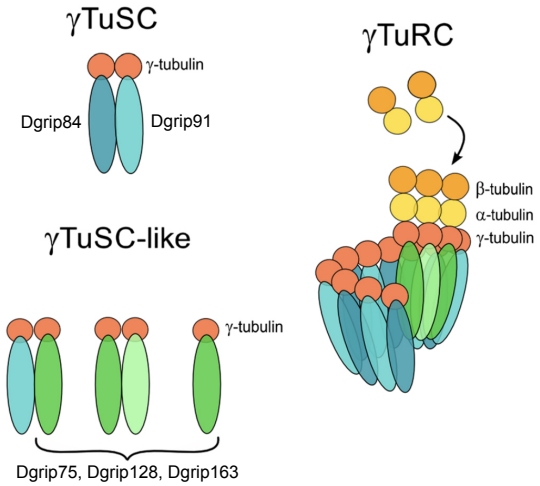


Figure 12. γ-TuRC assembly

γTuSC are composed of two γ-tubulin ring complex proteins: Dgrip84 and Dgrip91, (in Drosophila) and two molecules of γ-tubulin. Different γTuSC-like structures are formed by assembly of different γ-tubulin ring complex proteins. γ-TuRC assembly through association of multiple γ-TuSCs complexes, promoting interaction with αβ-tubulin. Modified from (Sulimenko et al., 2017).

This ring complex functions as the template for protofilament nucleation, while establishing MT polarity. The plus-end positioned away from the ring, is the most dynamic extremity and faces the cortex or the chromosomes during mitosis. The minus-end, less dynamic is positioned near the nucleation site. The presence of γ-TuRCs in certain cellular regions, like centrosomes maintain nucleation restricted to these spots, preventing therefore spontaneous MT polymerization.

Although centrosomes are well known for their role in regulating mitosis and nucleating MTs, they are also required for other cell functions such as control of cell shape and polarity, adhesion and motility as well as cilia formation in the case of centrioles (Bettencourt-Dias and Glover, 2007; Lattao et al., 2017). Even if centrosomes are involved in mitotic spindle assembly during cell division, they are not essential. In the absence of centrosomes in *Drosophila*, studied in contexts of Sas-4 or Cnn mutations, cells still assembled a functional bipolar mitotic spindle and accomplished cell division (Basto et al., 2006; Megraw et al., 2001). This is also seen

without any treatments, for example in the oocyte in the majority of animal species, where meiosis routinely occurs without centrosomes (Dumont and Desai, 2012; Heald et al., 1997).

Non-centrosomal microtubule organizing centers (ncMTOCs)

As mentioned above, MTs can be nucleated in the absence of centrosomes, which is normal referred to as non-centrosomal MTOCs (ncMTOCs).

The Chromatin pathway:

Chromatin-mediated MT nucleation occurs after activation of local MT nucleation on the chromatin through increase in concentration of a GTP-bound form of the Ras-related nuclear protein (Ran-GTP) (Gadde and Heald, 2004; Tillery et al., 2018). This promotes the release of spindle assembly factors that promote MT nucleation near chromosomes. This pathway was described in the *Drosophila* syncytial embryo and in female oocytes from different animals (Dumont and Desai, 2012; Hayward and Wakefield, 2014).

The Augmin pathway:

Pre-existing MTs can function as nucleation spots, mostly through the activity of the Augmin complex. This complex consists of eight subunits required to recruit γ-TuRC to pre-existing MTs, essential to initiate branching nucleation of interphase cortical MTs (Goshima et al., 2008; Tillery et al., 2018). This pathway is involved in the non-centrosomal MTs nucleation in neurons for example (Sánchez-Huertas et al., 2016).

The Golgi apparatus:

The Golgi apparatus represent a well-established ncMTOC, with important functions in Golgi organization, polarized transport, cell motility, and cell differentiation (Tillery et al., 2018). MT nucleation from the Golgi apparatus requires the A-kinase Anchoring Protein (AKAP450) which recruits γ-TuRCs to the Golgi. Golgi membranes can serve as ncMTOC in different types of cells such as muscle cells and pancreatic β cells (Rivero et al., 2009; Wu et al., 2016).

Nuclear envelope (NE):

The NE is considered one of the most common ncMTOC. It has been described in different organisms and cells such as in fission yeast *Schizosacchoromyces pombe*, where γ-TuRCs are recruited to the NE to nucleate MTs (Bao X X et al., 2018).

In *Drosophila,* acentrosomal polyploid cells constitute the larval fat body, an organ with metabolic functions similar to the liver. In these cells, MTs are nucleated from the NE and radiate toward the cytoplasm (Sun et al., 2019; Zheng et al., 2020). This requires the activity of different proteins, like the MT binding protein Ninein (Nin) and the calmodulin-regulated spectrin-associated protein- Patronin. These two proteins cooperate to recruit, assemble and stabilize MT minus-ends at the NE ensuring its perinuclear nucleation. Another protein Minispindles (Msps- the human ch-TOG orthologue) ensures MT elongation forming their typical radial structure (Zheng et al., 2020). Another important protein is called Shot, a Spectraplakin family member (Sun et al., 2019; Zheng et al., 2020). This protein is recruited to the NE with the help of a Nesprin-like protein, Muscle-specific protein 300 kDa (Msp300), to ensure the stabilization of the perinuclear MTs (Sun et al., 2019; Zheng et al., 2020). This perinuclear MT nucleation is essential for nuclear positioning in the center of the cell, since disruption of the MT cytoskeleton, by either MT-severing enzyme (Spastin) or knocking down MT subunits, leads to defects in nuclear positioning (Zheng et al., 2020).

In *Drosophila*, SGs acentrosomal polyploid cells also nucleate MTs from the NE, assembling a similar perinuclear and radial organization at the NE as in the cells of *Drosophila* fat body (Zheng et al., 2020). However, the mechanism or the regulators involved in this nucleation are not well understood. The only protein shown to have a role in this cell type, is Shot, suggesting similar mechanisms underlying MT organization in both tissues (Sun et al., 2019).

In mammals, competent mouse oocytes presented MT astral nucleation from the PCM foci localized at the nucleus surface (Łuksza et al., 2013). This perinuclear MT organization is also responsible for the accurate nuclear positioning in the center of the cell, as MT depolymerization with nocodazole results in its mis-positioning (Łuksza et al., 2013). Finally, in skeletal muscle cells, which are also polyploid through fusion events of myotubes, several PCM proteins can be seen associated with the NE marking it as the ncMTOC to nucleate MTs in a γ-tubulin -dependent manner (Bugnard Elisabeth et al., 2005).

3.4. Centrosome number

3.4.1. Centrosome number regulation

Control of centriole duplication requires the restriction of nucleating one daughter centriole next to the mother centriole. The restriction mechanism is dependent among others, on the activity of the SCF E3 ubiquitin ligase. In flies, the F-box involved is a protein called Slimb. SCF^{slimb} mediates the proteolytic degradation of Plk4 (Cunha-Ferreira et al., 2009; Rogers et al., 2009). During mitosis, When Plk4 levels increase, reaching a certain level, it auto-phosphorylate its conserved degron on Ser293 and Thr297 (Cunha-Ferreira et al., 2013). Slimb is then able to bind to phosphorylated Plk4, promoting Plk4 ubiquitination and, degradation by the proteasome and so regulating centrosome number during cell cycle (Cunha-Ferreira et al., 2013, 2009; Rogers et al., 2009).

3.4.2. Centrosome amplification

Centrosome amplification can result from different mechanisms, such as centrosome overduplication, de novo centrosome formation, and polyploidization.

Altered expression levels of main proteins involved in the regulation of centrosome duplication can lead to centriole overduplication and excessive growth of procentrioles around one or both parental centrioles. This is the case of Plk4 overexpression that allows the nucleation and growth of more than one procentriole on the mother centriole resulting in centrosome amplifications in different cell types and species (Figure 13) (Basto et al., 2008; Bettencourt-Dias et al., 2005; Coelho et al., 2015; Habedanck et al., 2005; Peel et al., 2007).

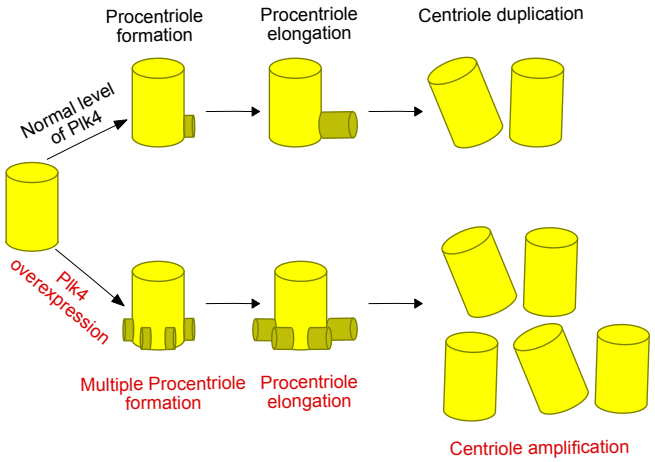


Figure 13. Centrosome amplification through Plk4 overexpression

In normal conditions, Plk4 is assembled in a one ring structure, which becomes restricted to a single dot promoting the formation of only one procentriole per parental centriole. Plk4 overexpression causes the assembly of multiple Plk4 dots leading to the formation of multiple sites for procentriole formation. This process results in centrosome amplification.

Centrosome amplification in cancer

As it was described in section 2.2, centrosome amplification is a common feature of cancer cells (D'assoro et al., 2002; Giehl et al., 2005; Godinho and Basto, 2025; Guo et al., 2007; Krämer et al., 2005; Morretton et al., 2022; Pihan German A. et al., 1998; Sato et al., 1999; Yongsheng Chan and Yongsheng Chan MBBS, 2011). Moreover, Plk4 expression is upregulated in human breast and colon cancers (Macmillan et al., 2001; Marina and Saavedra, 2014). Overexpressed Plk4 causes the nucleation and growth of more than one procentriole next to mature centrioles, resulting in total centrosome amplification.

In *Drosophila*, inducing centrosome amplification by overexpressing Plk4 in the larval brain or wing discs, showed potential for tumor formation upon transplantation assays into host flies (Basto et al., 2008; Sabino et al., 2015). In mice, global or transient centrosome amplification in different tissues, as for example in the mouse intestine, was sufficient to drive aneuploidy and the development of spontaneous tumors (Levine et al., 2017). In adult mouse skin, centrosome amplification promotes tumorigenesis in conditions of p53 depletion (Coelho et al., 2015; Kulukiana et al., 2015; Serçin et al., 2016).

Centrosome amplification beyond cancer

Although centrosome amplification showed a strong correlation with promoting tumorigenesis, this was not the only outcome when it was induced in vivo as its consequences depend on the organism and the tissue where it is induced. During mouse brain development, centrosome amplification in mouse neuronal stem cell led to multipolar mitosis. However, this caused high levels of aneuploidy, cell death and developmental defects as a drastic reduction in brain size, also known as microcephaly, but not cancer (Marthiens et al., 2013).

Centrosome amplification and mitochondria

Mitochondria

Before discussing possible consequences of centrosome amplification on mitochondria, I will introduce mitochondria structure and function.

Mitochondria are double-membraned organelles found in most eukaryotic cells and are often referred to as the “powerhouses of the cell” since they play a critical role in cellular respiration, as well as the production of cellular energy as adenosine triphosphate (ATP) (Benda C, 1898; Casanova et al., 2023; Chandel, 2021; Schenkel and Bakovic, 2014). Mitochondria are composed of three layers, the outer membrane, the inner membrane and the matrix (Figure 14).

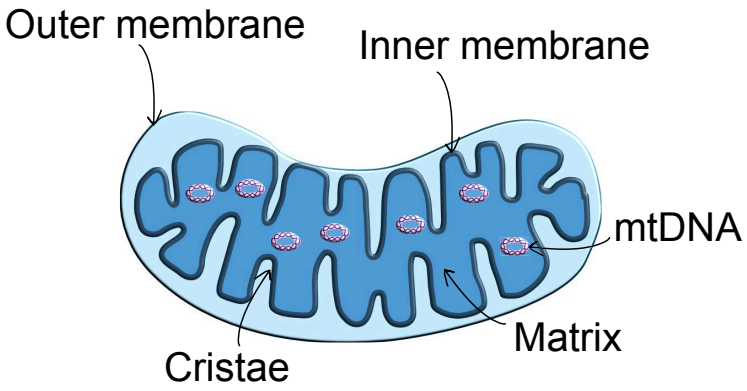


Figure 14. The structure of Mitochondria

Mitochondria are double membraned organelles.The inner membrane is folded in multiple cristae that all surround the matrix of the mitochondria containing the mitochondria DNA (mtDNA).

The outer mitochondrial membrane separates the intermembrane space from the cytosol and contains several pores, which facilitate the passage of ions and small uncharged particles (Chandel, 2021; Ellenrieder et al., 2019; Schenkel and Bakovic, 2014). The inner mitochondrial membrane separates the mitochondrial matrix from the intermembrane space. It is folded into several ridges (cristae), thought to increase its total surface area and is containing specialized protein complexes that regulate the transport of molecules and ions (Figure 15) (Chandel, 2021; Joubert and Puff, 2021; Kühlbrandt, 2015; Schenkel and Bakovic, 2014). The mitochondria matrix present at the centre of mitochondria contains the mitochondrial DNA (mtDNA), ribosomes and different enzymes required for mitochondria activity (Chandel, 2021; Schenkel and Bakovic, 2014).

Mitochondria play essential roles in generating nicotinamide adenine dinucleotide (NADH) and flavin adenine dinucleotide ($FADH_2$) during the Krebs cycle, also called the citric acid cycle (Figure 15) (Brown, 1992; Martínez-Reyes et al., 2016; Martínez-Reyes and Chandel, 2020; Osellame et al., 2012). This cycle takes place in the mitochondrial matrix and can be described as a series of chemical reactions that allow breaking down acetyl-CoA, which is the result of dehydrogenised pyruvate. This process is essential to produce GTP and energy-storing molecules like NADH and $FADH_2$. These molecules then help make more ATP in the next step of cellular respiration by pumping protons from the matrix into the intermembrane space through mitochondrial proton pumps (complexes I, III and IV) (Brown, 1992; Casanova et al., 2023; Chandel, 2021; Hroudová and Fišar, 2013; Nesci et al., 2021). Thus, creating a concentration proton gradient that will push the protons to flow back in the matrix resulting in an equal proton concentration in both sides.

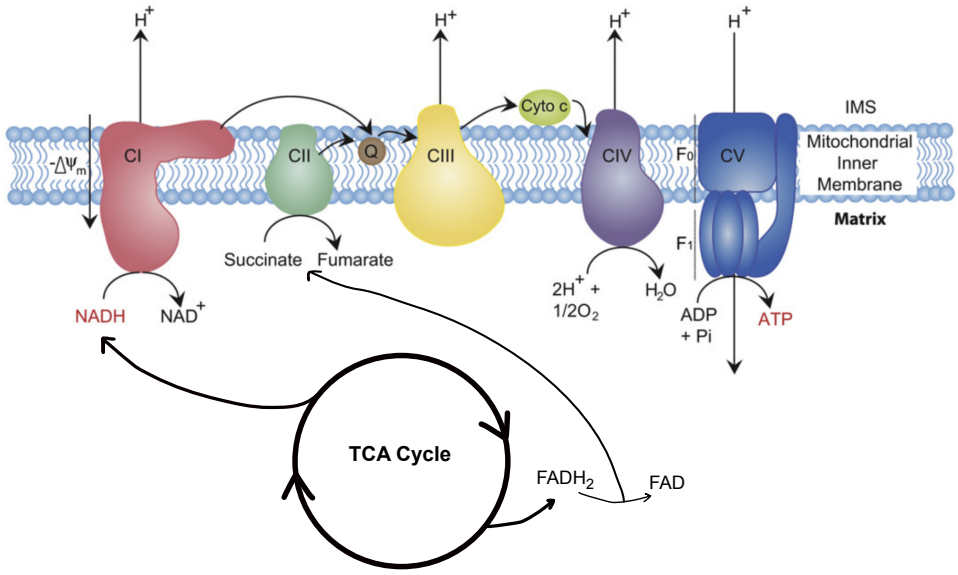


Figure 15. Mitochondria activity through its transmembrane complexes

The TCA cycle generates high-energy molecules, NADH and $FADH_2$ that transfer electrons to the mitochondrial electron transport chain, resulting in the generation of a proton motive force to drive ATP synthesis via complex V (ATP synthase). Modified from (Osellame et al., 2012).

In the mitochondrial inner membrane, a transmembrane enzyme called ATP synthase, or complex V can be found (Figure 15) (Casanova et al., 2023; Chandel, 2021; Jonckheere et al., 2012). ATP synthase is a large protein complex composed of two parts, F_0 and F_1. F_0 is embedded in the inner membrane and acts as a proton channel. On the other hand, F_1 is attached to F_0 and protrudes into the matrix and is responsible for the actual synthesis of ATP (Jonckheere et al., 2012; Nakamoto et al., 2008; Noji and Yoshida, 2001; Stock Daniela et al., 1999). When protons diffuse from the intermembrane space back in the matrix, ATP synthase uses their kinetic energy to convert adenosine diphosphate ADP and inorganic phosphate (P_i) into ATP, in a process called oxidative phosphorylation (OXPHOS) (Brown, 1992; Hroudová and Fišar, 2013; Kadenbach et al., 2010; Nesci et al., 2021). Mitochondrial ATP production is considered as the main energy source for intracellular metabolic pathways and this production requires oxygen as the electron transport chain can only work if oxygen is present (Chandel, 2021; Hroudová and Fišar, 2013; Reynafarje and Ferreira, 2008).

If oxygen is not present, electrons do not flow and protons are not pumped, preventing ATP synthase of producing ATP (St-Pierre et al., 2000).

Interestingly, mitochondria are dynamic organelles that are continually undergoing fission and fusion (Scott and Youle, 2010; Westermann, 2012, 2010). Both processes are energy-dependent and rely on specialized proteins and regulators, allowing the mitochondrial network to adapt its shape, size, number, and contents to changing metabolic demands. Fission involves the separation of the outer and inner mitochondrial membranes, producing two distinct mitochondria. It is essential for increasing mitochondrial number during high energy demands and for their proper distribution during cell division, as mitochondria cannot be formed de novo. In contrast, fusion is the process by which two mitochondria and their outer and inner membranes fuse to form a single, large mitochondrion. This process acts as a protective mechanism by mixing contents and diluting damaged components to preserve function.

In certain cell types, such as neurons, mitochondria are transported within the cell, promoting the intracellular distribution of mitochondria to sites of high ATP consumption (Guo et al., 2005; López-Doménech et al., 2018; Melkov and Abdu, 2018; Pilling et al., 2006; Stowers et al., 2002). This bidirectional transport is carried out via MTs and is executed by two main motor proteins, Dynein and Kinesin (Figure 16) (Pilling et al., 2006).

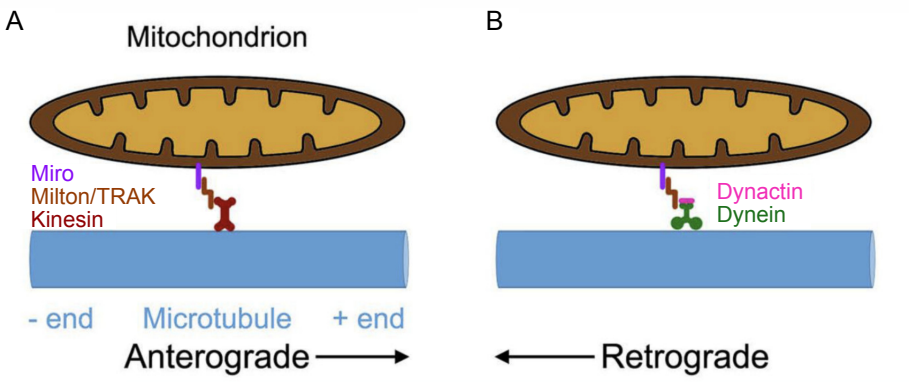


Figure 16. Transport of mitochondria by MTs

A- Anterograde transport of the mitochondria on the MTs, through a kinesin-Milton/track - Miro complex. B- Retrograde transport, promoted with the same Miro-Milton/TRAK complex but interacting with Dynactin-Dynein, instead of kinesin. Modified from (Smith and Gallo, 2018).

Kinesin 1 ensures plus-end-directed or anterograde transport. Kinesin is connected to MTs and the mitochondrial outer membrane while interacting with the mitochondrial protein Miro and the motor adaptor Milton (Figure 16A) (human homologue of TRAK) (Guo et al., 2005; López-Doménech et al., 2018; Stowers et al., 2002). Miro is a mitochondrial outer membrane GTPase protein that possesses a domain capable of binding cytosolic Ca^{2+} (Wang and Schwarz, 2009). This binding induces a conformational change that modifies the kinesin-Milton-Miro complex and stops anterograde transport of mitochondria. Regarding minus-end-directed or retrograde transport, dynein binds to the dynactin complex. Together, they interact with the Miro-Milton complex ensuring mitochondria retrograde transport (Figure 16B) (Melkov and Abdu, 2018; Pilling et al., 2006).

Mitochondria are involved in many different pathways, such as stress responses and apoptosis by releasing cytochrome C and other pro-apoptotic factors to initiate programmed cell death (Chandel, 2021, 2014; Hüttemann et al., 2011). Mitochondria are also involved in calcium signaling by buffering intracellular calcium (Ca^{2+}), essential for signaling and metabolism (Chandel, 2021; Jouaville et al., 1999; Rizzuto et al., 2012).

Consequences of centrosome amplification on mitochondria

Interestingly, it has been recently shown that centrosome amplification induces defects in mitochondria organization, distribution and activity. Cells with amplified centrosomes exhibited increased tubulin acetylation, which enhances kinesin-1-mediated transport (Monteiro et al., 2023). These changes lead to the displacement of different organelles, including mitochondria towards the cell periphery, which may affect cellular functions and responses (Monteiro et al., 2023). A recent study from our lab has linked centrosome amplification in ovarian cancer cells to mitochondrial outer membrane permeabilization priming, a critical event in apoptosis (Edwards et al., 2024; Lemasters, 2007; Tait and Green, 2010). This priming event enhanced the cell response to chemotherapy promoting cell death through cytochrome C and consequently caspase activation (Edwards et al., 2024).

Centrosome amplification in programmed polyploid cells

Certain programmed polyploid cells contain extra centrosomes, which does not necessarily result in genetic instability or transformation. This is the case of megakaryocytes, for example. These cells undergo polyploidization and the number of centrosomes (Becker et al., 2024). These amplified centrosomes undergo clustering and are required in the platelet production, as genetic ablation of these centrosomes in mice lead to reduced platelet formation (Becker et al., 2024).

Another example are the osteoclast polyploid cells that result from macrophage fusion and are known to control bone resorption, a process that involves destruction of the bone tissue and mineral release inducing calcium transfer from bone tissue to the blood (Soysa et al., 2012). Osteoclasts also show centrosome amplification that cluster to nucleate MT filaments and ensure proper functioning, as impairing centrosome clustering, by pharmacological inhibition, significantly reduced bone resorption (Philip et al., 2022).

Centrosome amplification control

Centrosome amplification can lead to multipolar cell division, which may represent a significant barrier to daughter cell survival. This problem can be overcome by centrosome clustering (Kalkan et al., 2022; Krämer et al., 2011; Marthiens et al., 2012). Centrosomes can coalesce into two main poles for pseudo-bipolar spindle formation, making it a great mechanism employed by cells with amplified centrosomes, to avoid the detrimental effects of multipolar mitosis.

Centrosome clustering was initially described in N115 mouse neuroblastoma cells, where centrosomes cluster to assemble a pseudo-bipolar spindle allowing chromosome segregation into two daughter cells (Ring et al., 1982). Subsequently, many cancer cell lines with high levels of centrosome amplification have been shown to efficiently cluster centrosomes, as they only rarely undergo multipolar divisions and when they do so, aneuploid daughter cells are mostly unviable (Bill R. Brinkley, 2001; Kwon et al., 2008; Quintyne NJ, 2005; Ring et al., 1982). Therefore, targeting this clustering mechanism by therapeutic drugs against clustering motors, to force multipolarity and ultimately cell death, marks a good strategy against cancer cells that frequently present centrosome amplification (Myers and Collins, 2016; Sabat-Pospiech et al., 2019).

The mechanism underlying centrosome clustering was reported to rely on MT-based motors and MT-bundling proteins that organize spindle poles in cells with extra centrosomes (Goshima et al., 2005; Kwon et al., 2008; Leber et al., 2010; Quintyne NJ, 2005). Genome-wide RNAi screens showed that SAC contributes first to this process by delaying the onset of anaphase until all chromosomes are properly aligned providing sufficient time for centrosome clustering and reorganization of multipolar spindles into pseudo-bipolar structures (Kwon et al., 2008; Leber et al., 2010). In *Drosophila* cells, a minus-end directed motor protein, non-claret disjunctional (Ncd/ human homologue of HSET) is responsible for centrosome clustering to suppresses multipolarity upon centrosome amplification (Basto et al., 2008; Chavali et al., 2016; Goshima et al., 2005; Karabay and Walker, 1999; Kwon et al., 2008). Another identified motor is the minus-end directed motor dynein, which depletion prevents centrosome clustering thus promoting spindle multipolarity in tumor cells as well as in non-transformed cells with extra centrosomes (Leber et al., 2010; Quintyne NJ, 2005). During mitosis, dynein recruits the nuclear mitotic apparatus protein (NUMA) to spindle poles, tethering MT minus ends to the centrosomes (Quintyne NJ, 2005).

A different way to overcome centrosome amplification is to limit the number of active spindle poles. This is achieved through centrosome inactivation. This was mainly described in *Drosophila* neuroblasts, and observed in wing discs, upon centrosome amplification, where un-clustered centrosomes displayed reduced MT-nucleation capacity (Basto et al., 2008; Sabino et al., 2015).

3.4.3. Centrosome loss

Although centrosomes are considered as well-conserved organelles that maintain a regulated level of stability across many cell cycles to support various cellular functions, they can be eliminated under specific circumstances. This process was first recognized by Theodor Boveri while studying animal oocytes, but then observed in a range of cell types across different organisms, with a significant variation in the underlying mechanisms promoting centrosome loss (Summarized in Table 3) (Borrego-Pinto et al., 2016; Boveri T, 1887; Hannaford and Rusan, 2024; Hinnant et al., 2020; Kalbfuss and Gönczy, 2023a, 2023b; Lu and Roy, 2014; Marie Pierron, 2020; Pimenta-Marques et al., 2016; Schoborg and Rusan, 2016; Woglar et al., 2024).

Naegleria gruberi

The single-celled eukaryote *Naegleria gruberi*, differentiates from an amoeboid form, an irregular and dynamic state during feeding process, to a flagellate form, an elongated and moving state in research to better environments. During this differentiation, centrioles undergo a cycle of elimination and de novo assembly (Fulton, 1977; Woglar et al., 2024). While transitioning from the flagellate to the amoeba state, both flagella and centrioles are eliminated in a process that only takes 90 minutes. In a recent study, centriole elimination was shown to be dependent on lysosome- and proteasome- in this organism (Woglar et al., 2024). In the initial steps of this process, centrioles are detached from the plasma membrane after flagella internalization and are then located inside the cell marking the initiation of elimination. Interestingly, there is not a single mechanism involved in centriole elimination afterwards. Centrioles undergoing elimination were seen to be ubiquitinated by either an autophagy-linked Lysine 63 (K63) polyubiquitination or a proteasome-promoting Lysine 48 (K48) polyubiquitination (Dósa and Csizmadia, 2022; Grice and Nathan, 2016; Woglar et al., 2024). The major pathway was dependent on lysosome degradation, since inhibiting lysosome activity by blocking lysosomal acidification using Bafilomycin A1, prevented centriole elimination in ~90% of the cells (Mauvezin and Neufeld, 2015; Woglar et al., 2024). The remaining centrioles were eliminated by proteasome degradation, since the use of proteasome inhibitor- Bortezomib- slowed down centriole elimination (Chen et al., 2011; Woglar et al., 2024). Interestingly, it was shown that a small fraction of centrioles can also be shed into the extracellular space to be captured by another cell where it will be eventually eliminated (Woglar et al., 2024).

Starfish oocytes

In starfish oocytes, centrioles are eliminated during meiosis in a different mechanism than the one described in the *Naegleria gruberi*. Interestingly, daughter centrioles do not undergo maturation into mother centrioles which results in the same number of centrioles, two mothers and two daughters, during starfish oocyte meiosis (Borrego-Pinto et al., 2016; Zhang et al., 2004). During meiosis I, both mother and daughter centriole localize near the plasma membrane to be subsequently extruded into the first polar body (Borrego-Pinto et al., 2016; Schoborg and Rusan, 2016; Zhang et al., 2004). During meiosis II, the remaining centrioles organize a new spindle with the mother centriole facing the plasma membrane to be then extruded into the second

polar body (Borrego-Pinto et al., 2016; Schoborg and Rusan, 2016; Zhang et al., 2004). This specific positioning is mediated by dynein-driven transport, and the mother-specific appendages serve as an anchor of the mother centriole to the plasma membrane (Borrego-Pinto et al., 2016). The remaining daughter centriole in the zygote is eliminated after losing its MT-nucleating activity before the first embryonic cleavage (Borrego-Pinto et al., 2016; Zhang et al., 2004). Retaining the centrioles in the zygote, by preventing polar body extrusion, using latrunculin B for example, showed a normal deactivation and elimination of daughter centrioles but maintenance of active mother centrioles that will then contribute to the spindle assembly resulting in multipolar spindles in the zygote (Borrego-Pinto et al., 2016; Zhang et al., 2004).

C. elegans

Embryos

In *C. elegans* embryos, ~88% of cells lose centrioles during embryogenesis (Kalbfuss and Gönczy, 2023b). Further detailed lineage analysis showed that centriole elimination is programmed and stereotyped in a way that it is dependent on specific timing and on cell fate. These findings were challenged by artificially imposing alterations in the fate of progenitor cells. Indeed, changing cell fate was sufficient to alter centriole fate (Kalbfuss and Gönczy, 2023b). In conclusion, these experiments show that cells that maintain centrioles are the ones that will continue to proliferate at later stages of development. However, intestinal cells that will later undergo endoreplication cycles, only maintain their centrioles at the first stages of development (Kalbfuss and Gönczy, 2023b; Lu and Roy, 2014).

Intestinal cells

During late first larval stages (L1), intestinal cells terminate nuclear divisions and prepare to undergo endoreplication cycles. At this stage, γ-tubulin previously associated with centrioles will disperse in the cytoplasm ensuring inactivation of the centrioles as active MTOCs (Lu and Roy, 2014). During endoreplication cycles, centrioles no longer duplicate. The elimination of the remaining centrioles is triggered by downregulation and degradation of Spd-2, through Plk1 phosphorylation and proteasome degradation respectively (Lu and Roy, 2014).

Oocytes

During oogenesis, centrioles are eliminated when the MT associated protein SAS-1 is lost. This event triggers the disassembly of other components ensuring the loss of the central tube (Pierron et al., 2023). In sas-1 mutant cells, the organization of the central tube is disrupted, and these centrioles undergo elimination earlier in development (Pierron et al., 2023). The loss of the central tube results in organelle widening, followed by MT disassembly, thus all remaining proteins start to move gradually to the plasma membrane, in a MT- and dynein- dependent manner (Pierron et al., 2023).

Drosophila melanogaster

Nurse cells

During early oogenesis, a 16-cell cyst is formed, from which only one cell is designated to become the oocyte, and the remaining 15 cells differentiate into nurse cells (Hannaford and Rusan, 2024; Hinnant et al., 2020). These nurse cells play an essential role in supplying maternally derived proteins and RNAs to the oocyte. This process is depedent on MTs that traverses cytoplasmic bridges, known as ring canals (Hannaford and Rusan, 2024; Hinnant et al., 2020). Interestingly, EM studies documented that during development, centrosomes migrate from nurse cells through the ring canals to be clustered in the oocyte, where they will be eliminated afterwards (Mahowald and Strassheim, 1970). Centrosome migration is first supported by localization to a microtubule-rich structure known as the fusome in a Shot-dependent manner (Röper and Brown, 2004). Shot is a fusome component and as mentioned previously, can have important functions in MT cytoskeleton organization. The transport of centrosomes along the ring canal is supported by the Dynein motor (Bolívar Jorge et al., 2001; Röper and Brown, 2004).

Oocytes

Centrosomes migrate from nurse cells into the oocyte to cluster in a large MTOC before undergoing elimination (Pimenta-Marques et al., 2016). A recent study characterized both centriolar and PCM protein behavior. It was shown that at mid stages of development, PCM components disappear while centriolar proteins were kept stable (Pimenta-Marques et al., 2016). At later stages, PCM components levels decrease concomitantly with the loss of centriolar components (Pimenta-Marques et

al., 2016). One major regulator of this process is the kinase Polo, which is essential for PCM recruitment and maintenance at the centrioles . Interestingly, downregulation of Polo resulted in earlier centriole loss (Pimenta-Marques et al., 2016). In contrast, when Polo was ectopically tethered to centrioles by fusing it to the centriole targeting domain PACT, which prevented PCM removal, centrosomes were maintained in the oocyte leading to a failure in zygotic development (Pimenta-Marques et al., 2016).

Others

Centriole elimination was reported in different tissues without proper explanation of the mechanism underlying this process, such as follicle cells, midgut enterocytes, polyploid enterocytes of the hindgut, malpighian tubule cells, SG secretory cells, fat body cells and wing epidermal cells (Kalbfuss and Gönczy, 2023a; Mahowald et al., 1979; Mogensen and Tucker, 1987; Schoenfelder et al., 2014; Zheng et al., 2020a).

Vertebrates: human and mouse

Centrosomes are eliminated from oocytes during meiotic prophase I in what remains a poorly understood mechanism, that starts with inactivation of MTOC activity by PCM disassembly followed by centriole degradation (Aljiboury and Hehnly, 2023; Gruss, 2018). Skeletal myotubes and muscle fibers were also reported to lose their centrosomes during their development (Kalbfuss and Gönczy, 2023a; Przybylski, 1971).

Table 3. Mechanisms of centrosome elimination in different organisms

Species	Cell type	When?	Mechanism of centrosome elimination
Naegleria gruberi		transition from flagellate to amoeba state	Autophagy- and Proteasome-linked polyubiquitination Lysosome and proteasome degradation Shedding into the extracellular space
Starfish	Oocytes	During Meiosis	Meiosis I: two centrioles are extruded in the first polar body Meiosis II: mother centriole extruded in the second polar body in a dynein mediated process. Daughter centriole degradation
C. elegans	Intestinal cells	During endoreplication	In L1: γ-tubulin is dispersed in the cytoplasm → centriole inactivation During endoreplication: Centriole eliminated by downregulation and degradation of Spd-2 by Plk1 phosphorylation and proteasome degradation
	Oocytes	During oogenesis	Loss of Sas-1→ loss of the central tube MT disassembly → proteins dispersion in the plasma membrane, in a MT- and dynein-dependent manner
Drosophila melanogaster	Nurse cells	During oogenesis	Centrosomes migrate from nurse cells through the ring canals → centrosomes clustered in the oocyte Shot and Dynein dependent mechanism

Drosophila melanogaster	Oocytes	Mid and late stages of oogenesis	Loss of Polo → PCM loss → centrioles degradation
	Follicle cells Midgut enterocytes Polyploid enterocytes of the hindgut Malpighian tubule cells Salivary gland secretory cells Fat body cells Wing epidermal cells		Not described
Human and mouse	Oocytes	Meiotic prophase I	PCM disassembly →centriole degradation
	Skeletal myotubes Muscle fibers	After fusion	Not described

4. Myosin II

Myosins are cytoskeletal actin-based motor proteins that convert chemical energy derived from ATP hydrolysis into mechanical force allowing them to move along actin filaments (Coluccio LM., 2008; Rayment I et al., 1993; Vale' and Goldsteint, 1990). The myosin superfamily consists of more than 25 different classes where most family members share the same structure composition, with variations in the organization of certain domains (Coluccio Lynne M., 2008; Vale' and Goldsteint, 1990). Generally, myosins consist of three domains: one amino-terminal (N-terminal) motor domain, the neck domain and the carboxy-terminal (C-terminal) tail domain (Coluccio LM., 2008; Rayment I et al., 1993; Vale' and Goldsteint, 1990). In this section, I will describe the structure and main functions of non-muscle myosin II (MyoII).

4.1. MyoII structure

MyoII is an hexameric complex composed of two heavy chains (MHCs, ~200-230kDa each), consisting of two motor domains and a coiled-coil tail domain, plus two essential light chains (ELCs, ~17 kDa each) and two regulatory light chains (RLCs, ~20 kDa each), both localized in the neck domain (Figure 17) (Chinthalapudi and Heissler, 2024; Coluccio Lynne M., 2008; Franke et al., 2006; Heissler and Manstein, 2013; Liu et al., 2008; Quintanilla et al., 2023; Rayment Ivan et al., 1993; Tan et al., 1992).

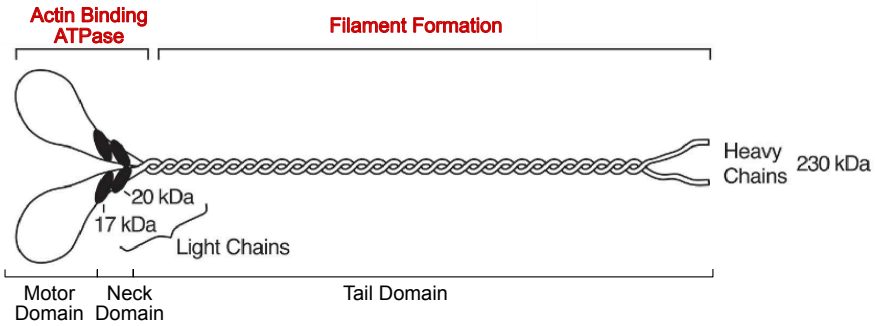


Figure 17. The overall organization of the MyoII motor

The drawing of a MyoII molecule showing the heavy chain dimer with two motor domains and two pairs of light chains. Their corresponding functions are annotated. Modified from (Coluccio Lynne M., 2008).

4.1.1. Motor domain

The N-terminal motor domain is a globular ~15 nm domain. Its detailed structure was first described in 1993, by high-resolution X-ray crystallography (Rayment I et al., 1993). This technique revealed that the MyoII motor domain presented a conserved structure with a length of 165 Å, a width of 65 Å, and a thickness of approximately 40 Å (Rayment I et al., 1993). In more detail, the motor domain is composed of a seven-stranded β-sheet surrounded by α-helices on each side which extends to the C-terminus of the heavy chain (Chinthalapudi and Heissler, 2024; Coluccio Lynne M., 2008; Rayment Ivan et al., 1993). These helices are arranged in a way to constitute four functional subdomains: the N-terminal subdomain (Nter), the upper 50 kDa subdomain (U50), the lower 50 kDa subdomain (L50), and the converter subdomain (Figure 18) (Chinthalapudi and Heissler, 2024; Coluccio LM., 2008; Rayment I et al., 1993). Each of these subdomains contributes to the functional core of MyoII, by promoting binding to actin filaments and hydrolyzing ATP to generate mechanical force.

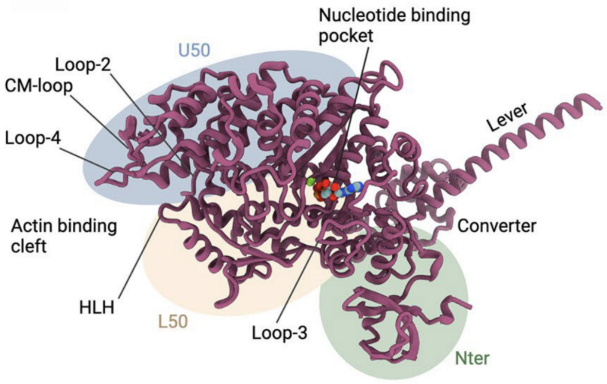


Figure 18. The structure of MyoII motor domain

Key structural features of the MyoII motor domain highlighting the four functional subdomains: Nter, U50, L50 and the converter (Chinthalapudi and Heissler, 2024).

The motor domain contains a nucleotide binding pocket and a binding region for filamentous actin located on opposite sides of the protein. The U50 subdomain composes parts of the nucleotide binding pocket which includes three conserved structural motifs required for binding and hydrolyzing ATP (Chinthalapudi and Heissler, 2024; Coluccio LM., 2008; Rayment Iv et al., 1993). The first motif is the Phosphate-binding loop (P-loop) and, as its name suggests, recognizes and binds the phosphate

groups of ATP (or ADP in the inactive state) (Chinthalapudi and Heissler, 2024; Coluccio LM., 2008). This interaction stabilizes nucleotide binding within the motor domain and initiates conformational changes in the second motif, switch-1 loop. Upon switch-1 detection of ATP binding, it regulates nucleotide binding and hydrolysis by structural rearrangements of another loop, switch-2, driving the myosin ATPase cycle (Chinthalapudi and Heissler, 2024; Coluccio LM., 2008; Furch et al., 1999; Koppole et al., 2007). A long α-helix, called relay helix, connects the nucleotide binding pocket, through its switch-2 loop, to the converter subdomain. This connection serves to transmit conformational changes to the lever arm (the neck domain) in order to initiate the mechanochemical cycle of MyoII (described in section 4.2) (Chinthalapudi and Heissler, 2024; Coluccio Lynne M., 2008; Koppole et al., 2007). On the other side of the motor domain, at more than 40 Å from the nucleotide binding pocket, structural elements of the U50 and the L50 connected with loop-2, form the actin binding region (Chinthalapudi and Heissler, 2024; Coluccio LM., 2008; Koppole et al., 2007; Rayment I et al., 1993). This region is split by a deep cleft extending from the nucleotide binding pocket to the actin binding site, which opens and closes in response to ATP binding (Chinthalapudi and Heissler, 2024; Coluccio LM., 2008; Rayment I et al., 1993).

4.1.2. Neck domain

The neck domain is composed α-helices reaching ~10 Å long localized distally to the myosin motor domain and features two binding sites specific for light chains. Each one of these binding sites is a ~24 amino acid domain usually with the common core sequence IQXXXRGXXXR, and so called based on the first two conserved residues, isoleucine and glutamine, IQ-motifs (Chinthalapudi and Heissler, 2024; Coluccio LM., 2008). The neck domain serves as a lever arm essential in the progression of the mechanochemical cycle of MyoII. Two distinct light chains are specific for MyoII, the RLC binding to the head-distal IQ-motif and the ELC binding to the head-proximal IQ-motif.

RLC is also referred to as the phosphorylatable light chain, since its phosphorylation increases MyoII actin-activated ATPase activity and when it is unphosphorylated, MyoII is unable to move actin filaments thus preventing force generation (Karess et al., 1991; Tan et al., 1992).

In *Drosophila*, the RLC is encoded by the gene *spaghetti squash* (*sqh*) located on the X chromosome at region 5E1. Activation of MyoII depends on phosphorylation at Serine 21 and Threonine 20 (T20S21) (Karess et al., 1991). Two well-known kinases involved in the regulation of MyoII activity by RLC phosphorylation, are the Ca^{2+}- calmodulin dependent myosin light chain kinase (MLCK) and Rho-associated protein kinase (ROCK in mammals and Rok in *Drosophila*) (Amano et al., 1996; Leung et al., 1995; Matsui et al., 1996; Takai Y et al., 1995; Tan et al., 1992; Tansey et al., 1994). Increased intracellular Ca^{2+} promotes its binding to the calcium modulating protein, calmodulin, to activate MLCK. MLCK is then able to phosphorylate the RLC at specific sites in order to increase MyoII ATPase activity as well as promoting MyoII assembly into bipolar filaments and actomyosin contraction (MyoII activation cycle is described in section 4.2) (Chinthalapudi and Heissler, 2024; Tan et al., 1992; Tansey et al., 1994). In parallel, Rho (Rho1 in *Drosophila* and RhoA in mammals) is a small GTPase from the Ras superfamily, which has a GDP-bound inactive and GTP-bound active forms (Nobes and Hall, 1994; Takai Y et al., 1995). GTP-Rho activates Rho-kinase which will subsequently phosphorylate RLC promoting the activation of myosin ATPase (Amano et al., 1996; Leung et al., 1995; Matsui et al., 1996). Importantly, RLC phosphorylation is reversible by opposing activities of myosin light chain phosphatase (MLCP) in a tightly controlled pathway to regulate MyoII dynamics and assembly. Activated Rho-kinase not only phosphorylates RLC, but it is also responsible for the inhibition of myosin phosphatase by phosphorylating the myosin phosphatase target subunit 1 (MYPT1), also known to phosphorylate myosin-binding subunit (MBS) (Chinthalapudi and Heissler, 2024; Kazushi Kimura, 1996). Protein phosphatase 1 (PP1) has been identified as the serine/threonine protein phosphatase that dephosphorylates RLC in order to inactivate MyoII promoting relaxation of actomyosin structures (Chinthalapudi and Heissler, 2024; Hartshorne D J et al., 1998; Wera and Hemmingst, 1995). In *Drosophila*, a specific isoform of PP1, PP1β, was identified as regulator of MyoII activity since its loss lead to increased levels of phosphorylated Sqh and actin disorganization in egg chambers (Vereshchagina et al., 2004). All these phenotypes were rescued and suppressed by reducing the amount of active myosin, using a nonphosphorylatable form of Sqh by alanine substitution at the phosphorylation sites (Vereshchagina et al., 2004).

ELC binds to the second IQ motif and interacts with the long α-helix of the heavy chain providing structural support and stabilization of the neck region (Chinthalapudi and Heissler, 2024; Coluccio Lynne M., 2008; Franke et al., 2006; Rayment Ivan et al., 1993). Although ELC does not undergo regulatory modifications as the RLC, it plays a critical role in transmitting structural conformation during mechanochemical force production. In *Drosophila*, ELC is encoded by the *essential light chain-cytoplasmic* gene (*mlc-c*) and it contains 147 amino acids (Edwards et al., 1995; Franke et al., 2006). Both *sqh*/RLC and *mlc-c*/ELC are bound to the heavy chain independently of each other, since in absence of *sqh*, heavy chains form aggregates in embryos, but *mlc-c* still binds to these aggregates independently of *sqh* (Edwards et al., 1995).

4.1.3. Tail domain

The tail domain represents the C-terminal domain of MyoII heavy chain (encoded by *zipper/zip* in *Drosophila*), containing ~800 residues with a heptad repeat and alternating charge distributions ensuring its self-association through hydrophobic interactions in both parallel and antiparallel fashion (Chinthalapudi and Heissler, 2024; Coluccio Lynne M., 2008; Quintanilla et al., 2023; Young et al., 1993). This results in an extended ~160 nm long α-helical structure that ends in a short non-helical tailpiece (NHT) (Chinthalapudi and Heissler, 2024; Cohen and Parry, 1990; Franke et al., 2006). This organization represents a coiled-coil structure resulting in the formation of an elongated MyoII hexameric complex of ~525 kDa that is referred to as the monomer (Chinthalapudi and Heissler, 2024; Franke et al., 2006). The tail domain is not only essential for the assembly of MyoII hexameric structure but is also critical for higher order oligomerization of MyoII into ~300 nm long bipolar filaments through the self-assembly of monomers via tail-tail interactions, essential for contractile force generation (Chinthalapudi and Heissler, 2024; Franke et al., 2006).

Importantly, the tail domain changes its conformation depending on the state of MyoII, autoinhibited or filamentous. In the inactive state, the two motor domains interact asymmetrically and are stabilized by hydrophobic interactions, with one head blocked from binding actin “blocked head”, while the other one is partially accessible but still inhibited “the free head” (Chinthalapudi and Heissler, 2024; Wendt et al., 2001,

1999). In parallel, the tail folds into three approximately equal size segments, loops around the motor domains, and folds back on itself preventing filament assembly and inhibiting ATPase activity (Burgess et al., 2007; Chinthalapudi and Heissler, 2024; Liu et al., 2003; Quintanilla et al., 2023). Upon RLC phosphorylation and MyoII activation, the tail unfolds allowing filament assembly via the exposed tail domains and thus enabling motor activity and function (Chinthalapudi and Heissler, 2024; Quintanilla et al., 2023; Roger Craig, 1983).

4.2. MyoII mechanochemical cycle

Different techniques including crystallography, cryo-electron microscopy and kinetic studies revealed a specific mechanochemical cycle where MyoII activity transitions through four major structural states (Chinthalapudi and Heissler, 2024; Fischer et al., 2005; Lynne M. Coluccio, 2008; Quintanilla et al., 2023; Lymn and Taylor, 1971). The key point in this cycle is that the binding of actin and the binding of nucleotides (ATP) to MyoII are antagonistic, meaning that ATP binding to actomyosin causes actin dissociation (Figure 19). This communication involves the opening and closing of the cleft between U50 and L50 domains of the MyoII head.

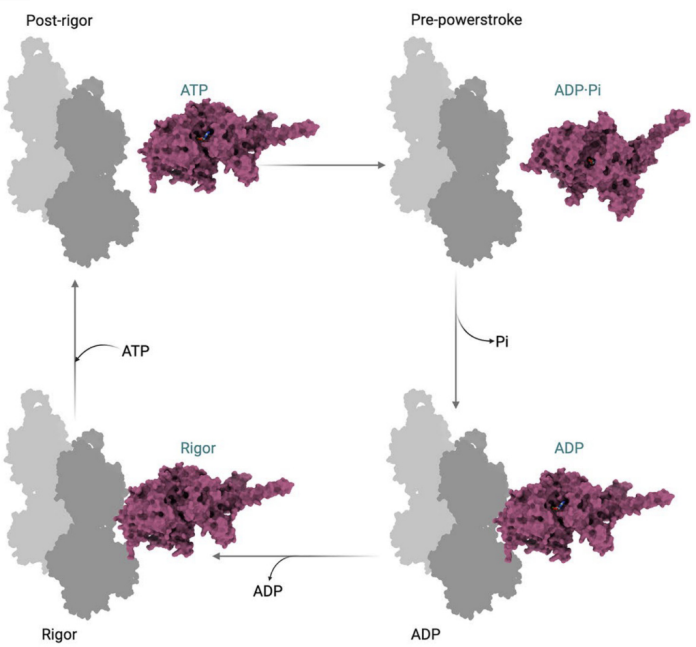


Figure 19. The mechanochemical cycle of MyoII

On the bottom left, at rigor state, in the absence of ADP and ATP, the MyoII motor domain binds actin. ATP binding to MyoII motor domain causes MyoII dissociation from the actin filament in the post-rigor state. ATP is the hydrolyzed to ADP-Pi in the pre-power stroke state. In this state, MyoII binds weakly to actin during the power stroke phase until the release of ADP and the restart of the cycle (Chinthalapudi and Heissler, 2024).

State 1 - Rigor State: Strong binding to actin

The first state of the cycle is marked by the nucleotide-free rigor state where the open nucleotide binding pocket is associated with the converter and the lever arm in the 'down' position. In the absence of ATP from the pocket present in the motor domain, MyoII is tightly binding to actin filaments.

State 2 - Post-rigor: ATP binding

Next, ATP binds to the nucleotide binding site, the ATPase site, inducing conformational changes in the actin-binding site, causing the dissociation of MyoII head from the actin filament.

State 3 - Pre-powerstroke: ATP hydrolysis – ADP, Pi binding

On the detached head, MyoII hydrolyzes ATP to ADP and Pi inducing conformational changes, linked to the converter and the lever arm in the 'up' position. The head stores the energy released by ATP hydrolysis and these changes promote a pre-powerstroke state, where ADP, Pi binding to MyoII form a stable intermediate with weak actin affinity.

State 4 - Powerstroke: Pi release

Once one of the head docks properly on the actin filament, Pi is released. Pi release strengthen the binding of the MyoII head to actin filaments and trigger the force generating powerstroke that ensures the displacement of both proteins one specific distance. At the end of the powerstroke, ADP is dissociated which allows a new ATP molecule to bind to the MyoII and the cycle starts again.

4.3. MyoII function

MyoII proteins play a role in several fundamental cellular and developmental processes such as tissue morphogenesis, cytokinesis, cell-cell adhesion, cell migration and is also involved in the activation of the autophagy pathway. In this section I will describe certain functions relevant to my work.

4.3.1. Morphogenesis

One of the key mechanisms driving morphogenesis is the generation of contractile forces driven by MyoII motor proteins that will interact with the filaments of actin composing the cell cortex. This drives filament sliding and contraction. Together MyoII and actin form an actomyosin network responsible for the generation of mechanical tension, playing a central role in shaping cells and tissues during morphogenesis (Guillot and Lecuit, 2013; Heer and Martin, 2017; Miao and Blankenship, 2020; Munjal and Lecuit, 2014; Röper, 2013).

Interestingly, actomyosin networks are organized in two main structural types relevant to morphogenesis. These differ significantly in their dynamics, spatial organization, and biological functions: pulsatile flows and supracellular cables. Actomyosin pulsatile flows are highly dynamic, transient and relatively disorganized contractions, characterized by the periodic accumulation and dispersal of both actin and MyoII, often associated with apical cell surfaces within individual cells (Miao and Blankenship, 2020; Munjal and Lecuit, 2014). Highly dynamic pulses of MyoII ensure rapid oscillating activity that mediates lasting changes in cell surfaces through its conserved unidirectional movement along actin filaments, without backtracking. In general, pulsatile actomyosin networks coordinate morphogenetic events through mechanical signaling, driving local shape changes in cells such as apical constriction during *Drosophila* embryonic SGs development mediated by the dynamic MT cytoskeleton (describe more in detail in section 6) (Booth et al., 2014). This process is also involved in other processes such as tissue invagination, symmetry breaking, or cell intercalation. In contrast, actomyosin supracellular cables are continuous, stable and coordinated junctional structures that span across multiple cells (Miao and Blankenship, 2020; Munjal and Lecuit, 2014; Röper, 2013). Therefore, these processes involve the coordination between the cytoskeletons of neighboring cells

forming tension cables over many cells to entire tissues. Actomyosin cables were mainly described during wound healing where certain main cables “actin purse-strings”, formed at the leading edge of the wound boundary. This mediates cell migration and remodeling of adhesive networks necessary for wound closure through mechanical tension (Abreu-Blanco et al., 2012; Miao and Blankenship, 2020; Röper, 2013). These structures also play a role during dorsal closure, tissue folding and boundary formation of different tissues and organisms (Franke et al., 2005; Miao and Blankenship, 2020; Röper, 2013, 2012).

Importantly, in certain cases, both pulsatile actomyosin and supracellular cables collaborate in the same tissues and even in the same cell type in order to remodel and shape tissue morphogenesis. This is the case of *Drosophila* embryos, during the shrinkage of dorsal-ventral-oriented junctions that are firstly produced by the flow of actomyosin pulses from apical cell surfaces toward these junctions (Rauzi et al., 2010).

Cytokinesis

As described above (in section 1.1.1), cytokinesis is the final stage of cell division marking the event of a single cell cytoplasm separation into two daughter cells. A critical player in this process is MyoII which its involvement and localization were described in the 1970’s, following MyoII signal throughout cytokinesis and its importance in maintaining these events (Fujiwara and Pollard, 1977; Mabuchi and Okuno, 1976).

Interestingly, MyoII was noticed to localized first around the equator during late anaphase, setting the point for the ring assembly, marking therefore the site for cleavage furrowing. This process was disrupted in the absence of MyoII (Fujiwara and Pollard, 1977; Mabuchi and Okuno, 1976). Subseqeuntly, many studies described in more detail the essential role and involvement of MyoII during cytokinesis in different organisms (Eggert et al., 2004; Karess et al., 1991; Manstein et al., 1989; Shelton et al., 1999; Takeda et al., 2003). In mitosis, actomyosin accumulates at the equator in order to mark the region from which the contractile ring will be assembled (Cabernard, 2012; Coluccio Lynne M., 2008; D’Avino et al., 2015; Heissler and Manstein, 2013). This localization is controlled by kinesin-6 activity and driven by two cooperative mechanisms that result in a converging actomyosin flow (Dean and Spudich, 2006; Jordan and Canman, 2012; Murthy and Wadsworth, 2005; Piekny et al., 2005; Vale et

al., 2009). First, Rho-dependent activation of MyoII promotes the recruitment of MyoII at the equator and then astral MTs inhibit MyoII recruitment outside of this zone. During cytokinesis, the contractile ring, composed of actomyosin as well as associated regulatory and scaffolding proteins, is formed perpendicular and equatorially at the cell cortex. Then, MyoII uses energy from ATP hydrolysis to move along actin filaments, causing the ring to constrict and generating the contractile force needed to pinch the plasma membrane inward and divide the cytoplasm (Cabernard, 2012; Coluccio Lynne M., 2008; D'Avino et al., 2015; Heissler and Manstein, 2013; Wang, 2005).

4.3.2. Secretion

Another key cellular process influenced by MyoII is secretion, particularly the mechanism of exocytosis, where cells deliver different molecules to the extracellular space (Bhat and Thorn, 2009; Biton et al., 2023; Heissler and Manstein, 2013; Masedunskas et al., 2011; Miklavc et al., 2015; Nightingale et al., 2011; Rousso et al., 2016; Segal et al., 2018). Several studies described the involvement of actomyosin in large secretory vesicles (LSVs) exocytosis, specifying its recruitment once the LSVs fuse with the apical surface in order to extrudes the cargo (Biton et al., 2023; Rousso et al., 2016; Segal et al., 2018; Segawa and Yamashina, 1989; Valentijn et al., 2000).

Drosophila SGs are highly secretory tissues (described in section 6), and several studies highlighted MyoII, or in more detail the actomyosin network, requirement in different steps of vesicle secretion (Biton et al., 2023; Rousso et al., 2016; Segal et al., 2018). For example, adhesive glycoproteins secretion (also known as the glue) starts first by fusion of the Rho1-enriched vesicle containing these cargos to the apical membrane (Rousso et al., 2016; Segal et al., 2018). This fusion activates Rho1, triggering actin-polymerizing activity of formin Diaphanous (Dia) and the recruitment of MyoII (Rousso et al., 2016; Segal et al., 2018). Therefore, Dia will promote the assembly of an actin coat that will recruit the Rho GTPase activating protein (RhoGAP), RhoGAP71E also known as Cumberland GAP (C-GAP) (Segal et al., 2018). This protein will inactivate Rho1, by its conversion from an active GTP-bound to an inactive GDP-bound state (Mason et al., 2016; Sailem et al., 2014; Segal et al., 2018). Finally, inactivated Rho1 results in actin disassembly, a critical aspect of the secretory process as only then the actomyosin-mediated vesicle constriction is achieved (Segal et al., 2018).

4.3.3. Activation of phagophore formation

Interestingly, one recent study revealed an essential role of MyoII in the early stages of autophagy during the initiation and expansion of a double-membrane structure, the phagophore (also known as the isolation membrane). The phagophore is involved in autophagy, which will be described more in detail in section 5) (Tang et al., 2011; Tang and Chen, 2011). In both *Drosophila* fat body cells and mammalian epithelial cells, the serine/threonine kinase Atg1/Ulk1 (*Drosophila*/mammalian) responsible for the induction of autophagy, promotes MyoII activation under starvation conditions. Atg1/Ulk1 phosphorylates and activates a novel myosin light chain kinase, Spaghetti-squash activator “Sqa” in *Drosophila* and zipper-interacting protein kinase “ZIPK” in mammalian cells (Tang et al., 2011; Tang and Chen, 2011). This kinase phosphorylates the RLCs inducing MyoII activation thus promoting its assembly into bipolar filaments and its interaction with actin filaments (Tang et al., 2011; Tang and Chen, 2011). In *Drosophila* fat body cells and mammalian MCF7 cells, MyoII inhibition or depletion of Sqa/ZIPK disrupts autophagosome formation, by clear reduction in their size and number, in response to starvation (Tang et al., 2011; Tang and Chen, 2011). In mammalian cells, the actomyosin network shuttles a membrane protein essential in supplying lipids to forming autophagosomes, Atg9-containing membranes between the trans-Golgi network (TGN) and to the sites of autophagosome nucleation (Tang et al., 2011; Tang and Chen, 2011).

5. Cellular trafficking and secretion

5.1. ESCRT-dependent membrane dynamics

The endosomal sorting complex required for transport - ESCRT machinery is essential for membrane remodeling events including multivesicular bodies (MVBs) formation, cytokinetic abscission, and certain exocytosis processes (Henne et al., 2011; Vietri et al., 2020). The ESCRT pathway consists of five distinct complexes: ESCRTs -0, -I, -II, -III, and vacuolar protein sorting (Vps4) (Figure 20). Each of these complexes is composed of different subunits and their nomenclature is largely conserved between mammals and *Drosophila* (Henne et al., 2011; Vietri et al., 2020).

5.1.1. ESCRT complex composition

ESCRT-0 consists of two subunits, the hepatocyte growth factor regulated tyrosine kinase substrate (HRS) and the signal transducing adaptor molecule (STAM) (Asao et al., 1997; Henne et al., 2011). ESCRT-I was the first ESCRT complex to be described and it consists of four subunits, Vps23 (Tsg101 in mammals), Vps28, Vps37 and multi-vesicular body 12 (Mvb12) (Curtiss et al., 2007; Henne et al., 2011; Katzmann et al., 2001). ESCRT-II is a Y-shaped complex consisting of one subunit of each Vps22 and Vps36, and two subunits of Vps25 (Babst et al., 2002b; Henne et al., 2011). These three complexes are involved in cargo recognition and early sorting.

ESCRT-III is considered the key complex in the ESCRT pathway as it is the complex responsible for membrane remodeling and scission (Eikenes et al., 2015; Henne et al., 2011; Park et al., 2024). This complex consists of four subunits that share the common name of charged multivesicular body protein (CHMP), CHMP6, Shrub (CHMP4 in mammals), CHMP3 and CHMP2. Interestingly, ESCRT-III does not form a stable, cytoplasmic complex as it alternates between an autoinhibited ‘‘closed’’ state and an active “open” state depending on its conformation (Henne et al., 2011; Lata et al., 2008; Park et al., 2024). Mainly, ESCRT-III proteins possess an N-terminal α-helix region rich in positively charged amino acids and a C-terminal α-helix region abundant in negatively charged amino acids. The C-terminal end contains a MT interacting and trafficking domain-interacting motif (MIM), which enables interactions with proteins

containing a MT interacting and trafficking domain (MIT) such as the Vps4 protein (Guo and Xu, 2015; Han et al., 2015). Once these regions interact together, resulting in a folded form of the proteins, they mark the autoinhibited conformation of ESCRT-III. Its activation only occurs when the ESCRT-II subunit Vps25 binds to CHMP6, initiating ESCRT-III recruitment and complex formation upon Shrub homo-oligomerization. Shrub is essential to recruits the ESCRT-III adaptor protein, apoptosis-linked gene-2 interacting protein X (ALIX), which then stabilizes Shrub filaments (Henne et al., 2011; Park et al., 2024). There are several ‘‘accessory’’ ESCRT-III subunits that govern ESCRT-III activity, such as the increased sodium tolerance 1 (Ist1), CHMP1, Vps twenty-associated 1 (Vta1 - LIP5 in mammals), and Vps60 (CHMP5 in mammals) (Henne et al., 2011; Park et al., 2024). Finally, the Vps4 is a multimeric mechanoenzyme, characterized by a class I ATPase associated with various cellular activities ATPase (AAA-ATPase) activity (Adell et al., 2014; Henne et al., 2011; Scott A, 2005).

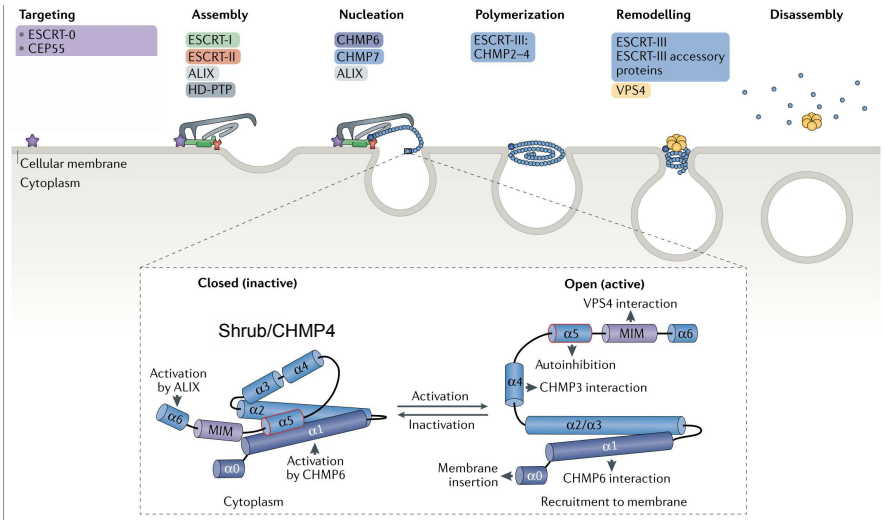


Figure 20. Membrane remodeling promoted by ESCRT complex assembly

Scheme representing all key protein and complexes required for ESCRT- III targeting, nucleation and polymerization during membrane remodeling. Starting by target recognition by ESCRT-0 or CEP55 (in mammals) or Pavarotti (in Drosophila). Then recruitment of ESCRT-I and ESCRT-II serving as a bridge to recruit and connect ESCRT-III to the target with the help of ALIX and other proteins. The interaction with VPS4 promotes ECRT-III activity in membrane scission. Modified from (Vietri et al., 2020).

5.1.2. ESCRT function and pathway

As mentioned above, the ESCRT machinery plays crucial roles in various cellular processes. Each process is accomplished through distinct pathway established by compartment-specific factors that assemble molecular scaffolds to recruit the downstream ESCRT components (Figure 20).

MVB formation process

HRS subunit of the ESCRT-0 identifies and clusters ubiquitinated membrane proteins on endosomes (Babst, 2011). Importantly, ESCRT-III does not directly interact with targeting factors, and therefore relies on bridging or assembly factors to establish this connection. This is the role of ESCRT- I and ESCRT- II in this context. ESCRT-0 recruits ESCRT-I that interacts at opposite ends with both ESCRT-0 and ESCRT-II (Babst et al., 2002b). The coordinated action of these three complexes induces curvature of the endosomal membrane around the ubiquitinated proteins, initiating the formation of intraluminal vesicles (ILVs) (Babst, 2011; Henne et al., 2011; Schöneberg et al., 2016). ESCRT-III, the final complex in the pathway, polymerizes into a filamentous spiral at the neck of the two lipid bilayer sheets, bringing them together, and thereby trapping the cargoes within the ILVs (Babst et al., 2002a; Wollert et al., 2009). Following this assembly, Vps4 is recruited to ESCRT-III through interactions with Vta1 and by binding its N-terminal MIT domain with the C-terminal MIM sequences present in the ESCRT-III subunits. The AAA-ATPase activity of Vps4 then promotes ATP hydrolysis necessary for removal and recycling of ESCRT-III subunits from the membrane, therefore facilitating membrane scission (Adell et al., 2014; Guo and Xu, 2015; Han et al., 2015).

Cytokinesis

In the final stage of cytokinesis, a thin intercellular membrane bridge, known as the midbody, must be severed to allow complete separation of the two daughter cells. This critical step is mediated by several proteins including the centralspindlin protein Pavarotti, and in mammals this process is CEP55 dependent (Lie-Jensen et al., 2019). When ALIX is recruited, a spiral-like structure at the abscission site is assembled, thus mediating Shrub recruitment through interactions with ESCRT-II components (Lie-Jensen et al., 2019). Then, Shrub recruits other ESCRT-III proteins

and polymerizes to form filaments that together with the activity of Vps4 results in a series of rings to construct ESCRT filaments in order to accomplish cytokinetic abscission.

5.2. Rab-mediated secretion

The Rab (Ras-related protein in brain) family of proteins belongs to the Ras superfamily of small GTPase proteins. With approximately 70 Rab proteins identified in humans, grouped into 44 subfamilies, they represent the largest family of small GTPases (Pfeffer, 2017; Pylypenko et al., 2018; Sannerud et al., 2003). This diversity reflects the complexity of membrane trafficking. Rab proteins are small monomeric GTPase of about 20-25 kDa, that contain a conserved globular G-domain of about 180 amino acids characterized by a six-stranded β-sheet flanked by five α-helices (Vetter, 2014).

Rab proteins function as molecular switches, cycling between an active GTP-bound state and an inactive GDP-bound state (Figure 21) (Hutagalung and Novick, 2011; Stenmark, 2009). This cycling is tightly regulated by specific regulatory proteins. The GTPase-activating protein (GAPs) accelerate the hydrolysis of GTP to GDP, converting Rabs to their inactive GDP-bound form. In this state, Rab proteins are cytosolic and in complex with Rab GDP dissociation inhibitor (GDI), which prevents premature membrane association. Reactivation occurs when guanine exchange factors (GEFs) catalyze the GDP-GTP exchange. In this state, Rab proteins are released from GDI and inserted into target membranes. This process is facilitated by geranylgeranyl transferase (GGT), which adds 20-carbon isoprenoid group on one or two C-terminal cysteines of the Rab, promoting its anchoring to the membrane. This cycle starts over with the extraction of the Rab proteins from membranes by GDI binding.

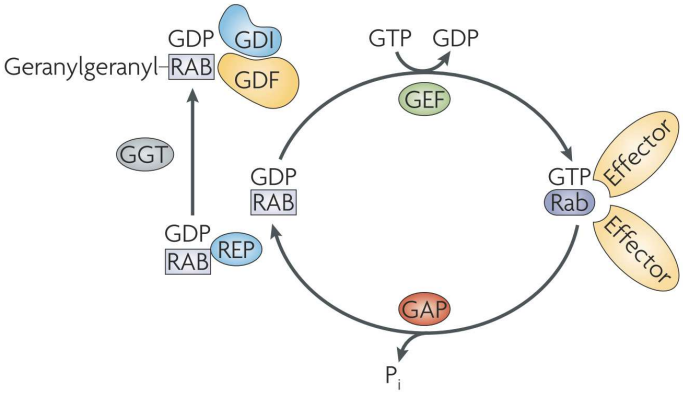


Figure 21. The Rab activation cycle

In the inactive GDP-bound state, Rab is in complex with Rab GDI. Reactivation through the exchange of GDP for GTP, is catalyzed by a GEF protein. The GTP-bound 'active' conformation is recognized by multiple effector proteins and is converted back to the GDP-bound 'inactive' form through hydrolysis of GTP stimulated by GAP. Modified from (Stenmark, 2009).

Interestingly, Rab proteins are key regulators of intracellular membrane trafficking by coordinating various steps including vesicle budding, movement along cytoskeletal tracks, tethering to target membranes as well as membrane fusion (Kasai et al., 2012). Moreover, studies performed in *Drosophila* as well as in other eukaryotes highlighted a conserved function of different Rab proteins in the secretion pathway (Caviglia et al., 2019). Their function is achieved by ensuring that proteins and membranes are accurately delivered to their specific cellular compartments in order to undergo secretion.

I will mention two of these Rab proteins that were used in my PhD work- Rab6 and Rab7. In the *Drosophila* oocyte, Rab6 cooperates with the conserved adaptor protein Bicaudal-D (BicD) to ensure proper delivery of secretory pathway components (Januschke et al., 2007). One of these components is the transforming growth factor β (TGF-β) homolog Gurken, to the plasma membrane marking a crucial step for establishing oocyte polarity (Januschke et al., 2007). In human epithelial cells, Rab6 regulates post-Golgi secretion by mediating exocytosis localization on specific hotspots juxtaposed to focal adhesions, therefore promoting proper protein secretion (Brault et al., 2022; Fourriere et al., 2019).

In *Drosophila* fat body cells, Rab7 can influence secretion by regulating the maturation and fusion of multivesicular endosomes that contribute to exosome-

mediated secretion (Zhou et al., 2023). In other contexts, Rab7 regulates exosomal secretion in different cell type. For example, in MCF-7 cells (a human breast cancer cell line), Rab7 regulates secretion of exosomes containing the cytoplasmic adaptor protein syntenin, and the transmembrane protein, syndecan (Baietti et al., 2012; Hessvik and Llorente, 2018).

5.3. Autophagy

Autophagy is a conserved cellular process by which cells eliminate unwanted cytoplasmic components, such as misfolded proteins or damaged organelles, by delivering them to lysosomes for degradation and recycling. So far, three main types of autophagy have been described: macroautophagy, microautophagy, and chaperone-mediated autophagy (Gohel et al., 2020; Maruzs et al., 2019; McPhee and Baehrecke, 2009). In this section, I am describing and focusing on macroautophagy.

Macroautophagy is the main autophagic pathway by which targeted cytoplasmic constituents are enclosed within double-membrane vesicles known as autophagosomes, before fusing with lysosomes for degradation and recycling (Gohel et al., 2020; Maruzs et al., 2019; McPhee and Baehrecke, 2009). Here, I will refer to macroautophagy with the term autophagy for simplicity.

5.3.1. Molecular mechanisms

Autophagy is mediated by a subset of autophagy-related proteins (ATGs) encoded by the evolutionarily conserved ATG gene family, playing essential and distinct roles through all different stages of the autophagic process (Figure 22) (Gohel et al., 2020; Klionsky et al., 2003; McPhee and Baehrecke, 2009).

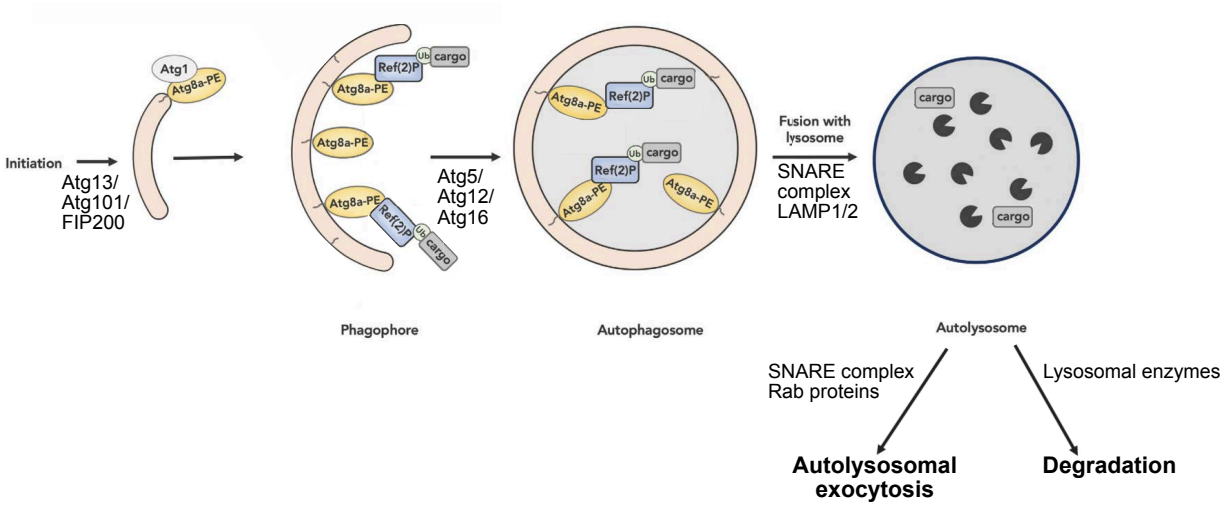


Figure 22. The machinery involved in autophagy

The selective autophagic pathway starts with phagophore formation promoted by Atg1 and other Atg proteins. Atg8a binding to the phagophore membrane, together with a cargo receptor, Ref(2)P for example, allows the capture of the targeted cargo into the phagophore. With the cooperation of different Atg proteins, the phagophore membrane closes forming the autophagosome. With the help of the SNARE complex and LAMP proteins, the autophagosome fuses with a lysosome forming an autolysosome. This cargo is either degraded within the lysosome or transported and exocytosis outside the cell. Exocytosis will rely on SNARE and Rab proteins. Modified from (Gohel et al., 2020).

Induction of autophagy

The primary pathway regulating autophagy induction involves the protein kinase target of rapamycin (TOR) that plays a central role in nutrient sensing (Gohel et al., 2020; Jung et al., 2010; Noda and Ohsumi, 1998; Pattingre et al., 2008). When nutrients are available, TOR is activated via the class I phosphatidylinositol-3-kinase (PI3K) signaling pathway. Active TOR inhibits autophagy by direct directly phosphorylating and repressing a serine/threonine kinase Atg1 (ULK1 in mammals). Under nutrient-deprived conditions, TOR becomes inactivated, relieving its repression of Atg1 and thereby inducing autophagy (Gohel et al., 2020; Jung et al., 2010; Kamada et al., 2010; Pattingre et al., 2008). However, when the autophagic pathway is more selective, it is initiated by cargo recognition independently of nutrient conditions. In this case, selective cargo receptors such as the refractory to sigma P, Ref(2)P (p62 in mammals) recognizes ubiquitinated or tagged substrates and then binds to the light chain 3 (LC3)

family protein Atg8a (Gohel et al., 2020; Jain et al., 2015; Nezis et al., 2008). A scaffold protein, Huntingtin, interacts with Ref(2)P and also mediates autophagy induction by binding Atg1 and releasing it from mTOR inhibition (Gohel et al., 2020; Rui et al., 2015).

Initiation - Phagophore formation

Upon activation, Atg1 assembles into a protein kinase complex with Atg13, Atg101 and the FAK family kinase-interacting protein of 200 kDa, FIP200 (Kamada et al., 2010; Levine and Klionsky, 2004; Mizushima, 2010). This complex promotes the formation of a double membrane structure known as the phagophore or isolation membrane around the cargo, representing the initial step in autophagosome formation.

Elongation - Autophagosome closure

Next, the phagophore starts to elongate around the cargo. The membrane-associated Atg8a is then linked to the phagophore membrane through a process involving two ubiquitin-like conjugation systems, Atg5 and Atg12 (Gohel et al., 2020; Kraft et al., 2012; Levine and Klionsky, 2004; Reid et al., 2022). Subsequently, these two proteins bind Atg16 creating a larger complex that assembles on the outer surface of the phagophore, aiding in phagophore expansion. This complex drives phagophore membrane curvature allowing its eventual closure into a mature autophagosome. After vesicle formation, the complex dissociates and is released into the cytosol.

Fusion with the lysosome - Autolysosome

Once the autophagosome is formed, it must be transported to fuse with the lysosome, forming an autolysosome, in order to deliver its enclosed cargo for recycling (Gohel et al., 2020). This process involves several key protein families. Rab proteins for example, facilitate this step by recruiting effector tethering proteins that help bring the autophagosome closer to the lysosome (Gohel et al., 2020; Hutagalung and Novick, 2011). Fusion of the two membranes is then mediated by the coordinated action of Soluble NSF Attachment Protein Receptor (SNARE) proteins, which form a complex bridging the autophagosome and lysosomal membranes (Gohel et al., 2020; Gu et al., 2019). In addition, a member of the ADP ribosylation factor (Arfs) GTPase family protein, Arl8 is responsible for the proper spatial distribution of lysosomes through its

activity as a lysosomal GTPase (Boda et al., 2019). This distribution plays a critical role in promoting autophagosome-lysosome fusion in fat cells under starvation for example.

Furthermore, the lysosomal-associated membrane protein 1, LAMP1 and its paralog LAMP2 share a common structure comprising a large luminal domain, a single transmembrane domain and a small 11 residues long cytosolic C-terminus tail (Eskelinen, 2006; Huynh et al., 2007). Together, these proteins serve a critical function in the fusion process, since their absence impair Rab proteins recruitment and prevents autolysosome formation.

5.3.2. Outcome of the autophagic pathway

When autophagosomes fuse with lysosomes, their inner membrane and enclosed cargo are broken down by lysosomal enzymes, releasing amino acids, lipids, and carbohydrates, which can then be recycled and reused by the cell.

However, autophagy is not exclusively coupled with cargo degradation. Emerging evidence shows that, autophagy can serve as an “unconventional secretion” pathway that leads to the secretion of cytosolic proteins or the release of enclosed material from the cell, rather than their degradation (Figure 22). This is also known as secretory autophagy (Claude-Taupin et al., 2017; New and Thomas, 2019; Rabouille, 2017; Walter Nickel and Catherine Rabouille, 2009).

Several distinct mechanisms of secretory autophagy have been identified; however, the one I am interested into describing here is through lysosomal exocytosis. This process requires the transport of lysosomes, or autolysosome, to the vicinity of the plasma membrane, where they fuse and release their contents into the extracellular space (Brooks et al., 2012; Claude-Taupin et al., 2017). The fusion step requires the SNARE complex as in classical exocytosis. Specifically, the lysosomal v-SNARE, VAMP7 interacts with different plasma membrane t-SNAREs, such as syntaxins, promoting membrane fusion (Szule and Coorssen, 2003; Vats and Galli, 2022; Verderio et al., 2012). In addition to the SNARE machinery, several Rab proteins, such as Rab27, regulate lysosomal exocytosis by promoting lysosome docking and fusion with the plasma membrane (Shen et al., 2016; Underwood et al., 2020).

6. *Drosophila* Salivary glands

6.1. *Drosophila* as a model system

Drosophila melanogaster, also known as the fruit fly, has been a key model organism in developmental genetics research for over a century. Many characteristics make it an ideal organism for the study of animal development and behavior, neurobiology, and even as a model to understand human genetic diseases.

6.1.1. *Drosophila* genome

The haploid genome of *Drosophila* consists of only four chromosomes: one pair of sex chromosomes (XX or XY for females and males respectively) and three autosomes. Among the autosomes, chromosome 4 is the smallest and is predominantly composed of heterochromatin. In contrast, chromosomes 2 and 3 are large and metacentric, with the centromeres located near the center of two left and right arms, named 2L, 3L and 2R, 3R, respectively (Deng et al., 2007). Importantly, this simplified genome structure facilitates genetic crosses. Despite its small number of chromosomes, the *Drosophila* genome exhibits high gene density and significant homology with the human genome, with nearly 75% of human disease- related genes having functional orthologues in *Drosophila* (Pandey and Nichols, 2011; Yamamoto et al., 2014).

6.1.2. *Drosophila* life cycle

Another advantage of *Drosophila* is its relatively rapid life cycle, from egg fertilization to adult life, that only takes about 10 days at 25°C (Figure 23) (Campos-Ortega, 1986; Hartenstein and Campos-Ortega, 1984).

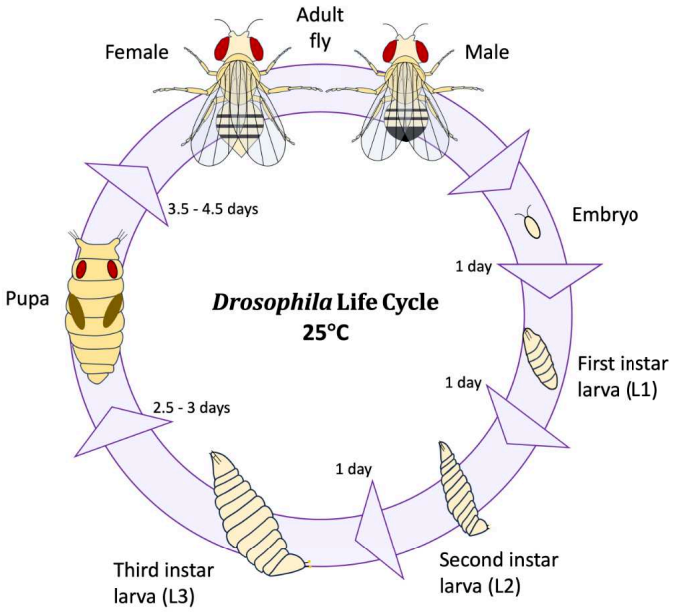


Figure 23. *Drosophila* life cycle at 25°C

The female fly lay an egg that will develop into an embryo after fertilization. After 24 hours, the embryo hatches into a first instar larva (L1). The larva then undergoes two molts, L1 to L2 (~24 h) and L2 to L3 (~24 h). L3 lasts for 3 days before staring pupa stage for 3-4 days until adult fly eclosion.

After fertilization, embryogenesis takes place over a ~20- 24 hour (h) period split into well documented stages of development, where each stage is characterized by different developmental events. Up to stage 4 of development these stages cover synchronized nuclear divisions, resulting in a multinucleated syncytium. This is followed by a cellularization process, where individual cells are formed. During these early stages, the embryo is transcriptionally silent and relies on maternal gene products to support early developmental processes (Laver et al., 2015; Lécuyer et al., 2007; Thomsen et al., 2010). Starting from stage 6, a series of morphogenetic movements begins, starting by a ventral and cephalic furrow formation. At stage 10-11, the embryo is divided into 14 distinct regions known as parasegments (PS), which are specified by a cascade of gene expression and interactions along the anterior-posterior axis. Along the ventral side, a prominent structure called the ventral midline, composed of two rows of elongated cells, extends the length of the embryo. This structure is later internalized and contributes to the formation of the central nervous system (Klämbt et al., 1991). Following this stage, the embryo undergoes a series of

coordinated developmental processes, beginning with organogenesis and germ band (posterior region of the embryo) retraction between stages 11 and 13 (Saunders, 2021). These are followed by key morphogenetic events during stages 14 to 17, including dorsal closure and the internalization of the embryo's head regions, commonly referred to as head involution. After completing embryogenesis, the embryo hatches into its first-instar larval stage (L1), which lasts approximately 24 h, marking the start of active feeding and growth (Fernández-Moreno et al., 2007). The larva then undergoes two molts, L1 to L2 (~24 h) and L2 to L3 (~24 h), each accompanied by shedding of the mouth parts as well as the larval cuticle. The L3 stage lasts about 48-72 h, and during the last ~24 h, the larva enters a wandering stage, during which it stops feeding and starts searching for a site to pupariate. Then the larva is immobile, and its cuticle starts hardening forming a prepupa. The next process, called pupation, is characterized by a new molt and the formation of the pupal case, an external protective layer of the pupa. This stage lasts ~4 days before the adult emerges from the pupal case (Fernández-Moreno et al., 2007).

6.1.3. Genetic tools

UAS-GAL4 system

The UAS-Gal4 system is a powerful genetic approach developed in 1993 that enables spatial and temporal expression or knockdown of specific genes (Brand and Perrimon, 1993). There are two major components of this system: the yeast transcription activator protein Gal4 (driver) and the upstream activating sequence (UAS) (responder), to which the Gal4 specifically binds and activates transcription (Brand and Perrimon, 1993; Fischer et al., 1988). In the driver line, Gal4 is placed downstream of a promoter region for a particular gene that is designed to drive the expression of GAL4 in a tissue-specific manner. However, the responder line carries either a gene of interest, or an RNA interference (RNAi) construct targeted to specific mRNAs, placed downstream of UAS sequences. Crossing two parental lines produces offspring in which Gal4 binds to the UAS region, activating the expression or knockdown of the target gene according to the pattern dictated by the promoter upstream of Gal4.

Due to the separation of the Gal4 driver from the UAS responder in different transgenic lines, the Gal4/UAS system can promote both mis-expression or overexpression of various genes at the same time, using the same promoter.

Balancer Chromosomes

Balancer chromosomes are multiply inverted and rearranged chromosomes widely used in *Drosophila* to suppress crossing over with the homologous chromosome, thus maintaining specific genetic configurations (Crown et al., 2018; Miller et al., 2019; Muller, 1918; Novitski Ani Braver, 1954; Sturtevart, 1921). Common balancer lines such as First Multiple 7 (FM7; X chromosome), Curly of Oster (CyO; II chromosome), and Third Multiple 6 (TM6; III chromosome), were used in my PhD work to maintain mutations and transgenes in a stable heterozygous state (Crown et al., 2018; Miller et al., 2019). Importantly, recessive lethal or sterile mutations are combined with balancers, ensuring that they are not transmitted homozygously and therefore maintain heterozygosity of deleterious mutations in stock populations (Miller et al., 2019). Moreover, certain balancer chromosomes also carry fluorescent tags allowing easy identification of balancer heterozygotes. These are very useful as they are selected for or against, informing on the genotype (Casso et al., 2000; Halfon et al., 2002).

6.2. Salivary glands

Drosophila SGs are paired tubular structures connected to the larval and embryonic mouth via a Y-shaped duct system (Sidor and Röper K., 2016). The proximal region consists of a common duct branching from the pharynx and divides into two individual ducts connected to the secretory tubes. Structurally, SGs originate from a single-layered epithelium surrounding the embryo, the ectoderm, and comprise three distinct cell types: secretory tube cells, duct cells (both common and individual), and imaginal ring cells (Sidor and Röper, 2016). Both secretory and duct cells undergo endoreplication cycles, becoming large and polyploid, while imaginal ring cell nuclei remain small and diploid (Edgar and Orr-Weaver, 2001; Yang and Deng, 2018). In this section, I will present a detailed overview of SGs development from embryonic to adult stages, highlighting its functional roles throughout development.

6.2.1. SG development

During Embryogenesis (Figure 24)

SG primodia specification and placode formation

During stage 10 of embryogenesis, the SG primordia are specified as two groups of approximately 100 cells each, located in the ventral region of PS2. This specification is controlled by the upstream action of the homeotic gene Sex combs reduced (Scr), which is expressed throughout the ectoderm of PS2 but induces SG fate only in ventral cells (Panzer et al., 1992; Riley et al., 1987). The transcription factor Teashirt (Tsh) ensures that Scr expression is confined to PS2 by repressing it in the adjacent PS3 (Taghli-Lamallem et al., 2007). The dorsal-ventral limits of SG formation are further defined by the transcription factor dorsal (dl), which specifies ventral cell fates by repressing the expression of a signaling molecule that specifies dorsal fates, decapentaplegic (dpp) (Irish and Gelbart, 1987; Ray et al., 1991). In the dorsal region of PS2, high dpp signaling blocks SG development, thereby restricting SG fate to the ventral ectoderm where Scr is active and dpp is repressed (Henderson et al., 1999; Isaac and Andrew, 1996; Panzer et al., 1992).

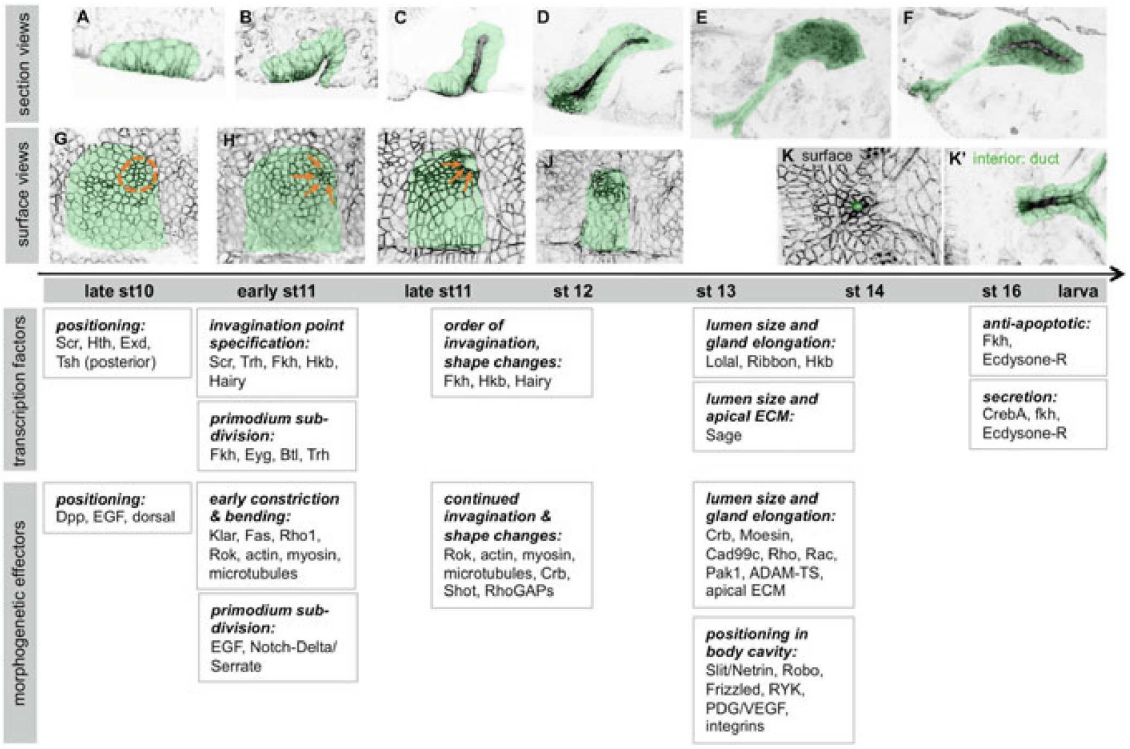


Figure 24. *Drosophila* embryonic SG development

During embryogenesis, SG development starts with placode formation, following apical constriction and tissue invagination and elongation until reaching its final posterior positioning in the embryo. These processes are controlled by different transcription factors throughout embryogenesis (Sidor C. and Röper K., 2016).

The SG primodium is subdivided into three distinct regions, presumptive secretory cells, imaginal ring cells and duct cells. In association with the two broadly expressed transcription factors Extradenticle (Exd) and Homothorax (Hth), Scr promotes the expression of SG specific genes that cooperate in order to promote this subdivision. These include *fork head* (*fkh*), *Cyclic-AMP response element binding protein A* (*crebA*), *Sage, huckebein* (*hkb*), *trachealess* (*trh*), *eyegone* (*eyg*), *dead ringer* (*dri*), *breathless* (*btl*) *and Serrate* (*ser*) (Andrew et al., 2000; Chandrasekaran and Beckendorf, 2003; Haberman et al., 2003; Henderson and Andrew, 2000; Jones et al., 1998; Myat et al., 2000; Panzer et al., 1992). Fkh is essential for initiating SG development and later promotes secretory cell identity while repressing duct fate within the dorsal secretory domain (Myat and Andrew 2000a; Weigel et al., 1969). Simultaneously, ventral EGF signaling suppresses secretory gene expression and inhibits Fkh, enabling the expression of duct specific genes, such as *dri, ser, btl, trh,* and *eyg* (Haberman et al., 2003; Isaac and Andrew, 1996; Jones et al., 1998; Kuo Y. M.; Jones et al., 1996). At the boundary between secretory and duct regions, imaginal ring cells are specified, in a process requiring Ser expression and involving eyg, acting downstream or in parallel, along with Notch signaling (Haberman et al., 2003; Jones et al., 1998). Imaginal ring cells later form the adult gland during metamorphosis. Following the specification of the SG primordium, the epithelium is thickened as cells transition from a cuboidal to a columnar shape, leading to the formation of the SG placode (Myat and Andrew 2000b).

Tissue invagination

At stage 11, a tightly regulated sequence of cellular and molecular events drives tissue invagination, beginning with cell elongation, basal nuclear migration, and localized apical constriction. This constriction begins in the dorso-posterior corner of the placode, where a small group of cells forms the initial invagination pit and then

expands radially, recruiting neighboring cells to bend and form a tube with apically oriented lumen (Sawyer et al., 2010).

As mentioned in section 4, the pulsatile activity of apically enriched actomyosin networks, represent a key mediator of this morphogenetic process. The actomyosin cytoskeleton is organized into a mid-apical meshwork, and its localization and dynamics depend on MTs, which reorient along the apico-basal axis during stage 11 to support contractility and apical tension (Booth et al., 2014). The transmembrane protein Crumbs (Crb), apically enriched in placodal cells, regulates apical membrane size and tissue polarity. Interestingly, Crb anisotropic distribution at the placode border is critical for the positioning of the MyoII activator, Rok, as Crb and downstream modulator regulate Rok residence time by affecting its dissociation rate through phosphorylation (Röper, 2012; Sidor et al., 2020).

The precise positioning of the invagination pit is pre-patterned by the transcription factors Hkb and Fkh. Together, these transcription factors drive the selective activation of downstream morphogenetic modules, initiating localized apical-medial actomyosin contraction at the site of the future pit (Sánchez-Corrales et al., 2021).

Tissue elongation and posterior positioning

As cells internalize through the invagination pit, their apical domains expand again, contributing to lumen formation and growth (Myat MM and Andrew D J, 2002). By late stage 12, all secretory cells are internalized, and the tube extends to contact the circular visceral mesoderm (CVM), which surrounds the developing gut. Contact with the CVM guides the distal gland cells posteriorly, and they migrate to their final position (Bradley et al., 2003; Vining et al., 2005). Simultaneously, the proximal portion of the secretory tube separates from the ectoderm, with individual ducts forming from cells of the posterior ventral primordium. Tube elongation is driven by anisotropic apical expansion along the proximal-distal axis and by convergent extension movements in the proximal region (Myat MM and Andrew D J, 2002).

Centrosome and MT behavior during embryonic development:

Notably, early in SG morphogenesis, placodal cells are the first to complete all embryonic divisions and enter G1 phase, becoming postmitotic (Callaini et al., 1997; Edgar and D, 1989). They then proceed to cycles of endoreduplication giving rise to

polytene chromosomes in larval stages (described in section 1) (Edgar and Orr-Weaver, 2001; Rudkin, 1972). These post-mitotic placodal cells exhibit centrosome asymmetry characterized by differential accumulation of centrosomal proteins such as Cnn, γ-tubulin, Polo kinase, and centrobin (Gillard et al., 2021). This organization leads to an asymmetric MT nucleation capacity; specifically, only the daughter centriole retains the ability to nucleate MTs at the onset of tube formation (Figure 25) (Gillard et al., 2021). Unlike in previous cycles, at the end of the last mitosis, cells inherit two isolated centrioles without associated procentrioles, which is accompanied by a loss of nucleation capacity in the centrobin-poor centrosome, a crucial change for proper morphogenesis (Gillard et al., 2021). MT minus ends are then released by katanin-severing at the active centrosome (Gillard et al., 2021). By the activity of the apical-medial Patronin, MTs are then captured and stabilized, promoting the assembly of a longitudinal MT network essential for apical constriction and SG tube formation (Booth et al., 2014; Gillard et al., 2021).

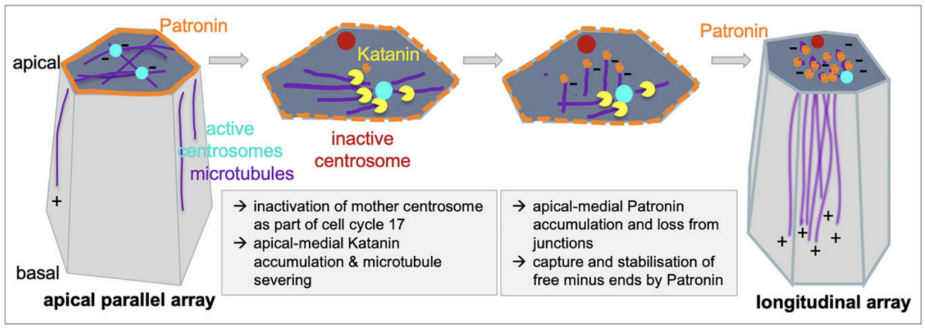


Figure 25. Centrosome and MT behavior in SG cells during early embryogenesis
MTs are nucleated from the active centrosomes in an apical parallel array. Upon inactivation of the Centrobin-depleted centrosome, MT nucleation is restricted to a single centrosome. Apical-medial Katanin accumulation drives MT severing at the active centrosome. This promotes the capture of MT minus-ends by Patronin (localized apically), resulting in a longitudinal MT arrangement (Gillard et al., 2021).

During larval stages (Figure 26)

In L1, SGs are positioned bilaterally beneath the body wall muscles, connected anteriorly to the digestive tract by their ducts, and associated with the fat body along their lobes (Ashburner et al., 1989). At this stage, gland growth occurs primarily by cell volume increase and nuclear enlargement, due to endoreplication, with few vacuoles present within the cells (Edgar and Orr-Weaver, 2001; Urata et al., 1995). In L2, the

glands continue to enlarge, with an increase in the number of vacuoles and the initial appearance of granules. During L3, an anteroposterior gradient in cell size and nuclear volume appears, followed by a progressive accumulation of cytoplasmic granules from anterior to posterior.

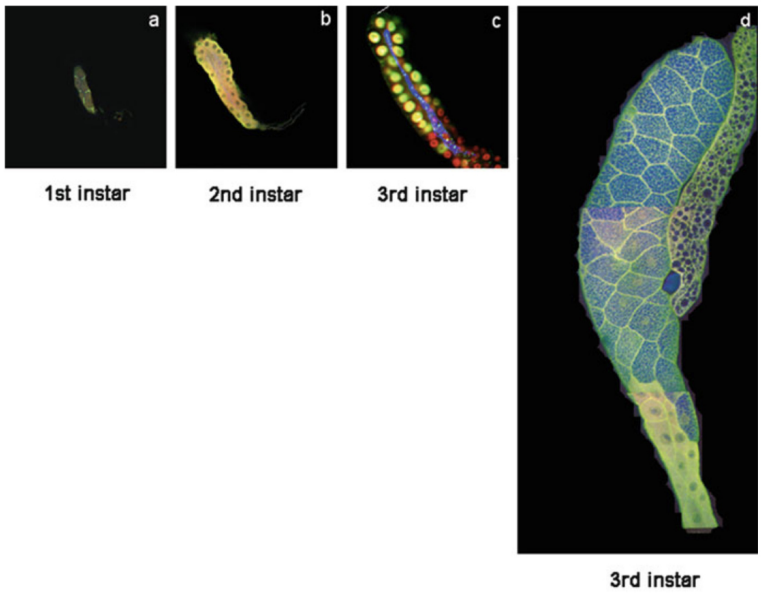


Figure 26. The development of *Drosophila* larval SGs

L1, L2, early and late L3 SGs showing the obvious increase in cell size through development resulting in total tissue size increase (Farkaš, 2016).

When the larva stops feeding, the size of posterior cell nuclei stabilizes while anterior nuclei continue to enlarge, with a continued increase in cell and vacuole volume until pupa formation, where the glands reach their maximum size and polyteny.

During pupation

During early pupal development, most larval SG cells undergo programmed cell death (PCD), leaving only imaginal ring diploid cells that will proliferate and differentiate into adult SGs upon metamorphosis. This PCD is initiated by a pulse of ecdysone, which triggers transcriptional repression of Fkh (Cao et al., 2007; Renault et al., 2001). In addition, the hormone-induced transcription factor E93 plays a crucial role during this process by promoting the expression of pro-apoptotic RHG (reaper, hid, grim) genes (Lam et al., 2022). Prior to the ecdysone pulse, apoptosis is actively inhibited by the Fkh-activated transcription factor Senseless (Sens), which inhibits the proapoptotic genes (Chandrasekaran and Beckendorf, 2003).

During adulthood (Figure 27)

SGs in the adult fly are still poorly studied and their precise function is unclear. All information that we can obtain relates with their structure. Mainly, they form tubes that connect to one another via ducts, that forms a single duct that continues along an appendage, proboscis, found on the head of the fly for olfactory and feeding purposes (Wells and Andrew, 2015). Each adult SG contain three morphologically distinct regions: a coiled distal region, a straight medial region, and a short proximal region (Riparbelli, 1993).

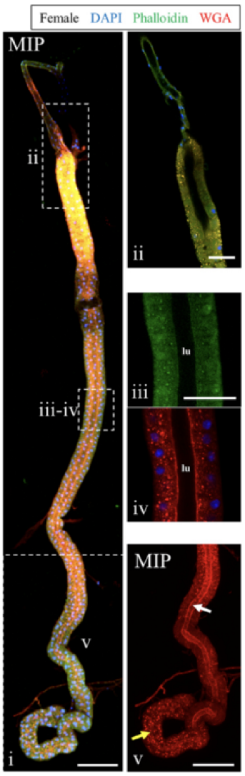


Figure 27. The structure of *Drosophila* adult SGs

Entire female adult SG. Cropped images are shown for the duct/proximal SG (ii), central region (iii and iv), and the distal coiled region (v). The lumen in shown in (iii and iv) with the abreviation "lu". Modified from (Wells and Andrew, 2015).

6.2.2. SG function

SGs are sequentially producing three types of secretions from L3 until the late prepupal stage:

Growth factors

A recent study revealed that SG ablation in *Drosophila* results in reduced pupal volume, reduced wing disc (~50%), fat body cells (~20%), and larval brain (~40%), and reduced adult size, weight, and wing size (Li et al., 2022). This growth delay is related to SG production of a hormone that regulates growth by modulating nutrient-sensing pathways, including insulin/insulin-like growth factor (IIS) signaling and mechanistic target of rapamycin (mTOR). In the larval brain, insulin-producing cells (IPCs) secrete insulin-like peptide 2 (Dilp2), a critical systemic growth regulator. Both Dilp2 release and IIS/mTOR pathway activity are controlled by a SG-derived secreted factor (Sgsf). This factor is secreted into the hemolymph and is essential for normal growth signaling, as mutants lacking Sgsf exhibit reduced Dilp2 expression and decreased IIS/mTOR activity (Li et al., 2022).

Glue proteins

Drosophila SGs are specialized secretory organs that synthesize and secrete glue proteins, called salivary gland secretion (Sgs) proteins, in the second half of L3 to enable the pupa to adhere to a solid surface during metamorphosis (Borne et al., 2020; Farkaš, 2016; Mach et al., 1996).

Glue protein synthesis involves protein folding in the endoplasmic reticulum, glycosylation of certain proteins in the Golgi apparatus, and packaging into secretory granules. These granules, initially about 1μm in diameter, fuse to form mature granules of 3–8μm, with each gland producing about 2,500–3,000 granules (Farkaš, 2016; Ji et al., 2018). Finally, the granules are exocytosed into the lumen in an actomyosin dependent mechanism (described in section 4), and the glue is expelled during pupation.

This intense secretory activity is supported by a highly upregulated secretory machinery, orchestrated by two key transcriptional modules, CrebA and the co-expression of Fkh and Sage. CrebA directly activates genes encoding components of the secretory pathway, and Fkh/Sage together regulate the expression of SG-specific cargo protein proteins and their modifiers (Fox et al., 2013, 2010; Mach et al., 1996).

Apocrine secretion

During prepupal stage, SGs engage in apocrine secretion, a distinct cellular process in which portions of the cytoplasm detach along with the secretory material, resulting in partial cytoplasmic loss (Farkaš et al., 2014). The apocrine mechanism has a crucial role in protecting the organism during this transient developmental phase. Studies have demonstrated that flies deficient in apocrine secretion exhibit significantly reduced survival rates after infection with bacteria, fungi, or yeast (Beňová-Liszeková et al., 2021).

Thesis outlines

This manuscript resumes the experimental findings obtained during my thesis in the laboratory of Renata Basto at the Institut Curie in Paris, France. My work is organized around two main questions presented as a single project in the form of an article containing an abstract, introduction, materials and methods, and discussion in ***Chapter 3 and 4 - Results***.

Further, in ***Chapter 1 - Introduction,*** *I presented* a comprehensive view *of the relevant literature* required to understand this project. In chapter 2, I described the methods used throughout this study. Finally, in ***Chapter 5 - Discussion and Perspectives***, I identify some of the questions raised by this study.

The data provided in ***Chapter 3 - Results*** - originate from a project that aimed to investigate the mechanisms underlying centrosome elimination in programmed polyploid cells while highlighting the main reason promoting this elimination. Polyploidy is a well-known process resulting in the generation of cells containing multiple copies of all chromosomes highlighted by a significant increase in cell size and gaining various functions. Thus, it is interesting to understand and characterize the various changes that the cell undergoes throughout the transition from diploid to a polyploid status. Importantly, one surprising change that occurs in different examples of polyploid cells (especially endoreplicating cells) is centrosome loss. Centrosomes are known as the main MT organizing center (MTOC) that ensure the assembly of a bipolar mitotic spindle during cell division. To analyze these changes in the polyploid background, I used *Drosophila* salivary glands as model system. This tissue undergoes several rounds of endoreplication to achieve high levels of ploidy, with complete loss of centrosomes in early stages of development. However, the mechanism and the reasons underlying this elimination process remain poorly understood. To answer these questions, I used different genetic tools, live imaging approaches, super-resolution microscopy combined with tissue clearing and electron microscopy. These analyses uncover a novel mechanism of centrosome elimination dependent on non-muscle myosin II (MyoII), together with secretory autophagy, autolysosome exocytosis and proteasomal degradation. Further analyzes of the

whole cytoskeleton, revealed that centrosome elimination in salivary gland cells is required from proper mitochondria organization and metabolic activity.
These findings gave rise to a first author article entitled “A novel mechanism for centrosome expulsion ensures metabolic activity in polyploid cells”, submitted in bioRxiv (2025.08.01.668089; doi: https://doi.org/10.1101/2025.08.01.668089).

Chapter 2 – Material and Methods

1. Fly husbandry

1.1. Fly culture

For all experiments performed on larvae, flies were raised in plastic vials containing homemade standard *Drosophila* rich culture medium (0.75% agar, 3.5% organic wheat flour, 5% yeast, 5.5% sugar, 2.5% nipagin, 1% penicillin-streptomycin (Gibco #15140), and 0.4% propanic acid). Fly stocks and experimental crosses were maintained at 22ºC. Stocks were maintained using balancer inverted chromosomes to prevent recombination. In all experiments, larvae were staged to obtain comparable stages of development. Egg collection was performed at 22°C for 24 hours (h). Mid-Late third instar larvae (L3) salivary glands (SGs) were dissected after 7 days of development. Pre-pupae larvae were dissected after 9 days (by choosing immobilized larvae on the wall of the tube).

1.2. Fly stocks

BL = Bloomington Drosophila Stock Center (Indiana University, IN, USA).

Stock Name	Chromosome	Source	Reference
wild-type (WT) - w1118		BL3605	
Driver			
Fkh-Gal4	II	BL78061	(Chandrasekaran and Beckendorf, 2005)
Fluorescent proteins			
Fkh-GFP	II	BL43951	(Sánchez-Corrales et al., 2021)
Sas-4 – GFP	II	Raff lab	(Peel et al., 2007)
MyoII-mCherry (T20S21)	III	Basto lab	This work
iMyoII-mCherry (A20A21)	III	Basto lab	This work
aMyoII-mCherry (E20E21)	III	Basto lab	This work
UAS-CL1-GFP	II	Pandey lab	(McPhee et al., 2013)
UAS-Polo-PACT-GFP	II	Bettencourt-Dias lab	(Pimenta-Marques et al., 2016)
Mutants			
sqh^{1} (*MyoII*^{mut})	X	Karess Lab	(Karess et al., 1991)
atg5^{5cc5} (*atg5*^{mut})	X	BL91419	(Kim et al., 2016)
alix^{1} (*alix*^{mut})	III	BL85211	(Eikenes et al., 2015)
Plk4OE	III	Raff lab	(Basto et al., 2008)
RNAi Lines			
UAS-Syx16-RNAi	III	BL25884	(Csizmadia et al., 2022)
UAS-Rab27-RNAi	III	BL35774	(Corrigan et al., 2014)
UAS-Chmp2b-RNAi	II	BL38375	(Mathieu et al., 2022)
UAS-Shrub-RNAi, UAS-Chmp2b-RNAi	III	Huynh lab (CIRB, Paris, France)	(Eikenes et al., 2015)
UAS-Rab6-RNAi	III	BL35744	(Zhou et al., 2023)
UAS-Rab7-RNAi	III	BL27051	(Zhou et al., 2023)

2. Immunofluorescence experiments

2.1. Immunofluorescence of *Drosophila* SGs whole mount preparations

L3 SGs were dissected in fresh PBS (Phosphate- Buffered Saline 10X, VWR #L182-10) and fixed for 40 minutes (min) at room temperature (RT) in 4% paraformaldehyde (EMS #15710) diluted in PBS. Fixed tissues were washed 3x15min in PBST 0.3% (PBS and 0,3% Triton X-100, Euromedex #2000-C) and incubated for 1h in blocking solution (PBST + 5% normal goat serum (NGS), Gibco #10098792). SGs were washed 3x15min, in PBST 0.3%. For antibody staining, tissues were incubated in primary antibodies at the appropriate dilution in the blocking solution, overnight at 4ºC in a humid chamber. After washes in PBST 0.3% 3x15min, tissues were incubated in secondary antibodies diluted in the blocking solution, protected from light in a humid chamber for 4h at 25°C. Tissues were then washed with PBST 0.3% 3x15min, rinsed in PBS and incubated with DAPI (4′,6-diamidino-2-phenylindole; 1:1000, Thermo Fisher Scientific #D1306), protected from light. SGs were then rinsed in PBS and mounted in clearing solution (Rapiclear 1.49 Sunjin Lab #RC149002).

2.2. Clearing experiment on L3 SGs for microtubule staining

For labelling the microtubule (MT) cytoskeleton, we used a clearing protocol that permeabilizes and improves antibody penetration generating tissues with lower fluorescence background levels. L3 SGs were fixed with 4% paraformaldehyde for 3h on a shaker at RT, then washed with PBS 4x30min. Tissues were transferred into a PBST 2% solution (PBS and 2% Triton X-100) on a shaker for 2h at RT for permeabilization and then washed again with PBS for 4x30min. The solution was changed to a freshly prepared blocking buffer- 10% NGS, 1% Triton X-100, 2.5% DMSO (Sigma #276855) and 0.2% sodium azide (Sigma #71289) in PBS- on a shaker for 24h at 4ºC in a humid chamber. In the following day, primary antibodies were added to the antibody buffer- 1% NGS, 0.2% Triton X-100, 2.5% DMSO and 0.2% sodium azide in PBS. Samples were placed on a shaker for 24h at 4ºC in a humid chamber. Samples were washed with a freshly autoclaved washing buffer- 3% NaCl (Honeywell Research Chemicals #31434) and 0.2% Triton X-100 in PBS- 3x 1h at RT and then

incubated with secondary antibodies also diluted in antibody buffer. Samples were placed on a shaker for 24h at 4ºC in a humid chamber. They were washed again with PBS 4x30min at RT. Tissues were then rinsed in PBS and incubated with DAPI (1:1000) at RT for 1h, rinsed again with PBS and incubated in the clearing solution for 1h before being mounted in the clearing solution.

2.3. Embryo culture and collection

Embryos were collected following ON egg laying on agar apple juice plates (topped with yeast paste) that were made by mixing two autoclaved agar solutions (18g in 600ml distilled water) at 60ºC, with 40g saccharose (Fisher chemicals #S/8600/60) in 400ml apple juice solution, followed by a 20ml of a 20% Nipagine solution (methyl 4 hydroxybenzoate; Sigma #H5501). Embryos were fixed either using formaldehyde or methanol, according to the requirements.

<u>The use of Formaldehyde fixative allows phalloidin labeling.</u>

After collection, embryos were collected with a small amount of detergent solution (PBST 0.05%), and transferred to an Eppendorf before being dechorionated in 50% freshly diluted bleach for 3min, then washed extensively with water and fixed in 2:1 mixture of Heptane and 4% methanol-free formaldehyde (EMS #15686) for 25min and devitellinized in a 50% mix of 90% ethanol (Avantor Sciences #20821.310) and heptane (Dutscher #446951) with vigorous shaking for 30 seconds (sec). Embryos were then rinsed twice with PBT 0.3% and incubated for 1h at 4ºC on a rotator in blocking solution- 0.5% BSA (Euromedex #04-100-812-C) and 0.3% Triton X-100 in PBS. They were then labelled with phalloidin and primary antibodies in the blocking solution, ON at 4ºC with rotation. The next day, embryos were washed with blocking solution 3x30min at RT and secondary antibodies were added to the blocking solution for 3h at RT, protected from light with rotation. Embryos were washed with the blocking solution 3x20min at RT, rinsed twice with PBS, incubated in DAPI (1:1000) for 20min at RT, protected from the light and then mounted in a homemade mounting medium (HMMM) (1.25% n-propyl gallate (Sigma #P3130), 75% glycerol (bidistilled, 99.5%, VWR #24388-295), 23.75% H2O).

For methanol Fixation (used for Lamp1 staining)

Embryos were collected as before. Embryos were transferred into an Eppendorf with 1:1 mixture of heptane and methanol-EGTA solution (heptane, 97% methanol (Honeywell #603-001-00-X) and 3% 0.5M EGTA (Euromedex #1310-B), shaked for 30sec and then the solution was replaced with methanol. Embryos were stored at 4ºC. For labelling, embryos were rehydrated with PBT 0.5% on a rotator 2x15min and then incubated in a blocking solution (5% BSA in PBS) 2x30min at RT on a rotator and incubated with primary antibodies diluted in the following blocking solution (5% BSA in PBST 0.05%), ON on a rotator at 4ºC. The next day, embryos were washed with PBST 0.05% 3x20min at RT and then incubated with secondary antibodies diluted in the same blocking solution for 2h with rotation at RT protected from light. Embryos were then washed for 20min with PBST 0.05% at RT and incubated in DAPI (1:1000) for 20min at RT, protected from light and then mounted in HMMM.

2.4. DNA Fluorescent In Situ Hybridization (FISH)

After fixation with 4% paraformaldehyde for 40min and washed with PBST 0.3% 3x15min, SGs were rinsed 3x in PBS, washed for 5min in 2xSSCT (2X Saline Sodium Citrate (Euromedex #EU0300-A) 0,1% Tween-20 (Sigma Aldrich #P1379), diluted in water, then for another 5min in 2xSSCT/50% formamide (Sigma Aldrich #47671) and transferred in pre-warmed 2xSSCT/50% formamide and pre-hybridized for 3min at 92°C. In the meantime, DNA probes diluted in the Hybridization Buffer (20%dextransulfate (Sigma Aldrich #D8906), 2xSSCT, 50%formamide, 0,5mg/ml salmon DNA sperm (Sigma Aldrich #D1626) were denatured at 92°C. After supernatant removal, SGs were incubated with the probe solutions and hybridized for 5min at 92°C and 5h at 37°C. Samples were rinsed at RT, washed for 10min at 60°C in a 60°C pre-warmed 2xSSCT solution and for another 5min at RT in 2xSSCT. Finally, after rinsing in PBS, SGs were incubated in DAPI (1:1000) for 20min at RT and mounted in HMMM. DNA probes (Sigma-Aldrich) used in this study were designed to recognize sequences localized on chromosome II and III, coupled with Cy3 fluorescent dye (40ng/µl) and Cy5 fluorescent dye (80ng/µl), respectively respectively as described in (Goupil et al., 2022).

3. Primary and secondary antibodies

Antibody	Dilution	Source	Identifier
Primary antibodies			
Guinea pig anti- Sas-4	1/500	Raff J.W. Lab	(Basto et al., 2006)
Rabbit anti- Plp	1/1000	Raff J.W. Lab	(Martinez-Campos et al., 2004)
Guinea pig anti- Cnn	1/500	Raff J.W. Lab	(Lucas and Raff, 2007)
Mouse monoclonal anti-γTub	1/500	Sigma-Aldrich	T5326
Rat monoclonal anti-RFP	1/500	Chromotec	5F8
Chicken polyclonal anti-GFP	1/1000	Abcam	ab13970
Rabbit polyclonal anti-Lamp1	1/250	Abcam	ab30687
Mouse monoclonal anti-ATP5A (15H4C4)	1/100	Abcam	ab14748
Rabbit polyclonal anti-aPKC (C-20)	1/500	Santa-Cruz	sc-216
Mouse monoclonal anti-α-Tubulin	1/500	Sigma	T9026
Rabbit Ub-K48 Recombinant Rabbit Monoclonal Antibody (5Y8J0)	1/200	Invitrogen	MA5-35382
Mouse Ubiquitin monoclonal antibody (P4D1)	1/500	Enzo Life Sciences	BML-PW0930-0100
Rabbit Anti-Myosin Light Chain Antibody, phospho-specific (Ser19)	1/200	EMB millipore	ab3381
Alexa Fluor™ Plus 555 Phalloidin	1/250	Thermo Scientific	A30106
Alexa Fluor™ Plus 647 Phalloidin	1/250	Thermo Scientific	A30107
Secondary antibodies			
Goat anti-Rat IgG (H+L) Cross-Adsorbed Secondary Antibody, Alexa Fluor 546	1/250	Thermo Fisher Scientific	A11081
Goat anti-Mouse IgG (H+L) Highly Cross-Adsorbed Secondary Antibody, Alexa Fluor 546	1/250	Thermo Fisher Scientific	A11030

Goat anti-Guinea Pig IgG (H+L) Highly Cross-Adsorbed Secondary Antibody, Alexa Fluor 488	1/250	Thermo Fisher Scientific	A11073
Goat anti-Rabbit IgG (H+L) Highly Cross-Adsorbed Secondary Antibody, Alexa Fluor 647	1/250	Thermo Fisher Scientific	A21245
Goat anti-Chicken IgY (H+L) Secondary Antibody, Alexa Fluor 488	1/250	Thermo Fisher Scientific	A11039

4. MG-132 treatment for proteasome activity inhibition

L3 SGs were dissected in Schneider's *Drosophila* medium used for live imaging (described above) and incubated for 3h at 25°C in Schneider's medium with MG-132 20 µg/ml (Selleck Chemicals #S2619, diluted in DMSO). Control SGs were incubated for 3h at 25°C in Schneider's medium with DMSO 20 µg/ml. Tissues were washed 3x in PBS and were fixed and stained as described above.

5. SeaHorse Assays

Real-time ATP production rate was measured on a SeaHorse XFPro Analyzer. The day before, the SeaHorse cartridge was hydrated using calibrant (Agilent #100840-000) and placed in an incubator at 25˚C without CO_2. The SeaHorse was also set at 25ºC. The morning of the experiment, L3 SGs were dissected and placed directly in the bottom of a SeaHorse 96-well plate (Agilent #103792-100) containing SeaHorse XF DMEM (Agilent #103575-100) supplemented with 10mM glucose (Agilent #103577-100), 1mM pyruvate (Agilent #103578-100) and 2mM glutamine (Agilent #103579-100). After measuring basal metabolism, a mitochondrial stress test was performed by successive injection of oligomycin 15µM (Sigma-Aldrich #O4876-5MG, stock at 30mM in ethanol) then rotenone 50mM (Sigma-Aldrich #R8875-1G, stock at 50mM in chloroform) and antimycin A 5µM (Sigma-Aldrich #A8674-25MG, stock at 0.5mg/mL in DMSO) combined together for the second injection. For each step, oxygen consumption rate (OCR), and the flux of protons- the extracellular acidification rate (ECAR) was measured during twelve cycles to ensure that steady-state values were reached once the drug had fully penetrated the tissue.

6. Conventional transmission electron microscopy (EM)

L3 SGs were dissected in Schneider's *Drosophila* Medium used for live imaging (described above) and embedded in low-melting agarose (2% w/v, Thermofisher Scientific #16520050). Tissues were fixed in 2.5% glutaraldehyde (EMS, Cat #16120), in Cacodylate buffer 100mM pH 7.2 (EMS, Cat #12300), ON at 4°C and then rinsed 3x/5min in 100mM cacodylate buffer pH 7.2 at RT. Tissues were next incubated in 1%

OsO4 (EMS, Cat #19150), 1.5% potassium ferrocyanure (Sigma #702587) in 100mMcacodylate buffer pH 7.2, 45 min at 4°C. Rinsed again 3x5min in H2O at RT and dehydrated at RT successively 15 min in 40% ethanol, 15 min in 70% ethanol, 15 min in 90% ethanol, 15min in 95% ethanol, 3 x 15min in 100% ethanol, 10 min in acetone. Infiltrate with EMbed 812 (EMbed 812 Embedding Kit, EMS cat #14120) resin successively with EPON 30% for 30min, epon 50 % for 30min, epon 70% for 1h and epon overnight. Samples are then deposited in a flat embedding mold filled with pure epon and set to polymerize for 48h in an oven at 60°C. Then, ultrathin epon sections (70 nm) of SGs were prepared with an ultramicrotome (UCT, Leica Microsystems), and contrasted with uranyle acetate and lead citrate (Delta Microscopies, ref 11300) before observation at an 80 kV transmission electron microscope (Tecnai Spirit G2; Thermo Fisher Scientific) equipped with a 4k CCD camera (Quemesa, Soft Imaging System).

7. Molecular Biology

7.1. Molecular cloning

Three constructs containing the *spaghetti squash (sqh)* gene- here referred to as MyoII- with a m-Cherry in tag in frame at the C-terminus were synthetized and mutagenized by Genescript (Rijswijk, Netherlands). WT MyoII (T20S21) was synthetized from 5' UTR to the residue before the stop codon. The mutant versions were generated using standard procedures. MyoII AA where alanines replaced T20 and S21- inactive MyoII and MyoII EE (constitutively active MyoII), where glutamic acids replaced T20 and S21 sequences in this order: The constructs contained from 5' to 3' the following restriction enzymes: SpeI- MyoII - Linker - mCherry - BamHI -3'. After confirmation of the full-length sequences by Sanger sequencing, 2µg of all constructs were digested for 1h at 37°C with 5U SpeI and 5U BamHI, restriction enzymes (New England Biolabs) with 3 µL Cutsmart Buffer (New England Biolabs) in 30 µL total volume. In parallel, a pBlueScript II SK(+) (PBSK+) vector, containing MyoII endogenous promoter sequence - a kind gift by A. Martin (MIT, Cambridge, USA) (Vasquez et al., 2014)- was also digested for 1h at 37°C with SpeI and BamHI, restriction enzymes. Digestion products were ligated in a 1:3 ratio of vector:insert

diluted in TE (10 mM Tris-HCl, pH 8.0, 1 mM EDTA) buffer in total volume of 5µL, and 5µL of ligation mix (Takara, 6023), for 1h at RT. The ligation mixture was transformed by mixing 2µL of the ligation with 50µl *E. coli* competent cells (Dh5α, NEB 5-alpha competent E.coli, subcloning efficiency, C2988), placed on ice for 30min, then heat shock at 42°C for 30 secs and again on ice for 5 min. 400µL of RT SOC was added to the mixture and incubated on a shaker (250rpm) for 1h at 37°C. This mixture was then spread on pre-warmed LB with the appropriate selection plates and incubated at 37°C ON. The next day, several positive colonies were collected and purified by Miniprep (17106, QIAGEN) based on the kit protocol. Constructs were first verified using restriction profile and subsequently one positive clone was Sanger sequenced by Eurofins Genomics (Ebersberg, Germany).

The WT MyoII, MyoII AA and MyoII EE, including MyoII sequences were then inserted in a P[acman] plasmid. P[acman] and all MyoII constructs were digested with AscI and NotI restriction enzymes (New England Biolabs) for 1h at 37°C, ligated in a 1:6 ratio of vector:insert for 1h at RT. The ligation products were used to transform TransforMax EPI300 *E. coli* (C300C105, Epicentre). The P[acman] vectors were purified from several clones and insert presence was tested by restriction enzyme digestion with AscI and NotI enzymes. One clone was used to generate transgenic flies by PhiC31 integrase-mediated transgenesis on ChIII- insertion site- 9750 by BestGene (CA, United States).

7.2. Synthetized/mutagenized sequences:

7.2.1. For WT MyoII-mCherry:

SpeI – WT MyoII (**Phosphorylation site**) - **Linker** - mCherry - **BamHI**

ACTAGTGCCACCAGCTCCATAGGCCGGCTCCATTTAGCTCCATTAACCGCATCA
GAACCACCAATCCAACAGCAACCATGTCATCCCGTAAGACCGCCGGACGTCGC
GCCACCACCAAGAAGCGCGCCCAACGCGCC**ACCTCC**AATGTGTTCGCCATGTT
CGATCAGGCGCAGATTGCCGAGTTCAAGGAGGCATTCAACATGATCGACCAGA
ACCGTGATGGCTTCGTCGAGAAGGAGGATCTGCACGACATGCTGGCCTCGCTG
GGCAAGAACCCAACGGACGACTATCTCGATGGCATGATGAACGAAGCGCCCG
GACCCATCAACTTCACCATGTTCCTCACGCTCTTCGGCGAGCGGCTGCAGGGC
ACCGATCCCGAGGATGTGATCAAGAACGCCTTCGGCTGCTTCGACGAGGAGAA

TATGGGCGTCCTGCCCGAGGATCGTCTGAGGGAGCTGCTGACCACCATGGGT
GATCGGTTCACAGACGAGGATGTATGTTGTCAAGTTGTTTACGATATCAAGTCG
GAGTGTGCCCTTACAACTTCTTTTCCATTTACATTCACAGGTGGACGAGATGTAT
CGGGAGGCGCCCATCAAGAACGGTCTGTTCGACTACCTCGAATTCACGCGCAT
CCTTAAGCACGGTGCCAAGGACAAGGATGAGCAGGTCGACGGTATCGATGTCG
CCACC**ggaggcacgggaggcacc**atggtgagcaagggcgaggaggataacatggccatcatcaaggagtt
catgcgcttcaaggtgcacatggagggctccgtgaacggccacgagttcgagatcgagggcgagggcgagggcc
gcccctacgagggcacccagaccgccaagctgaaggtgaccaagggtggcccctgcccttcgcctgggacatcc
tgtcccctcagttcatgtacggctccaaggcctacgtgaagcaccccgccgacatccccgactacttgaagctgtcctt
ccccgagggcttcaagtgggagcgcgtgatgaacttcgaggacggcggcgtggtgaccgtgacccaggactcctc
cctgcaggacggcgagttcatctacaaggtgaagctgcgcggcaccaacttcccctccgacggccccgtaatgcag
aagaagaccatgggctgggaggcctcctccgagcggatgtaccccgaggacggcgccctgaagggcgagatca
agcagaggctgaagctgaaggacggcggccactacgacgctgaggtcaagaccacctacaaggccaagaagc
ccgtgcagctgcccggcgcctacaacgtcaacatcaagttggacatcacctcccacaacgaggactacaccatcgt
ggaacagtacgaacgcgccgagggccgccactccaccggcggcatggacgagctgtacaagCATTCGTAG
AATTG**GGATCC**

7.2.2. For MyoII AA - mCherry: (Inactive MyoII - iMyoII)

SpeI – MyoII “AA” (**Phosphorylation site**) - **Linker** - mCherry - **BamHI**

ACTAGTGCCACCAGCTCCATAGGCCGGCTCCATTTAGCTCCATTAACCGCATCA
GAACCACCAATCCAACAGCAACCATGTCATCCCGTAAGACCGCCGGACGTCGC
GCCACCACCAAGAAGCGCGCCCAACGCGCC**GCCGCC**AATGTGTTCGCCATGT
TCGATCAGGCGCAGATTGCCGAGTTCAAGGAGGCATTCAACATGATCGACCAG
AACCGTGATGGCTTCGTCGAGAAGGAGGATCTGCACGACATGCTGGCCTCGCT
GGGCAAGAACCCAACGGACGACTATCTCGATGGCATGATGAACGAAGCGCCC
GGACCCATCAACTTCACCATGTTCCTCACGCTCTTCGGCGAGCGGCTGCAGGG
CACCGATCCCGAGGATGTGATCAAGAACGCCTTCGGCTGCTTCGACGAGGAGA
ATATGGGCGTCCTGCCCGAGGATCGTCTGAGGGAGCTGCTGACCACCATGGG
TGATCGGTTCACAGACGAGGATGTATGTTGTCAAGTTGTTTACGATATCAAGTC
GGAGTGTGCCCTTACAACTTCTTTTCCATTTACATTCACAGGTGGACGAGATGT
ATCGGGAGGCGCCCATCAAGAACGGTCTGTTCGACTACCTCGAATTCACGCGC
ATCCTTAAGCACGGTGCCAAGGACAAGGATGAGCAGGTCGACGGTATCGATGT
CGCCACC**ggaggcacgggaggcacc**atggtgagcaagggcgaggaggataacatggccatcatcaagg

agttcatgcgcttcaaggtgcacatggagggctccgtgaacggccacgagttcgagatcgagggcgagggcgagg
gccgcccctacgagggcacccagaccgccaagctgaaggtgaccaagggtggcccccctgcccttcgcctgggac
atcctgtcccctcagttcatgtacggctccaaggcctacgtgaagcaccccgccgacatccccgactacttgaagctgt
ccttccccgagggcttcaagtgggagcgcgtgatgaacttcgaggacggcggcgtggtgaccgtgacccaggactc
ctccctgcaggacggcgagttcatctacaaggtgaagctgcgcggcaccaacttcccctccgacggccccgtaatgc
agaagaagaccatgggctgggaggcctcctccgagcggatgtaccccgaggacggcgccctgaagggcgagat
caagcagaggctgaagctgaaggacggcggccactacgacgctgaggtcaagaccacctacaaggccaagaa
gcccgtgcagctgcccggcgcctacaacgtcaacatcaagttggacatcacctcccacaacgaggactacaccatc
gtggaacagtacgaacgcgccgagggccgccactccaccggcggcatggacgagctgtacaagCATTCGT
AGAATTG**GGATCC**

7.2.3. For MyoII EE - mCherry: (Constitutively active MyoII - aMyoII)

SpeI – MyoII “EE” (**Phosphorylation site**) - Linker - mCherry - **BamHI**

ACTAGTGCCACCAGCTCCATAGGCCGGCTCCATTTAGCTCCATTAACCGCATCA
GAACCACCAATCCAACAGCAACCATGTCATCCCGTAAGACCGCCGGACGTCGC
GCCACCACCAAGAAGCGCGCCCAACGCGCC**GAGGAG**AATGTGTTCGCCATGT
TCGATCAGGCGCAGATTGCCGAGTTCAAGGAGGCATTCAACATGATCGACCAG
AACCGTGATGGCTTCGTCGAGAAGGAGGATCTGCACGACATGCTGGCCTCGCT
GGGCAAGAACCCAACGGACGACTATCTCGATGGCATGATGAACGAAGCGCCC
GGACCCATCAACTTCACCATGTTCCTCACGCTCTTCGGCGAGCGGCTGCAGGG
CACCGATCCCGAGGATGTGATCAAGAACGCCTTCGGCTGCTTCGACGAGGAGA
ATATGGGCGTCCTGCCCGAGGATCGTCTGAGGGAGCTGCTGACCACCATGGG
TGATCGGTTCACAGACGAGGATGTATGTTGTCAAGTTGTTTACGATATCAAGTC
GGAGTGTGCCCTTACAACTTCTTTTCCATTTACATTCACAGGTGGACGAGATGT
ATCGGGAGGCGCCCATCAAGAACGGTCTGTTCGACTACCTCGAATTCACGCGC
ATCCTTAAGCACGGTGCCAAGGACAAGGATGAGCAGGTCGACGGTATCGATGT
CGCCACC**ggaggcacgggaggcacc**atggtgagcaagggcgaggaggataacatggccatcatcaagg
agttcatgcgcttcaaggtgcacatggagggctccgtgaacggccacgagttcgagatcgagggcgagggcgagg
gccgcccctacgagggcacccagaccgccaagctgaaggtgaccaagggtggcccccctgcccttcgcctgggac
atcctgtcccctcagttcatgtacggctccaaggcctacgtgaagcaccccgccgacatccccgactacttgaagctgt
ccttccccgagggcttcaagtgggagcgcgtgatgaacttcgaggacggcggcgtggtgaccgtgacccaggactc
ctccctgcaggacggcgagttcatctacaaggtgaagctgcgcggcaccaacttcccctccgacggccccgtaatgc
agaagaagaccatgggctgggaggcctcctccgagcggatgtaccccgaggacggcgccctgaagggcgagat

caagcagaggctgaagctgaaggacggcggccactacgacgctgaggtcaagaccacctacaaggccaagaa
gcccgtgcagctgcccggcgcctacaacgtcaacatcaagttggacatcacctcccacaacgaggactacaccatc
gtggaacagtacgaacgcgccgagggccgccactccaccggcggcatggacgagctgtacaagCATTCGT
AGAATTG**GGATCC**

8. Live imaging of *Drosophila* embryos

A glue solution containing double side sticking tape diluted in heptane was prepared with rotation. The glue solution was then spread on a on a glass-bottom 35 mm dish (MatTek Corporation #P35G-1.5-14-C) and once dried, embryos were placed on the plate and rolled on the glue, to remove the chorion. Subsequently, embryos were positioned ventrally, facilitating visualization of SGs. Embryos were covered with oil 10S Voltalef (VWR BDH Prolabo). Images were acquired with 100x/1.4 NA oil objective, at time intervals of 30 sec and 20 to 40 Z-stacks of 0.2µm.

9. Image acquisition and analysis

Image analysis and quantifications were performed using Image J software V2.1.0/1.53c, and Imaris software v.9.8.2 (Bitplane, RRID:SCR_007370).

9.1. L3 SGs Image acquisition and super-resolution

L3 SGs images were acquired using a Nikon Ti2-E fully motorized inverted microscope equipped with a 40x/1.3 NA and 100×/1.4 NA Plan-Apochromat oil immersion objectives and a Prime95B sCMOS camera (Teledyne Photometrics). Optical sectioning was performed via a Nano-Z500 piezoelectric stage (Mad City Labs). Excitation was provided by a laser combiner (Gataca Systems) comprising 405, 491, 561, and 642 nm laser diodes (150 mW each), coupled to a Yokogawa W1 spinning disk confocal head through a single-mode fiber. Multi-dimensional image acquisition was carried out in streaming mode using MetaMorph software (version 7.10.5, Molecular Devices). For super-resolution imaging, the Live SR module (Gataca Systems) was used in conjunction with the W1 spinning disk system. This module is based on structured illumination with the optical reassignment technique and online

processing leading to a two-time resolution improvement. The method called multifocal SIM (MSIM) allows combining the doubling resolution together with the physical optical sectioning of confocal microscopy. Acquired images were processed and reconstructed using Gataca's proprietary software integrated within the MetaMorph environment.

9.2. Embryonic SGs Images acquisition

Images from embryos were acquired using a Nikon Ti2-E fully motorized inverted microscope equipped with the Nikon AXR line scanning confocal and 20x/0.8 NA and 60x/1.42 NA objectives. Optical sectioning was performed via a NanoScan SP Z 600um piezoelectric stage (Prior). Excitation was provided by Nikon laser combiner comprising 405, 488, 561, and 640 nm laser diodes (150 mW each). Multi-dimensional image acquisition was carried by resonant scanner with NIS software (version 6.10.01 (Build 2027) Patch 01, Nikon). Acquired images were processed by the "Denoise.ai" module of Nikon.

9.3. Imaris

For the 3D reconstruction, images were converted in Imaris files using ImarisFileConverter 9.9.1 (Bitplane, RRID:SCR_007370). Then, images were imported into Imaris software v.9.8.2 (Bitplane, RRID:SCR_007370). 3D views were generated using Imaris software with surface module and saved as TIFF and mp4.

9.4. Analysis

9.4.1. Quantification of the frequency of events

Image analysis and quantifications were performed using Fiji software. Centrosomes in the embryonic SGs, were manually counted following the signal of Sas-4 and their localization was manually determined and confirmed by 3D reconstructions. Centrosomes were classified as being positioned in the cell, at the apical membrane (when in close proximity with the apical membrane) or in the lumen.

In L3 SGs, the number of cells with or without centrosomes was counted manually by identifying centrosomes using two centrosomal markers (Plp and Sas-4).

9.4.2. Characterization of centrosomes in L3 SGs

To quantify the presence/absence or distribution of centrosomes in the SG lumen, a max projection was performed on all slices comprising the lumen. The luminal region was selected using the polygon selection tool. On both Sas-4 and Plp channels, centrosomes were identified, and their surface area was measured using the 3D object counter mode with adjusted threshold. For the centrosomes that were localized around or near the lumen in Rab27-RNAi and Syx16-RNAi conditions, a max projection was generated as before. Then, using the line tool, the area around the lumen was selected and the fluorescence mean intensity was measured for both centrosomal markers (Plp and Sas-4).

9.4.3. Mitochondria characterization

From immunostained data

SG cells were cropped using a macro adapted from Anne-Sophie Mace, a research engineer at the Institut PICT platform. The macro selected the center plane of the cell, and mitochondria were identified using the analyze particle module on Fiji. Parameters like area, circularity and solidity (two indices informing on object circularity and invaginations, respectively) were obtained with the measurement tool from ImageJ.

From EM data

Mitochondria were identified in EM images based on their typical structure. Using the polygon selection tool and the measurement tool from ImageJ, parameters like area, circularity and solidity were obtained.

9.4.4. Ubiquitin fluorescence signal quantification

Centrosomes were identified either in the cell (*MyoII*^{mut}) or in the Lumen of WT SGs, with two centrosome markers (Plp and Sas-4). Each centrosome was selected using

the polygon selection tool, and the mean intensity of both ubiquitin markers was measured.

9.4.5. Statistical analysis

The statistical significance was calculated using GraphPad Prism (RRID:SCR_002798) version 7 for Mac, GraphPad Software, La Jolla California USA, www.graphpad.com. The statistical test used for each experiment is indicated in the figure legends. Each representative image originates from the analyzed dataset and are representative of the associated quantifications.

Chapter 3 - Results

A novel mechanism for centrosome expulsion ensures metabolic activity in polyploid cells

Riham Salame[1], Simon Gemble[1], Anthony Simon[1], Lin Jawish[1], Anne-Sophie Mace[2] Ptissam Bergman[3], Graca Raposo[3], Clotilde Cadart[4], and Renata Basto[1, *]

1- Biology of Centrosomes and Genetic Instability lab, Institut Curie, Centre National de la Recherche Scientifique (CNRS) Unité Mixte de Recherche 144 (UMR144), Université Paris Sciences et Lettres (PSL Research University), Paris, France.
2- Cell and Tissue Imaging Facility (PICT-IBiSA), Institut Curie,CNRS UMR144 PSL Research University, Paris, France.
3- Structure and Membrane Compartments lab, Institut Curie, CNRS UMR144, PSL Research University, Paris, France.
4- Université Paris Cité, CNRS, Inserm, Institut Cochin, F-75014 Paris, France.

* Corresponding author: renata.basto@curie.fr

1. Abstract:

Programmed polyploidy is often linked to increase cell size to support enhanced metabolism, barrier function or regeneration. In certain polyploid cells, the cytoskeleton is drastically remodeled- most notably by eliminating centrosomes. However, the purpose and mechanisms underlying centrosome elimination have remained unclear. We investigated this question in *Drosophila* acentrosomal salivary glands (SGs), a physiological polyploid model where cells reach high chromosome content through endoreplication. Using genetic tools, live imaging approaches, super-resolution microscopy combined with tissue clearing and electron microscopy, our study uncovers a novel centrosome elimination pathway *in vivo*. This process requires non-muscle myosin II (MyoII) activity and the macroautophagic machinery to drive centrosome release into the lumen via autolysosomal exocytosis. Failure to eliminate centrosomes disrupts the mitochondria network, impairing respiration and ATP production. Our findings reveal a previously unknown mechanism that removes centrosomes through the secretory autophagy pathway to protect mitochondrial function and support the high metabolic demands of polyploid cells.

2. Introduction

Centrosomes are the main microtubule (MTs) organizing centers (MTOC) of animal cells, with key roles in polarity establishment, cell migration and cell division (Conduit et al., 2015). Each centrosome contains two centrioles that recruit and organize the pericentriolar material (PCM), which is the site for MT nucleation (Ibrahim et al., 2009; Paintrand et al., 1992). Most cycling cells maintain stable centrosomes numbers through the tight control of the centriole duplication machinery along the cell cycle (Fu et al., 2015; Sullenberger and Loncarek, 2022). Moreover, surveillance mechanisms discard cells with abnormal centrosome number. Differentiated cells, such as neurons keep centrosomes, even if MTs are nucleated from alternative MTOCs, whereas multiciliated cells, massively amplify centrioles to be able to grow multiple cilia (Brooks and Wallingford, 2014; Petry and Vale, 2015; Spassky and Meunier, 2017). In most animal oocytes, centrosomes are eliminated before fertilization (Borrego-Pinto et al., 2016; Kalbfuss and Gönczy, 2023a; Pierron et al., 2023; Pimenta-Marques et al., 2016; Zhang et al., 2004). All these examples relate to diploid/haploid cells that through differentiation pause the cell cycle in G0 or G1.

Polyploid cells contain more than two sets of all chromosomes. Physiological polyploidy is associated with cell size increase and increase in metabolic capacity, barrier function or even regeneration (Orr-Weaver, 2015; Øvrebø and Edgar, 2018). Interestingly, many polyploid cells generated through endoreplication, such as *Drosophila* salivary glands, ring gland cells or cells from the fat body do not contain centrosomes (Kalbfuss and Gönczy, 2023a; Sun et al., 2019; Zheng et al., 2020). This is also the case of *Drosophil*a and mammalian muscle cells, which are multinucleated, but in this case formed through cell fusion (Kalbfuss and Gönczy, 2023a; Przybylski, 1971). Why and how certain polyploid cells lose their centrosomes is unknow. Here we investigated the mechanisms involved in centrosome elimination in *Drosophila* salivary gland (SG) polyploid cells. These are highly secretory tissues, which undergo up to 10 rounds of endoreplication generating cells with 1024C-2048C (C-value representing the DNA content in the haploid genome) with the chromosomes attached one to another - polytene chromosomes (Edgar and Orr-Weaver, 2001; Hammond and Laird, 1985; Pierce et al., 2004). We found that during embryogenesis, centrosomes are released into the lumen in a process dependent on non-muscle myosin II (MyoII)

activity and autolysosomal exocytosis, to be subsequently targeted for degradation by the proteasome. Strikingly, our work shows that if centrosomes are maintained in SG cells, the mitochondrial network appears fragmented, and cells display reduced oxygen consumption rates. This study provides a direct link between centrosome elimination in programmed polyploid cells and metabolic processes essential for their function and homeostasis.

3. Results

3.1. Centrosomes are released into the salivary gland lumen during embryonic development

To investigate the steps involved in centrosome elimination in polyploid cells from *Drosophila* salivary glands (SGs), we analyzed embryonic development after stage 10, when SG cells are specified (Booth et al., 2014; Gillard et al., 2021). In crowded wild type (WT) embryos, SGs were identified using an endogenous GFP tagged version of the transcription factor fork-head (Fkh) (Monn Monn Myat and Deborah J. Andrew, 2000; Sánchez-Corrales et al., 2021; Wcigel et al., 1989). Using antibodies that recognize the centriole and PCM proteins, Sas-4 and Pericentrin-like protein (Plp), respectively (Figure 1A-D, Supplementary Figure 1A), two centrosomes per cell were seen (Figure 1A and 1E) at stage 10, when the SG placode is formed (Booth et al., 2014; Gillard et al., 2021; Martinez-Campos et al., 2004; Peel et al., 2007). Around stage 11-12, when SG cells start to invaginate, due to apical constriction induced by actomyosin contraction (Abrams et al., 2003; Booth et al., 2014; Gillard et al., 2021), around 50% of the centrosomes were localized in close proximity to the apical membrane (Figure 1B and 1E). During stages 13-14, the SG secretory cells start to posteriorly elongate, forming a tube-like structure with a lumen (Abrams et al., 2003; Booth et al., 2014). At this stage, certain centrosomes could be noticed positioned in the lumen (Figure 1C and 1E) and at the later stages 15-17, the frequency of centrosomes in the lumen increased (Figure 1D-E).

These observations suggest that centrosomes translocate from the cell to the lumen of the SG, in a process that remains to be understood. Using time-lapse microscopy, we followed the dynamics of centrosomes in embryos expressing Sas-4-

GFP (Peel et al., 2007) and the regulatory light chain of non-muscle myosin II (NMMyoII) - Spaghetti squash (Jordan and Karess, 1997; Karess et al., 1991) fused to mCherry (MyoII-mCh) to label cell boundaries and the lumen border. Strikingly, centrosomes were seen lingering around the apical membrane in an erratic movement before being transported into the lumen (Figure 1F and Supplementary movie1).

The MyoII-mCh signals were relatively low and due to loss of the signal, we could only film for short periods of time. We also followed actin behavior using the LifeActin-RFP (Lu et al., 2021) reporter line, but the combination with Sas-4-GFP was not viable. We therefore labelled embryos with phalloidin to label actin and phospho-myosin (p-MyoII) antibodies, which reveal active MyoII. Analysis of actin vesicles positioned at the apical membrane of stage 15 embryos containing centrosomes showed that 50% displayed p-MyoII signals (Supplementary Figure 1B). Taking together, these results show that centrosomes are transported from SG cells to the lumen, in an expulsion trajectory using vesicles enriched with actin and active MyoII.

3.2. Centrosome expulsion depends on MyoII activity

To functionally test whether MyoII is involved in centrosome release into the SG lumen, we used a hypomorphic mutation in *spaghetti squash* (*sqh*^{mut}, here referred to as *MyoII*^{mut}) (Karess et al., 1991). Strikingly, *MyoII*^{mut} embryos at later developmental stages, contained centrosomes in SG cells and only a minor fraction was detected in the lumen (Figure 1G-H). Using three-dimensional (3D) reconstructions, the difference in luminal centrosome number was obvious between WT and *MyoII*^{mut} (Supplementary movies 2-3). Further, analysis of *MyoII*^{mut} SGs, showed that centrosomes were localized close to the apical membrane (Figure 1H), suggesting that their positioning at this location is independent of MyoII.

Unexpectedly, careful analysis of *MyoII*^{mut} SGs showed an increase in total centrosome number, when compared to WT SGs (Figure 1I). These observations, suggest that when centrosomes do not undergo their programmed elimination, through expulsion towards the lumen, they continue to duplicate throughout embryonic SG development, leading to centrosome amplification.

A prediction from the findings described above is that *MyoII*^{mut} SG cells at later developmental stages should contain centrosomes, while WT SGs should not. We analyzed both WT and *MyoII*^{mut} SGs, from third instar larval stages (L3) (Figure 2A

and Supplementary Figure 2A), labelled with different centrosome markers (Supplementary Figure 1D-F). As expected, in WT SGs, centrosomes were absent from SG cells, while they could still be noticed in the lumen (Figures 2B-C, Supplementary Figures 2B-D). In contrast, in *MyoII*^{mut} SGs, multiple centrosomes were readily identified in the large majority of SG cells (Figures 2B-C), while the lumen only occasionally contained centrosomes (Supplementary Figures 2B-C). We confirmed that the centrosomes present in SG cells, contained the canonical centriolar structures (Figure 2D) using an optically demodulated structured illumination technique (SIM) as described in (Fu and Glover, 2012).

While characterizing *MyoII*^{mut} SGs, we noticed a clear reduction in cell and nuclear size (Supplementary Figure 3A), suggesting defects in ploidy level, which were further confirmed by Fluorescent *in situ* Hybridization (FISH) (Supplementary Figure 3B-D). The decreased ploidy levels and cell growth suggest a role for MyoII in key cellular functions that are essential during SG development. To investigate if these unknow functions could contribute to the defects in centrosome elimination, we generated transgenic fly lines expressing MyoII under the control of its own promoter to avoid over-expressing conditions. Expression of WT MyoII and inactive MyoII (iMyoII), a MyoII mutant form that cannot be phosphorylated due to alanine substitutions at the phosphorylation site (A20A21 to replace T20S21) (Jordan and Karess, 1997), was analyzed in the *MyoII*^{mut} background. Cell and nuclear size defects were rescued to values comparable to WT SGs in both WT MyoII and iMyoII (Supplementary Figure 3A). However, while WT MyoII SGs displayed an impressive decrease in the number of cells containing centrosomes, SGs expressing iMyoII, maintained centrosomes (Figures 2B-C). Both WT MyoII and iMyoII SGs presented centrosomes in the lumen, even though at a decreased frequency in iMyoII compared to WT SGs (Supplementary Figure 2B-C). These data show that MyoII activity is required to promote centrosome expulsion from SG cells. Moreover, they show that failure to remove centrosomes from SG cells leads to centrosome amplification.

3.3. Centrosome release into the SG lumen does not require loss of Polo kinase activity

In *Drosophila* female oocytes, centrosome elimination occurs in a stepwise manner and depends on PCM removal in a Polo (Polo-like kinase 1)- loss dependent manner

(Pimenta-Marques et al., 2016). We tested the possible involvement of this mechanism in releasing centrosomes towards the SG lumen. Expression of Polo fused to the centriole targeting domain PACT (Polo-PACT), which inhibits PCM removal (Pimenta-Marques et al., 2016), did not perturb centrosome expulsion (Supplementary Figure 3E-G). We concluded that the same mechanism is not involved in favoring centrosome elimination through expulsion in SG polyploid cells.

3.4. Increasing MyoII activity can overcome the presence of extra centrosomes in SG cells

To test if increasing MyoII activity can overcome defects in centrosome expulsion we took advantage of Sak/PLK4 over-expression (Plk4OE), which leads to centrosome amplification in many different cells and tissues, leading to tumorigenesis (Basto et al., 2008; Bettencourt-Dias et al., 2005; Coelho et al., 2015; D'assoro et al., 2002; Levine et al., 2017; Peel et al., 2007). Analysis of Plk4OE SGs at L3 stages, showed cells containing centrosomes (Figures 2E-F and Supplementary Figures 1D-E). Further, centrosomes were also detected in the lumen (Supplementary Figure 2E-F), suggesting that a certain number of centrosomes was nevertheless released into the lumen in Plk4OE SGs and so the mechanism of elimination is present in Plk4OE SGs.

We next investigated whether increasing MyoII contributed to decrease the number of centrosomes in Plk4OE SG cells. We expressed a constitutively active MyoII (aMyoII) transgene, where the T20S21 residues were replaced by glutamic acid residues (E20E21) mimicking phosphorylation (Jordan and Karess, 1997). Importantly, this fully rescued the defects in centrosome elimination of Plk4OE SGs, while WT MyoII or iMyoII had no effect (Figures 2E-F). We concluded that MyoII activity is essential to promote centrosome expulsion in SG cells. A possible interpretation of these findings is that centrosome release towards the lumen is limited by the levels of active MyoII.

3.5. Luminal centrosomes are targeted for proteasome degradation

We next investigated the fate of luminal centrosomes in WT SGs, using two centrosome markers to detect co-localization and therefore identify bona fide centrosomes (Basto et al., 2008; Marthiens et al., 2013; Morretton et al., 2022). At L3

stages, a variety of sizes and structures could be detected in the WT SG lumen (Supplementary Figures 4A-C). These included centrioles, like the ones detected in cells in *MyoII*^{mut}, or in other tissues (Fu and Glover, 2012) and centrosome filaments, where beads like structures detected by centrosome markers appeared clustered in a filament pattern. Finally, extremely small structures were also seen. We called these centrosome dust, in light of their small size. At later developmental stages however, when the lumen becomes enlarged, no centrosome structures could be detected, suggesting the disappearance of centrosomes as larvae transition towards the pupal stage (Supplementary Figure 4D-E).

These results suggest an ongoing process of centrosome degradation. Recently, it has been shown that in *Naegleria gruberi,* centrosomes undergo ubiquitination, which promotes proteasome-mediated degradation (Woglar et al., 2024; Wojcik et al., 2000). To ascertain whether ubiquitination plays a role in promoting the disappearance of luminal centrosomes, we labelled WT SGs with antibodies that recognize ubiquitin moieties (P4D1) and K48 polyubiquitin (K48-Ub). In WT SGs, both markers co-localized with luminal centrosomes (Supplementary Figure 4F-H), suggesting indeed that these represent proteasome substrates (Finley et al., 1994; Grice and Nathan, 2016; V Chau, 1989). In *MyoII*^{mut} SGs however, only P4D1 co-localized with centrosomes in cells, whereas no K48-Ub signal could be identified in the lumen (Supplementary Figure 4F-H).

Proteasome-mediated degradation within the lumen necessitates the localization of the proteasome to this compartment. Several studies have described the presence of proteasomes in extracellular space such as blood, extracellular alveolar space or in the cerebrospinal fluid (Mueller et al., 2012; Sixt and Dahlmann, 2008; Sixt and Peters, 2010; Urs Sixt et al., 2007). Nevertheless, the presence of proteasome in the lumen of SGs, has never been reported. We therefore used a *Drosophila* proteasome-activity reporter line, where the proteasome substrate-CL1- is fused to GFP (McPhee et al., 2013), so that in the presence of the proteasome, GFP fluorescence intensity is not detected. At later developmental stages, GFP positive signals could be detected in a few SG cells, but not in the lumen (Supplementary Figure 4I), indicating proteasome activity.

To functionally test the possible role of the proteasome in L3 WT SGs, we used the proteasome inhibitor MG132 (Albornoz et al., 2019; Velentzas et al., 2011; Zhang et al., 2013) for three hours, to avoid toxic effects. Importantly, this short incubation

time was sufficient to completely alter the appearance of luminal centrosomes, which now could be seen forming large aggregates and filling the lumen entirely (Supplementary Figure 4J-K). Altogether, these results show that centrosome ubiquitination takes place in the SG lumen at late larval stages, which triggers their degradation in a proteasome dependent manner.

3.6. Secretory autophagy coupled with autolysosome exocytosis promotes centrosome expulsion from the cell

With the aim of identifying the mechanism responsible for centrosome expulsion from the cell into the lumen, we performed a candidate screen, where mutations or RNA interference (RNAi) of candidate genes were tested. We reasoned that if a given process involved in centrosome luminal release would be inhibited, centrosomes should be detected in SG cells at later larval stages as in *MyoII*^{mut} SG*s*. We tested components known to be involved in the biogenesis of MVBs and therefore altering their secretory properties, such as the endosomal sorting complexes required for transport (ESCRT) proteins (Colombo et al., 2013; Eikenes et al., 2015; Van Niel et al., 2018) and common secretory pathways (Bannykh et al., 1996).

Depletion of different ESCRT members or members of the secretory pathway (see methods) did not show any relevant difference in terms of centrosome behavior, as L3 SG cells did not contain centrosomes, but these could be detected in the lumen (Supplementary Figure 5A-C). It is worth noticing that SGs depleted for these components, presented abnormal organization of the polytene chromosome in the nucleus, attesting for an effect of the RNAi.

We next tested autophagy using an amorphic mutation in the *atg5* gene (*Atg5*^{mut}), which encodes a member of the autophagy complex, responsible for phagophore formation (Figure 3A) (Kim et al., 2016). Striking, similarly to *MyoII*^{mut} or Plk4OE SGs, *Atg5*^{mut} SGs cells contain multiple centrosomes (Figure 3B-C), suggesting a requirement for this pathway in centrosome elimination in SG cells. Further, this supports the findings describe above showing that if centrosomes are not eliminated from SG cells, they keep duplicating.

Selective autophagy has been shown to regulate centrosome number in cells that normally contain centrosomes (Holdgaard et al., 2019; Woglar et al., 2024; Wu et al., 2021), by degrading specific centrosomal proteins such as Cep63 (Watanabe et

al., 2016). Because in SGs, centrosomes are not degraded inside the cell but rather in the lumen, whereas in *Atg5^{mut}* SGs centrosomes are retained within the cell, we hypothesize that autophagy may function not as a degradative process but as a secretory one in respect to centrosome elimination in SGs. Indeed, autophagy can support secretory processes, such as autolysosomal exocytosis (Claude-Taupin et al., 2017; Ralhan et al., 2023; Sho et al., 2024). This process occurs through fusion of autophagosomes with lysosomes and subsequently with the plasma membrane, so that cellular content is released into the extra cellular space (Figure 3A).

To test the possible involvement of autolysosome exocytosis, we depleted Rab27 and Syntaxin (Syn)16. Rab27 is a small GTPase promoting lysosome docking at the plasma membrane, facilitating lysosomal exocytosis (Figure 3A) (D'Angelo et al., 2025; Delevoye et al., 2019). Syx16, is a Soluble N-ethylmaleimide-sensitive factor attachment protein receptors (SNARE) protein involved in autolysosome formation (Figure 3A) (Gu et al., 2019). Remarkably, depletion of Rab27 or Syx16 showed centrosomes positioned closely to the apical membrane (Figure 3B-D), suggesting failure in the fusion process.

One common way of detecting autolysosome exocytosis is by monitoring the localization of lysosomal associated membrane protein 1 (LAMP1), which is a key protein involved in lysosome docking at the cell membrane (Figure 3A) (Machado et al., 2015; Samie and Xu, 2014). Using LAMP1 antibodies, we characterized WT SGs, at embryonic stages 15-17, which corresponds to the stages where centrosomes are released into the lumen. Importantly, we found a high enrichment of LAMP1 vesicles at the apical membrane of SGs (Figure 3E). Strikingly, these vesicles also contained MyoII and centrosomes (Figure 3E-F). These results support the findings that MyoII activity, combined with secretory autophagy and autolysosome exocytosis cooperate to expulse centrosomes from SG cells towards the lumen.

3.7. Centrosome elimination is required for proper mitochondria organization and respiratory activity

A key unanswered question in the field of polyploidy is the underlying reason for centrosome elimination in certain polyploid cells. An obvious possibility is that the maintenance of centrosomes, that continue duplicating, may impact SG development or ploidy levels. *MyoII^{mut}* SG cells display reduced size and ploidy, when compared to

WT SG cells (Supplementary Figure 3A-D). However, Plk4OE SG cells contained centrosomes but normal ploidy levels and cell and nuclear size, when compared to WT (Supplementary Figure 3A-D), showing that lack of centrosome expulsion does not impair SG cell growth or ploidyzation.

We next hypothesized that the presence of centrosomes may hinder MT nucleation capacity from the nuclear envelope, typical of SG cells (Sun et al., 2019). Indeed, in muscle cells or in the *Drosophila* oocyte (Elisabeth Bugnard, 2005; Łuksza et al., 2013; Tavosanis and Gonzalez, 2003), MTs are nucleated from the nuclear envelope in the absence of centrosomes. Whether centrosome presence and nucleation from the nuclear envelope are mutually exclusive is unknown. In WT larval SGs, a highly organized MT ring could be readily identified. In sharp contrast however, *MyoII*^{mut} *SGs* lacked MT rings and displayed a very disorganized MT network (Supplementary Figure 6A-B). However, analysis of Plk4OE SGs showed an intact and perfectly arranged MT ring in cells that contain centrosomes (Supplementary Figure 6A-B). These results indicate that in polyploid cells, MTs can be nucleated by the nuclear envelope even when centrosomes are present. This suggests that the primary purpose of centrosome elimination in polyploid cells is not to enable MT nucleation from alternative MTOCs.

Recently, it has been shown that the presence of extra centrosomes-centrosome amplification- induces defects in mitochondria organization and activity (Edwards et al., 2024; Monteiro et al., 2023). Further, other studies have shown that in specialized cells like neurons or fibroblasts, MT motors regulate mitochondria motility and activity and defects in MT-dependent mitochondria transport can impair the function of this organelle (López-Doménech et al., 2018; Wang and Schwarz, 2009). We therefore characterized the mitochondrial network in WT, *MyoII*^{mut} , Plk4OE SGs using antibodies against the mitochondrial ATP synthase F1 Subunit Alpha (ATP5a). Interestingly, in WT SG cells, mitochondria appeared filamentous and formed a long and branched network, in which individual organelles displayed a high surface area (Figure 4A-B). In both *MyoII*^{mut} and Plk4OE SG cells however, mitochondria appeared fragmented and less branched with reduced surface area (Figure 4A-B). Analysis of the circularity and solidity parameters showed higher values in *MyoII*^{mut} and Plk4OE SG cells, when compared to WT SGs (Figure 4C-D), confirming a higher degree of branching in WT cells. Moreover, in electron microscopy (EM) experiments, mitochondria appeared smaller and circular in *MyoII*^{mut} SG cells

when compared to WT cells (Figure 4E-F and Supplementary Figure 6C-D). These results suggested that maintaining centrosomes in SGs impact mitochondria structure and network organization. We do not know the origin of these defects. Although we did not detect any obvious defect in cytoplasmic MTs in Plk4OE, defects in polarity or transport may account for the observed alterations in the mitochondria network.

Mitochondria are key organelles that produce energy through ATP synthesis (Arnold et al., 1998; Jonckheere et al., 2012; Jouaville et al., 1999; Osellame et al., 2012). Cells are thought to increase their ploidy to enable larger cell size, which may be linked to higher metabolic activity. We explore this possibility by measuring oxygen consumption rates (OCR) and mitochondrial ATP production rates using the Seahorse XF Analyzer. Strikingly, an important decrease in both OCR and mitochondrial ATP production rates was detected in *MyoII*^{mut} and Plk4OE SG cells, compared to the levels seen in WT SG cells (Figure 4G-H). Altogether, our findings uncovered a novel role for centrosome elimination in ensuring proper mitochondria organization to maintain metabolic and respiratory activity in polyploid SG cells.

4. Discussion

Our findings highlight the essential role of centrosome elimination in physiologically polyploid cells. They support a model (Figure 4I) in which centrosome removal depends on MyoII activity, which facilitates the transport of centrosomes from embryonic SG cells into the lumen. MyoII is known to function in autophagy, particularly in autophagosome formation (Tang et al., 2011), and our data show that inhibition of either MyoII or autophagy leads to the retention of centrosomes within the cell. Based on our results, we propose that autophagosomes containing centrosomes fuse with lysosomes to form autolysosomes, which are subsequently directed towards the plasma membrane, where they can undergo membrane fusion. This enables the release of centrosomes into the lumen, where they are eventually degraded by the proteasome during later developmental stages.

The strict requirement for complete centrosome elimination in these and other polyploid cells has remained unclear. Our findings suggest that centrosome retention disrupts mitochondrial network integrity, compromising the cell's ability to generate ATP at necessary levels. It remains unknown whether luminal centrosomes serve any biological function before their degradation.

Interestingly, recent studies have shown that human prostate and ovarian tumors often lose centrosomes (Morretton et al., 2022; Wang et al., 2020). Whether this phenomenon is linked to changes in mitochondrial respiratory activity remains to be determined but together, it exposes a requirement of centrosome loss that deserves attention. However, how ectopic presence of centrosomes affect mitochondria function remains to be understood. One possibility is that amplified centrosomes alter the polarity or properties of the MT cytoskeleton, which may impact fusion explaining the decrease in mitochondria size observed. Alternatively, the presence of extra centrosomes may influence other aspects of mitochondria biogenesis and function that remain to be understood. Importantly, this work uncovers a physiological requirement for centrosome elimination in cells undergoing extensive ploidy and cell size increase, particularly in support of large-scale metabolite production.

Acknowledgments

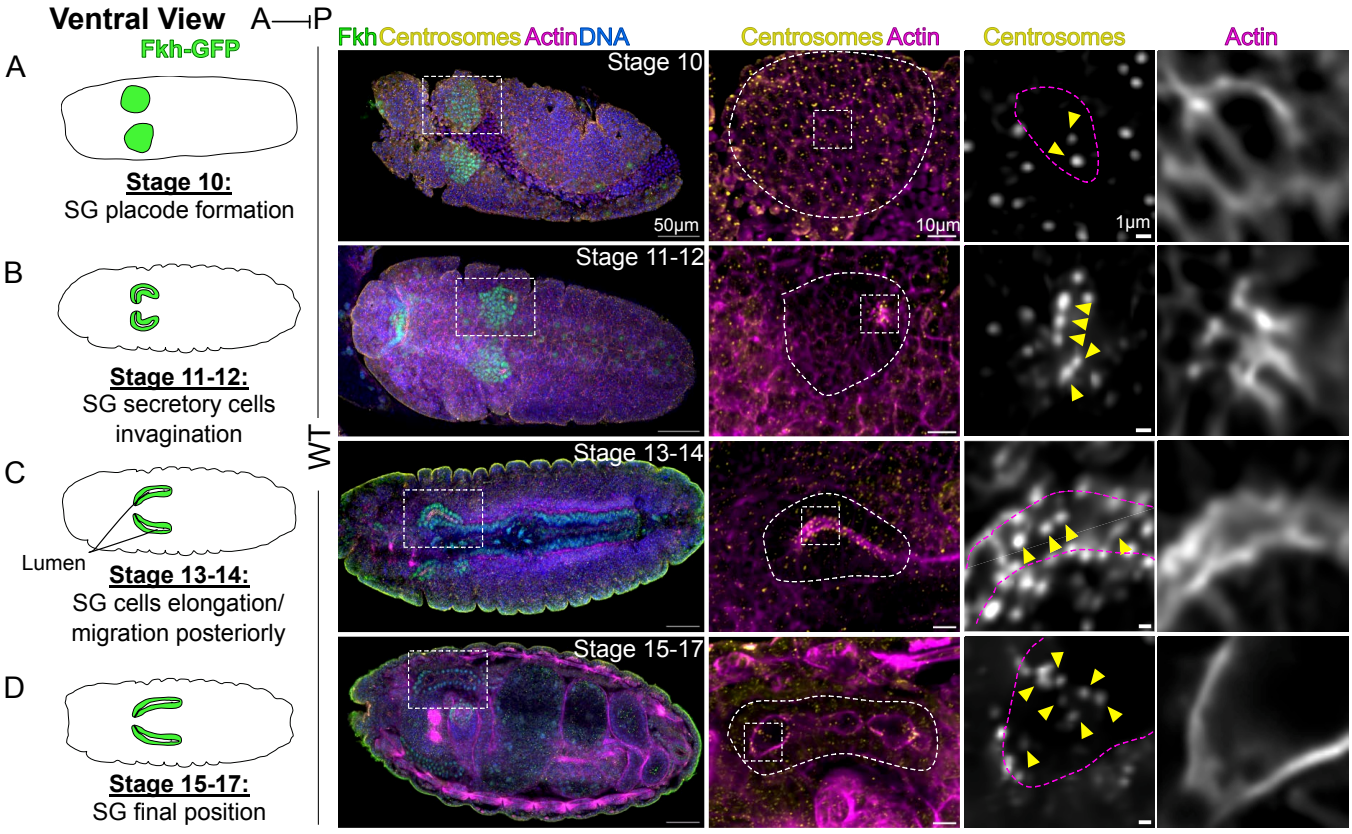
The authors acknowledge the Cell and Tissue Imaging (PICT-IBiSA) from Institut Curie, member of the national infrastructure France- BioImaging (https://ror.org/01y7vt929) supported by the French National Research Agency (ANR-24-INBS-0005 FBI BIOGEN) and V. Fraisier, C. Guedj. M. David, M. Cortes and A.S. Macé (PICT-IBiSA) for their continuous support on image acquisition and analysis. The authors thank B. Goud, F. Perez, Y. Bellaiche, J.L. Maitre (I. Curie), W. Marshall (UCSF) and M. Thery (IPGG) for helpful discussions. We are grateful to A.C. Gavin Perrin (UNIGEN) for bringing the lysosomal exocytosis pathway into our attention and for A. Echard for guidance throughout the project. We thank J. Mathieu, J. Schulman and U.B. Pandey for *Drosophila* stocks. We thank A.Martin for the plasmid containing MyoII endogenous promoter sequence. We thank V. Marthiens and A. Echard for comments on the manuscript. This work has been supported by the European Research Council ERC CoG (ChromoNumber-LS3, ERC-2016-COG for R.B.), the government through the Agence Nationale de la Recherche from France 2030 (ANR-23-CHBS-0012 for R.B), the Institut Curie and the CNRS. R.S salary was supported by the ERC-2016-COG and an FRM grant (FDT202404018667).

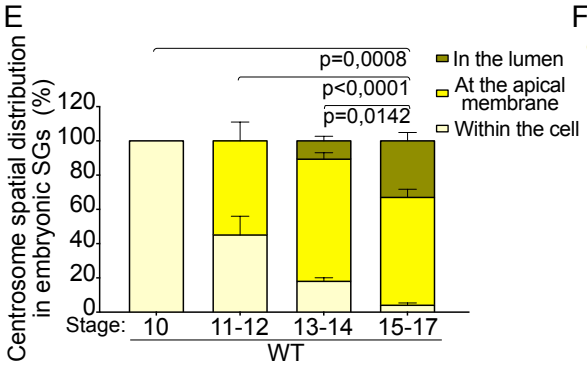
Author's contribution

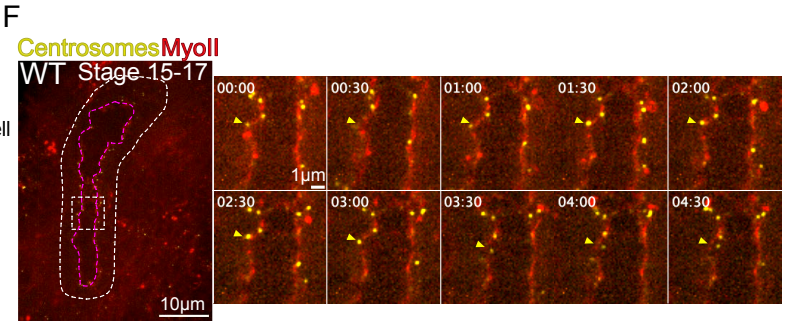
R.S. and R.B. conceived the project and wrote the manuscript. R.S. did most of the experiments and data analysis presented here with some help from A. S. L.J and S.G P.B. and G.R. contributed with the EM experiments and C.C with the seahorse measurements. R.B. obtained the funding used to develop this project. All authors read and commented on the manuscript.

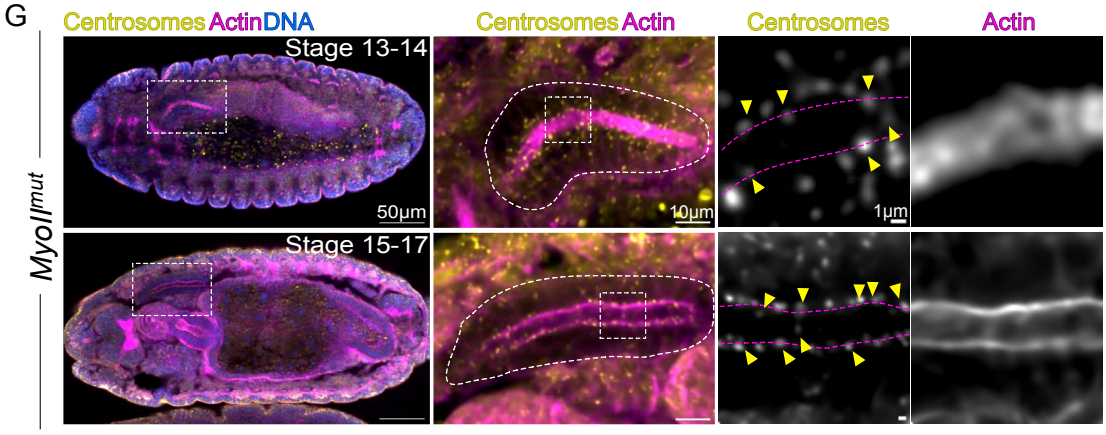
Chapter 4 - Figures

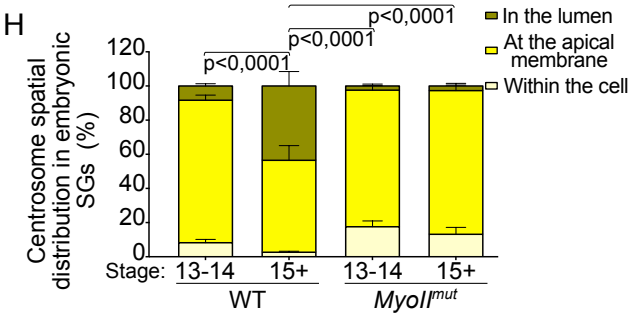
Figure 1


Ventral View A⟞P
Fkh-GFP
A
Stage 10:
SG placode formation
B
Stage 11-12:
SG secretory cells invagination
C
Lumen
Stage 13-14:
SG cells elongation/ migration posteriorly
D
Stage 15-17:
SG final position
WT
Fkh Centrosomes Actin DNA
Centrosomes Actin
Centrosomes
Actin
Stage 10
Stage 11-12
Stage 13-14
Stage 15-17
50µm
10µm
1µm


E
Centrosome spatial distribution in embryonic SGs (%)
p=0,0008
p<0,0001
p=0,0142
In the lumen
At the apical membrane
Within the cell
Stage: 10 11-12 13-14 15-17
WT


F
Centrosomes MyoII
WT Stage 15-17
10µm
1µm
00:00
00:30
01:00
01:30
02:00
02:30
03:00
03:30
04:00
04:30


G
MyoII mut
Centrosomes Actin DNA
Centrosomes Actin
Centrosomes
Actin
Stage 13-14
Stage 15-17
50µm
10µm
1µm


H
Centrosome spatial distribution in embryonic SGs (%)
p<0,0001
p<0,0001
p<0,0001
In the lumen
At the apical membrane
Within the cell
Stage: 13-14 15+ 13-14 15+
WT
MyoII mut

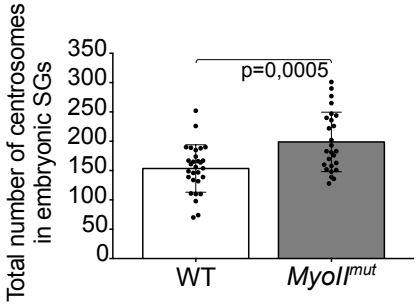

I
Total number of centrosomes in embryonic SGs
p=0,0005
WT
MyoII mut

Figure 1- Centrosomes are transported towards the SG lumen during embryonic development

(A-D) On the left, drawing depicting the indicated embryonic stages according to Fkh expression to label SGs. On the right representative immunostaining images showing low magnification views of embryos (left hand side) and higher magnification views (middle panels). Fkh in green, centrosomes in yellow, actin in magenta and DNA in blue. The white lines surround SGs, and the squares surround the region shown on the right-hand side, for centrosomes (top) and actin (bottom) depicted as separate panels in grey. In all insets, the yellow arrowheads point at centrosomes. In (A), the pink dashed line surrounds an SG cell. In (B), the centrosomes closely associated with the apical membrane during apical constriction. In (C-D) the pink dashed lines are marking the lumen. (E) Graph bar showing the centrosome spatial distribution in SGs across different developmental stages as indicated. (F) Stills of time lapse movie of embryonic SGs expressing Sas4-GFP to follow centrosomes (yellow) and Myosin II (MyoII)-mCherry transgene (red) at stage 15-17. On the left an overview of the entire SG. The white and magenta dashed line surrounds the SG and the lumen, respectively. The square indicates the region shown at higher magnification stills on the right. The yellow arrowheads points to the trajectory of a centrosome that is initially located at the apical membrane and that is subsequently translocated into the lumen. (G) On the left, representative images of *MyoII*^{mut} embryos of the indicated embryonic stages showing centrosomes (yellow), actin (magenta) and DNA (blue). In the middle panel, centrosomes and actin are shown. The white dashes lines surround SGs, and the white squares mark the regions shown on the right-hand insets for centrosomes (top) and actin (bottom) depicted as separate panels in grey. The yellow arrowheads indicate centrosomes and the pink dashed lines the lumen. (H) Bar and dot plot graph showing the centrosome spatial distribution in SGs in WT and *MyoII*^{mut} embryos at the indicated developmental stages. (I) Bar and dot plot graph showing the total number of centrosomes in SGs of the indicated genotypes. Bars show the mean ± SD. Statistical significance is shown, and it was determined by two-way ANOVA tests (E, H) and unpaired t-test (two-tailed) (I). Lines correspond to significant P value (in E and H, P value shown only for centrosomes in the lumen). For each graph, at least three experiments were quantified and a minimum of 10 embryos/stage (E), minimum of 13 embryos/stage (H) and minimum 26 embryos/stage (I) were analyzed per condition.

Figure 2

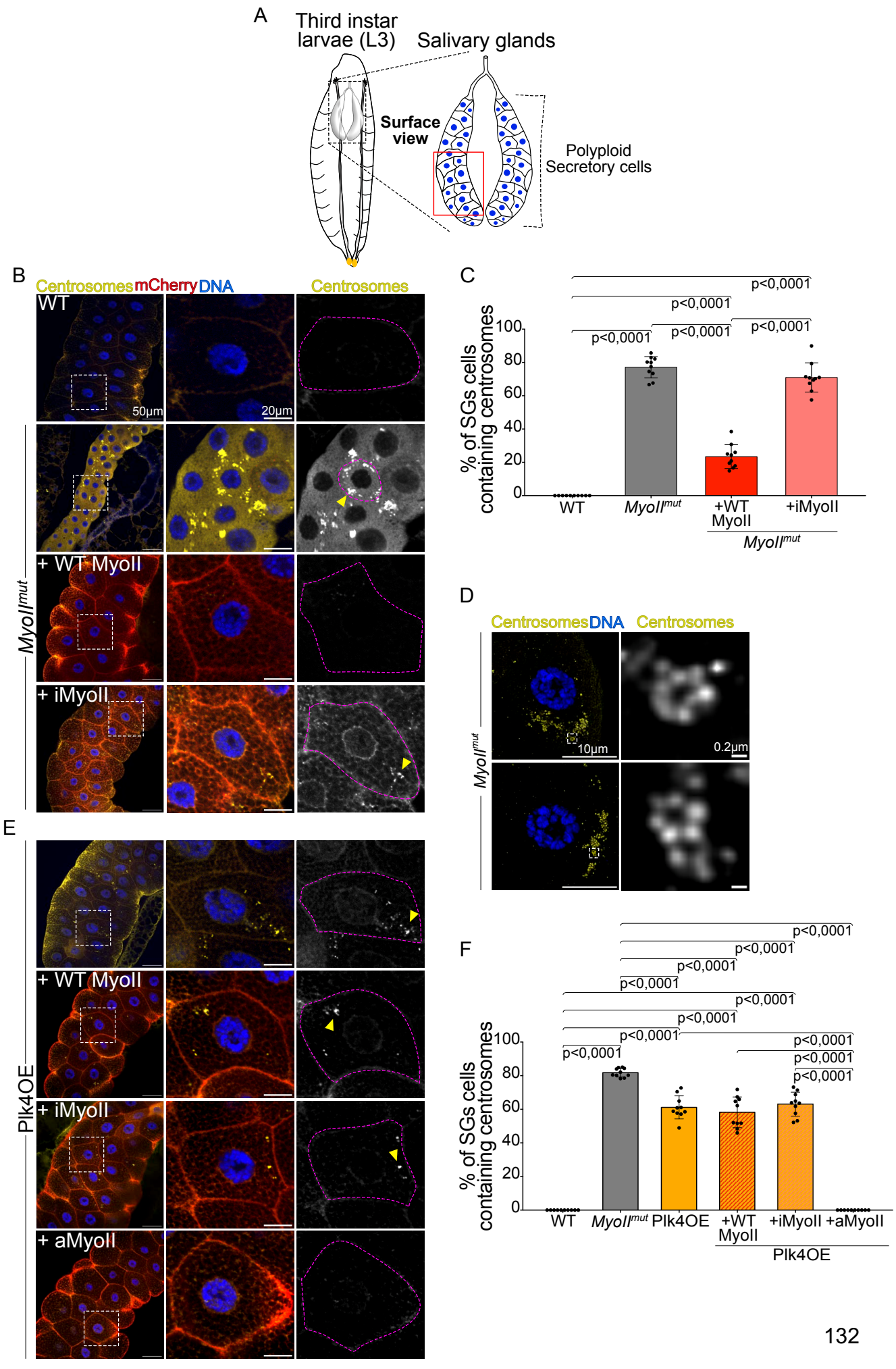

A
Third instar larvae (L3)
Salivary glands
Surface view
Polyploid Secretory cells
B
Centrosomes mCherry DNA
Centrosomes
WT
50µm
20µm
+ WT MyoII
+ iMyoII
MyoII^mut
C
p<0,0001
% of SGs cells containing centrosomes
100
80
60
40
20
0
WT
MyoII^mut
+WT MyoII
+iMyoII
MyoII^mut
D
Centrosomes DNA
Centrosomes
10µm
0.2µm
MyoII^mut
E
+ WT MyoII
+ iMyoII
+ aMyoII
Plk4OE
F
p<0,0001
% of SGs cells containing centrosomes
WT
MyoII^mut
Plk4OE
+WT MyoII
+iMyoII
+aMyoII
Plk4OE

Figure 2- Centrosome expulsion requires MyoII activity

(A) Schematic drawing of SGs from third instar larvae (L3). On the left an L3 larvae is depicted with anterior positioned at the top. On the right, the SG pair showing a top/surface view of polyploid secretory cells with nuclei depicted in blue. (B and E) On the left, representative immunostaining images of L3 SGs of the indicated genotypes. Centrosomes in yellow, mCherry tagged proteins in red and DNA in blue. The white squares mark the regions shown at higher magnification views in the middle panel. On the right, the centrosome channel is shown in grey. Pink dashed lines surround SG cells and yellow arrows point at centrosomes. (C and F) Bar and dot plot graphs showing the percentage of SGs cells with centrosomes of the indicated genotypes. (D) On the left, representative images of SG cells in *MyoII*^{mut} obtained by super resolution microscopy. Centrosomes (yellow) and DNA (blue). The white squares mark the regions shown at higher magnification views on the right panel. iMyoII=inactive MyoII; aMyoII= active MyoII; Statistical significance is shown and determined by ordinary one-way ANOVA test. Bars show the mean ± SD. For (C), at least three experiments and for (F) four experiments were quantified and 10 SGs were analyzed per condition.

Figure 3

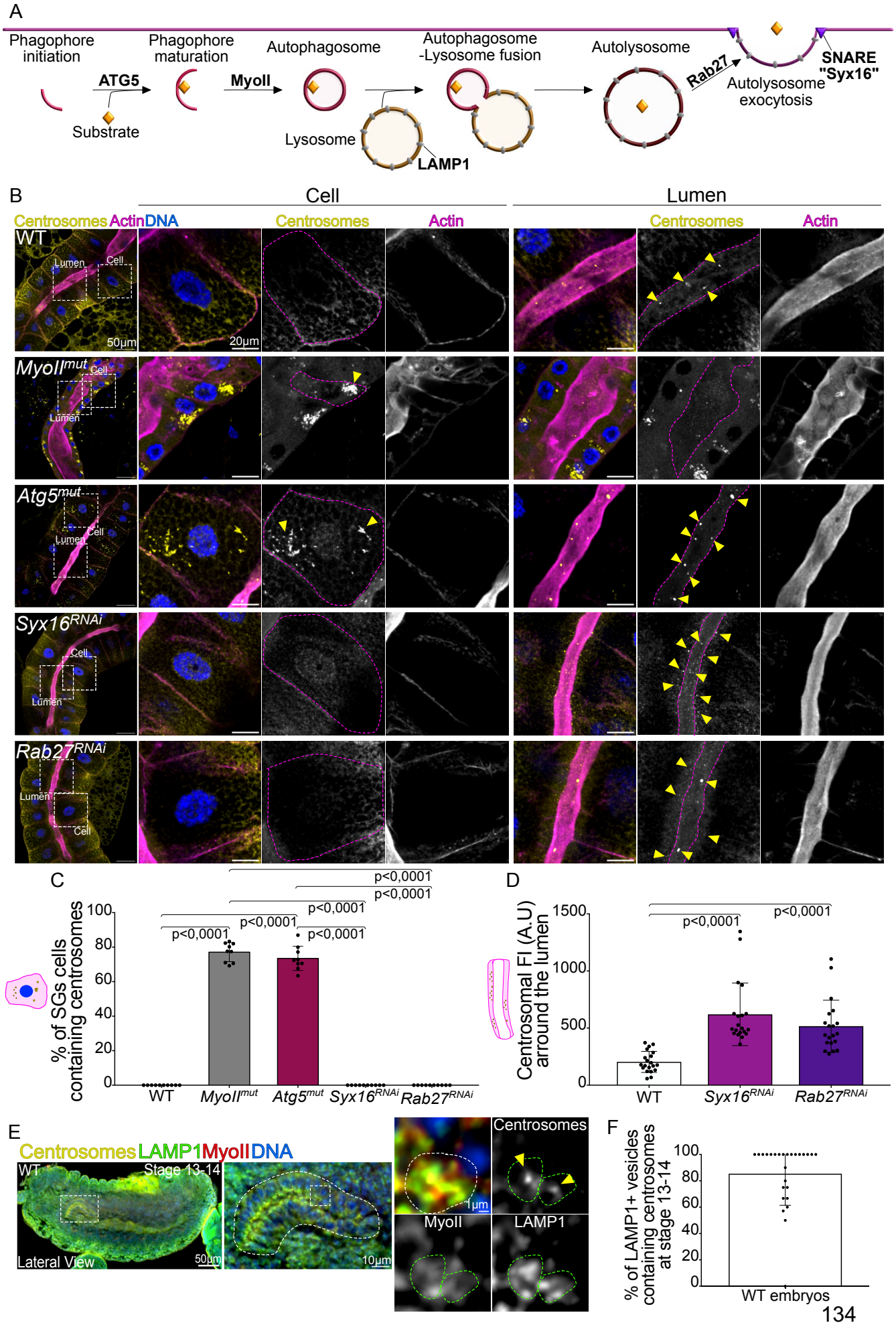

A
Phagophore initiation
ATG5
Substrate
Phagophore maturation
MyoII
Autophagosome
Lysosome
Autophagosome -Lysosome fusion
LAMP1
Autolysosome
Rab27
Autolysosome exocytosis
SNARE "Syx16"
B
Cell
Lumen
Centrosomes Actin DNA
Centrosomes
Actin
WT
MyoII mut
Atg5 mut
Syx16 RNAi
Rab27 RNAi
Lumen
Cell
50µm
20µm
C
% of SGs cells containing centrosomes
p<0,0001
WT
MyoII mut
Atg5 mut
Syx16 RNAi
Rab27 RNAi
D
Centrosomal FI (A.U) arround the lumen
p<0,0001
E
Centrosomes LAMP1 MyoII DNA
WT
Stage 13-14
Lateral View
50µm
10µm
Centrosomes
MyoII
LAMP1
1µm
F
% of LAMP1+ vesicles containing centrosomes at stage 13-14
WT embryos

Figure 3- Secretory Autophagy and Lysosomal Exocytosis Mediate Centrosome Delivery into the Lumen

(A) Schematic diagram of the main steps involved in autophagosome formation and lysosomal exocytosis. (B) On the left, illustrative low magnification immunostaining images of L3 SGs of the indicated genotypes. Centrosomes in yellow, actin in magenta and DNA in blue. The white squares mark the two SG regions that are shown at higher magnifications on the right as merged panels or as separate panels showing centrosomes and actin as indicated. These regions correspond to a cell (middle panels) and to the lumen (right panels). The dashed pink lines surround the cell, or the lumen and the yellow arrows point at centrosomes. (C-D) Bar and dot plot graphs showing the percentage of SGs cells with centrosomes (C) and the centrosomal fluorescence intensity (FI) in A.U. at the lumen (D). (E) On the left, representative immunostaining image of one embryo from stage 13-14 showing centrosomes in yellow, LAMP1 in green, MyoII in red and DNA in blue. The white dashed rectangle shows the SG region, shown at higher magnification on the right. The white dashed square shows the LAMP1 vesicles at higher magnification shown on the right in separate channels as indicated with green dashed lines marking the LAMP1 vesicle surrounding the centrosome. (F) Bar and dot plot graph showing the percentage of LAMP1+ vesicles containing centrosomes in WT embryos of stage 13-14. Statistical significance is shown, and it was determined by ordinary one-way ANOVA test (C-D) test. Bars show the mean ± SD. For (C), three experiments and for (D-F) two experiments were quantified and 10 SGs in (C-D) and 28 embryos in (F) were analyzed per condition.

Figure 4

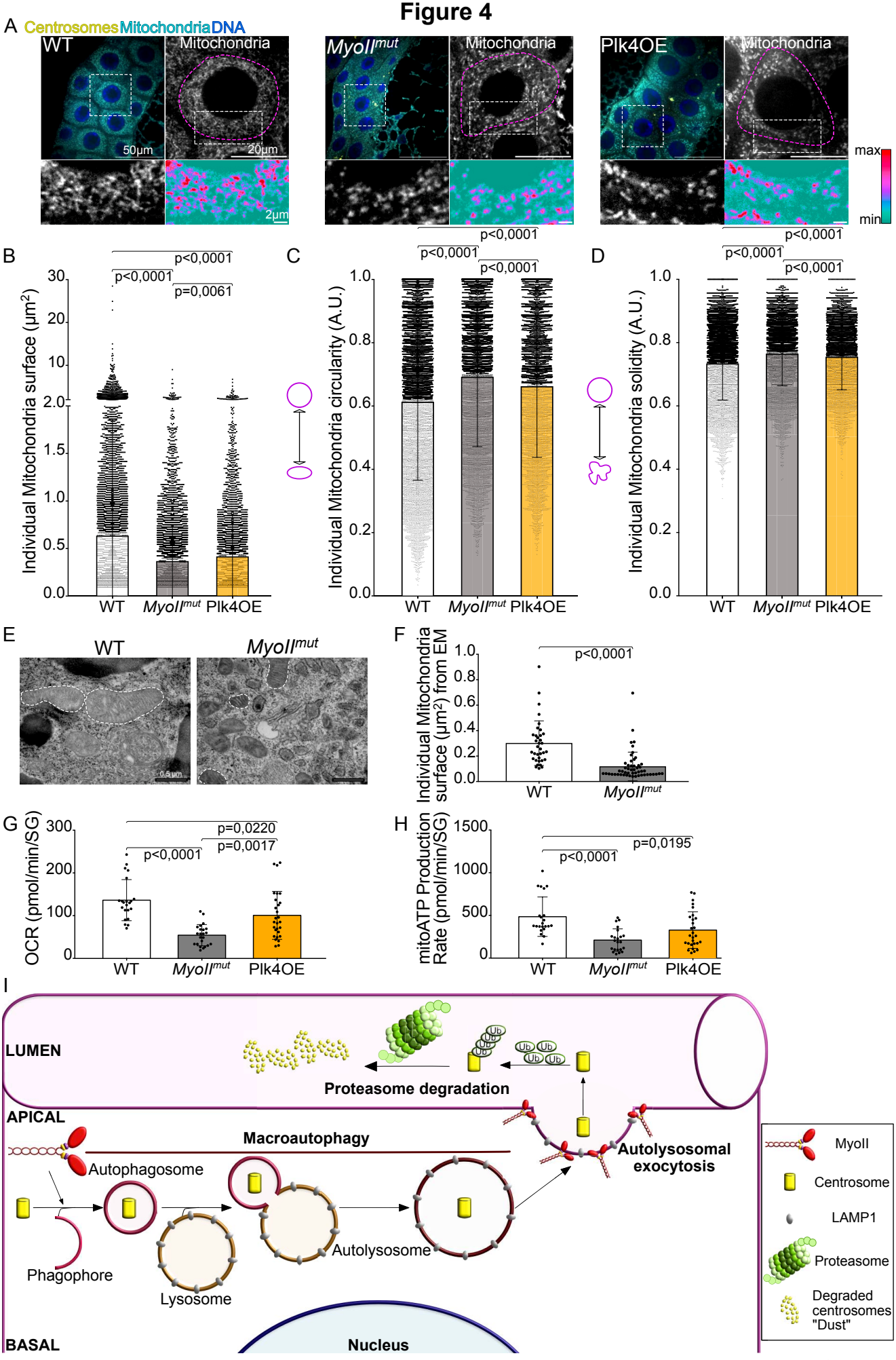
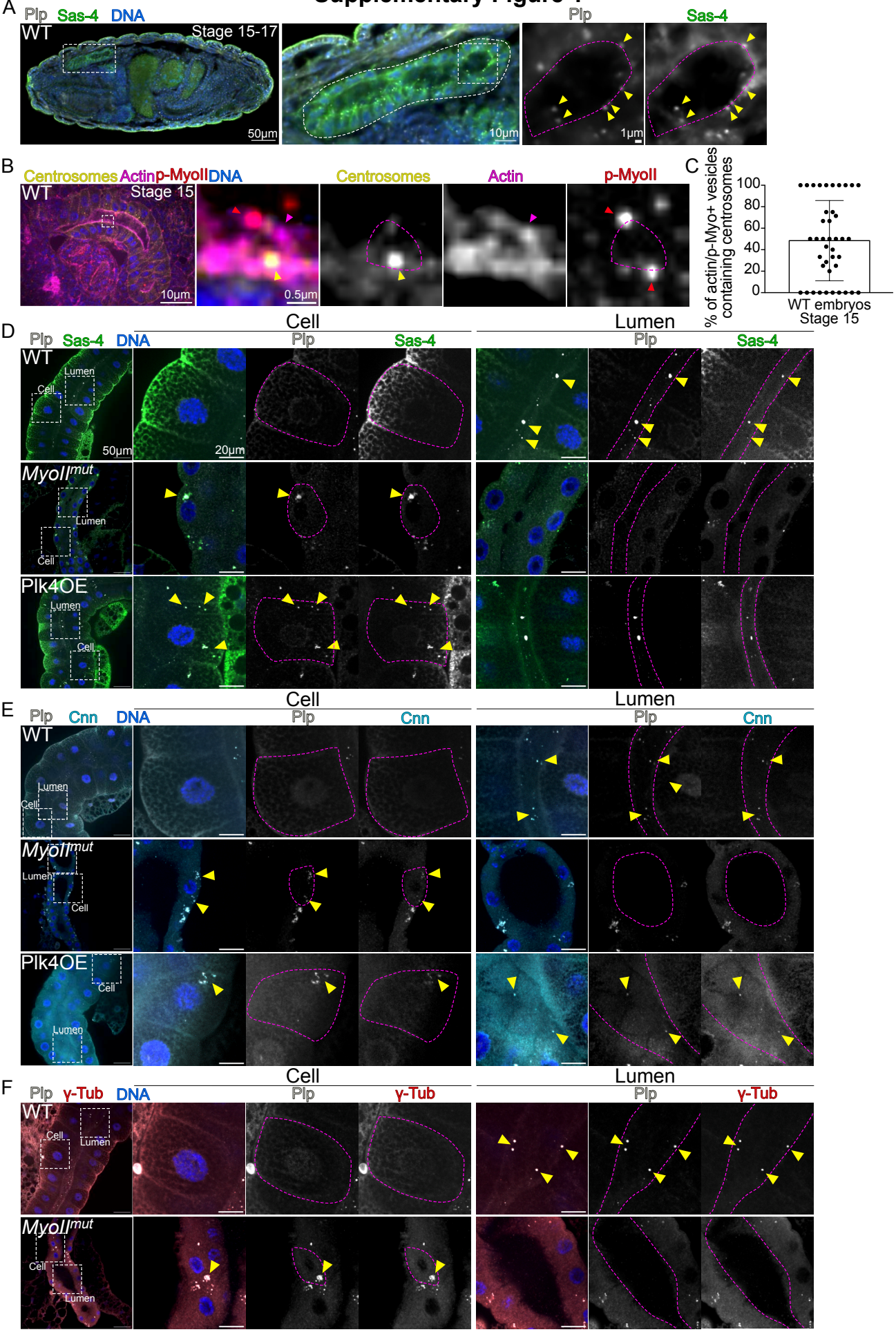

A
Centrosomes Mitochondria DNA
WT
Mitochondria
MyoII mut
Mitochondria
Plk4OE
Mitochondria
50µm
20µm
2µm
max
min
B
Individual Mitochondria surface (µm²)
p<0,0001
p<0,0001
p=0,0061
WT
MyoII mut
Plk4OE
C
Individual Mitochondria circularity (A.U.)
p<0,0001
p<0,0001
D
Individual Mitochondria solidity (A.U.)
p<0,0001
p<0,0001
E
WT
MyoII mut
0,5 µm
F
Individual Mitochondria surface (µm²) from EM
p<0,0001
G
OCR (pmol/min/SG)
p=0,0220
p=0,0017
p<0,0001
H
mitoATP Production Rate (pmol/min/SG)
p=0,0195
p<0,0001
I
LUMEN
Proteasome degradation
APICAL
Macroautophagy
Autophagosome
Autolysosomal exocytosis
Phagophore
Lysosome
Autolysosome
BASAL
Nucleus
MyoII
Centrosome
LAMP1
Proteasome
Degraded centrosomes "Dust"

Figure 4- Maintenance of centrosomes in SGs cells impacts the mitochondrial network and activity

(A) Illustrative immunofluorescence images of L3 SGs of the indicated genotypes showing centrosomes in yellow, mitochondria in cyan and DNA in blue on the left and mitochondria on the right in grey and in the Ice LUT bellow. The white dashed squares show the magnification regions. The pink dashed lines surround SG cells. (B-D) Bar and dot plot graphs showing individual mitochondria surface (B), circularity (C) and solidity (D) of the indicated genotypes. (E) Illustrative EM images of the indicated genotypes. White dashed lines surround mitochondria. (F) Bar and dot plot graphs showing individual mitochondria surface from EM data of the indicated genotypes. (G-H) Bar and dot plot graphs showing oxygen consumption rates (OCR) (G) and ATP production rates from mitochondria (H) in SG cells of the indicated genotypes. (I) Model representing the main findings of this study. During embryonic stages, MyoII functions together with the autophagy machinery and lysosomal exocytosis to transport centrosomes into the lumen of SGs. Centrosomes are then ubiquitinated and degraded by the proteasome machinery at later developmental stages. Statistical significance is shown and determined by ordinary one-way ANOVA tests (B-D and G-H) and Mann-Whitney test (F). Bars show the mean ± SD. For (B-D, G-H), three experiments and for (F) two experiments were quantified, and a minimum of 10 SGs (B-D), minimum 35 mitochondria (F) and minimum 22 SGs (G-H) was analyzed per condition.

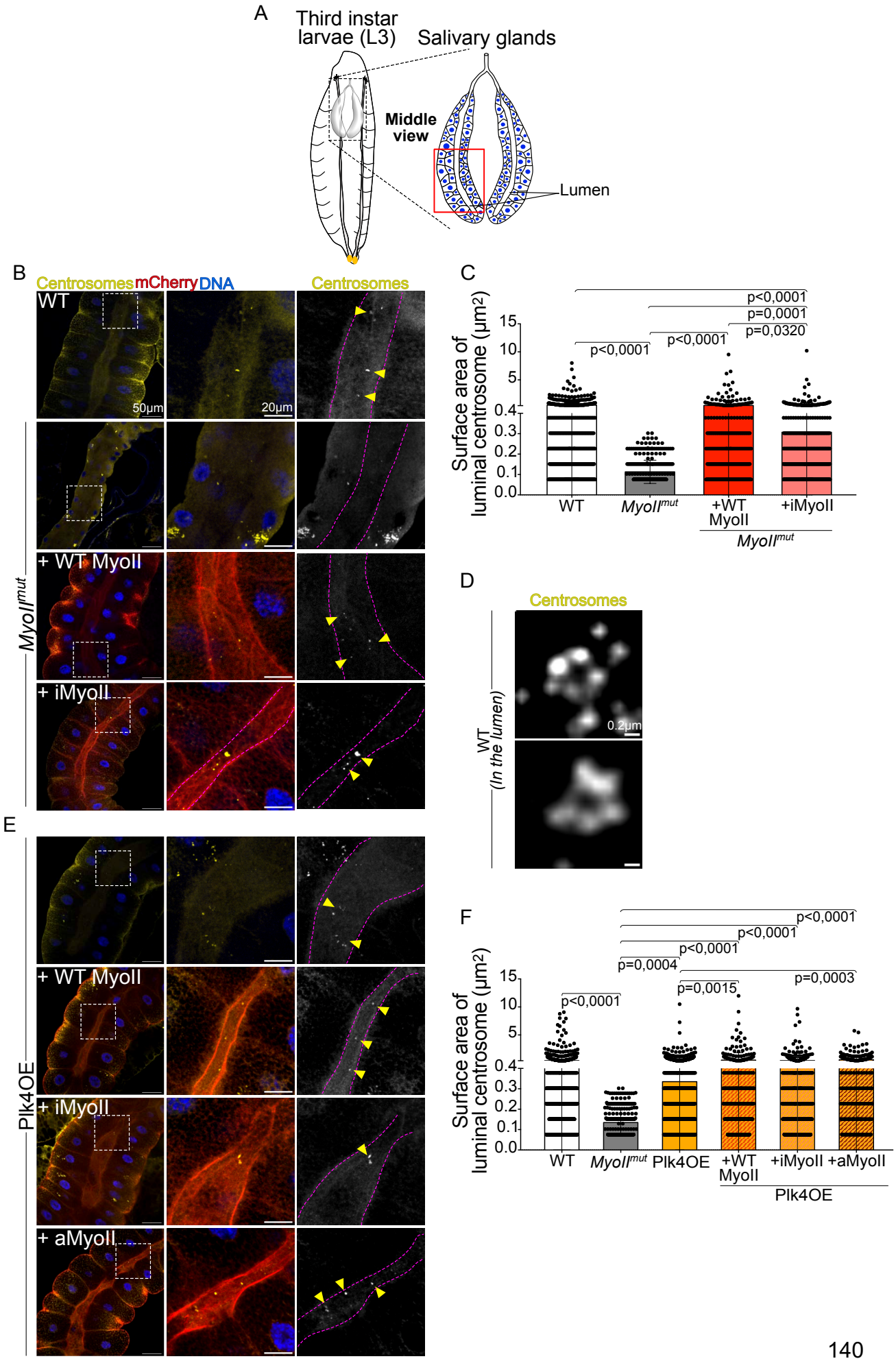
Supplementary Figure 1



Supplementary Figure 1- Validation of centrosome labeling with the use of two different centrosomal markers.

(A-B) Representative immunofluorescence images of WT embryos at stage 15-17 showing the co-localization of two centrosome markers- Plp in grey and Sas-4 in green (A) or centrosomes in yellow, Actin in magenta and p-Myo in red (B). DNA in blue. The white dashed rectangles and squares show the insets shown at higher magnifications on the right. In (A) the pink dashed lines surround SG cells, and the yellow arrowheads point at centrosomes. In (B), the white dashed circle surrounds actin/p-MyoII vesicle and the yellow, pink and red arrows point at centrosomes, one actin vesicle and foci of p-MyoII. (C) Bar and dot plot graph showing the percentage of actin/p-Myo+ vesicles containing centrosomes. (D) On the left, illustrative low magnification immunostaining images of L3 SGs of the indicated genotypes. Centrosomes are shown through the localization of two centrosome markers Plp (grey) and Sas-4 (green) DNA in blue. The white squares mark the two SG regions that are shown at higher magnifications on the right as merged panels or as separate panels showing centrosome markers in grey. These regions correspond to a cell (middle panels) and to the lumen (right panels). The pink dashed lines surround SG cells or the lumen. Yellow arrowheads point at centrosomes. (E) On the left, illustrative low magnification immunostaining images of L3 SGs of the indicated genotypes. Centrosomes are shown through the localization of two centrosome markers Plp (grey) and Cnn (Cyan) with DNA in blue. The white squares mark the two SG regions that are shown at higher magnifications on the right as merged panels or as separate panels showing centrosome markers in grey. These regions correspond to a cell (mid panels) and to the lumen (right panels). The pink dashed lines surround SG cells, or the lumen. Yellow arrowheads point at centrosomes. (F) On the left, illustrative low magnification immunostaining images of L3 SGs of the indicated genotypes. Centrosomes are shown through the localization of two centrosome markers- Plp (grey) and γ-tubulin (γ-tub) (red). DNA in blue. The white squares mark the two SG regions that are shown at higher magnifications on the right as merged panels or as separate panels showing centrosome markers in grey. These regions correspond to a cell (mid panels) and to the lumen (right panels). The pink dashed lines surround SG cells, or the lumen. Yellow arrowheads point at centrosomes. For (C) one experiment was quantified and 41 embryos were analyzed.

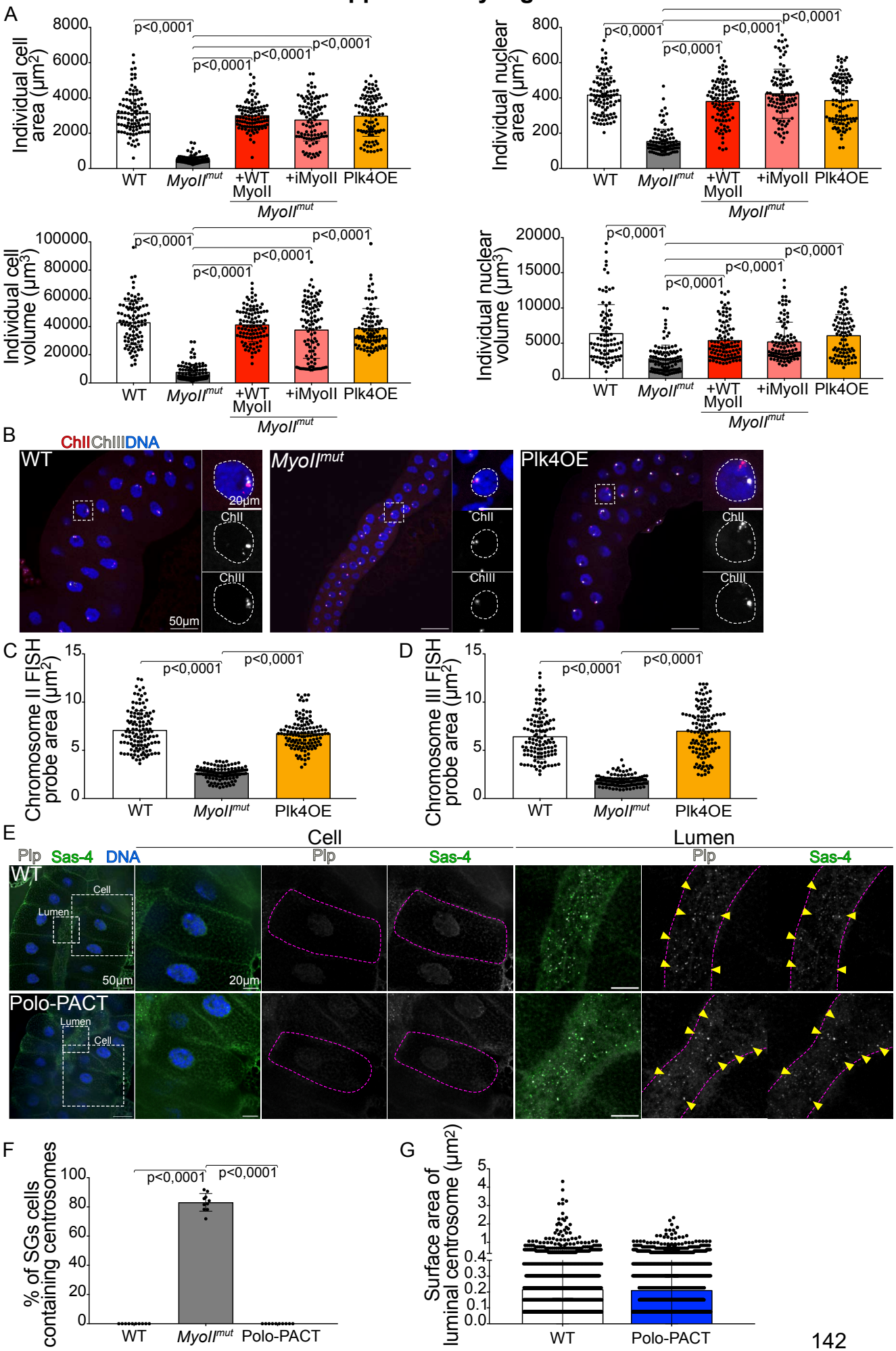
Supplementary Figure 2



Supplementary Figure 2- Characterization of centrosome behavior in larva SGs

(A) Schematic drawing of SGs in L3. On the left an L3 larvae is depicted with anterior positioned at the top. On the right, the SG pair showing a middle view of the polyploid secretory cells with nuclei depicted in blue and the tubular lumen. (B and E) On the left, representative immunostaining images of L3 SGs of the indicated genotypes. Centrosomes in yellow, mCherry-tagged proteins in red and DNA in blue. The white squares mark the luminal regions shown at higher magnification views in the mid panel. On the right, the centrosome channel is shown in grey. Pink dashed lines surround the lumen and yellow arrows point at centrosomes. (C and F) Bar and dot plot graphs showing the individual surface of luminal centrosomes of the indicated genotypes. (D) Representative images obtained by super resolution microscopy of WT luminal centrosomes. iMyoII=inactive MyoII; aMyoII= active MyoII; Statistical significance is shown and determined by ordinary one-way ANOVA tests. Bars show the mean ± SD. For (C), at least three experiments and for (F) four experiments were quantified and 10 SGs were analyzed per condition.

Supplementary Figure 3

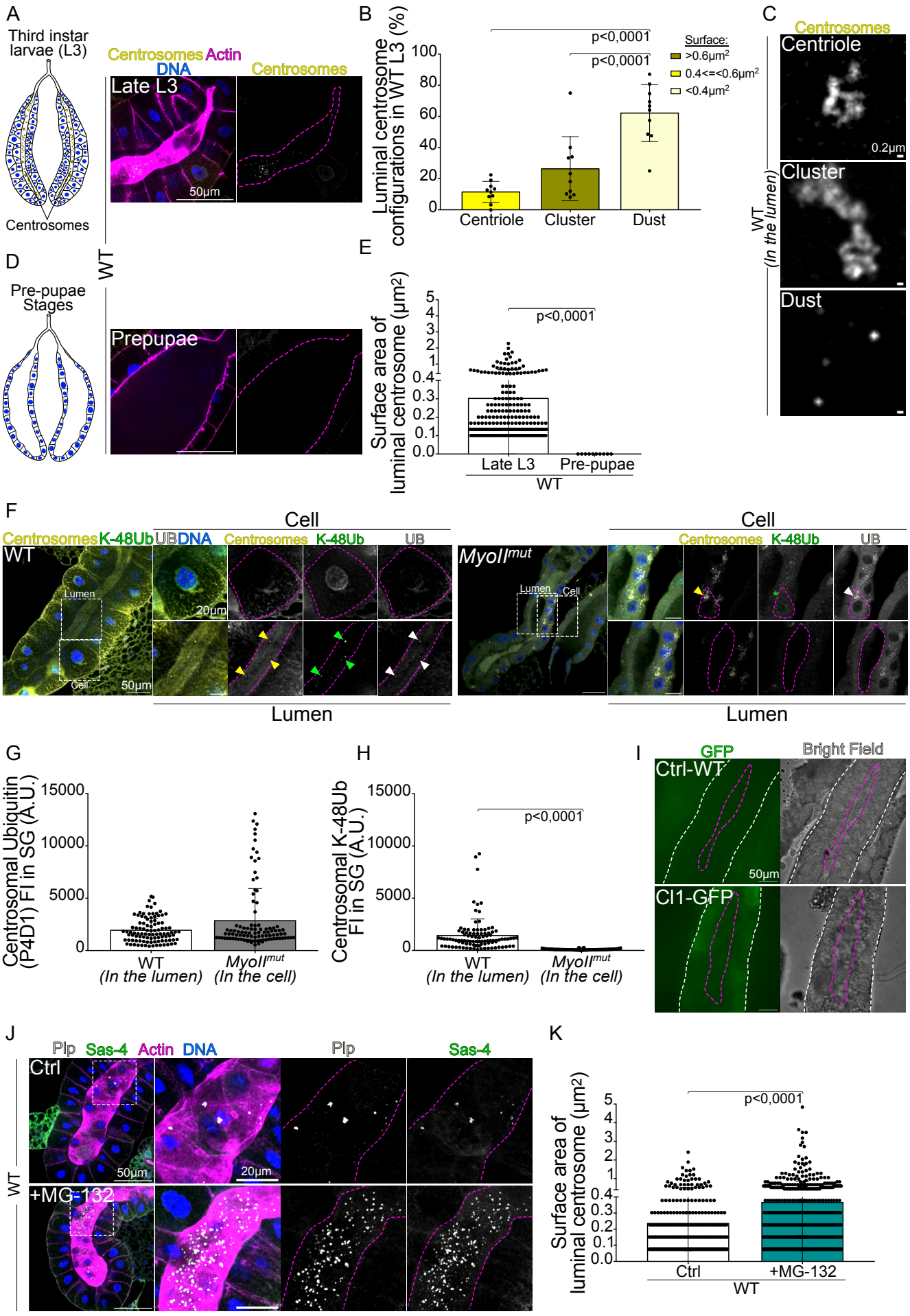


Supplementary Figure 3- Characterization of *MyoII*^{mut} and Plk4OE SGs

(A) Bar and dot plot graphs showing individual cell or nuclear area and volume of the indicated genotypes. (B) Representative immunostaining images of L3 SGs of the indicated genotypes showing FISH probes for Chromosome II (red) and Chromosome III (grey). DNA in blue. The white squares mark the cells shown on the right in merged panels or as separated panels in grey. (C-D) Bar and dot plot graphs showing Chromosome II (C) and Chromosome III (D) FISH probe area of the indicated genotypes. (E) Representative immunostaining images of L3 SGs of the indicated genotypes. Centrosomes are shown through the localization of two centrosome markers Plp (grey) and Sas-4 (green). DNA in blue. The white squares mark the two SG regions that are shown at higher magnifications on the right as merged panels or as separate panels showing centrosome markers in grey. These regions correspond to a cell (mid panels) and to the lumen (right panels). The pink dashed lines surround SG cells or the lumen. Yellow arrowheads point at centrosomes. (F) Bar and dot plot graph showing the percentage of SG cells containing centrosomes in the indicated genotypes. (G) Bar and dot plot graph showing the individual surface of luminal centrosomes of the indicated genotypes.

Statistical significance is shown and determined by ordinary one-way ANOVA tests (A, C, D, F) and Mann-Whitney test (G). Bars show the mean ± SD. For (A, C-D), three experiments and for (F-G) two experiments were quantified, and a minimum of 10 SGs was analyzed per condition.

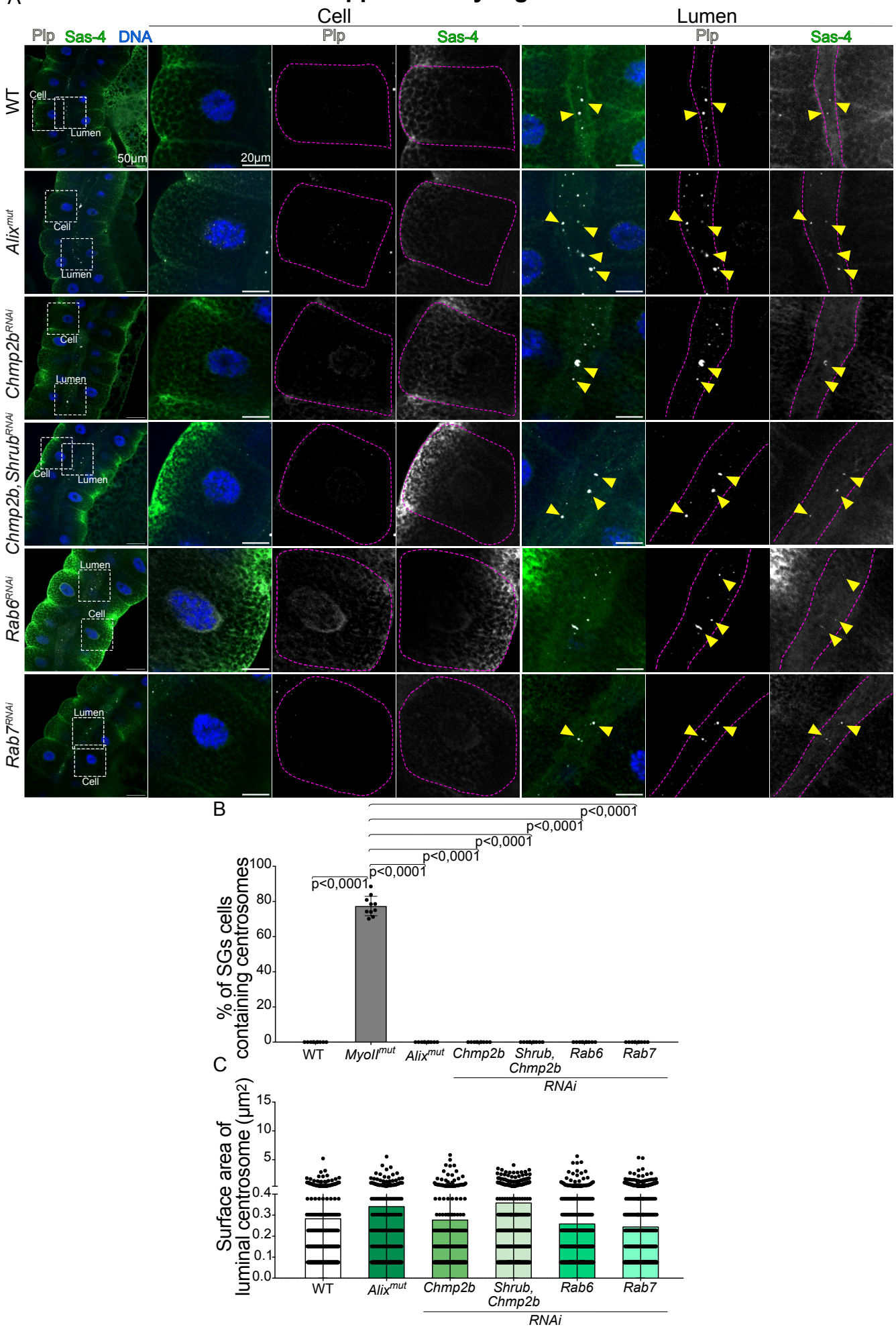
Supplementary Figure 4



Supplementary Figure 4- Centrosomes are degraded in the lumen of WT SGs

(A and D) Schematic drawing of L3 SGs (A) and pre-pupae stages SGs showing centrosomes localizing in a narrow lumen (A) or absent from a wide lumen (D). In both drawings, SGs are depicted with anterior positioned at the top and nuclei in blue. On the right, representative immunostaining images of WT L3 (A) and pre-pupal SGs (D) showing centrosomes in yellow, actin in magenta and DNA in blue in the first panel and centrosomes in the right panel. The pink dashed line marks the lumen. (B) Bar and dot plot graphs showing luminal centrosomal configurations in WT L3. (C) Illustrative super resolution images of luminal centrosomes as indicated. (E) Bar and dot plot graphs showing individual surface of luminal centrosome in WT at the indicated developmental stages. (F) On the left, of each panel representative immunostaining images of L3 SGs of the indicated genotypes. Centrosomes in yellow, K-48Ub and UB markers shown in green and grey respectively with DNA in blue. The white squares mark two regions shown as insets on the right-hand side. These correspond to cells (top) or luminal regions (bottom). Pink dashed lines surround the cell, or the lumen and the colored arrowheads point to the label of the same color. (G-H) Bar and dot plot graphs showing centrosomal P4D1 and K-48Ub FI (A.U.) in the indicated genotypes. (I) Representative images of a SGs expressing the proteasome activity reporter CI1-GFP compared to WT SGs. On the left, the GFP fluorescence is shown and, on the right, the corresponding bright field. The white and pink dashed lines surround SGs and the lumen. (J) Representative immunostaining images of WT L3 treated or not with the proteasome inhibitor MG-132, showing two centrosome markers- Plp (grey), Sas-4 (green), actin (magenta) and DNA in blue. The white squares mark the region shown at higher magnifications on the right as merged channels or individual centrosome labeling in grey channels. (K) Bar and dot plot graphs showing individual surface of luminal centrosome according to the indicated treatment. Statistical significance is shown and determined by ordinary one-way ANOVA tests (B) and Mann-Whitney test (E, G, H and K). Bars show the mean ± SD. For (B) four experiments, (E,G-H) two experiments and for (K) three experiments were quantified, and a minimum of 10 SGs was analyzed per condition.

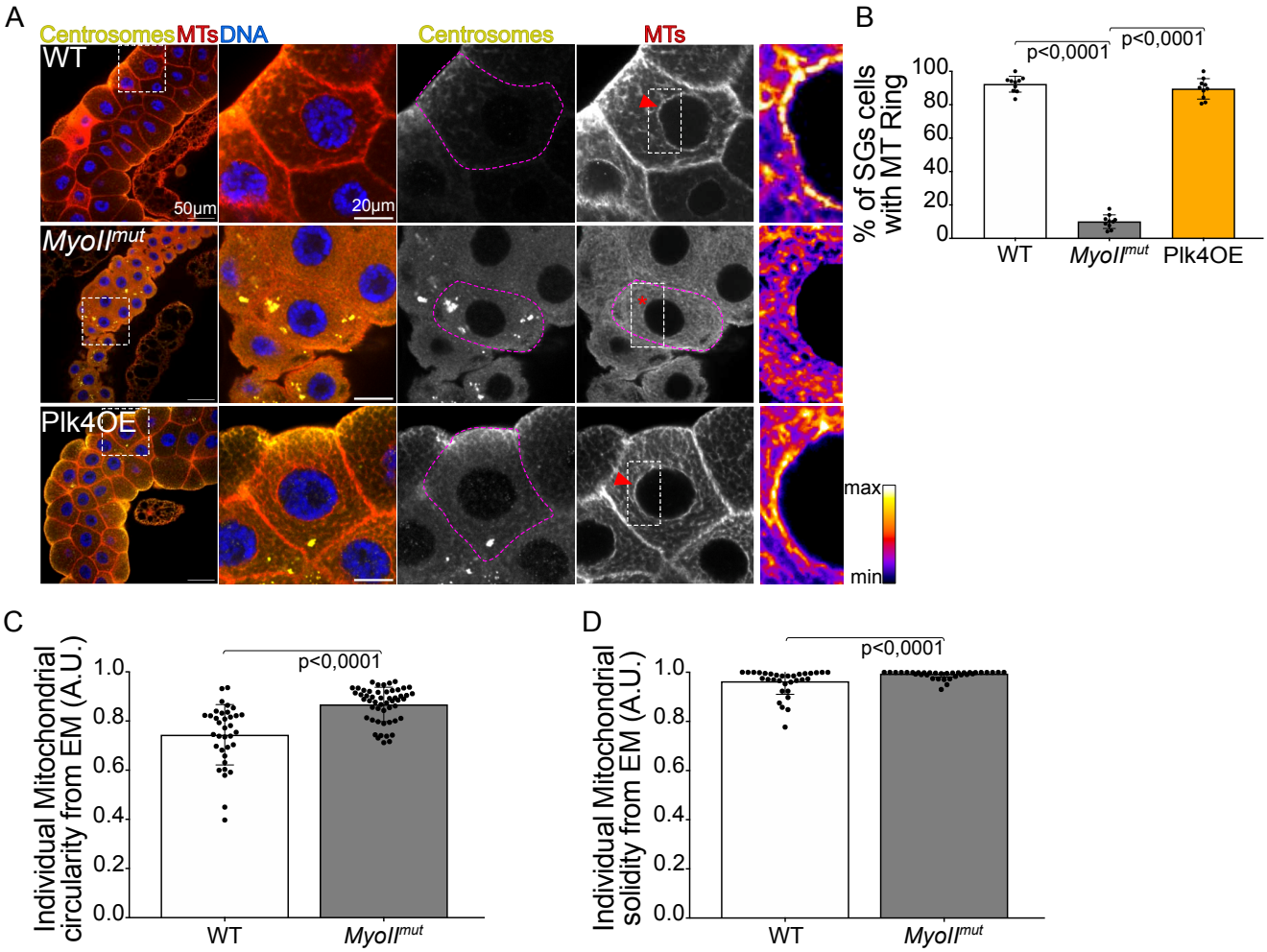
Supplementary Figure 5



Supplementary Figure 5- Analysis of centrosomal markers in different genotypes affecting secretion

(A) On the left, representative low magnification immunostaining images of L3 SGs of the indicated genotypes. Centrosomes are shown as co-localization of two centrosomal markers- Plp (grey) and Sas-4 (green) with DNA in blue. The white squares mark the two SG regions that are shown at higher magnifications on the right as merged panels or as separate panels showing Plp and Sas-4 in grey channels. These regions correspond to a cell (mid panels) and to the lumen (right panels). The dashed pink lines surround the cell, or the lumen and the yellow arrowheads point at centrosomes. (B and C) Bar and dot plot graphs showing the percentage of SGs cells containing centrosomes (B) and surface of luminal centrosome (C) of the indicated genotypes. Statistical significance is shown and determined by ordinary one-way ANOVA tests (B-C). Bars show the mean ± SD. For each graph, two experiments were quantified, and a minimum of 10 SGs was analyzed per condition.

Supplementary Figure 6



Supplementary Figure 6- Analysis of the MT cytoskeleton in SGs

(A) On the left, illustrative low magnification immunostaining images of L3 SGs of the indicated genotypes. Centrosomes in yellow, MTs in red and DNA in blue. The white squares mark a SG cell that is shown at higher magnifications on the right as merged panels or as separate panels showing centrosomes and MTs in grey channels. At the far right, a region displaying fire LUT of MTs is provided. (B) Bar and dot plot graphs showing the percentage of SG cells displaying a MT ring associated with the nuclear envelope in the indicated genotypes. (C and D) Bar and dot plot graphs showing individual mitochondrial circularity (C) and solidity (D) of the indicated genotypes. Statistical significance is shown and determined by ordinary one-way ANOVA test (B) and Mann-Whitney tests (C-D). Bars show the mean ± SD. For (B) three experiments and for (C-D) two experiments were quantified, and a minimum of 10 SGs was analyzed (B) and a minimum of 35 mitochondria (C-D).

Movie 1:

Time-lapse movie of embryos (either whole SG or partial SG) at stage 15-17, expressing Sas-4-GFP (yellow) and MyoII-mCherry (red). Yellow arrowhead pointing to the centrosome exiting the cell toward the lumen. Scale bar (10µm for whole SG and 1µm for the crop) and time interval of 30sec.

Movie 2:

3D reconstruction of WT embryonic SG at stage 13-14, showing the full SG (green), the lumen (magenta) and the centrosomes (color coded based on their distance to the lumen as indicated).

Movie 3:

3D reconstruction of *MyoII*^{mut} embryonic SG at stage 13-14, showing full SG (green), the lumen (magenta) and centrosomes (color coded based on their distance to the lumen as indicated).

Chapter 5 - Discussion

In the results section, I have described a novel mechanism that promotes centrosome elimination in *Drosophila* SG programmed polyploid cells. Interestingly, this process starts during embryogenesis with the release of centrosomes from the cell towards the lumen. This first step is achieved by the secretory autophagy pathway and controlled by MyoII activity. At late larval stages and just before pupariation, these luminal centrosomes are ubiquitinated and degraded by the proteasome. Importantly, centrosome elimination, in this condition, showed a critical role in maintaining metabolic and respiratory activity of the SG polyploid tissue.

1. Why reaching such high level of ploidy?

As I mentioned earlier in the introduction section, SG cells undergo several rounds of endoreplication to reach extreme high levels of ploidy when compared to other cells or tissues in *Drosophila* (Hammond and Laird, 1985; Lee et al., 2009; Rudkin, 1972). Even if we consider the advantages of polyploidy related with cell size parameters or capacity to produce metabolites, SGs appear quite unique. Other secretory tissues, such as the ring gland and fat body, also undergo endoreplication but not to the same extent as SGs (Lee et al., 2009; Orr-Weaver, 2015). This makes SGs a perfect model to study the regulation, characteristics, limitations and the physiological role of extreme polyploidy at the level of an organism.

One plausible explanation for the need of such high ploidy levels, is the functional demand for a high production and storage of secretory vesicles containing glue proteins. These are secreted into the lumen before pupariation (Beňo et al., 2024; Borne et al., 2020; Farkaš, 2016). Interestingly, the excessive rounds on endoreplication, somehow coordinate with the onset of secretory vesicle biogenesis and accumulation, since both processes evolve during L3. This may explain a possible link between both processes. On the other hand, if we consider fat body cells for example, they have lower storage capacity and lower ploidy levels, which are nevertheless sufficient to accomplish limited secretory function.

Another argument to consider is the fact that SG secretory cells must maintain direct contact with the lumen in order to secrete large amounts of glue effectively. Without this level of polyploidization, achieving the desired secretory output would

necessitate a larger number of cells. In this scenario a possible drawback would be the fact that not all cells will be directly connected to the apical membrane of the lumen.

2. Is there a relation between centrosome elimination and endoreplication?

Another common feature among SGs, fat body and ring gland polyploid cells in *Drosophila* is centrosome elimination. Interestingly, these are not the only endoreplicating cells that eliminate their centrosomes. Indeed, the majority of endoreplicating cells eventually lose their centrosomes. This was observed in *Drosophila* follicle cells and midgut, as well as in *C. elegans* intestinal cells (Kalbfuss and Gönczy, 2023a; Lu and Roy, 2014; Mahowald et al., 1979; Mogensen and Tucker, 1987; Schoenfelder et al., 2014; Zheng et al., 2020). However, the functional requirement for an active elimination mechanism, instead of centrosome inactivation or suppression of duplication for example, remains unknown.

It will be interesting to test requirement through the prism of at least two major hypotheses. The first one is that centrosomes are not inactivated or prevented from duplicating if remaining in the SG cells, because proteins involved in centrosome duplication have to be expressed. This would suggest that these proteins may have other functions such as regulating endoreplication or any other process required in these cells. In this context, centrosome elimination serves as a mechanism for the cell to prevent centrosome amplification during multiple rounds of endoreplication in the presence of these proteins. This could be tested by analyzing SG cell size and function in centriole duplication mutant genes such as *Sak/Plk4*, *Sas-6* or *Sas-4*.

The second hypothesis that I would like to test is whether, the endoreplicating cycle signals for centrosome elimination. This could be tested by inducing endoreplication in cells that never undergo endoreplication. Experimentally, this could be induced for example in *Drosophila* wing discs, where knockdown of Cyclin A, or of the transcription factor Myb, promote a switch to endoreplication (Rotelli et al., 2019b, 2019a).

3. Similar mechanisms for centrosome elimination in the fat body and ring gland polyploid cells?

An interesting observation while preforming different experiment during my thesis, was that *MyoII*^{mut} not only impaired centrosome elimination in SG cells but also in the fat body and ring gland cells. In both tissues, multiple centrosomes were distinguished, suggesting that a mechanism dependent on MyoII activity is present beyond SGs. Importantly, we know that these tissues do not contain a lumen and so the way cells in these tissues eliminate centrosomes, has to be different from the mechanisms described here in SG cells (Zhang Y, & and Xi Y., 2015; Quinn, L. et al., 2012).

To study the process of centrosome elimination in these cells, it will be interesting to analyze Atg, SNARE and Rab mutant/RNAi conditions in the fat body and ring gland cells. In addition, live imaging approaches of these tissues would allow to to directly assess the behavior and fate of these centrosomes. This will help to identify if centrosomes are somehow directly released into the hemolymph, like other secretory metabolites produced by these cells, or if they undergo elimination inside the cell as for example in *Drosophila* oocytes (Pimenta-Marques et al., 2016).

4. Direct function of MyoII on centrosomes?

While analyzing hundreds of SGs from different conditions and mutant backgrounds, a consistent unique difference in centrosome organization was observed in *MyoII*^{mut} SG cells. Specifically, centrosomes in *MyoII*^{mut} SG cells were highly clustered, instead of being more dispersed like seen in other conditions. These observations suggest a possible direct role for MyoII in regulating centrosome organization as an essential step for its elimination.

As mentioned above, MyoII is well known for its role during morphogenesis, secretion, cytoskeleton reorganization and autophagosome formation (Guillot and Lecuit, 2013; Masedunskas et al., 2011; Munjal and Lecuit, 2014; Rousso et al., 2016; Tang et al., 2011; Tang and Chen, 2011). Interestingly, certain studies have implicated MyoII in centriole separation and centrosome migration or displacement (Rosenblatt J et al., 2004; Vitiello E et al., 2019). Based on my observations from SG cells, it is tempting to propose that MyoII may have an additional role in promoting centriole

disengagement or promoting in a yet to be identified process - interaction with the autophagy machinery. To investigate this possibility, it will be interesting to increased autophagy in the *MyoII*^{mut} background, which may be achieved through Atg1 or Atg8a over-expression. Further, monitoring the dynamics and behavior of autophagy proteins during the expulsion process should be very informative. In this condition, if centrosomes remain in *MyoII*^{mut} SG cells, this imply that MyoII role in centrosome elimination is somehow through direct effect on the centrosome itself.

5. Why are centrosomes degraded in the lumen? Is there a function in glue biogenesis?

Another intriguing question is why centrosomes undergo this expulsion process into the lumen during embryonic stages to be ultimately degraded by the proteasome at L3 stages, which represents a gap of around 5 days. Since the autophagy and lysosomal pathways are present in these cells, why not simply being used these to promote degradation within the lysosomal compartment in the cell?

A possible explanation, accounting for the spatial and temporal gap between expulsion and degradation is that luminal centrosomes may play a role in glue biogenesis. This hypothesis may be tested by analyzing glue morphology and distribution in *MyoII*^{mut} SGs, where a very low number of centrosomes are detected in the lumen, while the large majority is maintained in cells. By following Sgs3 (Farkaš, 2016; Ji et al., 2018), a glue component, it will be interesting to identify possible defects in glue dynamics or ejection from the lumen to the exterior of the larva.

6. MyoII role in MT nucleation from the NE?

In addition to the maintenance of centrosomes detected in *MyoII*^{mut} SGs, MT nucleation from the NE was impaired in these cells. Initially, I reasoned that this defect resulted from the ectopic presence of centrosomes in the cell, but the lack of MT ring defects in Plk4OE SG cells, suggested otherwise.

Interestingly, MT nucleation or MT ring assembly, appears to be dependent on MyoII, but not on its activity. This is supported by the analysis of the expression of inactive MyoII (iMyoII) in the *MyoII*^{mut} background. In this condition, a MT ring co-

localizing with the NE was detected in the large majority of SG cells, even if centrosomes were maintained. Furthermore, analysis of the tagged versions of MyoII-mcherry and iMyoII-mcherry revealed localization at the NE in co-localization with the MT ring, suggesting that MyoII may have a role in recruiting nucleating factors allowing MT nucleation from the NE.

7. How do centrosomes influence the mitochondrial network?

This study has shown that both *MyoII*^{mut} and Plk4OE SGs showed defects in mitochondria structure and activity. It is however important to understand if this effect solely dependent on the ectopic presence of the centrosomes or if other indirect consequences of lacking MyoII and over-expressing Plk4 can lead to this type of defects. MyoII is implicated in many events has critical roles in cytoskeleton organization (Guillot and Lecuit, 2013; Heer and Martin, 2017; Miao and Blankenship, 2020; Munjal and Lecuit, 2014; Röper, 2013). Further, it is possible that overexpressing a kinase like Plk4 may have other consequences besides centrosome amplification.

To investigate whether the consequences observed on the mitochondria are solely dependent on centrosomes, I could combine both conditions with mutations in the *sas-4* gene (*sas-4*^{mut}). Sas-4 encodes a centriole protein that is essential for centriole duplication, thus *sas-4*^{mut} fail to duplicate centrosomes during *Drosophila* embryonic development (Basto et al., 2006). Indeed, I tried to test this possibility by combining *sas-4*^{mut} with *MyoII*^{mut}, but only rarely obtained larvae. In the few numbers of samples analyzed however, the mitochondria network appeared improved when compared to *MyoII*^{mut} alone. It will be important to analyze Plk4OE, *Sas4*^{mut} SGs and to perform OCR measures in seahorse assays.

While analyzing mitochondria by confocal and super-resolution microscopy, I observed that mitochondria could be noticed clustering in close proximity to centrosomes. Although I am not sure about the impact that this type of mitochondria clusters may have on their function, it is possible that this may affect fission and fusion resulting in respiratory defects as the ones identified by seahorse.

8. Do centrosomes disrupt mitochondrial function by altering the MT cytoskeleton?

Since mitochondria are transported by MTs (López-Doménech et al., 2018; Melkov and Abdu, 2018; Pilling et al., 2006; Smith and Gallo, 2018), it is evident to consider a link between centrosome maintenance, the MT cytoskeleton and the mitochondrial network. As explained above, the lack of any obvious defect in the MT cytoskeleton in Plk4OE SGs does not allow to conclude on such a role, at least in MT nucleation. An alternative possibility is that ectopic centrosomes disrupt MT polarity. To test this hypothesis, I tried to analyze the dynamics of EB1, a conserved plus end MT binding protein, in SG cell with and without centrosomes (Guru et al., 2022; Li et al., 2011; Rogers et al., 2002). However, due to the large size and dense cytoplasm of SG cells, it was technically challenging to detect EB1.

Another way to test this hypothesis would be to impair MT polarity in WT SGs, using genetic or pharmacological methods, such as knocking down motor protein like kinesin or dynein, or by colchicine/nocodazole treatment. Then I assess the impact on mitochondrial structure and metabolic activity. Moreover, these experiments may help to design other experiments where MT polarity defects may be rescued or manipulated at least in *MyoII*^{mut} or Plk4OE SGs.

References

Abdel-Monem, M., Durwald, H., Hoffmann-Berling, H., 1976. Enzymic Unwinding of DNA: 2. Chain Separation by an ATP-Dependent DNA Unwinding Enzyme. Eur J Biochem 65, 441–449. https://doi.org/10.1111/j.1432-1033.1976.tb10359.x

Abmayr, S.M., Pavlath, G.K., 2012. Myoblast fusion: Lessons from flies and mice. Development. https://doi.org/10.1242/dev.068353

Abrams, E.W., Vining, M.S., Andrew, D.J., 2003. Constructing an organ: The Drosophila salivary gland as a model for tube formation. Trends Cell Biol. https://doi.org/10.1016/S0962-8924(03)00055-2

Abreu-Blanco, M.T., Verboon, J.M., Liu, R., Watts, J.J., Parkhurst, S.M., 2012. Drosophila embryos close epithelial wounds using a combination of cellular protrusions and an actomyosin purse string. J Cell Sci 125, 5984–5997. https://doi.org/10.1242/jcs.109066

Adell, M.A.Y., Vogel, G.F., Pakdel, M., Müller, M., Lindner, H., Hess, M.W., Teis, D., 2014. Coordinated binding of Vps4 to ESCRT-III drives membrane neck constriction during MVB vesicle formation. Journal of Cell Biology 205, 33–49. https://doi.org/10.1083/jcb.201310114

Albornoz, N., Bustamante, H., Soza, A., Burgos, P., 2019. Cellular responses to proteasome inhibition: Molecular mechanisms and beyond. Int J Mol Sci 20. https://doi.org/10.3390/ijms20143379

Munden Alexander, Rong Zhan, Sun Amanda, Gangula Rama, Mallal Simon, Nordman Jared T, 2018. Rif1 inhibits replication fork progression and controls DNA copy number in Drosophila. Elife. https://doi.org/10.7554/eLife.39140.001

Aljiboury, A., Hehnly, H., 2023. The centrosome – diverse functions in fertilization and development across species. J Cell Sci. https://doi.org/10.1242/JCS.261387

Almeida, C., Costa, M., Wang, X.-F., Ellsworth, C., Deng, W.-M., 2021. Polyploidy in development and tumor models in Drosophila.

Amano, M., Ito, M., Kimura, K., Fukata, Y., Chihara, K., Nakano, T., Matsuura, Y., Kaibuchi, K., 1996. Phosphorylation and activation of myosin by Rho-associated kinase (Rho- kinase). Journal of Biological Chemistry 271, 20246–20249. https://doi.org/10.1074/jbc.271.34.20246

Anderson, C.T., Stearns, T., 2009. Centriole Age Underlies Asynchronous Primary Cilium Growth in Mammalian Cells. Current Biology 19, 1498–1502. https://doi.org/10.1016/j.cub.2009.07.034

Anderson, R.G.W., 1972. The three-dimensional structure of the basal body from the rhesus monkey oviduct.

Andreas Weiss, A.H.H.J. and C.F.L., 1999. Continuous Cyclin E expression inhibits progression through endoreduplication cycles in Drosophila. Process Safety and Environmental Protection 77, 371–372. https://doi.org/10.1016/s0957-5820(99)70836-0

Andrew, D.J., Henderson, K.D., Seshaiah, P., 2000. Salivary gland development in Drosophila melanogaster.

Aparicio, T., Ibarra, A., Méndez, J., 2006. Cdc45-MCM-GINS, a new power player for DNA replication. Cell Div. https://doi.org/10.1186/1747-1028-1-18

Arias, E.E., Walter, J.C., 2007. Strength in numbers: Preventing rereplication via multiple mechanisms in eukaryotic cells. Genes Dev. https://doi.org/10.1101/gad.1508907

Arnold, I., Pfeiffer, K., Neupert, W., Stuart, R.A., Schä Gger, H., 1998. Yeast mitochondrial F 1 F 0-ATP synthase exists as a dimer: identification of three dimer-specific subunits, The EMBO Journal.

Arroyo, M., Raychaudhuri, P., 1992. Retinoblastoma-repression of E2F-dependent transcription depends on the ability of the retinoblastoma protein to interact with E2F and is abrogated by the adenovirus E1A oncoprotein, Nucleic Acids Research.

Asao, H., Sasaki, Y., Arita, T., Tanaka, N., Endo, K., Kasai, H., Takeshita, T., Endo, Y., Fujita, T., Sugamura, K., 1997. Hrs is associated with STAM, a signal-transducing adaptor molecule. It's suppressive effect on cytokine-induced cell growth. Journal of Biological Chemistry 272, 32785–32791. https://doi.org/10.1074/jbc.272.52.32785

Ashburner, M.R.S.H. and K.G.Golic., 1989. Drosophila - A Laboratory Handbook. 2nd ed. - Cold Spring Harbor Laboratory Press.

Babst, M., 2011. MVB vesicle formation: ESCRT-dependent, ESCRT-independent and everything in between. Curr Opin Cell Biol. https://doi.org/10.1016/j.ceb.2011.04.008

Babst, M., Katzmann, D.J., Estepa-Sabal, E.J., Meerloo, T., Emr, S.D., 2002a. ESCRT-III: An Endosome-Associated Heterooligomeric Protein Complex Required for MVB Sorting, Developmental Cell.

Babst, M., Katzmann, D.J., Snyder, W.B., Wendland, B., Emr, S.D., 2002b. Endosome-Associated Complex, ESCRT-II, Recruits Transport Machinery for Protein Sorting at the Multivesicular Body, Developmental Cell.

Baietti, M.F., Zhang, Z., Mortier, E., Melchior, A., Degeest, G., Geeraerts, A., Ivarsson, Y., Depoortere, F., Coomans, C., Vermeiren, E., Zimmermann, P., David, G., 2012. Syndecan-syntenin-ALIX regulates the biogenesis of exosomes. Nat Cell Biol 14, 677–685. https://doi.org/10.1038/ncb2502

Bailey, E.C., Kobielski, S., Park, J., Losick, V.P., 2021. Polyploidy in tissue repair and regeneration. Cold Spring Harb Perspect Biol 13. https://doi.org/10.1101/cshperspect.a040881

Baines, K.J., Renaud, S.J., 2017. Transcription Factors That Regulate Trophoblast Development and Function, in: Progress in Molecular Biology and Translational Science. Elsevier B.V., pp. 39–88. https://doi.org/10.1016/bs.pmbts.2016.12.003

Bannykh, S.I., Rowe, T., Balch, W.E., 1996. The Organization of Endoplasmic Reticulum Export Complexes.

Barlow, P.W., Sherman, M.I., 1974. Cytological Studies on the Organization of DNA in Giant Trophoblast Nuclei of the Mouse and the Rat.

Barnum, K.J., O'Connell, M.J., 2014. Cell cycle regulation by checkpoints. Methods in Molecular Biology 1170, 29–40. https://doi.org/10.1007/978-1-4939-0888-2_2

Barr, A.R., Gergely, F., 2007. Aurora-A: The maker and breaker of spindle poles. J Cell Sci. https://doi.org/10.1242/jcs.013136

Basto, R., Brunk, K., Vinadogrova, T., Peel, N., Franz, A., Khodjakov, A., Raff, J.W., 2008. Centrosome Amplification Can Initiate Tumorigenesis in Flies. Cell 133, 1032–1042. https://doi.org/10.1016/j.cell.2008.05.039

Basto, R., Lau, J., Vinogradova, T., Gardiol, A., Woods, C.G., Khodjakov, A., Raff, J.W., 2006. Flies without Centrioles. Cell 125, 1375–1386. https://doi.org/10.1016/j.cell.2006.05.025

Bastock, R., St Johnston, D., 2008. Drosophila oogenesis. Current Biology. https://doi.org/10.1016/j.cub.2008.09.011

Batty, P., Gerlich, D.W., 2019. Mitotic Chromosome Mechanics: How Cells Segregate Their Genome. Trends Cell Biol. https://doi.org/10.1016/j.tcb.2019.05.007

Becker, I.C., Wilkie, A.R., Nikols, E., Carminita, E., Roweth, H.G., Tilburg, J., Sciaudone, A.R., Noetzli, L.J., Fatima, F., Couldwell, G., Ray, A., Mogilner, A., Machlus, K.R., Italiano, J.E., 2024. Cell cycle-dependent centrosome clustering precedes proplatelet formation, Sci. Adv.

Bell, S.D., Botchan, M.R., 2013. The minichromosome maintenance replicative helicase. Cold Spring Harb Perspect Biol 5. https://doi.org/10.1101/cshperspect.a012807

Belyaeva, E.S., Zhimulev, I.F., Volkova, E.I., Alekseyenko, A.A., Moshkin, Y.M., Koryakov, D.E., 1998. Su(UR)ES: A gene suppressing DNA underreplication in intercalary and pericentric heterochromatin of Drosophila melanogaster polytene chromosomes, Genetics Communicated by N. P. Dubinin, Russian Academy of Sciences.

Benda C, 1898. Ueber die Spermatogenese der Vertebraten und höherer Evertebraten. II. Theil- Die Histiogenese der Spermien.

Beňo, M., Beňová-Liszeková, D., Kostič, I., Šerý, M., Mentelová, L., Procházka, M., Šoltýs, J., Trusinová, L., Ritomský, M., Orovčík, L., Jerigová, M., Velič, D., Machata, P., Omastová, M., Chase, B.A., Farkaš, R., 2024. Gross morphology and adhesion-associated physical properties of Drosophila larval salivary gland glue secretion. Sci Rep 14. https://doi.org/10.1038/s41598-024-57292-8

Beňová-Liszeková, D., Mentelová, L., Babišová, K., Beňo, M., Pechan, T., Chase, B.A., Farkaš, R., 2021. An apocrine mechanism delivers a fully immunocompetent exocrine secretion. Sci Rep 11. https://doi.org/10.1038/s41598-021-95309-8

Berdnik, D., Knoblich, J.A., 2002. Drosophila Aurora-A Is Required for Centrosome Maturation and Actin-Dependent Asymmetric Protein Localization during Mitosis, Current Biology.

Bertoli, C., Skotheim, J.M., De Bruin, R.A.M., 2013. Control of cell cycle transcription during G1 and S phases. Nat Rev Mol Cell Biol. https://doi.org/10.1038/nrm3629

Bettencourt-Dias, M., Glover, D.M., 2007. Centrosome biogenesis and function: Centrosomics brings new understanding. Nat Rev Mol Cell Biol. https://doi.org/10.1038/nrm2180

Bettencourt-Dias, M., Rodrigues-Martins, A., Carpenter, L., Riparbelli, M., Lehmann, L., Gatt, M.K., Carmo, N., Balloux, F., Callaini, G., Glover, D.M., 2005. SAK/PLK4 is required for centriole duplication and flagella development. Current Biology 15, 2199–2207. https://doi.org/10.1016/j.cub.2005.11.042

Bhat, P., Thorn, P., 2009. Myosin 2 Maintains an Open Exocytic Fusion Pore in Secretory Epithelial Cells. Mol Biol Cell 20, 1795–1803. https://doi.org/10.1091/mbc.E08

Bielski, C.M., Zehir, A., Penson, A. V., Donoghue, M.T.A., Chatila, W., Armenia, J., Chang, M.T., Schram, A.M., Jonsson, P., Bandlamudi, C., Razavi, P., Iyer, G., Robson, M.E., Stadler, Z.K., Schultz, N., Baselga, J., Solit, D.B., Hyman, D.M., Berger, M.F., Taylor, B.S., 2018. Genome doubling shapes the evolution and prognosis of advanced cancers. Nat Genet 50, 1189–1195. https://doi.org/10.1038/s41588-018-0165-1

Bill R. Brinkley, 2001. Managing the centrosome numbers game: from chaos to stability in cancer cell division.

Binh, T.D., Nguyen, Y.D.H., Pham, T.L.A., Komori, K., Nguyen, T.Q.C., Taninaka, M., Kamei, K., 2022. Dysfunction of lipid storage droplet-2 suppresses endoreplication and induces JNK pathway-mediated apoptotic cell death in Drosophila salivary glands. Sci Rep 12. https://doi.org/10.1038/s41598-022-08299-6

Biton, T., Scher, N., Carmon, S., Elbaz-Alon, Y., Schejter, E.D., Shilo, B.Z., Avinoam, O., 2023. Fusion pore dynamics of large secretory vesicles define a distinct mechanism of exocytosis. Journal of Cell Biology 222. https://doi.org/10.1083/jcb.202302112

Blakely, C.M., Watkins, T.B.K., Wu, W., Gini, B., Chabon, J.J., McCoach, C.E., McGranahan, N., Wilson, G.A., Birkbak, N.J., Olivas, V.R., Rotow, J., Maynard, A., Wang, V., Gubens, M.A., Banks, K.C., Lanman, R.B., Caulin, A.F., St John, J., Cordero, A.R., Giannikopoulos, P., Simmons, A.D., MacK, P.C., Gandara, D.R., Husain, H., Doebele, R.C., Riess, J.W., Diehn, M., Swanton, C., Bivona, T.G., 2017. Evolution and clinical impact of co-occurring genetic alterations in advanced-stage EGFR-mutant lung cancers. Nat Genet 49, 1693–1704. https://doi.org/10.1038/ng.3990

Boda, A., Lőrincz, P., Takáts, S., Csizmadia, T., Tóth, S., Kovács, A.L., Juhász, G., 2019. Drosophila Arl8 is a general positive regulator of lysosomal fusion events. Biochim Biophys Acta Mol Cell Res 1866, 533–544. https://doi.org/10.1016/j.bbamcr.2018.12.011

Booth, A.J.R., Blanchard, G.B., Adams, R.J., Röper, K., 2014. A Dynamic microtubule cytoskeleton directs medial actomyosin function during tube formation. Dev Cell 29, 562–576. https://doi.org/10.1016/j.devcel.2014.03.023

Borne, F., Kovalev, A., Gorb, S., Courtier-Orgogozo, V., 2020. The glue produced by Drosophila melanogaster for pupa adhesion is universal. Journal of Experimental Biology 223. https://doi.org/10.1242/jeb.220608

Borrego-Pinto, J., Somogyi, K., Karreman, M.A., König, J., Müller-Reichert, T., Bettencourt-Dias, M., Gönczy, P., Schwab, Y., Lénárt, P., 2016. Distinct mechanisms eliminate mother and daughter centrioles in meiosis of starfish oocytes. Journal of Cell Biology 212, 815–827. https://doi.org/10.1083/jcb.201510083

Bradley, P.L., Myat, M.M., Comeaux, C.A., Andrew, D.J., 2003. Posterior migration of the salivary gland requires an intact visceral mesoderm and integrin function. Dev Biol 257, 249–262. https://doi.org/10.1016/S0012-1606(03)00103-9

Brand, H., Perrimon, N., 1993. Targeted gene expression as a means of altering cell fates and generating dominant phenotypes.

Brault, J., Bardin, S., Lampic, M., Carpentieri, J.A., Coquand, L., Penisson, M., Lachuer, H., Victoria, G.S., Baloul, S., El Marjou, F., Boncompain, G., Miserey-Lenkei, S., Belvindrah, R., Fraisier, V., Francis, F., Perez, F., Goud, B., Baffet, A.D., 2022. RAB6 and dynein drive post-Golgi apical transport to prevent neuronal progenitor delamination . EMBO Rep 23. https://doi.org/10.15252/embr.202254605

Brooks, D.A., Bader, C., Ng, Y.S., Brooks, R.D., Borlace, G.N., Shandal, T., 2012. At the Intersection of the Pathways for Exocytosis and Autophagy, in: Crosstalk and Integration of Membrane Trafficking Pathways. InTech. https://doi.org/10.5772/39111

Brooks, E.R., Wallingford, J.B., 2014. Multiciliated Cells. Current Biology. https://doi.org/10.1016/j.cub.2014.08.047

Brown, G.C., 1992. Control of respiration and ATP synthesis in mammalian mitochondria and cells, Biochem. J.

Brukman, N.G., Uygur, B., Podbilewicz, B., Chernomordik, L. V., 2019. How cells fuse. Journal of Cell Biology. https://doi.org/10.1083/jcb.201901017

Burgers, P.M.J., 2009. Polymerase dynamics at the eukaryotic DNA replication fork. Journal of Biological Chemistry. https://doi.org/10.1074/jbc.R800062200

Burgess, S.A., Yu, S., Walker, M.L., Hawkins, R.J., Chalovich, J.M., Knight, P.J., 2007. Structures of smooth muscle myosin and heavy meromyosin in the folded, shutdown state.

Cabernard, C., 2012. Cytokinesis in Drosophila melanogaster. Cytoskeleton. https://doi.org/10.1002/cm.21060

Callaini, G., Whitfield, W.G.F., Riparbelli, M.G., 1997. Centriole and Centrosome Dynamics during the Embryonic Cell Cycles That Follow the Formation of the Cellular Blastoderm in Drosophila, EXPERIMENTAL CELL RESEARCH.

Calvi, B.R., Lilly, M.A., Spradling, A.C., 1998. Cell cycle control of chorion gene amplification.

Campos-Ortega, J.A.H.V., 1986. The Embryonic Development of Drosophila melanogaster.

Cao, C., Liu, Y., Lehmann, M., 2007. Fork head controls the timing and tissue selectivity of steroid-induced developmental cell death. Journal of Cell Biology 176, 843–852. https://doi.org/10.1083/jcb.200611155

Carter, S.L., Cibulskis, K., Helman, E., McKenna, A., Shen, H., Zack, T., Laird, P.W., Onofrio, R.C., Winckler, W., Weir, B.A., Beroukhim, R., Pellman, D., Levine, D.A., Lander, E.S., Meyerson, M., Getz, G., 2012. Absolute quantification of somatic DNA alterations in human cancer. Nat Biotechnol 30, 413–421. https://doi.org/10.1038/nbt.2203

Casanova, A., Wevers, A., Navarro-Ledesma, S., Pruimboom, L., 2023. Mitochondria: It is all about energy. Front Physiol. https://doi.org/10.3389/fphys.2023.1114231

Casso, D., Âs, F.-A., Ârez-Weber, R., Kornberg, T.B., 2000. GFP-tagged balancer chromosomes for Drosophila melanogaster.

Caviglia, S., Flores-Benitez, D., Lattner, J., Luschnig, S., Brankatschk, M., 2019. Rabs on the fly: Functions of Rab GTPases during development. Small GTPases. https://doi.org/10.1080/21541248.2017.1279725

Chandel, N.S., 2021. Mitochondria. Cold Spring Harb Perspect Biol 13, 1–23. https://doi.org/10.1101/cshperspect.a040543

Chandel, N.S., 2014. Mitochondria as signaling organelles. BMC Biol. https://doi.org/10.1186/1741-7007-12-34

Chandrasekaran, V., Beckendorf, S.K., 2005. Tec29 controls actin remodelling and endoreplication during invagination of the Drosophila embryonic salivary glands. Development 132, 3515–3524. https://doi.org/10.1242/dev.01926

Chandrasekaran, V., Beckendorf, S.K., 2003. Senseless is necessary for the survival of embryonic salivary glands in Drosophila. Development 130, 4719–4728. https://doi.org/10.1242/dev.00677

Chavali, P.L., Chandrasekaran, G., Barr, A.R., Tátrai, P., Taylor, C., Papachristou, E.K., Woods, C.G., Chavali, S., Gergely, F., 2016. A CEP215-HSET complex links centrosomes with spindle poles and drives centrosome clustering in cancer. Nat Commun 7. https://doi.org/10.1038/ncomms11005

Chen, C., Yamashita, Y.M., 2021. Centrosome-centric view of asymmetric stem cell division: Centrosome asymmetry in stem cells. Open Biol. https://doi.org/10.1098/rsob.200314

Chen, D., Frezza, M., Schmitt, S., Kanwar, J., Dou, Q.P., 2011. Bortezomib as the First Proteasome Inhibitor Anticancer Drug: Current Status and Future Perspectives.

Chen, E.H., Olson, E.N., 2004. Towards a molecular pathway for myoblast fusion in Drosophila. Trends Cell Biol. https://doi.org/10.1016/j.tcb.2004.07.008

Chinthalapudi, K., Heissler, S.M., 2024. Structure, regulation, and mechanisms of nonmuscle myosin-2.

Chrétien, D., Buendia, B., Fuller, S.D., Karsenti, E., 1997. Reconstruction of the Centrosome Cycle from Cryoelectron Micrographs.

Claude-Taupin, A., Jia, J., Mudd, M., Deretic, V., 2017. Autophagy's secret life: Secretion instead of degradation. Essays Biochem. https://doi.org/10.1042/EBC20170024

Clurman, B.E., Sheaff, R.J., Thress, K., Groudine, M., Roberts I, J.M., 1995. Turnover of cyclin E by the ubiquitin-proteasome pathway is regulated by cdk2 binding andcyclin phosphorylation.

Coelho, P.A., Bury, L., Shahbazi, M.N., Liakath-Ali, K., Tate, P.H., Wormald, S., Hindley, C.J., Huch, M., Archer, J., Skarnes, W.C., Zernicka-Goetz, M., Glover, D.M., 2015. Over-expression of Plk4 induces centrosome amplification, loss of primary cilia and associated tissue hyperplasia in the mouse. Open Biol 5. https://doi.org/10.1098/rsob.150209

Cohen, C., Parry, D.A.D., 1990. α-Helical coiled coils and bundles: How to design an α-helical protein. Proteins: Structure, Function, and Bioinformatics. https://doi.org/10.1002/prot.340070102

Colombo, M., Moita, C., Van Niel, G., Kowal, J., Vigneron, J., Benaroch, P., Manel, N., Moita, L.F., Théry, C., Raposo, G., 2013. Analysis of ESCRT functions in exosome biogenesis, composition and secretion highlights the heterogeneity of extracellular vesicles. J Cell Sci 126, 5553–5565. https://doi.org/10.1242/jcs.128868

Conduit, P.T., Feng, Z., Richens, J.H., Baumbach, J., Wainman, A., Bakshi, S.D., Dobbelaere, J., Johnson, S., Lea, S.M., Raff, J.W., 2014a. The centrosome-specific phosphorylation of Cnn by Polo/Plk1 drives Cnn scaffold assembly and centrosome maturation. Dev Cell 28, 659–669. https://doi.org/10.1016/j.devcel.2014.02.013

Conduit, P.T., Richens, J.H., Wainman, A., Holder, J., Vicente, C.C., Pratt, M.B., Dix, C.I., Novak, Z.A., Dobbie, I.M., Schermelleh, L., Raff, J.W., 2014b. A molecular mechanism of mitotic centrosome assembly in Drosophila. Elife 3, 1–23. https://doi.org/10.7554/eLife.03399

Conduit, P.T., Wainman, A., Raff, J.W., 2015. Centrosome function and assembly in animal cells. Nat Rev Mol Cell Biol 16, 611–624. https://doi.org/10.1038/nrm4062

Corrigan, L., Redhai, S., Leiblich, A., Fan, S.J., Perera, S.M.W., Patel, R., Gandy, C., Mark Wainwright, S., Morris, J.F., Hamdy, F., Goberdhan, D.C.I., Wilson, C., 2014. BMP-regulated exosomes from Drosophila male reproductive glands reprogram female behavior. Journal of Cell Biology 206, 671–688. https://doi.org/10.1083/jcb.201401072

Craney, A., Rape, M., 2013. Dynamic regulation of ubiquitin-dependent cell cycle control. Curr Opin Cell Biol. https://doi.org/10.1016/j.ceb.2013.07.004

Crown, K.N., Miller, D.E., Sekelsky, J., Hawley, R.S., 2018. Local Inversion Heterozygosity Alters Recombination throughout the Genome. Current Biology 28, 2984-2990.e3. https://doi.org/10.1016/j.cub.2018.07.004

Csizmadia, T., Dósa, A., Farkas, E., Csikos, B.V., Kriska, E.A., Juhász, G., Lőw, P., 2022. Developmental program-independent secretory granule degradation in larval salivary gland cells of Drosophila. Traffic 23, 568–586. https://doi.org/10.1111/tra.12871

Cunha-Ferreira, I., Bento, I., Pimenta-Marques, A., Jana, S.C., Lince-Faria, M., Duarte, P., Borrego-Pinto, J., Gilberto, S., Amado, T., Brito, D., Rodrigues-Martins, A., Debski, J., Dzhindzhev, N., Bettencourt-Dias, M., 2013. Regulation of autophosphorylation controls PLK4 self-destruction and centriole number. Current Biology 23, 2245–2254. https://doi.org/10.1016/j.cub.2013.09.037

Cunha-Ferreira, I., Rodrigues-Martins, A., Bento, I., Riparbelli, M., Zhang, W., Laue, E., Callaini, G., Glover, D.M., Bettencourt-Dias, M., 2009. The SCF/Slimb Ubiquitin Ligase Limits Centrosome Amplification through Degradation of SAK/PLK4. Current Biology 19, 43–49. https://doi.org/10.1016/j.cub.2008.11.037

Curtiss, M., Jones, C., Babst, M., 2007. Efficient Cargo Sorting by ESCRT-I and the Subsequent Release of ESCRT-I from Multivesicular Bodies Requires the Subunit Mvb12 □ D. Mol Biol Cell 18, 636–645. https://doi.org/10.1091/mbc.E06

Hartshorne D J, Ito M, Erdödi F, 1998. Myosin light chain phosphatase: subunit composition, interactions and regulation.

Dang, F., Nie, L., Wei, W., 2021. Ubiquitin signaling in cell cycle control and tumorigenesis. Cell Death Differ. https://doi.org/10.1038/s41418-020-00648-0

D'Angelo, G., Stahl, P.D., Raposo, G., 2025. The cell biology of Extracellular Vesicles: A jigsaw puzzle with a myriad of pieces. Curr Opin Cell Biol. https://doi.org/10.1016/j.ceb.2025.102519

Stock Daniela, Leslie Andrew G. W., Walker John E., 1999. Molecular Architecture of the Rotary Motor in ATP Synthase, Plant Cell.

D'assoro, A.B., Lingle, W.L., Salisbury, J.L., 2002. Centrosome amplification and the development of cancer. Oncogene 21, 6146–6153. https://doi.org/10.1038/sj.onc

D'Avino, P.P., Giansanti, M.G., Petronczki, M., 2015. Cytokinesis in animal cells. Cold Spring Harb Perspect Biol 7. https://doi.org/10.1101/cshperspect.a015834

Davoli, T., De Lange, T., 2011. The causes and consequences of polyploidy in normal development and cancer. Annu Rev Cell Dev Biol 27, 585–610. https://doi.org/10.1146/annurev-cellbio-092910-154234

Dean, S.O., Spudich, J.A., 2006. Rho Kinase's role in Myosin recruitment to the equatorial cortex of mitotic Drosophila S2 cells is for Myosin regulatory light chain phosphorylation. PLoS One 1. https://doi.org/10.1371/journal.pone.0000131

Koepp DM, Schaefer LK, Ye X, Keyomarsi K, Chu C, Harper JW, Elledge SJ., 2001. Phosphorylation-dependent ubiquitination of cyclin E by the SCFFbw7 ubiquitin ligase.

Debec, A., Marcaillou, C., Bobinnec, Y., Borot, C., 1999. The centrosome cycle in syncytial Drosophila embryos analyzed by energy filtering transmission electron microscopy, Biology oj the Cell.

Dej, K.J., Spradling, A.C., 1998. The endocycle controls nurse cell polytene chromosome structure during Drosophila oogenesis.

Delevoye, C., Marks, M.S., Raposo, G., 2019. Lysosome-related organelles as functional adaptations of the endolysosomal system. Curr Opin Cell Biol. https://doi.org/10.1016/j.ceb.2019.05.003

Delgehyr, N., Rangone, H., Fu, J., Mao, G., Tom, B., Riparbelli, M.G., Callaini, G., Glover, D.M., 2012. Klp10A, a microtubule-depolymerizing kinesin-13, cooperates with CP110 to control drosophila centriole length. Current Biology 22, 502–509. https://doi.org/10.1016/j.cub.2012.01.046

Deng, Q., Zeng, Q., Qian, Y., Li, C., Yang, Y., 2007. Research on the Karyotype and Evolution of Drosophila melanogaster Species Group.

Desalvo, M.K., Mayer, N., Mayer, F., Bainton, R.J., 2011. Physiologic and anatomic characterization of the brain surface glia barrier of Drosophila. Glia 59, 1322–1340. https://doi.org/10.1002/glia.21147

Dewar, J.M., Walter, J.C., 2017. Mechanisms of DNA replication termination. Nat Rev Mol Cell Biol. https://doi.org/10.1038/nrm.2017.42

Dewhurst, S.M., McGranahan, N., Burrell, R.A., Rowan, A.J., Grönroos, E., Endesfelder, D., Joshi, T., Mouradov, D., Gibbs, P., Ward, R.L., Hawkins, N.J., Szallasi, Z., Sieber, O.M., Swanton, C., 2014. Tolerance of whole- genome doubling propagates chromosomal instability and accelerates cancer genome evolution. Cancer Discov 4, 175–185. https://doi.org/10.1158/2159-8290.CD-13-0285

Diehl, J.A., Cheng, M., Roussel, M.F., Sherr, C.J., 1995. Glycogen synthase kinase-3 regulates cyclin D1 proteolysis and subcellular localization, Kerkhoff and Rapp.

Dix, C.I., Raff, J.W., 2007. Drosophila Spd-2 Recruits PCM to the Sperm Centriole, but Is Dispensable for Centriole Duplication. Current Biology 17, 1759–1764. https://doi.org/10.1016/j.cub.2007.08.065

Dobbelaere, J., Josué, F., Suijkerbuijk, S., Baum, B., Tapon, N., Raff, J., 2008. A genome-wide RNAi screen to dissect centriole duplication and centrosome maturation in Drosophila. PLoS Biol 6, 1975–1990. https://doi.org/10.1371/journal.pbio.0060224

Donzelli, M., Draetta, G.F., 2003. Regulating mammalian checkpoints through Cdc25 inactivation. EMBO Rep. https://doi.org/10.1038/sj.embor.embor887

Dósa, A., Csizmadia, T., 2022. The role of K63-linked polyubiquitin in several types of autophagy. Biol Futur. https://doi.org/10.1007/s42977-022-00117-4

Dumont, J., Desai, A., 2012. Acentrosomal spindle assembly and chromosome segregation during oocyte meiosis. Trends Cell Biol. https://doi.org/10.1016/j.tcb.2012.02.007

Duncan H. Walker & James L. Maller, 1991. Role for cyclin A in the dependence of mitosis on completion of DNA replication.

Dzhindzhev, N.S., Tzolovsky, G., Lipinszki, Z., Abdelaziz, M., Debski, J., Dadlez, M., Glover, D.M., 2017. Two-step phosphorylation of Ana2 by Plk4 is required for the sequential loading of Ana2 and Sas6 to initiate procentriole formation. Open Biol 7. https://doi.org/10.1098/rsob.170247

Dzhindzhev, N.S., Tzolovsky, G., Lipinszki, Z., Schneider, S., Lattao, R., Fu, J., Debski, J., Dadlez, M., Glover, D.M., 2014. Plk4 phosphorylates ana2 to trigger SAS6 recruitment and procentriole formation. Current Biology 24, 2526–2532. https://doi.org/10.1016/j.cub.2014.08.061

Dzhindzhev, N.S., Yu, Q.D., Weiskopf, K., Tzolovsky, G., Cunha-Ferreira, I., Riparbelli, M., Rodrigues-Martins, A., Bettencourt-Dias, M., Callaini, G., Glover, D.M., 2010. Asterless is a scaffold for the onset of centriole assembly. Nature 467, 714–718. https://doi.org/10.1038/nature09445

Edgar, B.A., 2006. How flies get their size: Genetics meets physiology. Nat Rev Genet. https://doi.org/10.1038/nrg1989

Edgar B A, O'Farrell P H, 1989. Genetic Control of Cell Division Patterns in the Drosophila Embryo, Cell.

Edgar, B.A., Orr-Weaver, T.L., 2001. Endoreplication Cell Cycles: Review More for Less, Cell.

Edgar, B.A., Zielke, N., Gutierrez, C., 2014. Endocycles: A recurrent evolutionary innovation for post-mitotic cell growth. Nat Rev Mol Cell Biol. https://doi.org/10.1038/nrm3756

Edwards, F., Fantozzi, G., Simon, A.Y., Morretton, J.P., Herbette, A., Tijhuis, A.E., Wardenaar, R., Foulane, S., Gemble, S., Spierings, D.C.J., Foijer, F., Mariani, O., Vincent-Salomon, A., Roman-Roman, S., Sastre-Garau, X., Goundiam, O., Basto, R., 2024. Centrosome amplification primes ovarian cancer cells for

apoptosis and potentiates the response to chemotherapy. PLoS Biol 22. https://doi.org/10.1371/journal.pbio.3002759

Edwards, K.A., Chang, X.-J., Kiehart, D.P., 1995. Essential light myosin II chain of Drosophila nonmuscle, Journal of Muscle Research and Cell Motility.

Eggert, U.S., Kiger, A.A., Richter, C., Perlman, Z.E., Perrimon, N., Mitchison, T.J., Field, C.M., 2004. Parallel chemical genetic and genome-wide RNAi screens identify cytokinesis inhibitors and targets. PLoS Biol 2. https://doi.org/10.1371/journal.pbio.0020379

Eikenes, Å.H., Malerød, L., Christensen, A.L., Steen, C.B., Mathieu, J., Nezis, I.P., Liestøl, K., Huynh, J.R., Stenmark, H., Haglund, K., 2015a. ALIX and ESCRT-III Coordinately Control Cytokinetic Abscission during Germline Stem Cell Division In Vivo. PLoS Genet 11. https://doi.org/10.1371/journal.pgen.1004904

Bugnard Elisabeth, Zaal Kristien J M, Ralston Evelyn, 2005. Reorganization of microtubule nucleation during muscle differenciation.

Ellenrieder, L., Dieterle, M.P., Doan, K.N., Mårtensson, C.U., Floerchinger, A., Campo, M.L., Pfanner, N., Becker, T., 2019. Dual Role of Mitochondrial Porin in Metabolite Transport across the Outer Membrane and Protein Transfer to the Inner Membrane. Mol Cell 73, 1056-1065.e7. https://doi.org/10.1016/j.molcel.2018.12.014

Erenpreisa, J., Salmina, K., Huna, A., Jackson, T.R., Vazquez-Martin, A., Cragg, M.S., 2015. The “virgin birth”, polyploidy, and the origin of cancer.

Eskelinen, E.L., 2006. Roles of LAMP-1 and LAMP-2 in lysosome biogenesis and autophagy. Mol Aspects Med. https://doi.org/10.1016/j.mam.2006.08.005

Fangman, W.L., Brewer, B.J., 1992. A Question of Time: Replication Origins of Eukaryotic Chromosomes, Cell.

Farkaš, R., 2016. The Complex Secretions of the Salivary Glands of Drosophila Melanogaster, A Model System.

Farkaš, R., Ďatková, Z., Mentelová, L., Löw, P., Beňová-Liszeková, D., Beňo, M., Sass, M., Řehulka, P., Řehulková, H., Raška, O., Kováčik, L., Šmigová, J., Raška, I., Mechler, B.M., 2014. Apocrine secretion in drosophila salivary glands: Subcellular origin, dynamics, and identification of secretory proteins. PLoS One 9. https://doi.org/10.1371/journal.pone.0094383

Feng, Z., Caballe, A., Wainman, A., Johnson, S., Haensele, A.F.M., Cottee, M.A., Conduit, P.T., Lea, S.M., Raff, J.W., 2017. Structural Basis for Mitotic

Centrosome Assembly in Flies. Cell 169, 1078-1089.e13. https://doi.org/10.1016/j.cell.2017.05.030

Fernández-Moreno, M.A., Farr, C.L., Kaguni, L.S., Garesse, R., 2007. Drosophila melanogaster as a model system to study mitochondrial biology. Methods Mol Biol 372, 33–49. https://doi.org/10.1007/978-1-59745-365-3_3

Finley, D., Sadis, S., Monia, B.P., Boucher, P., Ecker, D.J., Crooke, S.T., Chau3, V., 1994. Inhibition of Proteolysis and Cell Cycle Progression in a Multiubiquitination-Deficient Yeast Mutant, MOLECULAR AND CELLULAR BIOLOGY.

Fischer, J.A., Giniger, E., Maniatis, T., & Ptashne, M., 1988. GAL4 activates transcription in Drosophila.

Fischer, S., rn Windshü gel, B., Horak, D., Holmes, K.C., Smith, J.C., 2005. Structural mechanism of the recovery stroke in the Myosin molecular motor.

Flemming Walther, 1882. Zellsubstanz, Kern und Zelltheilung.

Follette, P.J., Duronio, R.J., O'farrell, P.H., O'farrell, P., 1998. Fluctuations in Cyclin E levels are required for multiple rounds of endocycle S phase in Drosophila. Current Biology 8, 235–238.

Foster, D.A., Yellen, P., Xu, L., Saqcena, M., 2010. Regulation of G1 cell cycle progression: Distinguishing the restriction point from a nutrient-sensing cell growth checkpoint(s). Genes Cancer. https://doi.org/10.1177/1947601910392989

Fourriere, L., Kasri, A., Gareil, N., Bardin, S., Bousquet, H., Pereira, D., Perez, F., Goud, B., Boncompain, G., Miserey-Lenkei, S., 2019. RAB6 and microtubules restrict protein secretion to focal adhesions. Journal of Cell Biology 218, 2215–2231. https://doi.org/10.1083/jcb.201805002

Fox, R.M., Hanlon, C.D., Andrew, D.J., 2010. The CrebA/Creb3-like transcription factors are major and direct regulators of secretory capacity. Journal of Cell Biology 191, 479–492. https://doi.org/10.1083/jcb.201004062

Fox, R.M., Vaishnavi, A., Maruyama, R., Andrew, D.J., 2013. Organ-specific gene expression: The bHLH protein Sage provides tissue specificity to Drosophila FoxA. Development (Cambridge) 140, 2160–2171. https://doi.org/10.1242/dev.092924

Fraenkel, G., Brookes, V.J., 1953. The Process by Which the Puparia of Many Species of Flies Become Fixed to a Substrate.

Fragkos, M., Ganier, O., Coulombe, P., Méchali, M., 2015. DNA replication origin activation in space and time. Nat Rev Mol Cell Biol. https://doi.org/10.1038/nrm4002

Franke, J.D., Boury, A.L., Gerald, N.J., Kiehart, D.P., 2006. Native nonmuscle myosin II stability and light chain binding in Drosophila melanogaster. Cell Motil Cytoskeleton 63, 604–622. https://doi.org/10.1002/cm.20148

Franke, J.D., Montague, R.A., Kiehart, D.P., 2005. Nonmuscle myosin II generates forces that transmit tension and drive contraction in multiple tissues during dorsal closure. Current Biology 15, 2208–2221. https://doi.org/10.1016/j.cub.2005.11.064

Frawley, L.E., Orr-Weaver, T.L., 2015. Polyploidy. Current Biology. https://doi.org/10.1016/j.cub.2015.03.037

Friedberg, E.C., 2006. The eureka enzyme: the discovery of DNA polymerase.

Fu, J., Glover, D.M., 2012. Structured illumination of the interface between centriole and peri-centriolar material. Open Biol 2. https://doi.org/10.1098/rsob.120104

Fu, J., Hagan, I.M., Glover, D.M., 2015. The centrosome and its duplication cycle. Cold Spring Harb Perspect Med 5. https://doi.org/10.1101/cshperspect.a015800

Fu, J., Lipinszki, Z., Rangone, H., Min, M., Mykura, C., Chao-Chu, J., Schneider, S., Dzhindzhev, N.S., Gottardo, M., Riparbelli, M.G., Callaini, G., Glover, D.M., 2016. Conserved molecular interactions in centriole-to-centrosome conversion. Nat Cell Biol 18, 87–99. https://doi.org/10.1038/ncb3274

Fujiwara, K., Pollard, T.D., 1977. Fluorescent antibody localization of myosin in the cytoplasm, cleavage furrows, and mitotic spindle of human cells.

Fujiwara, T., Bandi, M., Nitta, M., Ivanova, E. V., Bronson, R.T., Pellman, D., 2005. Cytokinesis failure generating tetraploids promotes tumorigenesis in p53-null cells. Nature 437, 1043–1047. https://doi.org/10.1038/nature04217

Fulton, C., 1977. Intracellular Regulation of Cell Shape and Motility in Naegleria.First Insights and a Working Hypothesis, Journal of Supramolecular Structure.

Furch, M., Fujita-Becker, S., Geeves, M.A., Holmes, K.C., Manstein, D.J., 1999. Role of the Salt-bridge between Switch-1 and Switch-2 of Dictyostelium Myosin.

Fuse, N., Hirose, S., Hayashi, S., 1994. Diploidy of Drosophila imaginal cells is maintained by a transcriptional repressor encoded by escargot.

Gadde, S., Heald, R., 2004. Mechanisms and molecules of the mitotic spindle. Current Biology. https://doi.org/10.1016/j.cub.2004.09.021

Galletta, B.J., Fagerstrom, C.J., Schoborg, T.A., McLamarrah, T.A., Ryniawec, J.M., Buster, D.W., Slep, K.C., Rogers, G.C., Rusan, N.M., 2016. A centrosome interactome provides insight into organelle assembly and reveals a non-duplication role for Plk4. Nat Commun 7. https://doi.org/10.1038/ncomms12476

Gandarillas, A., Freije, A., 2014. Cycling up the epidermis: Reconciling 100 years of debate. Exp Dermatol 23, 87–91. https://doi.org/10.1111/exd.12287

Gandarillas, A., Sanz-Gómez, N., Freije, A., 2019. Polyploidy and the mitosis path to epidermal cell fate. Cell Cycle. https://doi.org/10.1080/15384101.2019.1568766

Ganem, N.J., Cornils, H., Chiu, S.Y., O'Rourke, K.P., Arnaud, J., Yimlamai, D., Théry, M., Camargo, F.D., Pellman, D., 2014. Cytokinesis failure triggers hippo tumor suppressor pathway activation. Cell 158, 833–848. https://doi.org/10.1016/j.cell.2014.06.029

Ganem, N.J., Godinho, S.A., Pellman, D., 2009. A mechanism linking extra centrosomes to chromosomal instability. Nature 460, 278–282. https://doi.org/10.1038/nature08136

Ganem, N.J., Pellman, D., 2007. Limiting the Proliferation of Polyploid Cells. Cell. https://doi.org/10.1016/j.cell.2007.10.024

Ganem, N.J., Storchova, Z., Pellman, D., 2007. Tetraploidy, aneuploidy and cancer. Curr Opin Genet Dev. https://doi.org/10.1016/j.gde.2007.02.011

Gartenmann, L., Vicente, C.C., Wainman, A., Novak, Z.A., Sieber, B., Richens, J.H., Raff, J.W., 2020. Drosophila Sas-6, Ana2 and Sas-4 self-organise into macromolecular structures that can be used to probe centriole/centrosome assembly. J Cell Sci 133. https://doi.org/10.1242/JCS.244574

Gatti, M., Giansanti, M.G., Bonaccorsi, S., 2000. Relationships Between the Central Spindle and the Contractile Ring During Cytokinesis in Animal Cells, Microsc. Res. Tech.

Gavet, O., Pines, J., 2010. Progressive Activation of CyclinB1-Cdk1 Coordinates Entry to Mitosis. Dev Cell 18, 533–543. https://doi.org/10.1016/j.devcel.2010.02.013

Geley, S., Kramer, E., Gieffers, C., Gannon, J., Peters, J.-M., Hunt, T., 2001. Anaphase-promoting Complex/Cyclosome-dependent Proteolysis of Human

Cyclin A Starts at the Beginning of Mitosis and Is Not Subject to the Spindle Assembly Checkpoint, The Journal of Cell Biology.

Gemble, S., Basto, R., 2020. CHRONOCRISIS: When Cell Cycle Asynchrony Generates DNA Damage in Polyploid Cells. BioEssays 42. https://doi.org/10.1002/bies.202000105

Gemble, S., Wardenaar, R., Keuper, K., Srivastava, N., Nano, M., Macé, A.S., Tijhuis, A.E., Bernhard, S.V., Spierings, D.C.J., Simon, A., Goundiam, O., Hochegger, H., Piel, M., Foijer, F., Storchová, Z., Basto, R., 2022. Genetic instability from a single S phase after whole-genome duplication. Nature 604, 146–151. https://doi.org/10.1038/s41586-022-04578-4

Gentric, G., Desdouets, C., 2014. Polyploidization in liver tissue. American Journal of Pathol-ogy. https://doi.org/10.1016/j.ajpath.2013.06.035ï

Gerlach, S.U., Eichenlaub, T., Herranz, H., 2018. Yorkie and JNK Control Tumorigenesis in Drosophila Cells with Cytokinesis Failure. Cell Rep 23, 1491–1503. https://doi.org/10.1016/j.celrep.2018.04.006

Gerlyng, P., Abyholm, A., Grotmol, T., Erikstein, B., Huitfeldt, H.S., Stokkel, T., Seglen, P. 0, 1993. Binucleation and polyploidization patterns in developmental and regenerative rat liver growth, Cell Prolif.

Pihan German A, Purohit Aruna, Wallace Janice, Knecht Hans, Woda Bruce, Quesenberry Peter, and Doxsey Stephen J, 1998. Centrosome defects and genetic instability in malignant tumors.

Giansanti, M.G., Bucciarelli, E., Bonaccorsi, S., Gatti, M., 2008. Drosophila SPD-2 Is an Essential Centriole Component Required for PCM Recruitment and Astral-Microtubule Nucleation. Current Biology 18, 303–309. https://doi.org/10.1016/j.cub.2008.01.058

Giehl, M., Fabarius, A., Frank, O., Hochhaus, A., Hafner, M., Hehlmann, R., Seifarth, W., 2005. Centrosome aberrations in chronic myeloid leukemia correlate with stage of disease and chromosomal instability. Leukemia 19, 1192–1197. https://doi.org/10.1038/sj.leu.2403779

Gillard, G., Girdler, G., Röper, K., 2021. A release-and-capture mechanism generates an essential non-centrosomal microtubule array during tube budding. Nat Commun 12. https://doi.org/10.1038/s41467-021-24332-0

Giono, L.E., Manfredi, J.J., 2006. The p53 tumor suppressor participates in multiple cell cycle checkpoints. J Cell Physiol. https://doi.org/10.1002/jcp.20689

Girard, F., Strausfeld, U., Fernandez, A., Lamb, N.J.C., 1991. Cyclin A Is Required for the Onset of DNA Replication in Mammalian Fibroblasts, Cell.

Glotzer, M., Murray, A.W., Kirschner, M.W., 1991. Cyclin is degraded by the ubiquitin pathway, NATURE ·.

Godinho, S.A., Basto, R., 2025. Centrosomes and cancer: balancing tumor-promoting and inhibitory roles. Trends Cell Biol. https://doi.org/10.1016/j.tcb.2025.02.009

Gohel, R., Kournoutis, A., Petridi, S., Nezis, I.P., 2020. Molecular mechanisms of selective autophagy in Drosophila, in: International Review of Cell and Molecular Biology. Elsevier Inc., pp. 63–105. https://doi.org/10.1016/bs.ircmb.2019.08.003

Goldstein, D.B., 1992. Heterozygote Advantage and the Evolution of a Dominant Diploid Phase.

Gopalakrishnan, J., Mennella, V., Blachon, S., Zhai, B., Smith, A.H., Megraw, T.L., Nicastro, D., Gygi, S.P., Agard, D.A., Avidor-Reiss, T., 2011. Sas-4 provides a scaffold for cytoplasmic complexes and tethers them in a centrosome. Nat Commun 2. https://doi.org/10.1038/ncomms1367

Goshima, G., Mayer, M., Zhang, N., Stuurman, N., Vale, R.D., 2008. Augmin: A protein complex required for centrosome-independent microtubule generation within the spindle. Journal of Cell Biology 181, 421–429. https://doi.org/10.1083/jcb.200711053

Goshima, G., Nédélec, F., Vale, R.D., 2005. Mechanisms for focusing mitotic spindle poles by minus end-directed motor proteins. Journal of Cell Biology 171, 229–240. https://doi.org/10.1083/jcb.200505107

Gottardo, M., Callaini, G., Riparbelli, M.G., 2015. The Drosophila centriole - conversion of doublets into triplets within the stem cell niche. J Cell Sci 128, 2437–2442. https://doi.org/10.1242/jcs.172627

Goupil, A., Heinen, J.P., Salame, R., Rossi, F., Reina, J., Pennetier, C., Simon, A., Skorski, P., Louzao, A., Bardin, A.J., Basto, R., Gonzalez, C., 2022. Illuminati: a form of gene expression plasticity in Drosophila neural stem cells. Development (Cambridge) 149. https://doi.org/10.1242/dev.200808

Goupil, A., Nano, M., Letort, G., Gemble, S., Edwards, F., Goundiam, O., Gogendeau, D., Pennetier, C., Basto, R., 2020. Chromosomes function as a barrier to mitotic spindle bipolarity in polyploid cells. Journal of Cell Biology 219. https://doi.org/10.1083/JCB.201908006

Gregg, T.G., Mccrate, A., Reveal, G., Hall, S., Rypstra, A.L., 1990. Insectivory and Social Digestion in Drosophila.

Grendler, J., Lowgren, S., Mills, M., Losick, V.P., 2019. Wound-induced polyploidization is driven by Myc and supports tissue repair in the presence of DNA damage. Development (Cambridge) 146. https://doi.org/10.1242/dev.173005

Grice, G.L., Nathan, J.A., 2016a. The recognition of ubiquitinated proteins by the proteasome. Cellular and Molecular Life Sciences. https://doi.org/10.1007/s00018-016-2255-5

Gruss, O.J., 2018. Animal female meiosis: The challenges of eliminating centrosomes. Cells 7. https://doi.org/10.3390/cells7070073

Gu, Y., Princely Abudu, Y., Kumar, S., Bissa, B., Choi, S.W., Jia, J., Lazarou, M., Eskelinen, E., Johansen, T., Deretic, V., 2019. Mammalian Atg8 proteins regulate lysosome and autolysosome biogenesis through SNARE s . EMBO J 38. https://doi.org/10.15252/embj.2019101994

Guarner, A., Morris, R., Korenjak, M., Boukhali, M., Zappia, M.P., Van Rechem, C., Whetstine, J.R., Ramaswamy, S., Zou, L., Frolov, M. V., Haas, W., Dyson, N.J., 2017. E2F/DP Prevents Cell-Cycle Progression in Endocycling Fat Body Cells by Suppressing dATM Expression. Dev Cell 43, 689-703.e5. https://doi.org/10.1016/j.devcel.2017.11.008

Guidotti, J.E., Brégerie, O., Robert, A., Debey, P., Brechot, C., Desdouets, C., 2003. Liver cell polyploidization: A pivotal role for binuclear hepatocytes. Journal of Biological Chemistry 278, 19095–19101. https://doi.org/10.1074/jbc.M300982200

Guillot, C., Lecuit, T., 2013. Mechanics of Epithelial Tissue Homeostasis and Morphogenesis.

Gunawardane, R.N., Martin, O.C., Cao, K., Zhang, L., Dej, K., Iwamatsu, A., Zheng, Y., 2000. Characterization and Reconstitution of Drosophila-Tubulin Ring Complex Subunits, The Journal of Cell Biology.

Guo, E.Z., Xu, Z., 2015. Distinct mechanisms of recognizing endosomal sorting complex required for transport III (ESCRT-III) protein IST1 by different microtubule interacting and trafficking (MIT) domains. Journal of Biological Chemistry 290, 8396–8408. https://doi.org/10.1074/jbc.M114.607903

Guo, H. qin, Gao, M., Ma, J., Xiao, T., Zhao, L. lin, Gao, Y., Pan, Q. jing, 2007. Analysis of the cellular centrosome in fine-needle aspirations of the breast. Breast Cancer Res 9. https://doi.org/10.1186/bcr1752

Guo, X., Macleod, G.T., Wellington, A., Hu, F., Panchumarthi, S., Schoenfield, M., Marin, L., Charlton, M.P., Atwood, H.L., Zinsmaier, K.E., 2005. The GTPase dMiro is required for axonal transport of mitochondria to drosophila synapses. Neuron 47, 379–393. https://doi.org/10.1016/j.neuron.2005.06.027

Guru, A., Saravanan, S., Sharma, D., Narasimha, M., 2022. The microtubule end-binding proteins EB1 and Patronin modulate the spatiotemporal dynamics of myosin and pattern pulsed apical constriction. Development (Cambridge) 149. https://doi.org/10.1242/dev.199759

Habedanck, R., Stierhof, Y.D., Wilkinson, C.J., Nigg, E.A., 2005. The Polo kinase Plk4 functions in centriole duplication. Nat Cell Biol 7, 1140–1146. https://doi.org/10.1038/ncb1320

Haberman, A.S., Isaac, D.D., Andrew, D.J., 2003. Specification of cell fates within the salivary gland primordium. Dev Biol 258, 443–453. https://doi.org/10.1016/S0012-1606(03)00140-4

Halfon, M.S., Gisselbrecht, S., Lu, J., Estrada, B., Keshishian, H., Michelson, A.M., 2002. New fluorescent protein reporters for use with the Drosophila Gal4 expression system and for vital detection of balancer chromosomes. Genesis (United States) 34, 135–138. https://doi.org/10.1002/gene.10136

Hammond, M.P., Laird, C.D., 1985. Control of DNA replication and spatial distribution of defined DNA sequences in salivary gland cells of Drosophila melanogaster.

Hamzah, M., Meitinger, F., Ohta, M., 2025. PLK4: Master Regulator of Centriole Duplication and Its Therapeutic Potential. Cytoskeleton. https://doi.org/10.1002/cm.22031

Han, H., Monroe, N., Votteler, J., Shakya, B., Sundquist, W.I., Hill, C.P., 2015. Binding of substrates to the central pore of the Vps4 ATPase is autoinhibited by the Microtubule Interacting and Trafficking (MIT) domain and activated by MIT Interacting Motifs (MIMs). Journal of Biological Chemistry 290, 13490–13499. https://doi.org/10.1074/jbc.M115.642355

Hannaford, M.R., Rusan, N.M., 2024. Positioning centrioles and centrosomes. Journal of Cell Biology. https://doi.org/10.1083/jcb.202311140

Hartenstein, V., Campos-Ortega, J.A., 1984. Early neurogenesis in wild-type Drosophila melanogaster, Arch Dev Biol.

Hartwell, L.H., Weinert, T.A., 1989. Checkpoints: Controls That Ensure the Order of Cell Cycle Events.

Hassel, C., Zhang, B., Dixon, M., Calvi, B.R., 2014. Induction of endocycles represses apoptosis independently of differentiation and predisposes cells to genome instability. Development (Cambridge) 141, 112–123. https://doi.org/10.1242/dev.098871

Hayward, D., Wakefield, J.G., 2014. Chromatin-mediated microtubule nucleation in Drosophila syncytial embryos. Commun Integr Biol 7. https://doi.org/10.4161/cib.28512

Heald, R., Tournebize, R., Habermann, A., Karsenti, E., Hyman, A., 1997. Spindle assembly in Xenopus egg extracts: Respective roles of centrosomes and microtubule self-organization. Journal of Cell Biology 138, 615–628. https://doi.org/10.1083/jcb.138.3.615

Hedgecock' And, E.M., White, J.G., 1985. Polyploid Tissues in the Nematode Caenorhabditis elegans, DEVELOPMENTAL BIOLOGY.

Heer, N.C., Martin, A.C., 2017. Tension, contraction and tissue morphogenesis. Development (Cambridge). https://doi.org/10.1242/dev.151282

Heissler, S.M., Manstein, D.J., 2013. Nonmuscle myosin-2: Mix and match. Cellular and Molecular Life Sciences. https://doi.org/10.1007/s00018-012-1002-9

Henderson, K.D., Andrew, D.J., 2000. Regulation and function of Scr, exd, and hth in the Drosophila salivary gland. Dev Biol 217, 362–374. https://doi.org/10.1006/dbio.1999.9560

Henderson, K.D., Isaac, D.D., Andrew, D.J., 1999. Cell Fate Specification in the Drosophila Salivary Gland: The Integration of Homeotic Gene Function with the DPP Signaling Cascade.

Henne, W.M., Buchkovich, N.J., Emr, S.D., 2011. The ESCRT Pathway. Dev Cell. https://doi.org/10.1016/j.devcel.2011.05.015

Herriage, H.C., Calvi, B.R., 2024. Premature endocycling of Drosophila follicle cells causes pleiotropic defects in oogenesis. Genetics 226. https://doi.org/10.1093/genetics/iyae009

Hershko, A., Pines, J., Tyers, M., Diffley, D.F.X., Yanagida, M., 1999. Mechanisms and regulation of the degradation of cyclin B, Endicott Source: Philosophical Transactions: Biological Sciences.

Hessvik, N.P., Llorente, A., 2018. Current knowledge on exosome biogenesis and release. Cellular and Molecular Life Sciences. https://doi.org/10.1007/s00018-017-2595-9

Hinnant, T.D., Merkle, J.A., Ables, E.T., 2020. Coordinating Proliferation, Polarity, and Cell Fate in the Drosophila Female Germline. Front Cell Dev Biol. https://doi.org/10.3389/fcell.2020.00019

Hirose, K., Payumo, A.Y., Cutie, S., Hoang, A., Zhang, H., Guyot, R., Lunn, D., Bigley, R.B., Yu, H., Wang, J., Smith, M., Gillett, E., Muroy, S.E., Schmid, T., Wilson, E., Field, K.A., Reeder, D.M., Maden, M., Yartsev, M.M., Wolfgang, M.J., Grützner, F., Scanlan, T.S., Szweda, L.I., Buffenstein, R., Hu, G., Flamant, F., Olgin, J.E., Huang, G.N., 2019. Evidence for hormonal control of heart regenerative capacity during endothermy acquisition.

Holdgaard, S.G., Cianfanelli, V., Pupo, E., Lambrughi, M., Lubas, M., Nielsen, J.C., Eibes, S., Maiani, E., Harder, L.M., Wesch, N., Foged, M.M., Maeda, K., Nazio, F., de la Ballina, L.R., Dötsch, V., Brech, A., Frankel, L.B., Jäättelä, M., Locatelli, F., Barisic, M., Andersen, J.S., Bekker-Jensen, S., Lund, A.H., Rogov, V. V., Papaleo, E., Lanzetti, L., De Zio, D., Cecconi, F., 2019. Selective autophagy maintains centrosome integrity and accurate mitosis by turnover of centriolar satellites. Nat Commun 10. https://doi.org/10.1038/s41467-019-12094-9

Hopfner, K.P., 2003. Chromosome Cohesion: Closing Time. Current Biology. https://doi.org/10.1016/j.cub.2003.10.045

Hroudová, J., Fišar, Z., 2013. Control mechanisms in mitochondrial oxidative phosphorylation. Neural Regen Res 8, 363–375. https://doi.org/10.3969/j.issn.1673-5374.2013.04.009

Hsu, W. Bin, Hung, L.Y., Tang, C.J.C., Su, C.L., Chang, Y., Tang, T.K., 2008. Functional characterization of the microtubule-binding and -destabilizing domains of CPAP and d-SAS-4. Exp Cell Res 314, 2591–2602. https://doi.org/10.1016/j.yexcr.2008.05.012

Hutagalung, A.H., Novick, P.J., 2011. Role of Rab GTPases in Membrane Traffic and Cell Physiology. https://doi.org/10.1152/physrev.00059.2009.-Intracellular

Hüttemann, M., Pecina, P., Rainbolt, M., Sanderson, T.H., Kagan, V.E., Samavati, L., Doan, J.W., Lee, I., 2011. The multiple functions of cytochrome c and their

regulation in life and death decisions of the mammalian cell: From respiration to apoptosis. Mitochondrion. https://doi.org/10.1016/j.mito.2011.01.010

Huynh, K.K., Eskelinen, E.L., Scott, C.C., Malevanets, A., Saftig, P., Grinstein, S., 2007. LAMP proteins are required for fusion of lysosomes with phagosomes. EMBO Journal 26, 313–324. https://doi.org/10.1038/sj.emboj.7601511

Hyun, S., 2018. Body size regulation by maturation steroid hormones: A Drosophila perspective. Front Zool. https://doi.org/10.1186/s12983-018-0290-9

Vorobjev I . A., and Chentsov Yu. S., 1982. Centrioles in the Cell Cycle. I. Epithelial Cells.

Ibrahim, R., Messaoudi, C., Chichon, F.J., Celati, C., Marco, S., 2009. Electron tomography study of isolated human centrioles. Microsc Res Tech 72, 42–48. https://doi.org/10.1002/jemt.20637

Irish, V.F., Gelbart, W.M., 1987. The decapentaplegic gene is required for dorsal-ventral patterning of the Drosophila embryo.

Isaac, D.D., Andrew, D.J., 1996. Tubulogenesis in Drosophila: a requirement for the trachealess gene product.

Rayment I, Rypniewski W R., Schmidt-Bdse K, Smith R, Tomchick D R., Benning M M., Winkelmann D A., Wesenberg G, Holden H M., 1993. Three-Dimensional Structure of Myosin Subfragment- 1- A Molecular Motor.

Jain, A., Rusten, T.E., Katheder, N., Elvenes, J., Bruun, J.A., Sjøttem, E., Lamark, T., Johansen, T., 2015. P62/sequestosome-1, autophagy-related gene 8, and autophagy in Drosophila are regulated by nuclear factor erythroid 2-related factor 2(NRF2), independent of transcription factor TFEB. Journal of Biological Chemistry 290, 14945–14962. https://doi.org/10.1074/jbc.M115.656116

Januschke, J., Nicolas, E., Compagnon, J., Formstecher, E., Goud, B., Guichet, A., 2007. Rab6 and the secretory pathway affect oocyte polarity in Drosophila. Development 134, 3419–3425. https://doi.org/10.1242/dev.008078

Andersen, J.S., Wilkinson Christopher J., Mayor Thibault, Mortensen Peter, Nigg Erich A. &, Mann Matthias, 2003. Proteomic characterization of the human centrosome by protein correlation profiling. Nature 426, 567–570. https://doi.org/10.1038/nature02163

Ji, S., Samara, N.L., Revoredo, L., Zhang, L., Tran, D.T., Muirhead, K., Tabak, L.A., Ten Hagen, K.G., 2018. A molecular switch orchestrates enzyme specificity and

secretory granule morphology. Nat Commun 9. https://doi.org/10.1038/s41467-018-05978-9

Jiang, Y.H., Wang, H.L., Peng, J., Zhu, Y., Zhang, H.G., Tang, F.Q., Jian, Z., Xiao, Y. Bin, 2020. Multinucleated polyploid cardiomyocytes undergo an enhanced adaptability to hypoxia via mitophagy. J Mol Cell Cardiol 138, 115–135. https://doi.org/10.1016/j.yjmcc.2019.11.155

Jonckheere, A.I., Smeitink, J.A.M., Rodenburg, R.J.T., 2012. Mitochondrial ATP synthase: Architecture, function and pathology. J Inherit Metab Dis. https://doi.org/10.1007/s10545-011-9382-9

Jones Nikolas A. ; Yien Ming Kuo; Y. Henry Sun and Steven K. Beckendorf, 1998. The Drosophila Pax gene eyegone is required for embryonic salivary duct development.

Jordan, P., Karess, R., 1997. Myosin Light Chain-activating Phosphorylation Sites Are Required for Oogenesis in Drosophila, The Journal of Cell Biology.

Jordan, S.N., Canman, J.C., 2012. Rho GTPases in animal cell cytokinesis: An occupation by the one percent. Cytoskeleton. https://doi.org/10.1002/cm.21071

Bolívar J, Huynh J-R, López-Schier H, González C, Johnston D St, and González-Reyes A, 2001. Centrosome migration into the Drosophila oocyte is independent of BicD and egl, and of the organisation of the microtubule cytoskeleton.

Jouaville, L.S., Pinton, P., Bastianutto, C., Rutter, G.A., Rizzuto, R., 1999. Regulation of mitochondrial ATP synthesis by calcium: Evidence for a long-term metabolic priming.

Joubert, F., Puff, N., 2021. Mitochondrial cristae architecture and functions: Lessons from minimal model systems. Membranes (Basel). https://doi.org/10.3390/membranes11070465

Jung, C.H., Ro, S.H., Cao, J., Otto, N.M., Kim, D.H., 2010. MTOR regulation of autophagy. FEBS Lett. https://doi.org/10.1016/j.febslet.2010.01.017

Kadenbach, B., Ramzan, R., Wen, L., Vogt, S., 2010. New extension of the Mitchell Theory for oxidative phosphorylation in mitochondria of living organisms. Biochim Biophys Acta Gen Subj. https://doi.org/10.1016/j.bbagen.2009.04.019

Kalbfuss, N., Gönczy, P., 2023a. Towards understanding centriole elimination. Open Biol. https://doi.org/10.1098/rsob.230222

Kalbfuss, N., Gönczy, P., 2023b. Extensive programmed centriole elimination unveiled in C. elegans embryos.

Kalkan, B.M., Ozcan, S.C., Quintyne, N.J., Reed, S.L., Acilan, C., 2022. Keep Calm and Carry on with Extra Centrosomes. Cancers (Basel). https://doi.org/10.3390/cancers14020442

Kamada, Y., Yoshino, K., Kondo, C., Kawamata, T., Oshiro, N., Yonezawa, K., Ohsumi, Y., 2010. Tor Directly Controls the Atg1 Kinase Complex To Regulate Autophagy. Mol Cell Biol 30, 1049–1058. https://doi.org/10.1128/mcb.01344-09

Kandoth, C., McLellan, M.D., Vandin, F., Ye, K., Niu, B., Lu, C., Xie, M., Zhang, Q., McMichael, J.F., Wyczalkowski, M.A., Leiserson, M.D.M., Miller, C.A., Welch, J.S., Walter, M.J., Wendl, M.C., Ley, T.J., Wilson, R.K., Raphael, B.J., Ding, L., 2013. Mutational landscape and significance across 12 major cancer types. Nature 502, 333–339. https://doi.org/10.1038/nature12634

Kannangara, J.R., Mirth, C.K., Warr, C.G., 2021. Regulation of ecdysone production in Drosophila by neuropeptides and peptide hormones. Open Biol. https://doi.org/10.1098/rsob.200373

Karabay, A., Walker, R.A., 1999. The Ncd Tail Domain Promotes Microtubule Assembly and Stability, Biochemical and Biophysical Research Communications.

Karess, R.E., Chang, X.-J., Edwards, K.A., Kulkarni, S., Aguilera, I., Kiehartt, D.P., 1991. The Regulatory Light Chain of Nonmuscle Myosin Is Encoded by spagheWsquash, a Gene Required for Cytokinesis in Drosophila, Cell.

Kasai, H., Takahashi, N., Tokumaru, H., 2012. Distinct initial SNARE configurations underlying the diversity of exocytosis. Physiol Rev 92, 1915–1964. https://doi.org/10.1152/physrev.00007.2012.-The

Katzmann, D.J., Babst, M., Emr, S.D., 2001. Ubiquitin-dependent sorting into the multivesicular body pathway requires the function of a conserved endosomal protein sorting complex, ESCRT-I. Cell 106, 145–155. https://doi.org/10.1016/S0092-8674(01)00434-2

Kazushi Kimura, M.I.M.A.K.C.Y.F.M.N.B.Y.J.F.T.N.K.O.A.I.K.K., 1996. Regulation of Myosin Phosphatase by Rho and Rho-Associated Kinase (Rho-Kinase).

Kerman, B.E., Cheshire, A.M., Andrew, D.J., 2006. From fate to function: The Drosophila trachea and salivary gland as models for tubulogenesis. Differentiation 74, 326–348. https://doi.org/10.1111/j.1432-0436.2006.00095.x

Khodjakov, A., Rieder, C.L., 1999. The Sudden Recruitment of-Tubulin to the Centrosome at the Onset of Mitosis and its Dynamic Exchange Throughout the Cell Cycle, Do Not Require Microtubules, The Journal of Cell Biology.

Kim, M., Sandford, E., Gatica, D., Qiu, Y., Liu, X., Zheng, Y., Schulman, B.A., Xu, J., Semple, I., Ro, S.H., Kim, B., Mavioglu, R.N., Tolun, A., Jipa, A., Takats, S., Karpati, M., Li, J.Z., Yapici, Z., Juhasz, G., Lee, J.H., Klionsky, D.J., Burmeister, M., 2016. Mutation in ATG5 reduces autophagy and leads to ataxia with developmental delay. Elife 5. https://doi.org/10.7554/eLife.12245.001

Kirsch-Volders, M., Mišík, M., Fenech, M., 2025. Tetraploidy in normal tissues and diseases: mechanisms and consequences. Chromosoma. https://doi.org/10.1007/s00412-025-00829-1

Kitagawa, D., Vakonakis, I., Olieric, N., Hilbert, M., Keller, D., Olieric, V., Bortfeld, M., Erat, M.C., Flückiger, I., Gönczy, P., Steinmetz, M.O., 2011. Structural basis of the 9-fold symmetry of centrioles. Cell 144, 364–375. https://doi.org/10.1016/j.cell.2011.01.008

Klämbt, C., Jacobs, J.R., Goodman, C.S., 1991. The Midline of the Drosophila Central Nervous System: A Model for the Genetic Analysis of Cell Fate, Cell Migration, and Growth Cone Guidance, Cell.

Klionsky, D.J., Cregg, J.M., Dunn, W.A., Emr, S.D., 2003. A Unified Nomenclature for Yeast Autophagy-Related Genes, Developmental Cell.

Kohlmaier, G., Lončarek, J., Meng, X., McEwen, B.F., Mogensen, M.M., Spektor, A., Dynlacht, B.D., Khodjakov, A., Gönczy, P., 2009. Overly Long Centrioles and Defective Cell Division upon Excess of the SAS-4-Related Protein CPAP. Current Biology 19, 1012–1018. https://doi.org/10.1016/j.cub.2009.05.018

Koppole, S., Smith, J.C., Fischer, S., 2007. The Structural Coupling between ATPase Activation and Recovery Stroke in the Myosin II Motor. Structure 15, 825–837. https://doi.org/10.1016/j.str.2007.06.008

Kraft, C., Kijanska, M., Kalie, E., Siergiejuk, E., Lee, S.S., Semplicio, G., Stoffel, I., Brezovich, A., Verma, M., Hansmann, I., Ammerer, G., Hofmann, K., Tooze, S., Peter, M., 2012. Binding of the Atg1/ULK1 kinase to the ubiquitin-like protein Atg8 regulates autophagy. EMBO Journal 31, 3691–3703. https://doi.org/10.1038/emboj.2012.225

Krämer, A., Maier, B., Bartek, J., 2011. Centrosome clustering and chromosomal (in)stability: A matter of life and death. Mol Oncol. https://doi.org/10.1016/j.molonc.2011.05.003

Krämer, A., Neben, K., Ho, A.D., 2005. Centrosome aberrations in hematological malignancies. Cell Biol Int. https://doi.org/10.1016/j.cellbi.2005.03.004

Kudryavtsev, B.N., Kudryavtseva, M. V, Sakuta, G.A., Stein, G.I., 1993. Virchow Archiv B Cell Pathology Including Molecular Padtolo~ Human hepatocyte polyploidization kinetics in the course of life cycle, Virchows Archiv B Cell Pathol.

Kühlbrandt, W., 2015. Structure and function of mitochondrial membrane protein complexes. BMC Biol. https://doi.org/10.1186/s12915-015-0201-x

Kulukiana, A., Holland, A.J., Vitrec, B., Naika, S., Cleveland, D.W., Fuchsa, E., 2015. Epidermal development, growth control, and homeostasis in the face of centrosome amplification. Proc Natl Acad Sci U S A 112, E6311–E6320. https://doi.org/10.1073/pnas.1518376112

Kuo Y M, Jones N, Zhou B, Panzer S, Larson V, Beckendorf S K, 1996. Salivary duct determination in Drosophila Roles of the EGF receptor signalling pathway and the transcription factors fork head and trachealess.

Kuznetsova, A.Y., Seget, K., Moeller, G.K., de Pagter, M.S., de Roos, J.A.D.M., Dürrbaum, M., Kuffer, C., Müller, S., Zaman, G.J.R., Kloosterman, W.P., Storchová, Z., 2015. Chromosomal instability, tolerance of mitotic errors and multidrug resistance are promoted by tetraploidization in human cells. Cell Cycle 14, 2810–2820. https://doi.org/10.1080/15384101.2015.1068482

Kwon, M., Godinho, S.A., Chandhok, N.S., Ganem, N.J., Azioune, A., Thery, M., Pellman, D., 2008. Mechanisms to suppress multipolar divisions in cancer cells with extra centrosomes. Genes Dev 22, 2189–2203. https://doi.org/10.1101/gad.1700908

Lam, G., Nam, H.J., Velentzas, P.D., Baehrecke, E.H., Thummel, C.S., 2022. Drosophila E93 promotes adult development and suppresses larval responses to ecdysone during metamorphosis. Dev Biol 481, 104–115. https://doi.org/10.1016/j.ydbio.2021.10.001

Lara-Gonzalez, P., Westhorpe, F.G., Taylor, S.S., 2012. The spindle assembly checkpoint. Current Biology. https://doi.org/10.1016/j.cub.2012.10.006

Lata, S., Mishra, R., Banerjea, A.C., 2018. Proteasomal degradation machinery: Favorite target of HIV-1 proteins. Front Microbiol 9. https://doi.org/10.3389/fmicb.2018.02738

Lata, S., Schoehn, G., Jain, A., Pires, R., Piehler, J., Gottlinger, H.G., Weissenhorn, W., 2008. Helical structures of ESCRT-III are disassembled by VPS4. Science (1979) 321, 1354–1357. https://doi.org/10.1126/science.1161070

Lattao, R., Kovács, L., Glover, D.M., 2017. The centrioles, centrosomes, basal bodies, and cilia of Drosophila melanogaster. Genetics 206, 33–53. https://doi.org/10.1534/genetics.116.198168

Laver, J.D., Marsolais, A.J., Smibert, C.A., Lipshitz, H.D., 2015. Regulation and Function of Maternal Gene Products During the Maternal-to-Zygotic Transition in Drosophila, in: Current Topics in Developmental Biology. Academic Press Inc., pp. 43–84. https://doi.org/10.1016/bs.ctdb.2015.06.007

Leber, B., Maier, B., Fuchs, F., Chi, J., Riffel, P., Anderhub, S., Wagner, L., Ho, A.D., Salisbury, J.L., Boutros, M., Krämer, A., 2010. Proteins required for centrosome clustering in cancer cells. Sci Transl Med 2. https://doi.org/10.1126/scitranslmed.3000915

Lécuyer, E., Yoshida, H., Parthasarathy, N., Alm, C., Babak, T., Cerovina, T., Hughes, T.R., Tomancak, P., Krause, H.M., 2007. Global Analysis of mRNA Localization Reveals a Prominent Role in Organizing Cellular Architecture and Function. Cell 131, 174–187. https://doi.org/10.1016/j.cell.2007.08.003

Lee, H.O., Davidson, J.M., Duronio, R.J., 2009. Endoreplication: Polyploidy with purpose. Genes Dev. https://doi.org/10.1101/gad.1829209

Lemasters, J.J., 2007. Modulation of mitochondrial membrane permeability in pathogenesis, autophagy and control of metabolism, in: Journal of Gastroenterology and Hepatology (Australia). Blackwell Publishing. https://doi.org/10.1111/j.1440-1746.2006.04643.x

Lerit, D.A., Jordan, H.A., Poulton, J.S., Fagerstrom, C.J., Galletta, B.J., Peifer, M., Rusan, N.M., 2015. Interphase centrosome organization by the PLP-Cnn scaffold is required for centrosome function. Journal of Cell Biology 210, 79–97. https://doi.org/10.1083/jcb.201503117

Leung, T., Manser, E., Tan, L., Lim, L., 1995. A novel serine/threonine kinase binding the ras-related RhoA GTPase which translocates the kinase to peripheral membranes. Journal of Biological Chemistry 270, 29051–29054. https://doi.org/10.1074/jbc.270.49.29051

Levine, B., Klionsky, D.J., 2004. Development by Self-Digestion: Molecular Mechanisms and Biological Functions of Autophagy, Developmental Cell.

Levine, M.S., Bakker, B., Boeckx, B., Moyett, J., Lu, J., Vitre, B., Spierings, D.C., Lansdorp, P.M., Cleveland, D.W., Lambrechts, D., Foijer, F., Holland, A.J., 2017. Centrosome Amplification Is Sufficient to Promote Spontaneous Tumorigenesis in Mammals. Dev Cell 40, 313-322.e5. https://doi.org/10.1016/j.devcel.2016.12.022

Li, H., O'Donnell, M.E., 2018. The Eukaryotic CMG Helicase at the Replication Fork: Emerging Architecture Reveals an Unexpected Mechanism. BioEssays 40. https://doi.org/10.1002/bies.201700208

Li, W., Miki, T., Watanabe, T., Kakeno, M., Sugiyama, I., Kaibuchi, K., Goshima, G., 2011. EB1 promotes microtubule dynamics by recruiting Sentin in Drosophila cells. Journal of Cell Biology 193, 973–983. https://doi.org/10.1083/jcb.201101108

Weng Li, Zhu Chenwen, Xu Jinhua, Du Wei, 2003. Critical role of active repression by E2F and Rb proteins in endoreplication during Drosophila development.

Li, Z., Qian, W., Song, W., Zhao, T., Yang, Y., Wang, W., Wei, L., Zhao, D., Li, Y., Perrimon, N., Xia, Q., Cheng, D., 2022. A salivary gland-secreted peptide regulates insect systemic growth. Cell Rep 38. https://doi.org/10.1016/j.celrep.2022.110397

Lie-Jensen, A., Ivanauskiene, K., Malerød, L., Jain, A., Tan, K.W., Laerdahl, J.K., Liestøl, K., Stenmark, H., Haglund, K., 2019. Centralspindlin Recruits ALIX to the Midbody during Cytokinetic Abscission in Drosophila via a Mechanism Analogous to Virus Budding. Current Biology 29, 3538-3548.e7. https://doi.org/10.1016/j.cub.2019.09.025

Limmer, S., Weiler, A., Volkenhoff, A., Babatz, F., Klämbt, C., 2014. The drosophila blood-brain barrier: Development and function of a glial endothelium. Front Neurosci. https://doi.org/10.3389/fnins.2014.00365

Lin, D.I., Barbash, O., Suresh Kumar, K.G., Weber, J.D., Harper, J.W., Klein-Szanto, A.J.P., Rustgi, A., Fuchs, S.Y., Diehl, J.A., 2006. Phosphorylation-dependent ubiquitination of cyclin D1 by the SCF FBX4-αBcrystallin complex.

Lin, Y.H., Zhang, S., Zhu, M., Lu, T., Chen, K., Wen, Z., Wang, S., Xiao, G., Luo, D., Jia, Y., Li, L., MacConmara, M., Hoshida, Y., Singal, A.G., Yopp, A., Wang, T., Zhu, H., 2020. Mice With Increased Numbers of Polyploid Hepatocytes Maintain Regenerative Capacity But Develop Fewer Hepatocellular Carcinomas Following Chronic Liver Injury. Gastroenterology 158, 1698-1712.e14. https://doi.org/10.1053/j.gastro.2020.01.026

Lingle, W.L., Barrett, S.L., Negron, V.C., D'assoro, A.B., Boeneman, K., Liu, W., Whitehead, C.M., Carol, R.¶, Salisbury, J.L., 2002. Centrosome amplification drives chromosomal instability in breast tumor development.

Liu, C., Huang, B., Wang, H., Zhou, J., 2021. The heterogeneity of megakaryocytes and platelets and implications for ex vivo platelet generation. Stem Cells Transl Med 10, 1614–1620. https://doi.org/10.1002/sctm.21-0264

Liu, J., 2022. Giant cells: Linking McClintock's heredity to early embryogenesis and tumor origin throughout millennia of evolution on Earth. Semin Cancer Biol. https://doi.org/10.1016/j.semcancer.2021.06.007

Liu, J., Wendt, T., Taylor, D., Taylor, K., 2003. Refined model of the 10 S conformation of smooth muscle myosin by cryo-electron microscopy 3D image reconstruction. J Mol Biol 329, 963–972. https://doi.org/10.1016/S0022-2836(03)00516-3

Liu, S.L., Fewkes, N., Ricketson, D., Penkert, R.R., Prehoda, K.E., 2008. Filament-dependent and -independent localization modes of Drosophila non-muscle myosin II. Journal of Biological Chemistry 283, 380–387. https://doi.org/10.1074/jbc.M703924200

Loftus, L. V., Amend, S.R., Pienta, K.J., 2022. Interplay between Cell Death and Cell Proliferation Reveals New Strategies for Cancer Therapy. Int J Mol Sci. https://doi.org/10.3390/ijms23094723

López, S., L.E.L., H.S. et al., 2020. Interplay between whole-genome doubling and the accumulation of deleterious alterations in cancer evolution. Nat Genet 52, 283–293. https://doi.org/10.1038/s41588-020-0584-7

López-Doménech, G., Covill-Cooke, C., Ivankovic, D., Halff, E.F., Sheehan, D.F., Norkett, R., Birsa, N., Kittler, J.T., 2018. Miro proteins coordinate microtubule- and actin-dependent mitochondrial transport and distribution. EMBO J 37, 321–336. https://doi.org/10.15252/embj.201696380

López-Schier, H., St. Johnston, D., 2001. Delta signaling from the germ line controls the proliferation and differentiation of the somatic follicle cells during Drosophila oogenesis. Genes Dev 15, 1393–1405. https://doi.org/10.1101/gad.200901

Losick, V.P., Fox, D.T., Spradling, A.C., 2013. Polyploidization and cell fusion contribute to wound healing in the adult Drosophila epithelium. Current Biology 23, 2224–2232. https://doi.org/10.1016/j.cub.2013.09.029

Losick, V.P., Jun, A.S., Spradling, A.C., 2016. Wound-induced polyploidization: Regulation by hippo and JNK signaling and conservation in Mammals. PLoS One 11. https://doi.org/10.1371/journal.pone.0151251

Lu, W., Lakonishok, M., Gelfand, V.I., 2021. Gatekeeper function for Short stop at the ring canals of the Drosophila ovary. Current Biology 31, 3207-3220.e4. https://doi.org/10.1016/j.cub.2021.05.010

Lu, Y., Roy, R., 2014. Centrosome/cell cycle uncoupling and elimination in the endoreduplicating intestinal cells of C. elegans. PLoS One 9. https://doi.org/10.1371/journal.pone.0110958

Lucas, E.P., Raff, J.W., 2007. Maintaining the proper connection between the centrioles and the pericentriolar matrix requires Drosophila Centrosomin. Journal of Cell Biology 178, 725–732. https://doi.org/10.1083/jcb.200704081

Łuksza, M., Queguigner, I., Verlhac, M.H., Brunet, S., 2013. Rebuilding MTOCs upon centriole loss during mouse oogenesis. Dev Biol 382, 48–56. https://doi.org/10.1016/j.ydbio.2013.07.029

Coluccio L M., 2008. Myosins.

Mabuchi, I., Okuno, M., 1976. The effect of myosin antibody on the division of starfish blastomeres.

Mach, V., Ohno, K., Kokubo, H., Suzuki, Y., 1996. The Drosophila Fork head factor directly controls larval salivary gland-specific expression of the glue protein gene Sgs3, Nucleic Acids Research.

Machado, E., White-Gilbertson, S., Van De Vlekkert, D., Janke, L., Moshiach, S., Campos, Y., Finkelstein, D., Gomero, E., Mosca, R., Qiu, X., Morton, C.L., Annunziata, I., D'Azzo, A., 2015. Regulated lysosomal exocytosis mediates cancer progression. Sci Adv 1. https://doi.org/10.1126/sciadv.1500603

Macmillan, J.C., Hudson, J.W., Bull, S., Dennis, J.W., Swallow, C.J., 2001. Comparative Expression of the Mitotic Regulators SAK and PLK in Colorectal Cancer, Anllals of Surgical Ollcology.

Magnaghi-Jaulin, L., Eot-Houllier, G., Gallaud, E., Giet, R., 2019. Aurora a protein kinase: To the centrosome and beyond. Biomolecules. https://doi.org/10.3390/biom9010028

Mahen, R., Jeyasekharan, A.D., Barry, N.P., Venkitaraman, A.R., 2011. Continuous polo-like kinase 1 activity regulates diffusion to maintain centrosome self-

organization during mitosis. Proc Natl Acad Sci U S A 108, 9310–9315. https://doi.org/10.1073/pnas.1101112108

Mahowald, A.P., Caulton, J.H., Edwards, M.K., Floyd, A.D., 1979. Loss of centrioles and polyploidization in follicle cells of Drosophila melanogaster, J histochem cytochem.

Mahowald, A.P., Strassheim, J.M., 1970. Intercellular migration of centrioles in the germarium of Drosophila melanogaster.

Manstein, D.J., Titus, M.A., De Lozannel, A., Spudich, J.A., 1989. Gene replacement in Dictyostelium: generation of myosin null mutants, The EMBO Journal.

Maqbool, S.B., Mehrotra, S., Kolpakas, A., Durden, C., Zhang, B., Zhong, H., Calvi, B.R., 2010. Dampened activity of E2F1-DP and Myb-MuvB transcription factors in Drosophilaendocycling cells. J Cell Sci 123, 4095–4106. https://doi.org/10.1242/jcs.064519

Marie Pierron, N.K.J.B.-P.P.L. and P.G., 2020. Centriole foci persist in starfish oocytes despite Polo like kinase 1 inactivation or loss of MT nucleation activity.

Marina, M., Saavedra, H.I., 2014. Nek2 and Plk4: prognostic markers, drivers of breast tumorigenesis and drug resistance.

Marthiens, V., Piel, M., Basto, R., 2012. Never tear us apart-the importance of centrosome clustering. J Cell Sci. https://doi.org/10.1242/jcs.094797

Marthiens, V., Rujano, M.A., Pennetier, C., Tessier, S., Paul-Gilloteaux, P., Basto, R., 2013. Centrosome amplification causes microcephaly. Nat Cell Biol 15, 731–740. https://doi.org/10.1038/ncb2746

Martinez-Campos, M., Basto, R., Baker, J., Kernan, M., Raff, J.W., 2004. The Drosophila pericentrin-like protein is essential for cilia/flagella function, but appears to be dispensable for mitosis. Journal of Cell Biology 165, 673–683. https://doi.org/10.1083/jcb.200402130

Martínez-Reyes, I., Chandel, N.S., 2020. Mitochondrial TCA cycle metabolites control physiology and disease. Nat Commun. https://doi.org/10.1038/s41467-019-13668-3

Martínez-Reyes, I., Diebold, L.P., Kong, H., Schieber, M., Huang, H., Hensley, C.T., Mehta, M.M., Wang, T., Santos, J.H., Woychik, R., Dufour, E., Spelbrink, J.N., Weinberg, S.E., Zhao, Y., DeBerardinis, R.J., Chandel, N.S., 2016. TCA Cycle and Mitochondrial Membrane Potential Are Necessary for Diverse Biological Functions. Mol Cell 61, 199–209. https://doi.org/10.1016/j.molcel.2015.12.002

Maruzs, T., Simon-Vecsei, Z., Kiss, V., Csizmadia, T., Juhász, G., 2019. On the fly: Recent progress on autophagy and aging in Drosophila. Front Cell Dev Biol. https://doi.org/10.3389/fcell.2019.00140

Masai, H., Matsumoto, S., You, Z., Yoshizawa-Sugata, N., Oda, M., 2010. Eukaryotic chromosome DNA replication: Where, when, and how? Annu Rev Biochem. https://doi.org/10.1146/annurev.biochem.052308.103205

Masedunskas, A., Sramkova, M., Parente, L., Sales, K.U., Amornphimoltham, P., Bugge, T.H., Weigert, R., 2011. Role for the actomyosin complex in regulated exocytosis revealed by intravital microscopy. Proc Natl Acad Sci U S A 108, 13552–13557. https://doi.org/10.1073/pnas.1016778108

Mason, F.M., Xie, S., Vasquez, C.G., Tworoger, M., Martin, A.C., 2016. RhoA GTPase inhibition organizes contraction during epithelial morphogenesis. Journal of Cell Biology 214, 603–617. https://doi.org/10.1083/jcb.201603077

Mathieu, J., Michel-Hissier, P., Boucherit, V., Huynh, J.-R., Huynh Deubiquitinase, J.-R., 2022. Deubiquitinase USP8 targets ESCRT-III to promote incomplete cell division. https://doi.org/10.1126/science.abg2653ï

Matsui, T., Amano, M., Yamamoto, T., Chihara, K., Nakafuku, M., Ito', M., Nakano1, T., Okawa2, K., Iwamatsu2, A., Kaibuchi3, K., 1996. Rho-associated kinase, a novel serine/threonine kinase, as a putative target for the small GTP binding protein Rho, The EMBO Journal.

Matsumoto, T., Wakefield, L., Peters, A., Peto, M., Spellman, P., Grompe, M., 2021. Proliferative polyploid cells give rise to tumors via ploidy reduction. Nat Commun 12. https://doi.org/10.1038/s41467-021-20916-y

Cottee M A, Muschalik N, Johnson S, Leveson J, Raff J W, Lea S M, 2015. The homo-oligomerisation of both Sas-6 and Ana2 is required for efficient centriole assembly in flies. https://doi.org/10.7554/eLife.07236.001

Mauvezin, C., Neufeld, T.P., 2015. Bafilomycin A1 disrupts autophagic flux by inhibiting both V-ATPase-dependent acidification and Ca-P60A/SERCA-dependent autophagosome-lysosome fusion. Autophagy 11, 1437–1438. https://doi.org/10.1080/15548627.2015.1066957

Mazzi, S., Lordier, L., Debili, N., Raslova, H., Vainchenker, W., 2018. Megakaryocyte and polyploidization. Exp Hematol. https://doi.org/10.1016/j.exphem.2017.10.001

Mccrann, D.J., Nguyen, H.G., Jones, M.R., Ravid, K., 2008. Vascular smooth muscle cell polyploidy: An adaptive or maladaptive response? J Cell Physiol. https://doi.org/10.1002/jcp.21363

McPhee, C.K., Baehrecke, E.H., 2009. Autophagy in Drosophila melanogaster. Biochim Biophys Acta Mol Cell Res. https://doi.org/10.1016/j.bbamcr.2009.02.009

McPhee, C.K., Balgley, B.M., Nelson, C., Hill, J.H., Batlevi, Y., Fang, X., Lee, C.S., Baehrecke, E.H., 2013. Identification of factors that function in Drosophila salivary gland cell death during development using proteomics. Cell Death Differ 20, 218–225. https://doi.org/10.1038/cdd.2012.110

Megraw, T.L., Kao, L.-R., Kaufman, T.C., 2001. Zygotic development without functional mitotic centrosomes.

Mehrotra, S., Maqbool, S.B., Kolpakas, A., Murnen, K., Calvi, B.R., 2008. Endocycling cells do not apoptose in response to DNA rereplication genotoxic stress. Genes Dev 22, 3158–3171. https://doi.org/10.1101/gad.1710208

Melissa E. Pepling, 2016. Nursing the oocyte. Science (1979). https://doi.org/10.1126/science.aad6284

Melkov, A., Abdu, U., 2018. Regulation of long-distance transport of mitochondria along microtubules. Cellular and Molecular Life Sciences. https://doi.org/10.1007/s00018-017-2590-1

Mennella, V., Keszthelyi, B., Mcdonald, K.L., Chhun, B., Kan, F., Rogers, G.C., Huang, B., Agard, D.A., 2012. Subdiffraction-resolution fluorescence microscopy reveals a domain of the centrosome critical for pericentriolar material organization. Nat Cell Biol 14, 1159–1168. https://doi.org/10.1038/ncb2597

Miao, H., Blankenship, J.T., 2020. The pulse of morphogenesis: Actomyosin dynamics and regulation in epithelia. Development (Cambridge). https://doi.org/10.1242/dev.186502

Moritz M, Braunfeld M, Sedat J W, Alberts B, & Agard D A, 1995. Microtubule nucleation by y-tubulin-containing rings in the centrosome.

Miklavc, P., Ehinger, K., Sultan, A., Felder, T., Paul, P., Gottschalk, K.E., Frick, M., 2015. Actin depolymerisation and crosslinking join forces with myosin II to contract actin coats on fused secretory vesicles. J Cell Sci 128, 1193–1203. https://doi.org/10.1242/jcs.165571

Miller, D.E., Cook, K.R., Scott Hawley, R., 2019. The joy of balancers. PLoS Genet. https://doi.org/10.1371/journal.pgen.1008421

Kim M, Fong C S, and Tsou M-F B, 2014. Centriole Duplication: When PLK4 Meets Ana2/STIL. Current Biology. https://doi.org/10.1016/j.cub.2014.09.064

Miyaoka, Y., Ebato, K., Kato, H., Arakawa, S., Shimizu, S., Miyajima, A., 2012. Hypertrophy and unconventional cell division of hepatocytes underlie liver regeneration. Curr Biol 22, 1166–1175. https://doi.org/10.1016/j.cub.2012.05.016

Mizushima, N., 2010. The role of the Atg1/ULK1 complex in autophagy regulation. Curr Opin Cell Biol. https://doi.org/10.1016/j.ceb.2009.12.004

Mogensen, M.M., Tucker, J.B., 1987. Evidence for microtubule nucleation at plasma membrane-associated sites in Drosophila.

Monn Monn Myat and Deborah J. Andrew, 2000. Fork head prevents apoptosis and promotes cell shape change during formation of the Drosophila salivary glands . Development.

Myat MM, Andrew D J, 2002. Epithelial Tube Morphology Is Determined by the Polarized Growth and Delivery of Apical Membrane, Cell.

Monteiro, P., Yeon, B., Wallis, S.S., Godinho, S.A., 2023. Centrosome amplification fine tunes tubulin acetylation to differentially control intracellular organization. EMBO J 42. https://doi.org/10.15252/embj.2022112812

Morgan, D. 0, 1995. Principles of CDK regulation.

Morretton, J., Simon, A., Herbette, A., Barbazan, J., Pérez-González, C., Cosson, C., Mboup, B., Latouche, A., Popova, T., Kieffer, Y., Macé, A., Gestraud, P., Bataillon, G., Becette, V., Meseure, D., Nicolas, A., Mariani, O., Vincent-Salomon, A., Stern, M., Mechta-Grigoriou, F., Roman Roman, S., Vignjevic, D.M., Rouzier, R., Sastre-Garau, X., Goundiam, O., Basto, R., 2022. A catalog of numerical centrosome defects in epithelial ovarian cancers. EMBO Mol Med 14. https://doi.org/10.15252/emmm.202215670

Mueller, O., Anlasik, T., Wiedemann, J., Thomassen, J., Wohlschlaeger, J., Hagel, V., Keyvani, K., Schwieger, I., Dahlmann, B., Sure, U., Sixt, S.U., 2012. Circulating extracellular proteasome in the cerebrospinal fluid: A study on concentration and proteolytic activity. Journal of Molecular Neuroscience 46, 509–515. https://doi.org/10.1007/s12031-011-9631-2

Müller, H., Schmidt, D., Steinbrink, S., Mirgorodskaya, E., Lehmann, V., Habermann, K., Dreher, F., Gustavsson, N., Kessler, T., Lehrach, H., Herwig, R., Gobom, J., Ploubidou, A., Boutros, M., Lange, B.M.H., 2010. Proteomic and functional analysis of the mitotic Drosophila centrosome. EMBO Journal 29, 3344–3357. https://doi.org/10.1038/emboj.2010.210

Muller, N.J., 1918. Genetic Variability, Twin Hybrids and Constant Hybrids, in a Case of Balanced Lethal Factors.

Munjal, A., Lecuit, T., 2014. Actomyosin networks and tissue morphogenesis. Development (Cambridge) 141, 1789–1793. https://doi.org/10.1242/dev.091645

Murthy, K., Wadsworth, P., 2005. Myosin-II-dependent localization and dynamics of F-actin during cytokinesis. Current Biology 15, 724–731. https://doi.org/10.1016/j.cub.2005.02.055

Myat M. M. & Andrew D. J., 2000a. Fork head prevents apoptosis and promotes cell shape change during formation of the Drosophila salivary glands.

Myat M. M. & Andrew D. J., 2000b. Organ shape in the Drosophila salivary gland is controlled by regulated, sequential internalization of the primordia. .

Myat, M.M., Isaac, P.P., Andrew, D.J., 2000. Early Genes Required for Salivary Gland Fate Determination and Morphogenesis in Drosophila melanogaster.

Myers, S.M., Collins, I., 2016. Recent findings and future directions for interpolar mitotic kinesin inhibitors in cancer therapy. Future Med Chem. https://doi.org/10.4155/fmc.16.5

Nakamoto, R.K., Baylis Scanlon, J.A., Al-Shawi, M.K., 2008. The rotary mechanism of the ATP synthase. Arch Biochem Biophys. https://doi.org/10.1016/j.abb.2008.05.004

Nandakumar, S., Grushko, O., Buttitta, L.A., 2020. Polyploidy in the adult drosophila brain. Elife 9, 1–25. https://doi.org/10.7554/ELIFE.54385

Nano, M., Gemble, S., Simon, A., Pennetier, C., Fraisier, V., Marthiens, V., Basto, R., 2019. Cell-Cycle Asynchrony Generates DNA Damage at Mitotic Entry in Polyploid Cells. Current Biology 29, 3937-3945.e7. https://doi.org/10.1016/j.cub.2019.09.041

Narbonne-Reveau, K., Senger, S., Pal, M., Herr, A., Richardson, H.E., Asano, M., Deak, P., Lilly, M.A., 2008. APC/CFzr/Cdh1 promotes cell cycle progression during the Drosophila endocycle. Development 135, 1451–1461. https://doi.org/10.1242/dev.016295

Nesci, S., Trombetti, F., Pagliarani, A., Ventrella, V., Algieri, C., Tioli, G., Lenaz, G., 2021. Molecular and supramolecular structure of the mitochondrial oxidative phosphorylation system: Implications for pathology. Life. https://doi.org/10.3390/life11030242

New, J., Thomas, S.M., 2019. Autophagy-dependent secretion: mechanism, factors secreted, and disease implications. Autophagy. https://doi.org/10.1080/15548627.2019.1596479

Nezis, I.P., Simonsen, A., Sagona, A.P., Finley, K., Gaumer, S., Contamine, D., Rusten, T.E., Stenmark, H., Brech, A., 2008. Ref(2)P, the Drosophila melanogaster homologue of mammalian p62, is required for the formation of protein aggregates in adult brain. Journal of Cell Biology 180, 1065–1071. https://doi.org/10.1083/jcb.200711108

Nguyen, Y.D.H., Pham, T.L.A., Nishihara, T., Kamei, K., Tran, D.B., 2024. Depletion of lipid storage droplet-1 delays endoreplication progression and induces cell death in Drosophila salivary gland. Arch Insect Biochem Physiol 116. https://doi.org/10.1002/arch.22132

Nightingale, T.D., White, I.J., Doyle, E.L., Turmaine, M., Harrison-Lavoie, K.J., Webb, K.F., Cramer, L.P., Cutler, D.F., 2011. Actomyosin II contractility expels von Willebrand factor from Weibel-Palade bodies during exocytosis. Journal of Cell Biology 194, 613–629. https://doi.org/10.1083/jcb.201011119

Nishiyama, T., 2018. Cohesion and cohesin-dependent chromatin organization.

Nobes, C., Hall, A., 1994. Regulation and function of the Rho subfamily of small CTPases, Current Opinion in Genetics and Development.

Noda, T., Ohsumi, Y., 1998. Tor, a phosphatidylinositol kinase homologue, controls autophagy in yeast. Journal of Biological Chemistry 273, 3963–3966. https://doi.org/10.1074/jbc.273.7.3963

Noji, H., Yoshida, M., 2001. The rotary machine in the cell, ATP synthase. Journal of Biological Chemistry. https://doi.org/10.1074/jbc.R000021200

Norbury, C., Nurse, P., 1992. Animal cell cycles and their control.

Nordman, J., Li, S., Eng, T., MacAlpine, D., Orr-Weaver, T.L., 2011. Developmental control of the DNA replication and transcription programs. Genome Res 21, 175–181. https://doi.org/10.1101/gr.114611.110

Nordman, J.T., Kozhevnikova, E.N., Verrijzer, C.P., Pindyurin, A. V., Andreyeva, E.N., Shloma, V. V., Zhimulev, I.F., Orr-Weaver, T.L., 2014. DNA copy-number

control through inhibition of replication fork progression. Cell Rep 9, 841–849. https://doi.org/10.1016/j.celrep.2014.10.005

Novak, Z.A., Conduit, P.T., Wainman, A., Raff, J.W., 2014. Asterless licenses daughter centrioles to duplicate for the first time in Drosophila embryos. Current Biology 24, 1276–1282. https://doi.org/10.1016/j.cub.2014.04.023

Novitski Ani Braver, E.G., 1954. An Analysis of Crossing over within a Heterozygous Inversion in Drosophila Melanogaster.

Ohta, M., Ashikawa, T., Nozaki, Y., Kozuka-Hata, H., Goto, H., Inagaki, M., Oyama, M., Kitagawa, D., 2014. Direct interaction of Plk4 with STIL ensures formation of a single procentriole per parental centriole. Nat Commun 5, 5267. https://doi.org/10.1038/ncomms6267

Ohta, M., Watanabe, K., Ashikawa, T., Nozaki, Y., Yoshiba, S., Kimura, A., Kitagawa, D., 2018. Bimodal Binding of STIL to Plk4 Controls Proper Centriole Copy Number. Cell Rep 23, 3160-3169.e4. https://doi.org/10.1016/j.celrep.2018.05.030

Ohtsubo, M., Theodoras, A.M., Schumacher, J., Roberts, J.M., Pagano, M., 1995. Human Cyclin E, a Nuclear Protein Essential for the G 1-to-S Phase Transition, MOLECULAR AND CELLULAR BIOLOGY.

Orr-Weaver, T.L., 2015. When bigger is better: The role of polyploidy in organogenesis. Trends in Genetics. https://doi.org/10.1016/j.tig.2015.03.011

Osellame, L.D., Blacker, T.S., Duchen, M.R., 2012. Cellular and molecular mechanisms of mitochondrial function. Best Pract Res Clin Endocrinol Metab. https://doi.org/10.1016/j.beem.2012.05.003

Øvrebø, J.I., Edgar, B.A., 2018. Polyploidy in tissue homeostasis and regeneration. Development (Cambridge). https://doi.org/10.1242/dev.156034

Paintrand, M., Moudjou, M., Delacroix, H., Bornens', M., 1992. Centrosome Organization and Centriole Architecture: Their Sensitivity to Divalent Cations, JOURNAL OF STRUCTURAL BIOLOGY.

Palazzo, R.E., Vogel, J.M., Schnackenberg, B.J., Hull, D.R., Wu, X., 2000. Centrosome Maturation.

Pandey, U.B., Nichols, C.D., 2011. Human disease models in drosophila melanogaster and the role of the fly in therapeutic drug discovery. Pharmacol Rev 63, 411–436. https://doi.org/10.1124/pr.110.003293

Pandit, S.K., Westendorp, B., De Bruin, A., 2013. Physiological significance of polyploidization in mammalian cells. Trends Cell Biol. https://doi.org/10.1016/j.tcb.2013.06.002

Pandit, S.K., Westendorp, B., Nantasanti, S., Van Liere, E., Tooten, P.C.J., Cornelissen, P.W.A., Toussaint, M.J.M., Lamers, W.H., De Bruin, A., 2012. E2F8 is essential for polyploidization in mammalian cells. Nat Cell Biol 14, 1181–1191. https://doi.org/10.1038/ncb2585

Panzer, S., Weigel, D., Beckendorf, S.K., 1992. Organogenesis in Drosophila melanogaster. embryonic salivary gland determination is controlled by homeotic and dorsoventral patterning genes, Development.

Pardee, A.B., 1989. G1 Events and Regulation of Cell Proliferation.

Park, J., Kim, J., Park, H., Kim, T., Lee, S., 2024. ESCRT-III: a versatile membrane remodeling machinery and its implications in cellular processes and diseases. Anim Cells Syst (Seoul). https://doi.org/10.1080/19768354.2024.2380294

Pattingre, S., Espert, L., Biard-Piechaczyk, M., Codogno, P., 2008. Regulation of macroautophagy by mTOR and Beclin 1 complexes. Biochimie 90, 313–323. https://doi.org/10.1016/j.biochi.2007.08.014

Peel, N., Stevens, N.R., Basto, R., Raff, J.W., 2007. Overexpressing Centriole-Replication Proteins In Vivo Induces Centriole Overduplication and De Novo Formation. Current Biology 17, 834–843. https://doi.org/10.1016/j.cub.2007.04.036ï

Pelletier, L., O'Toole, E., Schwager, A., Hyman, A.A., Müller-Reichert, T., 2006. Centriole assembly in Caenorhabditis elegans. Nature 444, 619–623. https://doi.org/10.1038/nature05318

Riley Peter D.; Carroll Sean B.; and Scott Matthew P., 1987. The expression and regulation of Sex combs reduced protein in Drosophila embryos.

Peter, M., Nakagawa, J., Dotie, M., Labbc, J.C., Nigg, E.A., 1990. In Vitro Disassembly of the Nuclear Lamina and M Phase-Specific Phosphorylation of Lamins by cdc2 Kinase, Cell.

Peters, J.M., Franke, W.W., Kleinschmidt, J.A., 1994. Distinct 19 S and 20 S subcomplexes of the 26 S proteasome and their distribution in the nucleus and the cytoplasm. Journal of Biological Chemistry 269, 7709–7718. https://doi.org/10.1016/s0021-9258(17)37345-3

Petry, S., Vale, R.D., 2015. Microtubule nucleation at the centrosome and beyond. Nat Cell Biol. https://doi.org/10.1038/ncb3220

Pfeffer, S.R., 2017. Rab GTPases: Master regulators that establish the secretory and endocytic pathways. Mol Biol Cell. https://doi.org/10.1091/mbc.E16-10-0737

Philip, R., Fiorino, C., Harrison, R.E., 2022. Terminally differentiated osteoclasts organize centrosomes into large clusters for microtubule nucleation and bone resorption. Mol Biol Cell 33. https://doi.org/10.1091/mbc.E22-03-0098

Piekny, A., Werner, M., Glotzer, M., 2005. Cytokinesis: Welcome to the Rho zone. Trends Cell Biol. https://doi.org/10.1016/j.tcb.2005.10.006

Pierce, S.B., Yost, C., Britton, J.S., Loo, L.W.M., Flynn, E.M., Edgar, B.A., Eisenman, R.N., 2004. dMyc is required for larval growth and endoreplication in Drosophila. Development 131, 2317–2327. https://doi.org/10.1242/dev.01108

Pierron, M., Woglar, A., Busso, C., Jha, K., Mikeladze-Dvali, T., Croisier, M., Gönczy, P., 2023. Centriole elimination during Caenorhabditis elegans oogenesis initiates with loss of the central tube protein SAS -1 . EMBO J 42. https://doi.org/10.15252/embj.2023115076

Pilling, A.D., Horiuchi, D., Lively, C.M., Saxton, W.M., 2006. Kinesin-1 and Dynein Are the Primary Motors for Fast Transport of Mitochondria in Drosophila Motor Axons. Mol Biol Cell 17, 2057–2068. https://doi.org/10.1091/mbc.E05-06

Pimenta-Marques, A., Bento, I., Lopes, C.A.M., Duarte, P., Jana, S.C., Bettencourt-Dias, M., 2016. A mechanism for the elimination of the female gamete centrosome in Drosophila melanogaster. Science (1979) 353. https://doi.org/10.1126/science.aaf4866

Pines, J., 1995. Cyclins and cyclin-dependent kinases: a biochemical view, Biochem. J.

Przybylski, R.J., 1971. Occurrence of centrioles during skeletal and cardiac myogenesis.

Pylypenko, O., Hammich, H., Yu, I.M., Houdusse, A., 2018. Rab GTPases and their interacting protein partners: Structural insights into Rab functional diversity. Small GTPases. https://doi.org/10.1080/21541248.2017.1336191

Quinn, L., Lin, J., Cranna, N., Amanda Lee, J. E., Mitchell, N., & H, R. (2012). Steroid Hormones in Drosophila: How Ecdysone Coordinates Developmental Signalling with Cell Growth and Division. In Steroids - Basic Science. InTech. https://doi.org/10.5772/27927

Quinn, M.E., Goh, Q., Kurosaka, M., Gamage, D.G., Petrany, M.J., Prasad, V., Millay, D.P., 2017. Myomerger induces fusion of non-fusogenic cells and is required for skeletal muscle development. Nat Commun 8. https://doi.org/10.1038/ncomms15665

Quintanilla, M.A., Hammer, J.A., Beach, J.R., 2023. Non-muscle myosin 2 at a glance. J Cell Sci 136. https://doi.org/10.1242/jcs.260890

Quintyne NJ, J.E.R.D.R.H.S.M.G.W.S.S., 2005. Spindle Multipolarity Is Prevented by Centrosomal Clustering. Science (1979) 307, 124–127. https://doi.org/10.1126/science.1103631

R. W. Lymn and E. W. Taylor, 1971. Mechanism of adenosine triphosphate hydrolysis by actomyosin. UTC.

Rabouille, C., 2017. Pathways of Unconventional Protein Secretion. Trends Cell Biol. https://doi.org/10.1016/j.tcb.2016.11.007

Ralhan, I., Chang, J., Moulton, M.J., Goodman, L.D., Lee, N.Y.J., Plummer, G., Amalia Pasolli, H., Matthies, D., Bellen, H.J., Ioannou, M.S., 2023. Autolysosomal exocytosis of lipids protect neurons from ferroptosis. Journal of Cell Biology 222. https://doi.org/10.1083/jcb.202207130

Oliveira R A, Nasmyth K, 2013. Cohesin cleavage is insufficient for centriole disengagement in Drosophila. Current Biology. https://doi.org/10.1016/j.cub.2013.05.055

Rauzi, M., Lenne, P.F., Lecuit, T., 2010. Planar polarized actomyosin contractile flows control epithelial junction remodelling. Nature 468, 1110–1115. https://doi.org/10.1038/nature09566

Ravid, K., Lu, J., Zimmet, J.M., Jones, M.R., 2002. Roads to polyploidy: The megakaryocyte example. J Cell Physiol. https://doi.org/10.1002/jcp.10035

Ray, R.P., Aroraf', K., Nusslein-Volhardt, C., Gelbart, W.M., 1991. The control of cell fate along the dorsal-ventral axis of the Drosophila embryo, Development.

Reed, B.H., Orr-Weaver, T.L., 1997. The Drosophila gene morula inhibits mitotic functions in the endo cell cycle and the mitotic cell cycle. Development 124, 3543–3553. https://doi.org/10.1242/dev.124.18.3543

Reid, S.E., Kolapalli, S.P., Nielsen, T.M., Frankel, L.B., 2022. Canonical and non-canonical roles for ATG8 proteins in autophagy and beyond. Front Mol Biosci. https://doi.org/10.3389/fmolb.2022.1074701

Renault, N., King-Jones, K., Lehmann, M., 2001. Downregulation of the tissue-specific transcription factor fork head by Broad-Complex mediates a stage-specific hormone response. Development 128, 3729–3737. https://doi.org/10.1242/dev.128.19.3729

Reynafarje, B.D., Ferreira, J., 2008. OXIDATIVE PHOSPHORYLATION: Kinetic and Thermodynamic Correlation between Electron Flow, Proton Translocation, Oxygen Consumption and ATP Synthesis under Close to In Vivo Concentrations of Oxygen, International Journal of Medical Sciences.

Ribatti, D., 2018. An historical note on the cell theory. Exp Cell Res. https://doi.org/10.1016/j.yexcr.2018.01.038

Ring, D., Hubble, R., Kirschner, M., 1982. Mitosis in a Cell with Multiple Centrioles, THE JOURNAL OF CELL BIOLOGY •.

Riparbelli, M.G., C.G., & D.R., 1993. Spatial organization of microtubules and microfilaments in larval and adult salivary glands of Drosophila melanogaster.

Rivero, S., Cardenas, J., Bornens, M., Rios, R.M., 2009. Microtubule nucleation at the cis-side of the golgi apparatus requires AKAP450 and GM130. EMBO Journal 28, 1016–1028. https://doi.org/10.1038/emboj.2009.47

Rizzuto, R., De Stefani, D., Raffaello, A., Mammucari, C., 2012. Mitochondria as sensors and regulators of calcium signalling. Nat Rev Mol Cell Biol. https://doi.org/10.1038/nrm3412

Roger Craig, R.S.& J.K.-J., 1983. Light-chain phosphorylation controls the conformation of vertebrate non-muscle and smooth muscle myosin molecules, J. Cell Bioi.

Rogers, G.C., Rusan, N.M., Roberts, D.M., Peifer, M., Rogers, S.L., 2009. The SCF Slimb ubiquitin ligase regulates Plk4/Sak levels to block centriole reduplication. Journal of Cell Biology 184, 225–229. https://doi.org/10.1083/jcb.200808049

Rogers, S.L., Rogers, G.C., Sharp, D.J., Vale, R.D., 2002. Drosophila EB1 is important for proper assembly, dynamics, and positioning of the mitotic spindle. Journal of Cell Biology 158, 873–884. https://doi.org/10.1083/jcb.200202032

Rojnuckarin, P., Drachman, J.G., Kaushansky, K., 1999. Thrombopoietin-Induced Activation of the Mitogen-Activated Protein Kinase (MAPK) Pathway in Normal Megakaryocytes: Role in Endomitosis.

Röper, K., 2013. Supracellular actomyosin assemblies during development. Dev Cell 23, 939–953. https://doi.org/10.1016/j.devcel.2012.09.013

Röper, K., 2012. Anisotropy of Crumbs and aPKC Drives Myosin Cable Assembly during Tube Formation. Dev Cell 23, 939–953. https://doi.org/10.1016/j.devcel.2012.09.013

Röper, K., Brown, N.H., 2004. A Spectraplakin Is Enriched on the Fusome and Organizes Microtubules during Oocyte Specification in Drosophila. Current Biology 14, 99–110. https://doi.org/10.1016/j.cub.2003.12.056

Roque, H., Saurya, S., Pratt, M.B., Johnson, E., Raff, J.W., 2018. Drosophila PLP assembles pericentriolar clouds that promote centriole stability, cohesion and MT nucleation. PLoS Genet 14. https://doi.org/10.1371/journal.pgen.1007198

Roque, H., Wainman, A., Richens, J., Kozyrska, K., Franz, A., Raff, J.W., 2012. Drosophila Cep135/Bld10 maintains proper centriole structure but is dispensable for cartwheel formation. J Cell Sci 125, 5881–5886. https://doi.org/10.1242/jcs.113506

Rosenblatt J, Cramer LP, Baum B, McGee KM. Myosin II-dependent cortical movement is required for centrosome separation and positioning during mitotic spindle assembly. Cell. 2004;117(3):361-372. doi:10.1016/S0092-8674(04)00341-1

Rotelli, M.D., Bolling, A.M., Killion, A.W., Weinberg, A.J., Dixon, M.J., Calvi, B.R., 2019a. An RNAi screen for genes required for growth of Drosophila wing tissue. G3: Genes, Genomes, Genetics 9, 3087–3100. https://doi.org/10.1534/g3.119.400581

Rotelli, M.D., Policastro, R.A., Bolling, A.M., Killion, A.W., Weinberg, A.J., Dixon, M.J., Zentner, G.E., Walczak, C.E., Lilly, M.A., Calvi, B.R., 2019b. A Cyclin A—Myb-MuvB—Aurora B network regulates the choice between mitotic cycles and polyploid endoreplication cycles. PLoS Genet 15. https://doi.org/10.1371/journal.pgen.1008253

Rousso, T., Schejter, E.D., Shilo, B.Z., 2016. Orchestrated content release from Drosophila glue-protein vesicles by a contractile actomyosin network. Nat Cell Biol 18, 181–190. https://doi.org/10.1038/ncb3288

Rubin, S.M., Sage, J., Skotheim, J.M., 2020. Integrating Old and New Paradigms of G1/S Control. Mol Cell. https://doi.org/10.1016/j.molcel.2020.08.020

Rudkin, G.T., 1972. Replication in Polytene Chromosomes.

Rui, Y.N., Xu, Z., Patel, B., Chen, Z., Chen, D., Tito, A., David, G., Sun, Y., Stimming, E.F., Bellen, H.J., Cuervo, A.M., Zhang, S., 2015. Huntingtin

functions as a scaffold for selective macroautophagy. Nat Cell Biol 17, 262–275. https://doi.org/10.1038/ncb3101

Baker S J, Fearon E R, Nigro J M, Hamilton S R, Preisinger A C, Jessup J M, Tuinen P van, Ledbetter D H, Barker D F, Nakamura Y, White R, Vogelstein B, 1987. Chromosome 17 Deletions and p53 Gene Mutations in Colorectal Carcinomas, Proc. Natl. Acad. Sci. U.S.A.

Sabat-Pospiech, D., Fabian-Kolpanowicz, K., Prior, I.A., Coulson, J.M., Fielding, A.B., 2019. Targeting centrosome amplification, an Achilles' heel of cancer. Biochem Soc Trans. https://doi.org/10.1042/BST20190034

Sabino, D., Gogendeau, D., Gambarotto, D., Nano, M., Pennetier, C., Dingli, F., Arras, G., Loew, D., Basto, R., 2015. Moesin is a major regulator of centrosome behavior in epithelial cells with extra centrosomes. Current Biology 25, 879–889. https://doi.org/10.1016/j.cub.2015.01.066

Sailem, H., Bousgouni, V., Cooper, S., Bakal, C., 2014. Cross-talk between Rho and Rac GTPases drives deterministic exploration of cellular shape space and morphological heterogeneity. Open Biol 4. https://doi.org/10.1098/rsob.130132

Samie, M.A., Xu, H., 2014. Thematic review series: Recent advances in the treatment of lysosomal storage diseases: Lysosomal exocytosis and lipid storage disorders. J Lipid Res. https://doi.org/10.1194/jlr.R046896

Sánchez-Corrales, Y.E., Blanchard, G.B., Röper, K., 2021. Correct regionalization of a tissue primordium is essential for coordinated morphogenesis. https://doi.org/10.7554/eLife

Sánchez-Huertas, C., Freixo, F., Viais, R., Lacasa, C., Soriano, E., Lüders, J., 2016. Non-centrosomal nucleation mediated by augmin organizes microtubules in post-mitotic neurons and controls axonal microtubule polarity. Nat Commun 7. https://doi.org/10.1038/ncomms12187

Sannerud, R., Saraste, J., Goud, B., 2003. Retrograde traffic in the biosynthetic-secretory route: Pathways and machinery. Curr Opin Cell Biol. https://doi.org/10.1016/S0955-0674(03)00077-2

Sato, N., Mizumoto, K., Nakamura, M., Nakamura, K., Kusumoto, M., Niiyama, H., Ogawa, T., Tanaka, M., 1999. Centrosome Abnormalities in Pancreatic Ductal Carcinoma.

Saunders, T.E., 2021. The early Drosophila embryo as a model system for quantitative biology. Cells and Development. https://doi.org/10.1016/j.cdev.2021.203722

Saunders, W., 2005. Centrosomal amplification and spindle multipolarity in cancer cells. Semin Cancer Biol. https://doi.org/10.1016/j.semcancer.2004.09.003

Saurya, S., Roque, H., Novak, Z.A., Wainman, A., Aydogan, M.G., Volanakis, A., Sieber, B., Pinto, D.M.S., Raff, J.W., 2016. Drosophila Ana1 is required for centrosome assembly and centriole elongation. J Cell Sci 129, 2514–2525. https://doi.org/10.1242/jcs.186460

Sawyer, J.M., Harrell, J.R., Shemer, G., Sullivan-Brown, J., Roh-Johnson, M., Goldstein, B., 2010. Apical constriction: A cell shape change that can drive morphogenesis. Dev Biol. https://doi.org/10.1016/j.ydbio.2009.09.009

Schaeffer, V., Althauser, C., Shcherbata, H.R., Deng, W.-M., Ruohola-Baker, H., 2004. Notch-Dependent Fizzy Related/Hec1/Cdh1 Expression Is Required for the Mitotic-to-Endocycle Transition in Drosophila Follicle Cells. Current Biology 14, 630–636. https://doi.org/10.1016/j

Scheer, U., 2014. Historical roots of centrosome research: Discovery of Boveri's microscope slides in Würzburg. Philosophical Transactions of the Royal Society B: Biological Sciences. https://doi.org/10.1098/rstb.2013.0469

Schenkel, L.C., Bakovic, M., 2014. Formation and regulation of mitochondrial membranes. Int J Cell Biol. https://doi.org/10.1155/2014/709828

Schmidt, T.I., Kleylein-Sohn, J., Westendorf, J., Le Clech, M., Lavoie, S.B., Stierhof, Y.D., Nigg, E.A., 2009. Control of Centriole Length by CPAP and CP110. Current Biology 19, 1005–1011. https://doi.org/10.1016/j.cub.2009.05.016

Schoborg, T.A., Rusan, N.M., 2016. Taking Centrioles to the Elimination Round. Dev Cell. https://doi.org/10.1016/j.devcel.2016.06.027

Schoenfelder, K.P., Fox, D.T., 2015. The expanding implications of polyploidy. Journal of Cell Biology. https://doi.org/10.1083/jcb.201502016

Schoenfelder, K.P., Montague, R.A., Paramore, S. V., Lennox, A.L., Mahowald, A.P., Fox, D.T., 2014. Indispensable pre-mitotic endocycles promote aneuploidy in the Drosophila rectum. Development (Cambridge) 141, 3551–3560. https://doi.org/10.1242/dev.109850

Schöneberg, J., Lee, I.H., Iwasa, J.H., Hurley, J.H., 2016. Reverse-topology membrane scission by the ESCRT proteins. Nat Rev Mol Cell Biol. https://doi.org/10.1038/nrm.2016.121

Schrock, M.S., Stromberg, B.R., Scarberry, L., Summers, M.K., 2020. APC/C ubiquitin ligase: Functions and mechanisms in tumorigenesis. Semin Cancer Biol. https://doi.org/10.1016/j.semcancer.2020.03.001

Schroeder, T.E., 1973. Actin in Dividing Cells: Contractile Ring Filaments Bind Heavy Meromyosin (cell division/cytokinesis/cleavage/HeLa cells/microfilament), Proc. Nat. Acoa. So. USA.

Scott A, G.J.S.-B.M.A.S.S.J.S.WI., 2005. Structure and ESCRT-III protein interactions of the MIT domain of human VPS4A.

Scott, I., Logan, D.C., 2004. The birth of cell biology. New Phytologist 163, 7–9. https://doi.org/10.1111/j.1469-8137.2004.01110.x

Scott, I., Youle, R.J., 2010. Mitochondrial fission and fusion. Essays Biochem 47, 85–98. https://doi.org/10.1042/BSE0470085

Sedat, J., Manuelidis, L., 1977. A direct approach to the structure of eukaryotic chromosomes. Cold Spring Harb Symp Quant Biol 42, 331–350. https://doi.org/10.1101/sqb.1978.042.01.035

Segal, D., Zaritsky, A., Schejter, E.D., Shilo, B.Z., 2018. Feedback inhibition of actin on Rho mediates content release from large secretory vesicles. Journal of Cell Biology 217, 1815–1826. https://doi.org/10.1083/jcb.201711006

Segawa, A., Yamashina, S., 1989. Roles of Microfilaments in Exocytosis: A New Hypothesis, CELL STRUCTURE AND FUNCTION.

Serçin, Ö., Larsimont, J.C., Karambelas, A.E., Marthiens, V., Moers, V., Boeckx, B., Le Mercier, M., Lambrechts, D., Basto, R., Blanpain, C., 2016. Transient PLK4 overexpression accelerates tumorigenesis in p53-deficient epidermis. Nat Cell Biol 18, 100–110. https://doi.org/10.1038/ncb3270

Shcherbata, H.R., Althauser, C., Findley, S.D., Ruohola-Baker, H., 2004. The mitotic-to-endrocycle switch in Drosophila follicle cells is executed by Notch-dependent regulation of G1/S, G2/M and M/G1 cell-cycle transitions. Development 131, 3169–3181. https://doi.org/10.1242/dev.01172

Shelton, C.A., Carter, J.C., Ellis, G.C., Bowerman, B., 1999. The Nonmuscle Myosin Regulatory Light Chain Gene mlc-4 Is Required for Cytokinesis, Anterior-Posterior Polarity, and Body Morphology during Caenorhabditis elegans Embryogenesis, The Journal of Cell Biology.

Shen, Y.T., Gu, Y., Su, W.F., Zhong, J. fei, Jin, Z.H., Gu, X.S., Chen, G., 2016. Rab27b is Involved in Lysosomal Exocytosis and Proteolipid Protein Trafficking

in Oligodendrocytes. Neurosci Bull 32, 331–340. https://doi.org/10.1007/s12264-016-0045-6

Sherr, C.J., 1994. Gl Phase Progression: Cycling on Cue, Cell.

Shibutani, S.T., de la Cruz, A.F.A., Tran, V., Turbyfill, W.J., Reis, T., Edgar, B.A., Duronio, R.J., 2008. Intrinsic Negative Cell Cycle Regulation Provided by PIP Box- and Cul4Cdt2-Mediated Destruction of E2f1 during S Phase. Dev Cell 15, 890–900. https://doi.org/10.1016/j.devcel.2008.10.003

Sho, T., Li, Y., Jiao, H., Yu, L., 2024. Migratory autolysosome disposal mitigates lysosome damage. J Cell Biol 223. https://doi.org/10.1083/jcb.202403195

Sidor C. and Röper K., 2016. Chapter 5- Genetic Control of Salivary Gland Tubulogenesis in Drosophila.

Sidor, C., Stevens, T.J., Jin, L., Boulanger, J., Röper, K., 2020. Rho-Kinase Planar Polarization at Tissue Boundaries Depends on Phospho-regulation of Membrane Residence Time. Dev Cell 52, 364-378.e7. https://doi.org/10.1016/j.devcel.2019.12.003

Sigrist, S.J., Lehner, C.F., 1997. Drosophila fizzy-related Down-Regulates Mitotic Cyclins and Is Required for Cell Proliferation Arrest and Entry into Endocycles, Cell.

Sixt, S.U., Dahlmann, B., 2008. Extracellular, circulating proteasomes and ubiquitin - Incidence and relevance. Biochim Biophys Acta Mol Basis Dis. https://doi.org/10.1016/j.bbadis.2008.06.005

Sixt, S.U., Peters, J., 2010. Extracellular alveolar proteasome: Possible role in lung injury and repair. Proc Am Thorac Soc. https://doi.org/10.1513/pats.200906-035JS

Smith, G.M., Gallo, G., 2018. The role of mitochondria in axon development and regeneration. Dev Neurobiol. https://doi.org/10.1002/dneu.22546

Smith, A. V, Orr-Weaver, T.L., 1991. The regulation of the cell cycle during Drosophila embryogenesis: the transition to polyteny, Development.

Soltis, D.E., Visger, C.J., Soltis, P.S., 2014. The polyploidy revolution then...and now: Stebbins revisited. Am J Bot 101, 1057–1078. https://doi.org/10.3732/ajb.1400178

Soysa, N.S., Alles, N., Aoki, K., 2012. Osteoclast formation and differentiation: An overview. Article in Journal of Medical and Dental Sciences. https://doi.org/10.11480/jmds.590301

Spassky, N., Meunier, A., 2017. The development and functions of multiciliated epithelia. Nat Rev Mol Cell Biol. https://doi.org/10.1038/nrm.2017.21

Spradling, A.C., 2017. Polytene Chromosome Structure and Somatic Genome Instability. Cold Spring Harb Symp Quant Biol 82, 293–304. https://doi.org/10.1101/sqb.2017.82.033670

Stebbins, G.L., 1938. The Significance of Polyploidy in Plant Evolution, Source: The American Naturalist.

Stenmark, H., 2009. Rab GTPases as coordinators of vesicle traffic. Nat Rev Mol Cell Biol. https://doi.org/10.1038/nrm2728

Stevens, N.R., Dobbelaere, J., Brunk, K., Franz, A., Raff, J.W., 2010a. Drosophila Ana2 is a conserved centriole duplication factor. Journal of Cell Biology 188, 313–323. https://doi.org/10.1083/jcb.200910016

Stevens, N.R., Roque, H., Raff, J.W., 2010b. DSas-6 and Ana2 Coassemble into Tubules to Promote Centriole Duplication and Engagement. Dev Cell 19, 913–919. https://doi.org/10.1016/j.devcel.2010.11.010

Storchova, Z., Pellman, D., 2004. From polyploidy to aneuploidy, genome instability and cancer. Nat Rev Mol Cell Biol. https://doi.org/10.1038/nrm1276

Stork, T., Engelen, D., Krudewig, A., Silies, M., Bainton, R.J., Klämbt, C., 2008. Organization and function of the blood-brain barrier in Drosophila. Journal of Neuroscience 28, 587–597. https://doi.org/10.1523/JNEUROSCI.4367-07.2008

Stowers, R.S., Megeath, L.J., Gó Rska-Andrzejak, J., Meinertzhagen, I.A., Schwarz, T.L., 2002. Axonal Transport of Mitochondria to Synapses Depends on Milton, a Novel Drosophila Protein, Neuron.

St-Pierre, J., Brand, M.D., Boutilier, R.G., 2000. Mitochondria as ATP consumers: Cellular treason in anoxia.

Sturtevart, A.H., 1921. A Case of Rearrangement of Genes in Drosophila.

Sulimenko, V., Hájková, Z., Klebanovych, A., Dráber, P., 2017. Regulation of microtubule nucleation mediated by γ-tubulin complexes. Protoplasma. https://doi.org/10.1007/s00709-016-1070-z

Sullenberger, C., Loncarek, J., 2022. Centrosomes and Centrioles, in: Encyclopedia of Cell Biology: Volume 1-6, Second Edition. Elsevier, pp. 151–163. https://doi.org/10.1016/B978-0-12-821618-7.00231-5

Sun, T., Song, Y., Dai, J., Mao, D., Ma, M., Ni, J.Q., Liang, X., Pastor-Pareja, J.C., 2019. Spectraplakin Shot Maintains Perinuclear Microtubule Organization in Drosophila Polyploid Cells. Dev Cell 49, 731-747.e7. https://doi.org/10.1016/j.devcel.2019.03.027

Szule, J.A., Coorssen, J.R., 2003. Revisiting the role of SNAREs in exocytosis and membrane fusion. Biochim Biophys Acta Mol Cell Res. https://doi.org/10.1016/S0167-4889(03)00095-8

Taghli-Lamallem, O., Gallet, A., Leroy, F., Malapert, P., Vola, C., Kerridge, S., Fasano, L., 2007. Direct interaction between Teashirt and Sex combs reduced proteins, via Tsh's acidic domain, is essential for specifying the identity of the prothorax in Drosophila. Dev Biol 307, 142–151. https://doi.org/10.1016/j.ydbio.2007.04.028

Tait, S.W.G., Green, D.R., 2010. Mitochondria and cell death: Outer membrane permeabilization and beyond. Nat Rev Mol Cell Biol. https://doi.org/10.1038/nrm2952

Takayama, Y., Kamimura, Y., Okawa, M., Muramatsu, S., Sugino, A., Araki, H., 2003. GINS, a novel multiprotein complex required for chromosomal DNA replication in budding yeast. Genes Dev 17, 1153–1165. https://doi.org/10.1101/gad.1065903

Takeda, K., Kishi, H., Ma, X., Yu, Z.X., Adelstein, R.S., 2003. Ablation and mutation of nonmuscle myosin heavy chain II-B results in a defect in cardiac myocyte cytokinesis. Circ Res 93, 330–337. https://doi.org/10.1161/01.RES.0000089256.00309.CB

Tamori, Y., Deng, W.M., 2013. Tissue Repair through Cell Competition and Compensatory Cellular Hypertrophy in Postmitotic Epithelia. Dev Cell 25, 350–363. https://doi.org/10.1016/j.devcel.2013.04.013

Tan, J.L., Ravid, S., Spudich, J.A., 1992. Control of nonmuscle myosins by phosphorylation.

Tanaka, S., Araki, H., 2013. Helicase activation and establishment of replication forks at chromosomal origins of replication. Cold Spring Harb Perspect Biol 5. https://doi.org/10.1101/cshperspect.a010371

Tang, H.W., Chen, G.C., 2011. Unraveling the role of myosin in forming autophagosomes. Autophagy. https://doi.org/10.4161/auto.7.7.15537

Tang, H.W., Wang, Y.B., Wang, S.L., Wu, M.H., Lin, S.Y., Chen, G.C., 2011. Atg1-mediated myosin II activation regulates autophagosome formation during starvation-induced autophagy. EMBO Journal 30, 636–651. https://doi.org/10.1038/emboj.2010.338

Tanos, B.E., Yang, H.J., Soni, R., Wang, W.J., Macaluso, F.P., Asara, J.M., Tsou, M.F.B., 2013. Centriole distal appendages promote membrane docking, leading to cilia initiation. Genes Dev 27, 163–168. https://doi.org/10.1101/gad.207043.112

Tansey, M.G., Luby-Phelps, K., Kamm, K.E., Stull, J.T., 1994. Ca2+-dependent phosphorylation of myosin light chain kinase decreases the Ca2+ sensitivity of light chain phosphorylation within smooth muscle cells. Journal of Biological Chemistry 269, 9912–9920. https://doi.org/10.1016/s0021-9258(17)36969-7

Tavosanis, G., Gonzalez, C., 2003. γ-tubulin function during female germ-cell development and oogenesis in Drosophila. Proc Natl Acad Sci U S A 100, 10263–10268. https://doi.org/10.1073/pnas.1731925100

Boveri T, 1887. Ueber den Antheil des Spermatozoon an der Teilung des Eies.

Thomsen, S., Anders, S., Janga, S.C., Huber, W., Alonso, C.R., 2010. Genome-wide analysis of mRNA decay patterns during early Drosophila development. Genome Biol 11. https://doi.org/10.1186/gb-2010-11-9-r93

Tillery, M.M.L., Blake-Hedges, C., Zheng, Y., Buchwalter, R.A., Megraw, T.L., 2018. Centrosomal and non-centrosomal microtubule-organizing centers (MTOCs) in Drosophila melanogaster. Cells. https://doi.org/10.3390/cells7090121

Trakala, M., Rodríguez-Acebes, S., Maroto, M., Symonds, C.E., Santamaría, D., Ortega, S., Barbacid, M., Méndez, J., Malumbres, M., 2015. Functional Reprogramming of Polyploidization in Megakaryocytes. Dev Cell 32, 155–167. https://doi.org/10.1016/j.devcel.2014.12.015

Uhlmann, F., 2001. Secured cutting: controlling separase at the metaphase to anaphase transition, EMBO reports.

Ullah, Z., Kohn, M.J., Yagi, R., Vassilev, L.T., DePamphilis, M.L., 2008. Differentiation of trophoblast stem cells into giant cells is triggered by p57/Kip2 inhibition of CDK1 activity. Genes Dev 22, 3024–3026. https://doi.org/10.1101/gad.1718108

Ullah, Z., Lee, C.Y., DePamphilis, M.L., 2009. Cip/Kip cyclin-dependent protein kinase inhibitors and the road to polyploidy. Cell Div. https://doi.org/10.1186/1747-1028-4-10

Underwood, R., Wang, B., Carico, C., Whitaker, R.H., Placzek, W.J., Yacoubian, T.A., 2020. The GTPase Rab27b regulates the release, autophagic clearance, and toxicity of alpha-synuclein. Journal of Biological Chemistry 295, 8005–8016. https://doi.org/10.1074/JBC.RA120.013337

Unhavaithaya, Y., Orr-Weaver, T.L., 2012. Polyploidization of glia in neural development links tissue growth to blood-brain barrier integrity. Genes Dev 26, 31–36. https://doi.org/10.1101/gad.177436.111

Urata, Y., Parmelee, S.J., Agard, D.A., Sedat, John W, Sedat, J W, 1995. A Three-Dimensional Structural Dissection of Drosophila Polytene Chromosomes.

Urs Sixt, S., Beiderlinden, M., Peter Jennissen, H., rgen Peters, J., 2007. Extracellular proteasome in the human alveolar space: a new housekeeping enzyme? Am J Physiol Lung Cell Mol Physiol 292, 1280–1288. https://doi.org/10.1152/ajplung.00140.2006.-We

Uzbekov, R., Prigent, C., 2022. A Journey through Time on the Discovery of cell cycle regulation. Cell Cycle Regulation. Cells 2022. https://doi.org/10.3390/cells11040704ï

V Chau, J.W.T.A.B.D.M.D.J.E.D.K.G.A.V., 1989. A Multiubiquitin Chain Is Confined to Specific Lysine in a Targeted Short-Lived Protein, Cold Spring Harbor Symp. Quant. Biol.

Vale', R.D., Goldsteint, L.S.B., 1990. One Motor, Many Tails: An Expanding Repertoire of Force-Generating Enzymes, Cell.

Vale, R.D., Spudich, J.A., Griffis, E.R., 2009. Dynamics of myosin, microtubules, and Kinesin-6 at the cortex during cytokinesis in Drosophila S2 cells. Journal of Cell Biology 186, 727–738. https://doi.org/10.1083/jcb.200902083

Valentijn, J.A., Valentijn, K., Pastore, L.M., Jamieson, J.D., 2000. Actin coating of secretory granules during regulated exocytosis correlates with the release of rab3D.

van Beneden E, N.A., 1887. Nouvelle recherches sur la fecondation et la division mitosique chez l'Ascaride megalocephale.

Van Breugel, M., Hirono, M., Andreeva, A., Yanagisawa, H.A., Yamaguchi, S., Nakazawa, Y., Morgner, N., Petrovich, M., Ebong, I.O., Robinson, C. V.,

Johnson, C.M., Veprintsev, D., Zuber, B., 2011. Structures of SAS-6 suggest its organization in centrioles. Science (1979) 331, 1196–1199. https://doi.org/10.1126/science.1199325

Van De Peer, Y., Mizrachi, E., Marchal, K., 2017. The evolutionary significance of polyploidy. Nat Rev Genet. https://doi.org/10.1038/nrg.2017.26

Van Niel, G., D'angelo, G., Raposo, G., 2018. Shedding light on the cell biology of extracellular vesicles. Nat Rev Mol Cell Biol 19, 213–228. https://doi.org/10.1038/nrm.2017.125ï

Vasquez, C.G., Tworoger, M., Martin, A.C., 2014. Dynamic myosin phosphorylation regulates contractile pulses and tissue integrity during epithelial morphogenesis. Journal of Cell Biology 206, 435–450. https://doi.org/10.1083/jcb.201402004

Vats, S., Galli, T., 2022. Role of SNAREs in Unconventional Secretion—Focus on the VAMP7-Dependent Secretion. Front Cell Dev Biol. https://doi.org/10.3389/fcell.2022.884020

Velentzas, P.D., Velentzas, A.D., Mpakou, V.E., Papassideri, I.S., Stravopodis, D.J., Margaritis, L.H., 2011. Proteasome inhibition induces developmentally deregulated programs of apoptotic and autophagic cell death during Drosophila melanogaster oogenesis . Cell Biol Int 35, 15–27. https://doi.org/10.1042/cbi20100191

Verderio, C., Cagnoli, C., Bergami, M., Francolini, M., Schenk, U., Colombo, A., Riganti, L., Frassoni, C., Zuccaro, E., Danglot, L., Wilhelm, C., Galli, T., Canossa, M., Matteoli, M., 2012. TI-VAMP/VAMP7 is the SNARE of secretory lysosomes contributing to ATP secretion from astrocytes. Biol Cell 104, 213–228. https://doi.org/10.1111/boc.201100070

Vereshchagina, N., Bennett, D., Szö, B., Kirchner, J., Gross, S., Vissi, E., White-Cooper, H., Alphey, L., 2004. The Essential Role of PP1 in Drosophila Is to Regulate Nonmuscle Myosin □ D. Mol Biol Cell 15, 4395–4405. https://doi.org/10.1091/mbc.E04

Vermeulen, K., Van Bockstaele, D.R., Berneman, Z.N., 2003. The cell cycle: a review of regulation, deregulation and therapeutic targets in cancer, Cell Prolif.

Vérollet, C., Colombié, N., Daubon, T., Bourbon, H.M., Wright, M., Raynaud-Messina, B., 2006. Drosophila melanogaster γ-TuRC is dispensable for targeting γ-tubulin to the centrosome and microtubule nucleation. Journal of Cell Biology 172, 517–528. https://doi.org/10.1083/jcb.200511071

Vetter, I.R., 2014. Ras Superfamily Small G Proteins: Biology and Mechanisms 1 General Features, Signaling.

Vietri, M., Radulovic, M., Stenmark, H., 2020. The many functions of ESCRTs. Nat Rev Mol Cell Biol. https://doi.org/10.1038/s41580-019-0177-4

Vining, M.S., Bradley, P.L., Comeaux, C.A., Andrew, D.J., 2005. Organ positioning in Drosophila requires complex tissue-tissue interactions. Dev Biol 287, 19–34. https://doi.org/10.1016/j.ydbio.2005.08.017

Vitiello E, Moreau P, Nunes V, et al. Acto-myosin force organization modulates centriole separation and PLK4 recruitment to ensure centriole fidelity. Nat Commun. 2019;10(1):52. doi:10.1038/s41467-018-07965-6

Von Stetina, J.R., Frawley, L.E., Unhavaithaya, Y., Orr-Weaver, T.L., 2018. Variant cell cycles regulated by Notch signaling control cell size and ensure a functional blood-brain barrier. Development (Cambridge) 145. https://doi.org/10.1242/dev.157115

Walczak, C.E., Cai, S., Khodjakov, A., 2010. Mechanisms of chromosome behaviour during mitosis. Nat Rev Mol Cell Biol. https://doi.org/10.1038/nrm2832

Walczak, C.E., Heald, R., 2008. Mechanisms of Mitotic Spindle Assembly and Function, in: International Review of Cytology. Academic Press Inc., pp. 111–158. https://doi.org/10.1016/S0074-7696(07)65003-7

Walter Nickel and Catherine Rabouille, 2009. Mechanisms of regulated unconventional protein secretion.

Wang, M., Nagle, R.B., Knudsen, B.S., Cress, A.E., Rogers, G.C., 2020. Centrosome loss results in an unstable genome and malignant prostate tumors. Oncogene 39, 399–413. https://doi.org/10.1038/s41388-019-0995-z

Wang, X., Schwarz, T.L., 2009. The Mechanism of Ca2+-Dependent Regulation of Kinesin-Mediated Mitochondrial Motility. Cell 136, 163–174. https://doi.org/10.1016/j.cell.2008.11.046

Wang, Y.L., 2005. The mechanism of cortical ingression during early cytokinesis: Thinking beyond the contractile ring hypothesis. Trends Cell Biol 15, 581–588. https://doi.org/10.1016/j.tcb.2005.09.006

Watanabe, Y., Honda, S., Konishi, A., Arakawa, S., Murohashi, M., Yamaguchi, H., Torii, S., Tanabe, M., Tanaka, S., Warabi, E., Shimizu, S., 2016. Autophagy controls centrosome number by degrading Cep63. Nat Commun 7. https://doi.org/10.1038/ncomms13508

Watson, E.D., Cross, J.C., 2005. Development of structures and transport functions in the mouse placenta. Physiology. https://doi.org/10.1152/physiol.00001.2005

Wcigel, D., Bellen, H.J., Jiirgens, G., Jiicklc, H., 1989. Primordium specific requirement of the homeotic gene fork head in the developing gut of the Drosophila embryo, Arch Dev Biol.

Weigel, D., Gerd, ', Irgens, J., Kiittner, F., Seifert, E., Jlckle, H., 1969. The Homeotic Gene fork head Encodes a Nuclear Protein and Is Expressed in the Terminal Regions of the Drosophila Embryo, Cell.

Weinberg, R.A., 1995. The Retinoblastoma Protein and Cell Cycle Control Review, Cell.

Weintraub, S.J., Prater, C.A., Dean, D.C., Rinnooy-Kan, C.Y., 1992. Retinoblastoma protein switches the E2F site from positive to negative element, 15. Kawabe, Y. & Ochi, A. 1 expo Med.

Welcker, M., Singer, J., Loeb, K.R., Grim, J., Bloecher, A., Gurien-West, M., Clurman, B.E., Roberts, J.M., 2003. Multisite Phosphorylation by Cdk2 and GSK3 Controls Cyclin E Degradation, Molecular Cell. Moreover.

Wells, M.B., Andrew, D.J., 2015. Salivary gland cellular architecture in the Asian malaria vector mosquito Anopheles stephensi. Parasit Vectors 8. https://doi.org/10.1186/s13071-015-1229-z

Wendt, T., Taylor, D., Messier, T., Trybus, K.M., Taylor, K.A., 1999. Visualization of Head-Head Interactions in the Inhibited State of Smooth Muscle Myosin, The Journal of Cell Biology.

Wendt, T., Taylor, D., Trybus, K.M., Taylor, K., 2001. Three-dimensional image reconstruction of dephosphorylated smooth muscle heavy meromyosin reveals asymmetry in the interaction between myosin heads and placement of subfragment 2.

Wera, S., Hemmingst, B.A., 1995. Serine/threonine protein phosphatases, Biochem. J.

Westermann, B., 2012. Bioenergetic role of mitochondrial fusion and fission, in: Biochimica et Biophysica Acta - Bioenergetics. pp. 1833–1838. https://doi.org/10.1016/j.bbabio.2012.02.033

Westermann, B., 2010. Mitochondrial fusion and fission in cell life and death. Nat Rev Mol Cell Biol. https://doi.org/10.1038/nrm3013

Wiese, C., Zheng, Y., 2006. Microtubule nucleation: γ-tubulin and beyond. J Cell Sci 119, 4143–4153. https://doi.org/10.1242/jcs.03226

Williams, B.C., Riedy, M.E., Williams, E. V, Gatti, M., Goldberg, M.L., Pasteur-Fondazione, I., Bolognetti, C., 1995. The Drosophila Kinesin-like Protein KLP3A Is a Midbody Component Required for Central Spindle Assembly and Initiation of Cytokinesis.

Woglar, A., Busso, C., Garcia-Rodriguez, G., Douma, F., Croisier, M., Knott, G., Gönczy, P., 2024. Mechanisms of axoneme and centriole elimination in Naegleria gruberi. EMBO Rep. https://doi.org/10.1038/s44319-024-00329-w

Wojcik, E.J., Glover, D.M., Hays, T.S., 2000. The SCF ubiquitin ligase protein Slimb regulates centrosome duplication in Drosophila, Current Biology.

Wold, M.S., 2025. REPLICATION PROTEIN A: A Heterotrimeric, Single-Stranded DNA-Binding Protein Required for Eukaryotic DNA Metabolism, Annu. Rev. Biochem.

Wollert, T., Wunder, C., Lippincott-Schwartz, J., Hurley, J.H., 2009. Membrane scission by the ESCRT-III complex. Nature 458, 172–177. https://doi.org/10.1038/nature07836

Wolthuis, R., Clay-Farrace, L., van Zon, W., Yekezare, M., Koop, L., Ogink, J., Medema, R., Pines, J., 2008. Cdc20 and Cks Direct the Spindle Checkpoint-Independent Destruction of Cyclin A. Mol Cell 30, 290–302. https://doi.org/10.1016/j.molcel.2008.02.027

Wu, J., de Heus, C., Liu, Q., Bouchet, B.P., Noordstra, I., Jiang, K., Hua, S., Martin, M., Yang, C., Grigoriev, I., Katrukha, E.A., Altelaar, A.F.M., Hoogenraad, C.C., Qi, R.Z., Klumperman, J., Akhmanova, A., 2016. Molecular Pathway of Microtubule Organization at the Golgi Apparatus. Dev Cell 39, 44–60. https://doi.org/10.1016/j.devcel.2016.08.009

Wu, Q., Yu, X., Liu, L., Sun, Shengrong, Sun, Si, 2021. Centrosome-phagy: implications for human diseases. Cell Biosci. https://doi.org/10.1186/s13578-021-00557-w

Xiang, J., Bandura, J., Zhang, P., Jin, Y., Reuter, H., Edgar, B.A., 2017. EGFR-dependent TOR-independent endocycles support Drosophila gut epithelial regeneration. Nat Commun 8. https://doi.org/10.1038/ncomms15125

Bao X X, Spanos C, Kojidani T, Lynch E M, Rappsilber J, Hiraoka Y, Haraguchi T, Sawin K E, 2018. Exportin Crm1 is repurposed as a docking protein to generate

microtubule organizing centers at the nuclear pore. https://doi.org/10.7554/eLife.33465.001

Takai Y, Sasaki T, Tanaka K, Nakanishi H, 1995. Rho as a regulator of the cytoskeleton.

Yamamoto, S., Jaiswal, M., Charng, W.L., Gambin, T., Karaca, E., Mirzaa, G., Wiszniewski, W., Sandoval, H., Haelterman, N.A., Xiong, B., Zhang, K., Bayat, V., David, G., Li, T., Chen, K., Gala, U., Harel, T., Pehlivan, D., Penney, S., Vissers, L.E.L.M., De Ligt, J., Jhangiani, S.N., Xie, Y., Tsang, S.H., Parman, Y., Sivaci, M., Battaloglu, E., Muzny, D., Wan, Y.W., Liu, Z., Lin-Moore, A.T., Clark, R.D., Curry, C.J., Link, N., Schulze, K.L., Boerwinkle, E., Dobyns, W.B., Allikmets, R., Gibbs, R.A., Chen, R., Lupski, J.R., Wangler, M.F., Bellen, H.J., 2014. A drosophila genetic resource of mutants to study mechanisms underlying human genetic diseases. Cell 159, 200–214. https://doi.org/10.1016/j.cell.2014.09.002

Yamano, H., 2019. APC/C: current understanding and future perspectives. F1000Res. https://doi.org/10.12688/f1000research.18582.1

Yang, S.A., Deng, W.M., 2018. Serrate/notch signaling regulates the size of the progenitor cell pool in Drosophila imaginal rings. Genetics 209, 829–843. https://doi.org/10.1534/genetics.118.300963

Zhang Y, & and Xi Y. (2015). Fat Body Development and its Function in Energy Storage and Nutrient Sensing in Drosophila melanogaster. Journal of Tissue Science & Engineering, 06(01). https://doi.org/10.4172/2157-7552.1000141

Zheng Y, Wong M L, Alberts B, & Mitchison T, 1995. Nucleation of microtubule assembly by a y-tubulin-containing ring complex, 72. McDonough, W. F. Earth planet. Sci. Lett. Spec. Pub. 42, Geol. Soc. Land.

Chan, J.Y., 2011. A Clinical Overview of Centrosome Amplification in Human Cancers, Int. J. Biol. Sci.

Young, P.E., Richman, A.M., Ketchum, A.S., Kiehart, D.P., 1993. Morphogenesis in Drosophila requires nonmuscle myosin heavy chain function.

Zack, T.I., Schumacher, S.E., Carter, S.L., Cherniack, A.D., Saksena, G., Tabak, B., Lawrence, M.S., Zhang, C.Z., Wala, J., Mermel, C.H., Sougnez, C., Gabriel, S.B., Hernandez, B., Shen, H., Laird, P.W., Getz, G., Meyerson, M., Beroukhim, R., 2013. Pan-cancer patterns of somatic copy number alteration. Nat Genet 45, 1134–1140. https://doi.org/10.1038/ng.2760

Zanet, J., Freije, A., Ruiz, M., Coulon, V., Sanz, J.R., Chiesa, J., Gandarillas, A., 2010. A mitosis block links active cell cycle with human epidermal differentiation and results in endoreplication. PLoS One 5. https://doi.org/10.1371/journal.pone.0015701

Zhai, Y., Kronebusch, P.J., Simon, P.M., Borisy, G.G., 1996. Microtubule Dynamics at the G2/M Transition: Abrupt Breakdown of Cytoplasmic Microtubules at Nuclear Envelope Breakdown and Implications for Spindle Morphogenesis, The Journal of Cell Biology.

Zhang, L., Tang, H., Kou, Y., Li, R., Zheng, Y., Wang, Q., Zhou, X., Jin, L., 2013. MG132-mediated inhibition of the ubiquitin-proteasome pathway ameliorates cancer cachexia. J Cancer Res Clin Oncol 139, 1105–1115. https://doi.org/10.1007/s00432-013-1412-6

Zhang, Q.Y., Tamura, M., Uetake, Y., Washitani-Nemoto, S., Nemoto, S.I., 2004. Regulation of the paternal inheritance of centrosomes in starfish zygotes. Dev Biol 266, 190–200. https://doi.org/10.1016/j.ydbio.2003.10.027

Zhang, S., Zhou, K., Luo, X., Li, L., Tu, H.C., Sehgal, A., Nguyen, L.H., Zhang, Y., Gopal, P., Tarlow, B.D., Siegwart, D.J., Zhu, H., 2018. The Polyploid State Plays a Tumor-Suppressive Role in the Liver. Dev Cell 44, 447-459.e5. https://doi.org/10.1016/j.devcel.2018.01.010

Zhang, Y., Wang, Z., Liu, D.X., Pagano, M., Ravid, K., 1998. Ubiquitin-dependent degradation of cyclin B is accelerated in polyploid megakaryocytes. Journal of Biological Chemistry 273, 1387–1392. https://doi.org/10.1074/jbc.273.3.1387

Zheng, L., Shen, B., 2011. Okazaki fragment maturation: Nucleases take centre stage. J Mol Cell Biol 3, 23–30. https://doi.org/10.1093/jmcb/mjq048

Zheng, Y., Buchwalter, R.A., Zheng, C., Wight, E.M., Chen, J. V., Megraw, T.L., 2020. A perinuclear microtubule-organizing centre controls nuclear positioning and basement membrane secretion. Nat Cell Biol 22, 297–309. https://doi.org/10.1038/s41556-020-0470-7

Zhou, L., Xue, X., Yang, K., Feng, Z., Liu, M., Pastor-Pareja, J.C., 2023. Convergence of secretory, endosomal, and autophagic routes in trans-Golgi–associated lysosomes. Journal of Cell Biology 222. https://doi.org/10.1083/jcb.202203045

Zielke, N., Kim, K.J., Tran, V., Shibutani, S.T., Bravo, M.J., Nagarajan, S., Van Straaten, M., Woods, B., Von Dassow, G., Rottig, C., Lehner, C.F., Grewal,

S.S., Duronio, R.J., Edgar, B.A., 2011. Control of Drosophila endocycles by E2F and CRL4 CDT2. Nature 480, 123–127. https://doi.org/10.1038/nature10579

Zimmet, J., Ravid, K., 2000. Polyploidy: Occurrence in nature, mechanisms, and significance for the megakaryocyte-platelet system, Experimental Hematology.

Zou, L., Mitchell, J., And, †, Stillman, B., 1997. CDC45, a Novel Yeast Gene That Functions with the Origin Recognition Complex and Mcm Proteins in Initiation of DNA Replication, MOLECULAR AND CELLULAR BIOLOGY.

Zybina, T.G., Zybina, E. V., 2005. Cell reproduction and genome multiplication in the proliferative and invasive trophoblast cell populations of mammalian placenta. Cell Biol Int. https://doi.org/10.1016/j.cellbi.2005.10.015

RÉSUMÉ

Les centrosomes sont les principaux centres organisateurs des microtubules (MTs) dans les cellules animales. Bien que le nombre de centrosomes soit normalement bien régulé, certaines cellules font exception. Par exemple, on observe une amplification du nombre de centrosomes dans les cellules multiciliées et une élimination programmée dans les cellules polyploïdes des glandes salivaires (SGs) de la *Drosophile*. Ce processus, dans les cellules polyploïdes s'accompagne souvent d'une perte des centrosomes par un mécanisme mal compris.

Pour étudier ce phénomène, j'ai utilisé les SGs de la *Drosophile* comme modèle. Ces tissus sécrétoires sont composés de cellules géantes polyploïdes, organisées autour d'un lumen dans lequel elles sécrètent une colle essentielle à la puparation. J'ai d'abord analysé le comportement des centrosomes au cours du développement embryonnaire des SGs. En utilisant des approches d'immunofluorescence et d'imagerie en direct, j'ai identifié un nouveau mécanisme d'élimination des centrosomes, qui commence lorsque les centrosomes se localisent à la membrane apicale au début du stade embryonnaire. Les centrosomes sont ensuite libérés dans le lumen à des stades ultérieurs de l'embryogenèse. En analysant la membrane des cellules des SGs, j'ai observé que les centrosomes étaient localisés dans des vésicules enrichies d'actin et myosine II active (MyoII). Ceci suggère un rôle de MyoII dans le processus d'élimination, ce qui a été confirmé en utilisant une mutation hypomorphe (*MyoII*^{mut}).

J'ai ensuite confirmé que l'activité de MyoII est essentielle pour l'élimination des centrosomes, car seul MyoII WT, et non MyoII inactif, pouvait sauver les phénotypes *MyoII*^{mut}. J'ai également utilisé une autre stratégie pour maintenir les centrosomes en surexprimant Sak/Plk4 (Plk4OE). Les centrosomes dans le lumen sont polyubiquitinés avant dégradation par le protéasome et disparition au stade de la prépupal. En utilisant différentes mutations, j'ai pu identifier l'implication de l'autophagie et de l'exocytose autolysosomale pour la libération des centrosomes dans le lumen. J'ai ensuite étudié la cause de l'élimination des centrosomes. Le maintien des centrosomes causait des défauts dans la structure et l'organisation des mitochondries. Ceci a été renforcé par des seahorse expériences montrant une réduction de la respiration et de la production d'ATP.

En conclusion, mon travail de doctorat a révélé un nouveau mécanisme impliqué dans l'élimination des centrosomes avec des fonctions clés dans la sauvegarde de l'organization des mitochondries assurant une production élevée d'énergie issue du métabolisme.

MOTS CLÉS

Centrosomes ; Polyploïdie ; Glande salivaires de la *Drosophile* ; Myosin II (MyoII) ; Autophagie ; Exocytose Lysosomal ; Protéasome ; Mitochondries

ABSTRACT

Centrosomes act as the main microtubule (MTs) organizing centers (MTOC) of animal cells. Although centrosome number is tightly regulated in the cell, many exceptions can be found. This is the case of centrosome amplification in multiciliated cells or centrosome elimination in programmed polyploid *Drosophila* salivary gland (SGs) cells. Interestingly, many polyploid cells lose their centrosomes in a not well understood mechanism.

With the aim of characterizing the mechanism of centrosome elimination, I used *Drosophila* SGs as a model system. These are highly secretory tissues composed of secretory cells surrounding a tubular lumen, in which they secrete a glue essentiel for pupariation.

I first analyzed centrosome behavior during embryonic SG development. Using immunofluorescence and live imaging approaches, I identified a model for centrosome elimination, that is initiated when centrosomes localize at the apical membrane at early embryonic stage. Then centrosomes are release into the lumen at later stages of embryogenesis. While analyzing the membrane behavior, I could detect that the centrosomes were engulfed in an actin vesicle enriched with active myosin II (MyoII). This suggested a possible role of MyoII in the elimination process, which was confirmed using a hypomorphic mutation (*MyoII*^{mut}).

I then confirmed that MyoII activity is essential for centrosome elimination as only wild type MyoII, not inactive MyoII, could rescue the *MyoII*^{mut} phenotypes in L3 SGs. I also used another strategy to maintain centrosomes, by overexpressing Sak/Plk4 (Plk4OE). Interestingly, centrosomes were present in Plk4OE SG cells, and they were only eliminated with the constitutive active MyoII, suggesting that centrosome elimination is a time restricted process dependent on MyoII activity. Centrosomes in the lumen were polyubiquitinated for proteasome degradation until they disappeared in prepupae stages. Using different mutations, I could identify the involvement of autophagy and autolysosome exocytosis in centrosome release in the lumen.

I next investigated the purpose of centrosome elimination in SG cells. Maintenance of centrosomes in SG cells caused defects in mitochondria structure and organization. This was reinforced with seahorse experiments showing reduced respiration and ATP production.

In conclusion my PhD work revealed a novel mechanism involved in centrosome elimination with key functions in safeguarding the mitochondria cytoskeleton ensuring high metabolic energy production.

KEYWORDS

Centrosomes ; Polyploidy ; *Drosophila* salivary glands ; Myosin II (MyoII) ; Autophagy ; Lysosomal exocytosis ; Proteasome, and Mitochondria